1-1-2015

Biochemical And Structural Characterization Of The Core Subunits Of Gpi Transamidase

Dilani G. Gamage
Wayne State University,

BIOCHEMICAL AND STRUCTURAL CHARACTERIZATION OF THE CORE SUBUNITS OF GPI TRANSAMIDASE

by

DILANI G GAMAGE

DISSERTATION

Submitted to the Graduate School

of Wayne State University,

Detroit, Michigan

in partial fulfillment of the requirements

for the degree of

DOCTOR OF PHILOSOPHY

2015

MAJOR: CHEMISTRY (Biochemistry)

Approved by:

_____

Advisor Date

_____

_____

_____

DEDICATION

To my loving parents K. M. Rathnaweera and G. G. Gunasena

My aunt D. C. Rathnaweera

My loving husband N. G. Wijesundara

My dissertation advisor Prof T. L. Hendrickson

ACKNOWLEDGMENTS

I would like to acknowledge my advisor, Professor Tamara L. Hendrickson for the constant support and advise given to me during last five years. Her mentorship, guidance and believing in me to be a good research scientist, allowed me be who I am today. With her enormous scientific knowledge and generosity I was able to learn a number of new skills and techniques. The excellent atmosphere she created in our lab reduced our working stress. Staying far away from our motherland, Sri Lanka, she once plays the role of a mother and a dear friend in many occasions. Her encouragement to build up self confident in me not only helped to achieve my targets in science, but also helped me to handle difficult situations in my life. With deepest gratitude, I sincerely thank you, Prof Tamara L. Hendrickson for giving me five blessed years at Wayne State University.

My sincere gratitude goes to my thesis committee, Professor Christine S. Chow, Professor Sarah Trimpin and Professor Rafael A. Fridman for the invaluable support and comments given throughout my Ph.D. period. I would like to thank my committee for being supportive and understanding me throughout these time to achieve my goals. Unless the time and efforts you have put together, I won't be able to fulfill my desires on time.

A numerous support was given by my talented colleagues, Dr. Yug Varma, Ms. Megan Ehrenworth, Dr. Keng-Ming Chang, Dr. Sandamali Ekanayaka, Dr. Liangjun Zhao, Dr. Gayathri Silva, Shirin Fathma, Nilesh Joshi, Sairaman Seetharaman, Travis Ness, Udumbara Rathnayaka, Whitney Wood,

Suwiman Subka and Aaron Sieg. I am thankful to all of them sharing the scientific knowledge and creating a friendly environment inside and outside the lab.

I also like to thank Professor Trimpin, Professor Plum, Professor Bhagwat, Professor Feig, professor Ahn and Professor Chow for allowing me to share some of the valuable instruments from your labs. I also would like to acknowledge members from the department of chemistry, for helping me in many ways. Also I'd like to thank to Wayne State University for providing funding and facilities to pursue my Ph.D.

My greatest gratitude goes to all of my Sri Lankan friends being with me during life's challenges and frustrations and remembering me the value of friendship specially in a country far away from the home land.

I would like to extend my deepest gratitude to my parents and my aunt for the sacrifices and efforts you have done on me to be who I'm today. Also I'm thankful to my loving brother and sister with their family for the help and support given to me throughout my life. Last but not least I am utterly grateful to my loving husband for the love, kindness and the support given to me throughout these years. I'm really grateful for your constant encouragement on my research and personal life. It's your belief in me that built myself confident.

TABLE OF CONTENTS

LIST OF TABLES

LIST OF FIGURES

LIST OF ABBREVIATIONS

Abz	2-aminobenzoic acid
ADH	Acohol dehydrogenase
APS	Ammonium peroxodisulfate
BME	β-mercaptoethanol
CA25	Campath-1 antigen
CAP-1	Channel activating protease-1
CF	Carboxyfluorescein
COPII	Coat protein II
CPY	Carboxypeptidase Y
CSE	Cigarette smoke extract
DIPEA	N,N-diisopropylethylamine
EDTA	Ethylenediaminetetraacetic acid
EGFR	Epidermal growth factor receptor
EGTA	Ethyleneglycoltetraacetic acid
Y21	Yapsin 2 protease
ER	Endoplasmic reticulum

ESI-IMS-MS	Electrospray ionization ion mobility separation mass spectrometry
FOXC2	Forkhead box protein C2
FR	Folate binding receptors
FRET	Fluorescence resonance energy transfer
GPAA1	Glycosylphosphatidylinositol anchor attachment 1
GPI	Glycosylphosphatidylinositol
GPI-T	Glycosylphosphatidylinositol transamidase
GSH	Reduced glutathione
GST	Glutathione S-Transferase
HA	Hemagglutinin
HBTU	*O*-(Benzotriazol-1-yl)-*N,N,N′,N′*-tetramethyluronium hexafluorophosphate
hDAF	Human decay accelerating factor
HPLC	High performance liquid chromatography
IPTG	Isopropyl-γ-D-1-thiogalactopyranoside
MW	Molecular weight
NBN	Nitrobenzonitrile
NMP	N-methyl-2-pyrrolidone

PAGE	Polyacrylamide gel electrophoresis
PAI	Plasminogen activator inhibitor
PBS	Phosphate buffered saline
PIG-K	Phosphatidylinositol glycan class K
PIG-S	Phosphatidylinositol glycan class S
PIG-T	Phosphatidylinositol glycan class T
PIG-U	Phosphatidylinositol glycan class U
PLAP	Placental alkaline phosphatase
PMSF	Phenylmethanesulfonylfluoride
PN-1	Protease nexin–1
PNH	Paroxysmal nocturnal hemoglobinuria
PSSM	Position-specific scoring matrix
RIPA	Radioimmunoprecipitation
SAD	Small amino acid domain
SAXS	Small angle X-ray scattering
SDS	Sodium dodecyl sulfate
Endo H	Endoglycosidase H
SEC	Size exclusion chromatography

SRP	Secretory recognition particle
TAP	Tandem affinity purification
TEMED	Tetramethylethylenediamine
TFA	Trifluoro Acetic acid
TIR	Toll/interleukin-1 receptor
TLC	Thin layer chromatography
TM	Transmembrane
UP30	Urokinase-type plasminogen-activated receptor
uPAR	Urokinase plasminogen-activated receptor
uPAS	Urokinase plasminogen activating system

CHAPTER 1

INTRODUCTION

GPI TRANSAMIDASE AND GPI ANCHORED PROTEINS: ONCOGENES AND BIOMARKERS FOR CANCER

Most of this chapter was published in an invited review: **Gamage, D. G.** and Hendrickson, T. L. "GPI transamidase and GPI anchored proteins: oncogenes and biomarkers for cancer." **2013**, *Crit. Rev. Biochem. Mol Biol.* 48(5): 446-464

1.1 Introduction

Cancer is caused by uncontrolled abnormal cell growth. According to statistics from the American Cancer Society, in the United States nearly one in two men and one in three women will develop a cancer in his or her lifetime. Cancer is also a public health threat worldwide. Geographic variations in cancer types and prevalence can arise from differences in regional lifestyle, genetics, diet and pollution, amongst other factors.[1]

In addition to the emotional toll of cancer on patients, family, and friends, statistics from the American Cancer Society illustrate the devastating economic impact of cancer worldwide, which stem from direct costs for medical care and rehabilitation and indirect costs from morbidity and mortality.[1] In order to reduce cancer mortality and improve each patient's quality of life, it is important to understand how different oncogenes and biomarkers participate in cancer onset, progression, and metastasis. Several well established cancer biomarkers, including the urokinase plasminogen-activated receptor (uPAR) and the folate

receptor, are *C*-terminally modified with a glycosylphosphatidylinositol (GPI) anchor.[2,3] This glycolipid anchor is clearly essential for proper translocation of these proteins; however, evidence supporting any further functional involvement for the GPI anchor, particularly with respect to tumor phenotypes, was minimal. In 2004, the discovery of the GPI anchor biosynthesis class U protein (PIG-U) as an oncogene in human bladder cancer opened a new door to the possibility that the enzyme involved in GPI anchoring, called GPI transamidase or GPI-T, might itself be tumorigenic.[4] PIG-U is one of the five subunits that comprise the human GPI-T although the function of PIG-U in this enzyme is unknown.[5] The reaction catalyzed by GPI-T and the chemical structure of a typical human GPI anchor are shown in Figure 1.1.

GPI membrane anchoring of proteins is an abundant phenomenon that specifically tethers proteins to lipid bilayers. Approximately 0.5% of all eukaryotic proteins are modified or predicted to be modified by GPI-T to contain a GPI anchor.[6] GPI anchored proteins are almost exclusively localized on the cell surface where they are non-covalently associated with the plasma membrane via the lipid portion of the anchor. GPI anchored proteins are engaged in diverse processes like immune recognition, cellular communication, signal transduction, and embryogenesis.[7,8,9,10,11] Loss of GPI anchoring is embryonically lethal to mammals and conditionally lethal to yeast.[10, 12,13] Defects in GPI anchor biosynthesis can cause diseases like paroxysmal nocturnal hemoglobinuria and hyperphosphatasia mental retardation syndrome and a mutation in the PIG-T

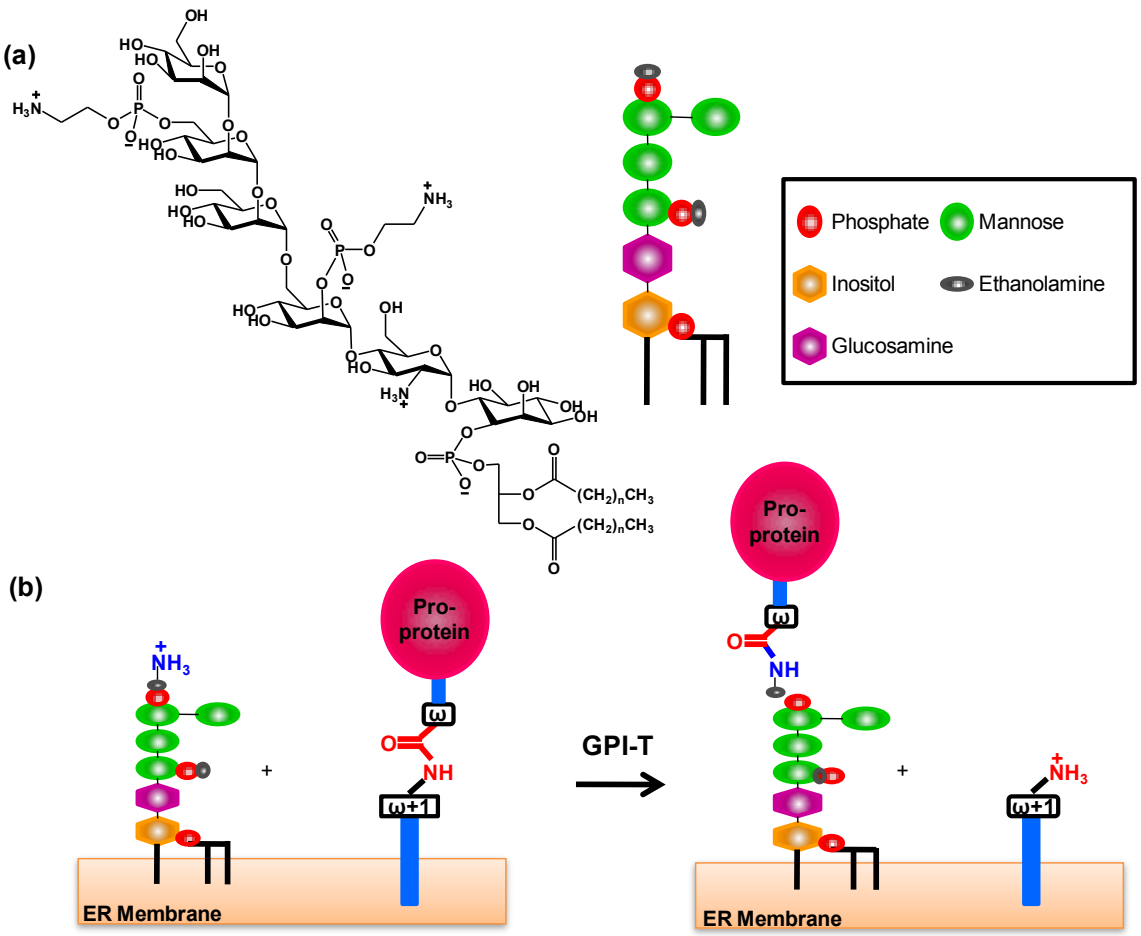

Figure 1.1: The chemical structure of the GPI anchor and the reaction catalyzed by GPI-T. (a) Left: The basic chemical structure of a human GPI anchor from nucleated cells is shown as a representative example. Right: A simplified cartoon representation of this GPI anchor. (b) The reaction catalyzed by GPI-T. GPI-T displaces the *C*-terminal signal sequence in the proprotein substrate with a GPI anchor, forming a new amide bond between the ω site carbonyl and the amine from the phosphoethanolamine group on the third mannose in the GPI anchor. Figure 1.5 shows the mechanism of this reaction in greater detail.

subunit of GPI-T is connected to an intellectual disorder.[14,15,16] These different diseases highlight the importance of GPI anchoring of proteins to normal cell biology. This introductory chapter focuses specifically on the connections that link GPI membrane anchoring to abnormal cell biology and cancer.

GPI-T is a complicated and poorly understood enzyme. GPI-T is a membrane bound, multi-subunit protein complex found in the endoplasmic reticulum (ER). This enzyme contains five known subunits, PIG-K, PIG-T, GPAA1, PIG-S, PIG-U in humans[5,12,17] (analogous to Gpi8, Gpi16, Gaa1, Gpi17 and Gab1 in yeast[5,12,18,19]). PIG-U, the last subunit of GPI-T was identified more than a decade ago and yet clear functional assignments for all but one of these subunits have remained elusive. The exception is PIG-K (Gpi8): this subunit comprises the catalytic machinery of the enzyme.[12,20] Understanding how changes in gene overexpression participate in tumor onset or progression is difficult without a clear picture of the enzyme itself in terms of its structure and function.

1.2 The GPI anchor: A substrate for GPI-T

GPI anchors contain a common core structure that is conserved across eukaryotes and contains an ethanolamine phosphate, three mannoses, a glucosamine and a phosphatidylinositol group (Figure 1.1). However, tissue- and species-specific core modifications and elaborations were identified in GPI anchors from different sources.[21,22,23,24,25] The complete biosynthetic pathway to

produce the GPI anchor was fully revealed by the early 2000's (Figure 1.2). This pathway requires more than 20 gene products, making GPI anchoring of proteins one of the most complex and metabolically expensive post-translational modifications.[9,26,27] The different enzymes involved in GPI biosynthesis have been characterized to varying extents. Most are hydrophobic and reside in the ER membrane (recently reviewed by Fujita and Kinoshita).[9]

GPI anchors are present in minute amounts in human and fungal cells and are also challenging to synthesize and purify. Due to this complexity, small nucleophiles like hydrazine, hydroxylamine, and biotin hydrazide were identified as useful GPI anchor mimics.[28] These GPI anchor surrogates were used early on to characterize the reaction catalyzed by GPI-T.

Because of limitations faced when isolating GPI anchors from their natural environments, it has remained challenging to understand the contributions made by different monosaccharides or modifications. Syntheses of short series of GPI anchor analogues have been reported.[29,30] Synthesis of the full-length CD52 peptide, with its *N*-linked glycan and most of its GPI anchor, was reported about 10 years ago and was recently followed up by the synthesis of a complete GPI anchor (from the human lymphocyte CD52 antigen).[31,32] These synthetic compounds (full-length anchors, synthetic GPI anchored proteins, anchor mimics and anchor analogues) can be used not only to better understand GPI-T but also to investigate the functions of GPI anchored proteins in cells and for vaccine development. In fact, synthetic GPI glycans were used in microarray studies to examine antitoxic malaria responses and to develop carbohydrate-based

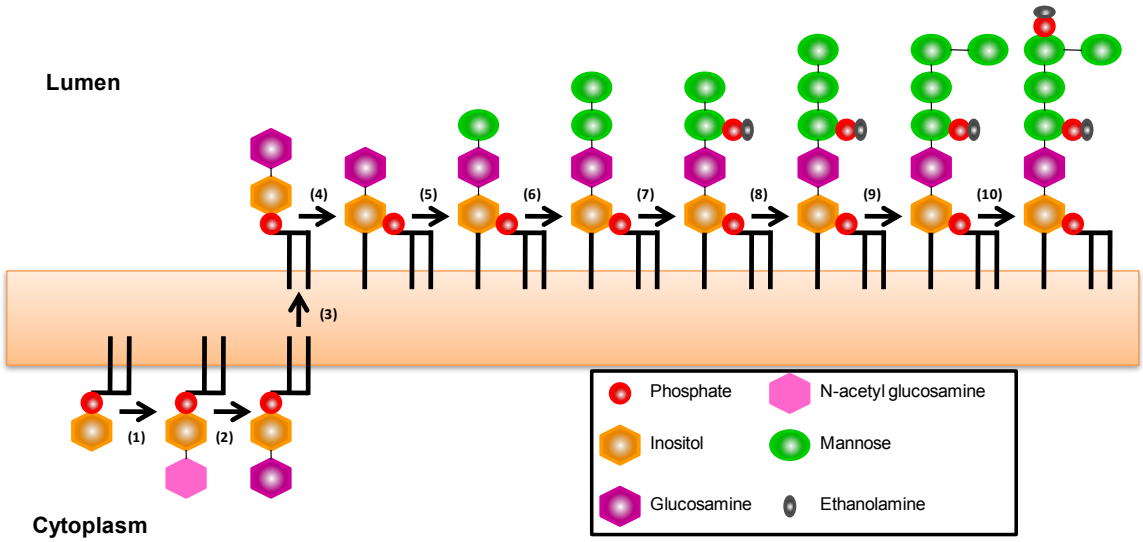

Figure 1.2: Biosynthetic pathway for GPI anchors in human nucleated cells. The GPI anchor is synthesized in the ER starting from phosphoinositol. At least ten enzymes are needed for this pathway; these enzymes are summarized in the table 1.1. The first two steps of the synthesis take place on the cytoplasmic side of the ER and steps 4 through 10 occur on the luminal side. Later steps in this pathway can vary in different types of cells.

vaccines to treat severe malaria.[33,34] Another recent study used an azide-labeled *N*-acetylgalactosamine analog (GalNAz) to understand the immobilization of GPI anchored proteins inside the cell as well as to analyze the functional roles of branch modifications.[35]

Defects in different GPI anchor biosynthetic steps cause several types of inheritable and acquired diseases. For a recent review see Almeida *et.al.*.[36] To our knowledge, defects in GPI anchor biosynthesis have not been directly linked to cancer onset or propagation. However, patients with paroxysmal nocturnal hemoglobinuria (PNH), a hemolytic disorder that results from a somatic mutation in *PIGA* (See Table 1.1), are at increased risk of developing acute leukemia.[14]

1.3 Protein substrates for GPI-T

Proteins designated to be GPI anchored are ribosomally synthesized as preproproteins and contain an *N*-terminal signal sequences targeting them for translocation into the ER. Historically, it has been assumed that substrates for GPI-T enter the ER via the secretory recognition particle (SRP).[37] However, a recent report made the compelling argument that these preproproteins are predominantly delivered to the ER by an SRP-independent pathway.[38] This process relies on recognition of both the *N*-terminal signal peptide and the *C*-terminal GPI-T-specific signal sequence (described below). Once the preproprotein is delivered to the ER, the *N*-terminal signal sequence is cleaved by signal peptidase. The resultant proprotein is recognized by GPI-T and the *C*-

Table 1.1: Enzymes involved in GPI anchor biosynthesis in human nucleated cells. Additional modification reactions are known to occur in other types of cells.

Step	Enzyme complex	Proteins involved
1	GPI-GlcNActransferase[39,40,41,42]	PIG-A, PIG-C, PIG-H, PIG-P, PIG-Q, PIG-Y, DPM2
2	GlcNAc-PI de-N-acetylase[41]	PIG-L
3	Flippase[43]	Unknown
4	Inositol acyltransferase[44]	PIG-W
5	α1-4 mannosyltransferase I[45,46]	PIG-M, PIG-X
6	α1-6 mannosyltransferase II[47]	PIG-V
7	EtNPtransferase I[48]	PIG-N
8	α1-2 mannosyltransferase III[49]	PIG-B
9	α1-2 mannosyltransferase IV[50]	PIG-Z
10	EtNPtransferase III[51]	PIG-O, PIG-F

terminal GPI-T signal sequence is displaced upon conversion to the mature GPI anchored protein (Figure 1.3 and Table 1.1). The use of an SRP-independent pathway for translocation to the ER clearly defines GPI membrane anchoring as a post-translational protein modification.

GPI-T recognizes and cleaves the *C*-terminal signal sequence of the proprotein at the ω-site, forming a new amide bond between the ω-site carbonyl and the appropriate amine on the GPI anchor. The ω-site is so named because it becomes the *C*-terminal residue of the mature GPI anchored protein. This residue is immediately followed by the ω+1 and ω+2 residues (and so forth towards the *C*-terminus); the remainder of this *C*-terminal sequence is composed of a hydrophilic spacer and a hydrophobic peptide.[52,53] Several studies have analyzed the identity of the ω-site amino acid and GPI-T's ability to tolerate substitutions. Most of this work relied on a protein construct called preprominiPLAP, a minimalistic version of human placental alkaline phosphatase. PreprominiPLAP promoted significant advances in the field because it contained an engineered poly-Met sequence suitable for metabolic labeling with ^{35}S-Met and it was significantly smaller than native PLAP so that the different processing intermediates could be resolved by gel electrophoresis (namely, the preproprotein, the proprotein, and the GPI anchored protein, as well as a truncated hydrolytic product).[54,55] Analysis of preprominiPLAP mutants revealed that alanine, cysteine, glycine, asparagine and serine are good ω-site candidates for human GPI-T. Similar results were obtained using human decay

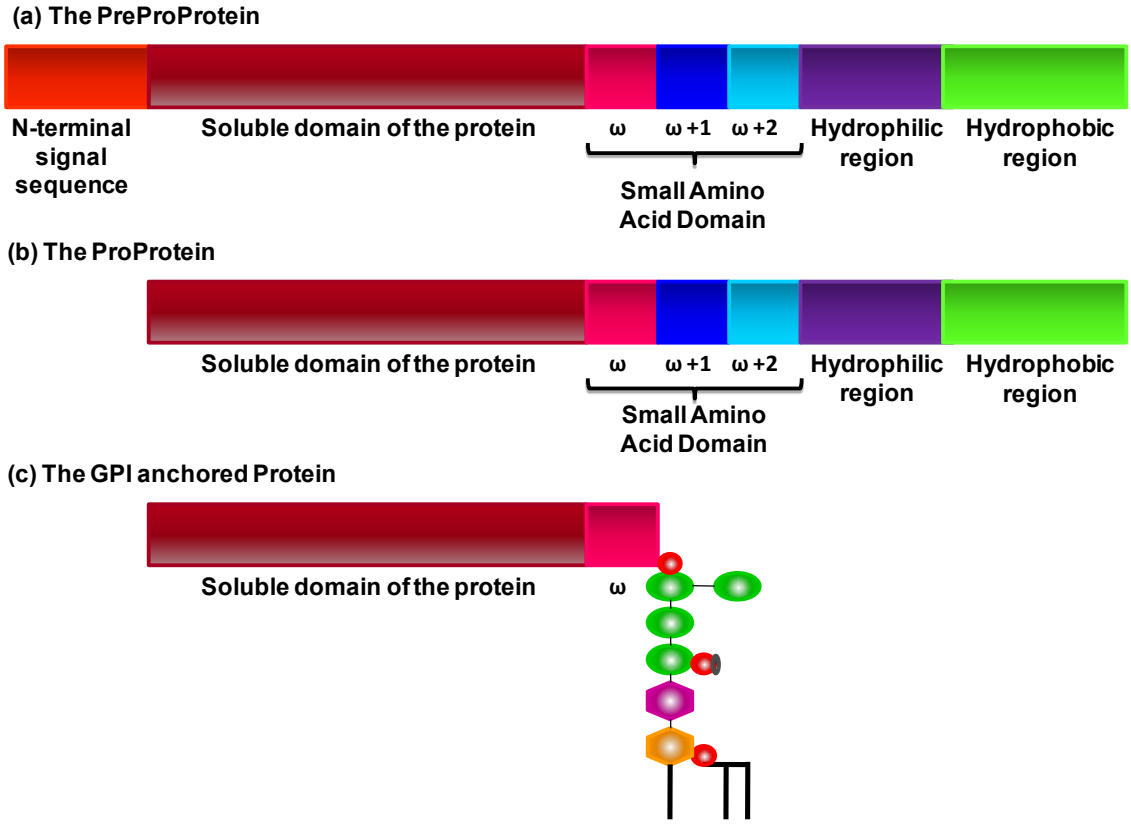

Figure 1.3: Cartoon schematic of a protein substrate for GPI-T and its processing intermediates. The preproprotein (a), which is destined for GPI anchoring, has an *N*-terminal signal sequence that is cleaved by signal peptidase to produce the proprotein (b). The GPI-T signal sequence on the *C*-terminus of this protein contains a hydrophilic region followed by a hydrophobic region. The signal sequence is cleaved by GPI-T between the ω and ω+1 amino acids to attach the GPI anchor, producing the mature, GPI anchored protein (c). (Refer to Figure 1.1 for the symbols used to designate the GPI anchor.)

accelerating factor (hDAF), another GPI anchored protein; in this case, aspartate was identified as a good ω-site but cysteine was not.[56,57] In general, the ω-site residue should be a small, hydrophilic amino acid.[54] The first web server to predict the presence and identity of ω sites in protein sequences was put forward in 1999, with a false positive prediction rate of only 0.3%.[58]

The ω+1 position is typically small but can be any amino acid other than proline. The requirements for ω+2 are much more stringent.[59,54] This position is almost always alanine, glycine or serine.[59,54] Because the ω to ω+2 positions tend to be small amino acids, this region has been referred to as the Small Amino acid Domain (SAD).[52,59]

The ω+2 residue is followed by the remainder of the GPI-T signal sequence. This peptide is typically between 18 and 32 amino acids long and ends at the *C*-terminus of the protein. It can be broken down into two sections, an 8-12 amino acid spacer sequence that is predominantly hydrophilic, followed by a 15-20 amino acid hydrophobic sequence.[37,52,53] Remarkably, the GPI-T *C*-terminal signal sequence does not contain a consensus motif. In fact, in one report, completely artificial signal sequences (e.g. Ser_3-Thr_8-Leu_{14}) were appended onto the *C*-terminus of CD46 and were shown to be viable, enabling GPI anchoring *in vivo*.[60] Consequently, recognition of this sequence by GPI-T is analogous to recognition of the *N*-terminal secretory signal sequence by signal peptidase, more than it is to the methods used by other co- and post-translational modification enzymes to select their substrates. Recent findings suggest that the hydrophobicity of the hydrophobic region needs to be marginal compared to type

II transmembrane anchors.[61] Similarly, the hydrophilic spacer lacks a consensus sequence, but the relative hydrophilicity and the length of the peptide play important roles.[53,60] Amino acids *N*-terminal to the ω-site are required for GPI anchoring but without sequence or size specificity.[37,53,62,63]

The smallest known GPI anchored protein is the CD52 or Campath-1 antigen. In humans, the full-length *CD52* gene encodes a 61 amino acid protein that begins with an *N*-terminal signal peptide that is 24 amino acids in length. CD52's *C*-terminal GPI-T signal sequence begins with the ω-site at Ser36 and proceeds to the *C*-terminus (Ser61). Thus, the proprotein is 37 amino acids long and the fully mature, GPI anchored protein contains only 12 amino acids.[64]

Despite the simplicity of the rules that define the GPI-T signal sequence, some studies have suggested that GPI-T shows species specificity for its protein substrates.[65,66,67] General and species-specific prediction algorithms have been developed and have revolutionized the ability of researchers to predict not only GPI anchoring but also the identity of the one or two most likely ω-sites.[58,68,69,70] One recent GPI-T signal peptide prediction tool demonstrates high accuracy using a position-specific scoring matrix (PSSM).[71,72] One thing that these *in silico* analyses suggest is the possibility that GPI-T recognizes and processes more than one ω-site in a single peptide, leading to subtle heterogeneity during maturation. (In other words, a protein substrate with two putative ω-sites might be processed at both positions so that a mixture is produced where the anchor can be attached at either ω-site.) To our knowledge, the experimental identification of processing at more than one ω-site has not yet been observed or

reported. However, very few efforts at genome-wide characterizations of anchored proteins, particularly with ω-site validation, have been reported, so this possibility cannot be rejected at the present time.

1.4 The GPI Transamidase Complex

Five GPI-T subunits have been identified so far, with homologues in eukaryotes ranging from yeast to humans; all five subunits are essential for the attachment of GPI anchors to proteins. As mentioned above, these subunits are called PIG-K, PIG-T, GPAA1, PIG-S, PIG-U in humans,[5,12,17,73] analogous to Gpi8, Gpi16, Gaa1, Gpi17, Gab1 in yeast, respectively.[5,12,17,18,19] In *Trypanosoma brucei*, PIG-U and PIG-T are replaced by TTA1 and TTA2, two unrelated subunits.[74] Table 1.2 summarizes the sizes of these different subunits as well as their predicted number of transmembrane domains and glycosylation sites for orthologs from humans, yeast, and *T. brucei*. For the remainder of this introductory chapter, we will use the names of the human GPI-T subunits unless specifically talking about an experiment conducted with GPI-T from other species.

Homologues of PIG-K, GPAA1, and PIG-T are conserved across eukaryotes. In yeast, these core subunits can be purified together as a complex.[18] In contrast, in humans, all five subunits can be isolated together.[5] Based on mutagenic analyses and its similarity to caspases, the PIG-K subunit

Table 1.2: Features of GPI-T from humans, *S. cerevisiae*, and *T. brucei*. Specific references are provided for publications where a given TM domain or glycosylation site was predicted or experimentally examined. Asterisks (*) indicate glycosylation sites or TM regions that were only predicted in the UniProt database.

Subunit	Size (kD)	Putative glycosylation sites	Transmembrane regions
Human			
PIG-K[75]	45.3	-	One*
GPAA1[76]	67.6	Two: N203, N517	Eight
PIG-S[75]	61.7	Two: N267*, N370*	Two*
PIG-T[77]	65.7	Three: N164, N291*, N327*	One*
PIG-U[75]	50.1	-	Nine*
S. cerevisiae			
Gpi8[78]	47.4	Three: N23[a], N256*, N346*	One*
Gaa1[79]	69.2	Two: N87, N383*[b]	Six
Gpi17[75]	60.8	Five: N100*, N170*, N228*, N247*, N299*	Two*
Gpi16[80]	68.8	Two: N28[a], N184*	One
Gab1[75]	44.7	-	Eight *
T. brucei			
TbGpi8[81]	36.7	One: N25	No
TbGaa1[82]	51.2	-	Six
TbGpi16[82]	75.8	-	One
TTA1[82]	41.9	Two: N79, N259	Two
TTA2[82]	45.6	-	Six

[a] In yeast, both Gpi8 and Gpi16 contain reasonable *N*-linked glycosylation sites within or immediately adjacent to their *N*-terminal signal peptides. These sites are listed here for completeness but they have not been characterized; they may not be glycosylated or may have been cleaved from the protein during *N*-terminal processing.
[b]N383 is predicted as a glycosylation site using UniProt[75] However, Hamburger *et al.* reported results that argue that this site is not glycosylated.[78-79] N383 lies between the second and third transmembrane domains of Gaa1 and is presumably inaccessible to the glycosylation machinery.

was identified as the catalytic active site and is the best characterized of the five known subunits.[20,83,84] Possible roles for some of the remaining subunits have been proposed and are discussed individually below. The hydrophobicity of the subunits, the complexity of the GPI-T enzyme, and poor expression levels of the different subunits have contributed to the lack of progress in further characterization of this enzyme. Another drawback has been the lack of a high-throughput assay for GPI-T. Nearly all methods to assay this enzyme's activity are both cumbersome and qualitative. Significant data is accumulating that supports the hypothesis that the GPI-T complex contains more than one copy of some or all of its subunits. In particular, native PAGE analysis of the pure, heterotrimeric GPI-T complex from yeast revealed that this complex resolves into two assemblies with molecular weights of ~430 and ~650 kD.[18] Given the molecular weights of the individual subunits, a complex of only ~240 kD is predicted. All three of these yeast GPI-T subunits (Gpi8, Gaa1, and Gpi16) contain probable glycosylation sites (See Table 1.2), but it seems unlikely that glycans could account for an increase in MW of the ~400 kD needed to explain the 650 kD complex. Thus, Conzelmann and colleagues proposed higher order

oligomerization for GPI-T.[18] The human GPI-T complex (from HeLA cells) has a velocity sedimentation value of 17S, also consistent with a globular complex with a mass of ~450 kD.[85] In this work, Gaa1 was also observed to interact with α- and β-tubulin; thus the possibility that tubulin is the source of the increase in the molecular weight of GPI-T in humans cannot be ruled out. (Tubulin was not apparent in the yeast GPI-T complex analyzed by native gel.) Additionally, PIG-K, the active site subunit of GPI-T, has sequence and putative structural similarity to caspases. The soluble domain of Gpi8 (the PIG-K ortholog from yeast) partly assembles into a homodimer when heterologously expressed in *Escherichia coli*, analogous to caspase dimerization.[83] Gpi16 is attached to Gpi8 by a known disulfide bond[86] (see below); thus, by analogy, the hypothesis that the Gpi8 homodimer is symmetrically modified by two Gpi16 subunits is intuitive. Gpi8 dimerization has recently been called into question (discussed further in the next section).[12, 84] Understanding the stoichiometry and organization of GPI-T is going to be crucial to understanding its function. Additional research is needed in this area.

The next sections summarize what is known about the structures and functions of the individual subunits of GPI-T. The possible functional roles for each subunit, as they are currently understood, are discussed individually here and are summarized for human GPI-T in Table 1.3. Their possible roles in cancer will be discussed later in this introductory chapter.

Table 1.3: Proposed functional roles for the five subunits of human GPI-T.

Subunit	Possible Roles or Functions
PIG-K[20,78,87]	Similarities to caspases and other cysteine proteases Contains all or some of the enzyme's catalytic machinery Attached to PIG-T by a disulfide bond
GPAA1[76]	May contain part of the active site and be involved in peptide binding and/or recognition
PIG-S[88,89]	Essential for thioester intermediate formation between PIG-K and the protein substrate
PIG-T[87,88]	Essential for carbonyl intermediate formation between PIG-K and the protein substrate Attached to PIG-K by a disulfide bond
PIG-U[5,90]	Loosely associated with the rest of the GPI-T complex Weak similarity to fatty acid elongases Possibly involved in lipid recognition or binding

1.4.1 The PIG-K (Gpi8) subunit

PIG-K is the catalytic subunit of GPI-T. This ~47 kD subunit nominally belongs to the C13 cysteine protease family.[12,20] PIG-K has a large soluble domain, oriented to the luminal side of the ER, and a single *C*-terminal transmembrane region (Figure 1.4 (a)).[12] The soluble domain has sequence similarity to caspases, a family of cysteine proteases that regulate cell death.[20] Analysis of conserved His and Cys residues indicated that His164 and Cys206 are the catalytic residues in human PIG-K (His157 and Cys199 in yeast).[20,91] By analogy to cysteine proteases, the histidine presumably deprotonates the cysteine, which nucleophilically attacks the amide bond between the ω and ω+1 residues, creating a thioester intermediate, which is subsequently converted to a new amide with the GPI anchor (Figure 1.5).[92]

A Rosetta-predicted structure of the soluble domain of yeast Gpi8 was built based on putative structural homology between caspases and Gpi8 (Figure 4 (b)).[83] This model positions the backbones of the two catalytic residues of GPI-T (His157 and Cys199) in similar locations and orientations as their counterparts in caspases. Caspases are active as homodimers, leading to the hypothesis that Gpi8 also assembles into a homodimer, an oligomerization step that may be essential for enzyme activity. Dimerization of the soluble domain of Gpi8 was observed by native PAGE and by mass spectrometry. Furthermore, dimerization was disrupted by the introduction of mutations at positions corresponding to the face of caspase dimerization. Significant Gpi8 monomer was also observed in this work, leading to the proposal that the Gpi8 dimer reflects the native

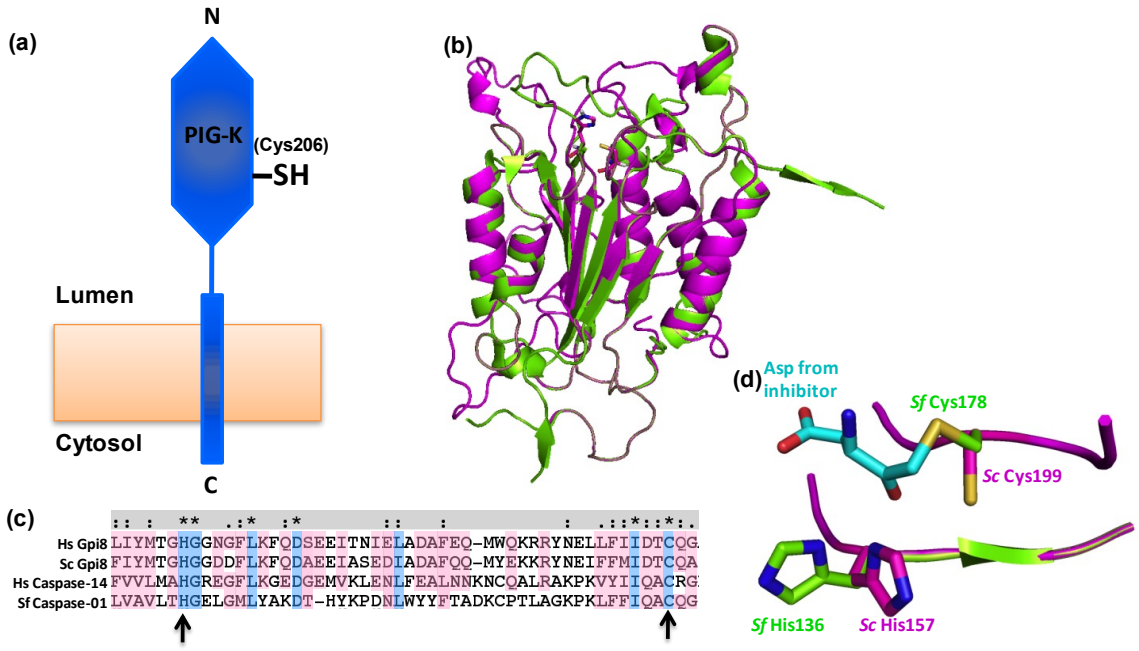

Figure 1.4: The PIG-K subunit. (a) PIG-K has a single soluble domain (~340 amino acids) and one transmembrane domain. Human PIG-K is not glycosylated however there are three sites of *N*-glycosylation in yeast Gpi8. The catalytic cysteine (Cys206 in humans) is noted. PIG-K is connected to PIG-T via a single disulfide bond (not shown). (b) The soluble domain of PIG-K has putative sequence and structural homology with caspases.[83, 93] The structure of caspase-1 from *Spodoptera frugiperda*(PDB: 1M72, green) is overlayed onto a Rosetta model of *S. cerevisiae* Gpi8 (magenta).[83] (c) The sequences for portions of the active site of human PIG-K (NP_005473), *S. cerevisiae* Gpi8 (NP_010618), human caspase-14 (NP_036246), and *S. frugiperda* caspase-1 (AAC47442) were aligned using Clustal W. Conserved residues are colored in blue, including the histidine and cysteine that form the catalytic dyad for each enzyme. Residues highlighted in magenta indicate positions that show similarity in at least three of the four sequences. (d) A close up of the catalytic dyads in *S. frugiperda* caspase-1 (green) and the model of *S. cerevisiae* Gpi8 (magenta) from panel B. The active site cysteine in caspase-1 is shown alkylated by an irreversible inhibitor. The model of Gpi8 places the His/Cys catalytic dyad within hydrogen bonding distance.

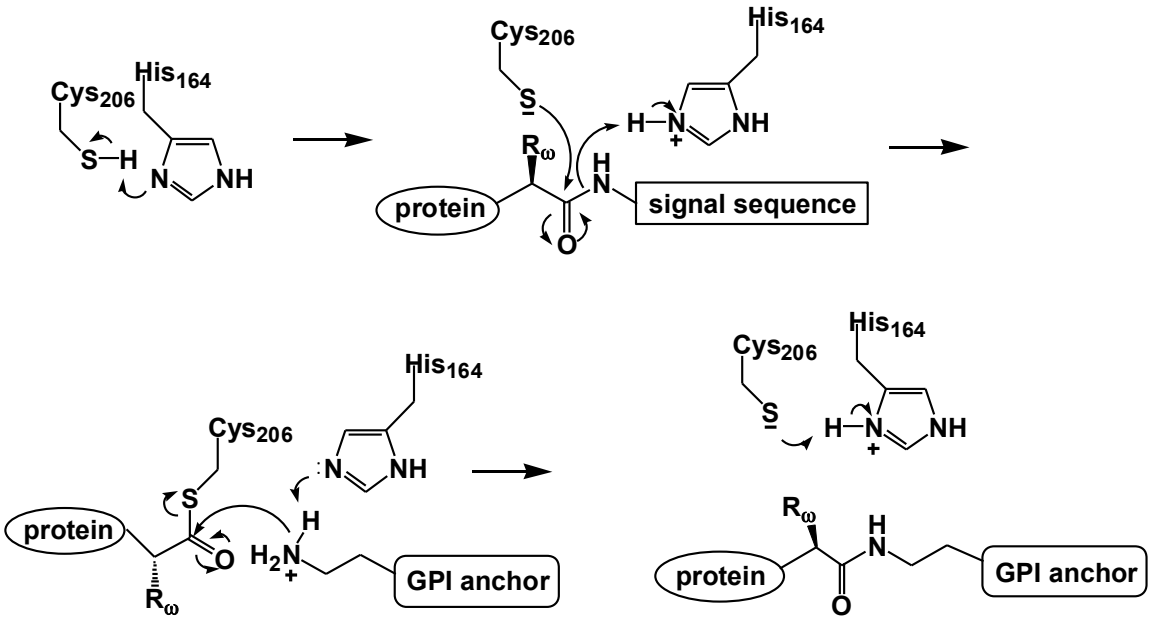

Figure 1.5: Proposed mechanism for GPI-T mediated protein transamidation.

oligomerization state and that the monomer represents poorly folded or misfolded Gpi8 as a consequence of heterologous expression in *E. coli*. Toh *et al.* recently reported a very similar isolation of the soluble domain of Gpi8.[84] However, they used size exclusion chromatography (SEC) to isolate only the monomeric form of Gpi8. It is unclear whether or not they examined their preparations for dimer and it is probable that the Gpi8 dimer was lost during SEC purification. As discussed above, clear evidence from two other research groups also support the hypothesis that GPI-T assembles into a higher order oligomer in yeast and in humans.[18,85] Consequently, the preponderance of available evidence argue that GPI-T assembles into a higher order oligomer. However, additional characterization of this enzyme's stoichiometry is clearly mandated.

1.4.2 The GPAA1 (Gaa1) subunit

GPAA1 (67 kD) was the first subunit identified in the GPI-T complex.[19] It has a single *N*-terminal TM domain, a soluble domain, and six *C*-terminal TM domains (Figure 1.6).[19] GPAA1 shares 25% sequence identity and 57% similarity with yeast Gaa1.[76] It assembles into a stable complex with Gpi16 and Gpi8 in yeast.[18] In human cells, GPAA1 associates with PIG-K, PIG-T, PIG-S and PIG-U and is essential for transamidase activity.[17,85,91] A portion of the soluble domain of yeast Gaa1 (residues 70-247) was characterized recently using small angle X-ray scattering (SAXS) providing a low resolution map of a fragment (residues 70-247) of this domain.[94]

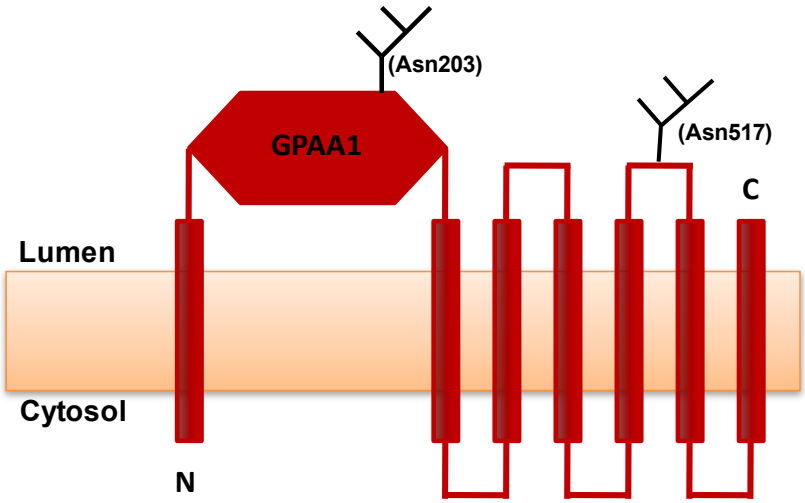

Figure 1.6: The GPAA1 structure. GPAA1 has one *N*-terminal transmembrane domain, a single soluble domain (~323 amino acids) and six *C*-terminal transmembrane domains.[95] Two *N*-linked glycosylation sites are found in GPAA1 at Asn203 and Asn517.

While its exact function is unknown, evidence suggests that GPAA1 recognizes and stabilizes the *C*-terminal signal sequence of the peptide substrate through a conserved Pro609 in the last transmembrane helix.[85,96,90] Additionally, photo cross linking studies also support the hypothesis that GPAA1 interacts with protein substrates for GPI-T. GPI-T from GPAA1 knockout mouse cells were still capable of generating the thioester intermediate between Gpi8 and a substrate protein, but this intermediate was not processed to the mature, GPI anchored protein.[91] Combined, these observations are consistent with GPAA1 containing part of the active site (in addition to Gpi8) and/or a substrate recognition domain. However, with all these finding, a recent paper claimed that GPAA1 is a M28 peptide synthetase that carry presumably a Zn^{2+} metal binding site and catalyzes peptide bond formation between the substrate and the GPI anchor.

1.4.3 The PIG-T (Gpi16) subunit

PIG-T is a 69 kD protein with a large *N*-terminal hydrophilic region and a *C*-terminal transmembrane domain (Figure 1.7).[17] A mutation in PIG-T is connected to a recessive intellectual disability syndrome, which, to our knowledge, is the only known GPI-T defect associated with a disease other than cancer.[16] In yeast, Gpi16 is co-purified along with GST-Gpi8 and Gaa1; in human all five subunits co-purify as a complex with GST-PIG-K.[5,18] Even though the exact function of this subunit is not clear, PIG-T is essential for formation of the carbonyl intermediate between Gpi8 and the protein substrate during transamidation (see Figure 1.5).[17] Some evidence suggests that PIG-T stabilizes

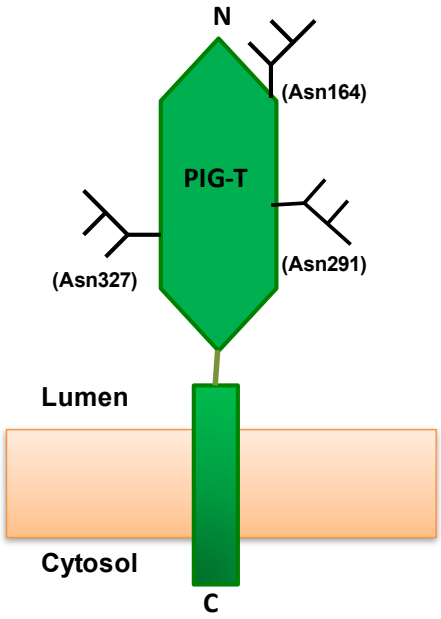

Figure 1.7: The PIG-T structure. PIG-T has one *N*-terminal soluble domain (~506 amino acids) and a single *C*-terminal transmembrane domain. PIG-T is connected to PIG-K via a disulfide bond (not shown). PIG-T has three *N*-linked glycosylation sites in its soluble domain.

PIG-K and GPAA1: When *PIG-T* was knocked out, reduced expression levels of the other GPI-T subunits were observed.[17] PIG-T makes a functionally relevant disulfide bond with PIG-K through two conserved cysteine residues, Cys^{92} (in PIG-K) and Cys^{182} (in PIG-T), making it the only subunit covalently linked to the catalytic subunit.[86] This linkage is not essential for the formation of the GPI-T complex, but is important for GPI-T activity.[86]

1.4.4 The PIG-S (Gpi17) subunit

PIG-S is a 61 kD protein with a large soluble domain in between two transmembrane regions (Figure 1.8).[17] In yeast, Gpi17 is essential for GPI-T activity, but it does not stably interact with the core GPI-T subunits (Gpi8, Gpi16, and Gaa1) and its exact function is unknown.[89] As observed with *PIG-T*, knockout of the *PIG-S* gene eliminated formation of the thioester intermediate between PIG-K and the proprotein substrate.[17] PIG-S is one of the subunits replaced by TTA1 and TTA2 in *T. brucei* (See Figure 1.8).

1.4.5 The PIG-U (Gab 1) subunit

PIG-U was the fifth (and presumably final) subunit identified as a component of GPI-T (Figure 1.8).[5] This 38 kD protein is highly hydrophobic and has between eight to ten transmembrane regions. Deletion of this gene inhibits the formation of cell surface GPI anchored proteins.[5] Vainauskas and Menon suggested that PIG-U is more loosely associated with the GPI-T complex than any of the other subunits, based on differential immunoprecipitation patterns with

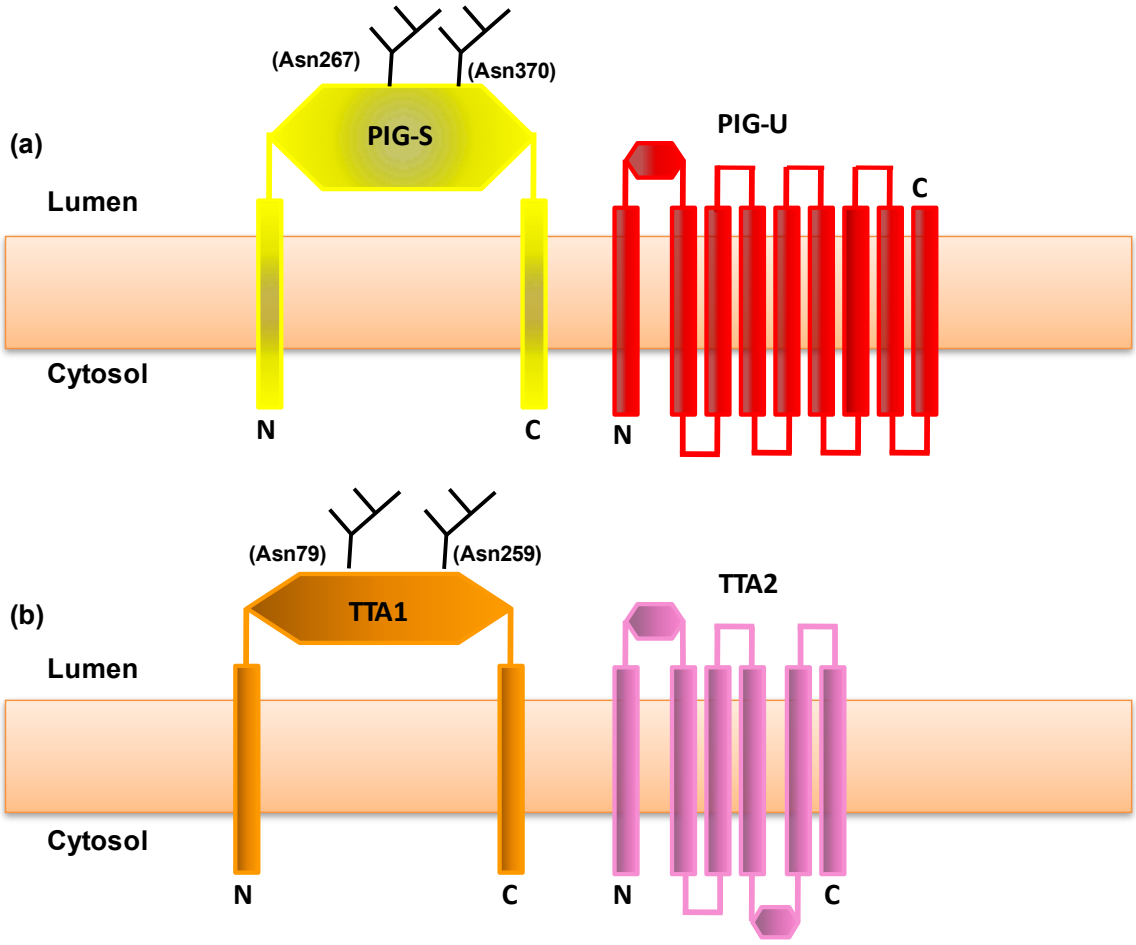

Figure 1.8: Subunits PIG-S and PIG-U are found in human GPI-T (a) and are replaced by TTA1 and TTA2 in *T. brucei* (b). PIG-S and TTA1 are not related in sequence but have topological similarities and both contain two putative glycosylation sites. PIG-U and TTA2 both have two small soluble domains and several transmembrane domains however they are topological dissimilar and do not share sequence similarity.

digitonin versus Nonidet-solubilized microsomes.[90] Although its contribution to the GPI-T complex is unknown, PIG-U does show weak sequence similarity with fatty acid elongases suggesting that it may be involved in recognition of the lipid portion of the GPI anchor.[5] PIG-U was the first GPI-T subunit found in human cancer.[4] Like PIG-S, PIG-U is also replaced by TTA1 and TTA2 in the *T. brucei* GPI-T (see Figure 1.8).

1.4.6 The TTA1 & TTA2 subunits

Two of the five human GPI-T subunits (PIG-S and PIG-U) are not conserved across all eukaryotes. In trypanosomes, these two subunits are replaced by the Trypanosomatid Transamidase 1 (TTA1) and Trypanosomatid Transamidase 2 (TTA2) proteins (Figure 1.8).[74] TTA1 has two transmembrane helices, one at each terminus. The intervening hydrophilic soluble region is predicted to face the luminal side of the ER and contain two *N*-glycosylation sites. TTA2 contains multiple transmembrane domains and a single soluble domain. TTA1 and TTA2 do not share sequence homology with any mammalian, yeast, plant, insect or nematode GPI-T subunits; however orthologs are present in *Leishmania major*. TTA1 and TTA2 are linked to each other through a disulfide linkage and knockout of either of these subunits inhibits the transfer of the GPI anchor onto its protein substrates.

The relevance of TTA1 and TTA2 to a discussion of GPI-T and cancer is not immediately obvious. However, these two trypanosomal subunits have replaced PIG-S and PIG-U, the same two subunits that do not co-purify as part of

a robust complex from *Saccharomyces cerevisiae*.[18] Even though we don't yet understand the impact of these observations, they do suggest that the roles of PIG-S and PIG-U in human GPI-T may be peripheral compared to those of PIG-K, PIG-T, and GPAA1. In other words, they hint that PIG-K, PIG-T, and GPAA1 may constitute the catalytic core of GPI-T for all species. While this hypothesis remains speculative, it is likely that these observations will ultimately contribute to our understanding of human GPI-T function and the roles of these subunits in cancer.

1.5 GPI-T and cancer

The amplification of oncogenes contributes to human carcinogenesis.[97] Chromosomes 8q and 20q are frequently amplified in many cancers including breast, bladder, ovarian and endometrioid carcinomas.[98,99,100,101,102] Out of the five GPI-T subunits, the genes encoding PIG-U, PIG-T and GPAA1 are localized in the 20q11, 20q13 and 8q24 chromosome regions, respectively, positions that are considered hotspots for most cancers.[103] The genes encoding PIG-K and PIG-S are located at 1p31 and 17p13, respectively.[103] Simple localization of a gene within an oncogenic amplicon is insufficient to identify an oncogene. Amplicons contain multiple genes, not all of which have increased copy numbers in the corresponding tumors nor are overexpressed to a significant degree. However, known oncogenic amplicons make useful starting points to identify new oncogenes and to better understand tumorigenesis.

The first hint for the importance of GPI-T in cancer was reported by Trink and colleagues in 2004, with their discovery of the first oncogenic GPI-T subunit, CDC91L1 (encoding PIG-U) in bladder cancer.[4] With this finding, the possibility of overexpression of other GPI-T subunits in different cancer types came into the picture. Another critical study showed that breast cancer cells have significantly elevated levels of cell surface GPI anchored proteins that are more typical of mesenchymal stem cells than of healthy breast tissue.[104] This finding is consistent with overexpression of one or more GPI-T subunits leading to up-regulation of GPI-T catalytic activity as a mechanism for tumor initiation or invasion. This section will discuss our current understanding of the overexpression of different GPI-T subunits in different cancer types, at both the mRNA and protein levels, and their importance as oncogenes or biomarkers. It is clear that a number of different downstream events can be activated or regulated by overexpression of different GPI-T subunits.

1.5.1 PIG-U and Cancer

PIG-U was the fifth subunit identified in the GPI-T complex, a hydrophobic protein that is essential for GPI-T activity.[5] Building on the discovery of germline translocation of the 20q11 chromosomal region in uroepithelial cancer, the *CDC91L1* (*PIG-U*) gene was characterized for its role in bladder cancer development.[4,105] This gene lies adjacent to the germline translocation site. Overexpression of PIG-U in mice induced tumorigenesis, providing strong evidence that this subunit acts as an oncogene.[4] Furthermore, forced

overexpression of PIG-U in cell culture induced an increase in cell growth rate and enhanced overexpression of proteins known to be GPI anchored. Of particular interest was the observed overexpression of urokinase plasminogen activated receptor (uPAR).[4] This GPI-anchored protein is a well-characterized oncogene for most cancers.[106,107] Increased STAT-3 phosphorylation was also observed as a downstream effect of uPAR overexpression, suggesting that tumorigenicity arises from perturbations in *JAK/stat* cell signaling.[4] In total, this report suggests that overexpression of PIG-U increases GPI-T activity and anchoring of substrate proteins although the mechanism by which activity is increased remains unknown, particularly since PIG-U is not the catalytic subunit of GPI-T.

A subsequent study concluded that *CDC91L1* is not overexpressed in urothelial cell carcinomas (where 2.4% overexpression of *CDC91L1* mRNA was observed compared to > 30% *CDC91L1* amplification in cell lines and primary bladder tumors.[4,108] Finally, a third group assessed a larger data set of bladder urothelial cell carcinoma. In this study, *CDC91L1* mRNA was overexpressed in 30.1% of tumors compared to healthy cells. PIG-U protein overexpression occurred in 75.3% of tumor samples.[109] These differences in overexpression levels of both mRNA and protein presumably arise from different factors such as tumor stage, age and gender of the patient, or other environmental factors that remain poorly understood.

Expression patterns for all five GPI-T subunits were analyzed in 19 different cancer types and compared to healthy tissues from the same organ and

the same patient using microarray technology.[103] Basal level expression of different subunits varied in different types of healthy tissue.[103] *PIG-U* mRNA was overexpressed in 60% of colon and ovarian cancer samples versus healthy tissue.[103] In lymph node tumors, PIG-U protein was expressed at moderate to low levels in 90% of malignant tissues, but was not detectable in the corresponding healthy tissues. Also a significant increase of PIG-U protein production was observed in both ovarian and breast cancer cells and overexpression occurred in 60% of large cell lung carcinoma cells.[103] PIG-U was overexpressed in 42% of breast cancer cells, as well as in prostate cancer.[103,110]

1.5.2 PIG-T and Cancer

The *PIGT* gene is also positioned in a chromosomal hot spot (chromosomal region 20q13.12). With the discovery of *PIG-U* as an oncogene, the possibility of other GPI-T subunits as oncogenes, including PIG-T, became relevant.[4,103] Overexpression of PIG-T was first found in human breast cancer. An increase in PIG-T expression correlated with downstream overexpression and phosphorylation of paxillin, a known cell invasion related and tumorigenic protein.[110,111,112]

In the same microarray report discussed for *PIG-U*, *PIG-T* mRNA overexpression was observed in 60% of uterine, 50% of thyroid and melanoma, and 30% of breast cancer samples compared to healthy tissues.[103] Significant PIG-T protein overexpression was observed in colon, thyroid, lung and

pancreatic cancers; overexpression at lower levels also occurred in both squamous cell carcinoma and lung adenocarcinoma cells.[103]

A combination of mass spectrometry, separate siRNA inhibition of PIG-T and GPAA1 expression, and separate overexpression of each of these subunits led to the identification of nineteen GPI anchored proteins that are specifically expressed in breast cancer cells and are either poorly expressed or not expressed in healthy breast tissue.[104] Eighteen of these biomarkers are present in mesenchymal stem cells, suggesting that all or some of these proteins facilitate dedifferentiation of breast cancer cells. Furthermore, reduction of either PIG-T or GPAA1 levels by siRNA reduced expression levels of the FOXC2 transcription factor by 80%. Overexpression (by viral infection) of either subunit increased expression of FOXC2 at both the mRNA and protein levels.[104] The authors posited that overexpression of either PIG-T or GPAA1 affects signal transduction pathways (presumably by increased expression of a GPI-anchored cell surface receptor) that leads to increased FOXC2 expression. FOXC2 is overexpressed in breast and colon cancers and is involved in mitochondrial biogenesis and increased cell metabolism.[104,113]

Cigarette smoke extract (CSE) induces cancer formation in head, neck, bladder and breast cells.[114] CSE also induces overexpression of three GPI-T subunits: PIG-T, PIG-U, and GPAA1.

1.5.3 GPAA1 and Cancer

Frequent amplification in chromosomal region 8q24 in different cancer types makes this region a chromosomal hotspot.[115,116,117,118] The *GPAA1* gene is in the 8q24.3 region and thus, like PIG-U, is a possible oncogene.[73,76]

GPAA1 mRNA levels were increased 69% in head and neck squamous carcinoma and 40% in uterine cancer cells.[103,119] Significant overexpression of GPAA1 protein was observed in ovary and thyroid cells, along with ~40% overexpression in prostate cancer and 10-20% in lung adenocarcinoma cases.[103] PCR-array profiling of 20 pairs of liver tissues (healthy vs. tumor samples) identified 117 genes with different expression levels, only seven of which were amplified in hepatocellular carcinoma and both hepatitis B virus positive carcinoma and hepatitis C virus positive carcinoma.[120] *GPAA1* was one of these seven genes. Amplification was observed at both the mRNA (75%) and protein levels (90%).[121]

When GPAA1 was overexpressed in breast cancer cells, levels of phosphorylated paxillin also increased, thereby activating Brk-mediated phosphorylation and promoting cell invasion that is linked to tumor metastasis (Figure 1.9).[110,112,122] Along with PIG-U and PIG-T, GPAA1 was overexpressed in the presence of CSE, which led to initiation of paxillin phosphorylation in head, neck, bladder and breast cancers.[114] GPAA1 overexpression led to its association with the epidermal growth factor receptor (EGFR) and EGFR phosphorylation in the presence of epidermal growth factor.[114] As a consequence, PIG-T and PIG-U were phosphorylated by EGFR. It was proposed

that this GPAA1-EGFR interaction and phosphorylation leads to phosphorylation of paxillin to induce cancer initiation.[114] GPAA1 overexpression was observed in a variety of different cancers that did not correlate with overexpression of other GPI-T subunits. The connection between GPAA1 and EGFR may explain this divergence.[114] Elevated levels of GPAA1 also increased FOXC2 protein levels.[104,113]

1.5.4 PIG-K and Cancer

Human PIG-K is the catalytic subunit of the GPI-T complex.[12,20] Compared to other subunits, PIG-K resides on a different chromosome (1p31.1), in a region that is frequently lost in various human cancers.[123] In breast cancer, PIG-K was overexpressed in both ovarian (64%) and uterine (67%) cancers.[103] However PIG-K was down-regulated 50% in both bladder and hepatocellular carcinoma cells and 40% in colon carcinoma cells, based on mRNA levels; similar down-regulation was observed at the protein level (40%, 100%, and 40% respectively).[103] In order to understand the reason for diminished PIG-K expression, all ten PIG-K exons were examined in samples from 45 different colorectal cancer patients. A single nucleotide polymorphism at position rs1048575 (outside the coding region), which changed C/C to either G/C or G/G, was identified that varied with race.[124] In contrast, PIG-K was undetectable in normal lymph node tissues but accumulated in 65% of lymph node cancer samples.[103]

Given the close connections between GPI-T and cancer in general, it is perhaps surprising that PIG-K, the catalytic subunit of GPI-T, is more likely to be down-regulated than up-regulated in many cancers. In yeast, depletion of Gpi8 causes changes in actin morphology (depletion of Gab1, but none of the other GPI-T subunits, showed similar effects).[125] These changes offer one possible scenario for how reduced Gpi8 expression might lead to downstream tumorigenesis without increasing GPI-T activity and anchoring of oncogenic GPI anchored proteins.

1.5.5 PIG-S and Cancer

The *PIG-S* gene resides in chromosomal region 17p13.2, a region lost in certain cancers.[123] However, PIG-S is overexpressed in breast cancer tissues compared to healthy tissues.[103] A significant overexpression of PIG-S protein was seen in thyroid cancer samples and mRNA levels of *PIG-S* were amplified 60% in lung, 40% in ovarian and liver, and 50% in thyroid cancers.[103]

1.6 How does GPI-T subunit overexpression lead to cancer?

Overexpression of each GPI-T subunit has been observed in one or more cancer types with different frequencies and different patterns. For example, in breast cancer samples, PIG-T, PIG-U and GPAA1 are commonly overexpressed compared to healthy tissue. In ovarian tumor samples, PIG-T, PIG-K, and GPAA1 were overexpressed. In some colon cancer samples, PIG-T is overexpressed, but PIG-K expression suppressed.[103] Table 1.4 highlights some

Table 1.4: Examples of reported changes in GPI-T subunit expression (compared to healthy cells of the same tissue).

Cancer Type	PIG-U	PIG-T	PIG-K	GPAA1	PIG-S
Bladder Cancer[103],[109]	↑↑↑		↓↓		
Breast Cancer[103],[126]	↑↑	↑↑	↑		↑
Colon cancer[103]		↑	↓↓		
Head and neck squamous carcinoma[119]				↑↑↑*	
Hepatocellular carcinoma[103]			↓↓↓		↑↑*
Hepatitis positive hepatocellular carcinoma[121]				↑↑↑	
Lymph node cancer[103]	↑		↑↑↑		
Lung carcinoma[103]	↑↑↑	↑		↑	↑↑↑*
Melanoma		↑↑*			
Ovarian cancer[103]	↑		↑↑↑	↑	↑↑*
Pancreas cancer[103]		↑			
Prostate cancer[103]	↑			↑↑	
Squamous cell carcinoma[103]		↑			
Thyroid cancer[103]		↑↑*		↑	↑↑*
Uterine cancer[103]		↑↑↑*	↑↑↑	↑↑*	

Symbols are as follows: ↑↑↑ indicates >50% overexpression; ↑↑ indicates 20-50% overexpression; ↑ indicates 0-20% overexpression; ↓↓↓ indicates >50% down-regulation; ↓↓indicates 20-50% down-regulation; * indicates data obtained from mRNA levels (all other data reflect characterization of protein expression levels).

examples of the patterns of subunit expression observed in different tumor types and samples.

The five GPI-T genes have the hallmarks of oncogenes, tumor biomarkers, and potential targets for the development of new chemotherapeutics. However, a great deal remains to be understood before GPI-T subunits can be used to detect or treat cancer. For example, how does overexpression of one subunit induce tumorigenesis? The work described above has led to proposals for different mechanisms (Figure 1.9). First, and most logically, overexpression of a GPI-T subunit can lead to increased GPI-T activity and increased presentation of GPI anchored proteins on the surface of cancer cells.

The observation that PIG-U overexpression increased uPAR cell surface presentation and *Jak/STAT* cell signaling supports this hypothesis.[4,107] So does the fact that GPAA1 overexpression in breast cancer correlated with increased cell surface presentation of 18 GPI anchored proteins involved in cell dedifferentiation.[104] Second, overexpression of GPI-T subunits can cause perturbations in cell signaling and transcription that facilitate tumor growth. Evidence is accumulating to support roles for GPI-T in modulating paxillin phosphorylation and overexpression of the FOXC2 transcription factor.[104,114] Neither paxillin nor FOXC2 is GPI anchored so the subunit overexpression

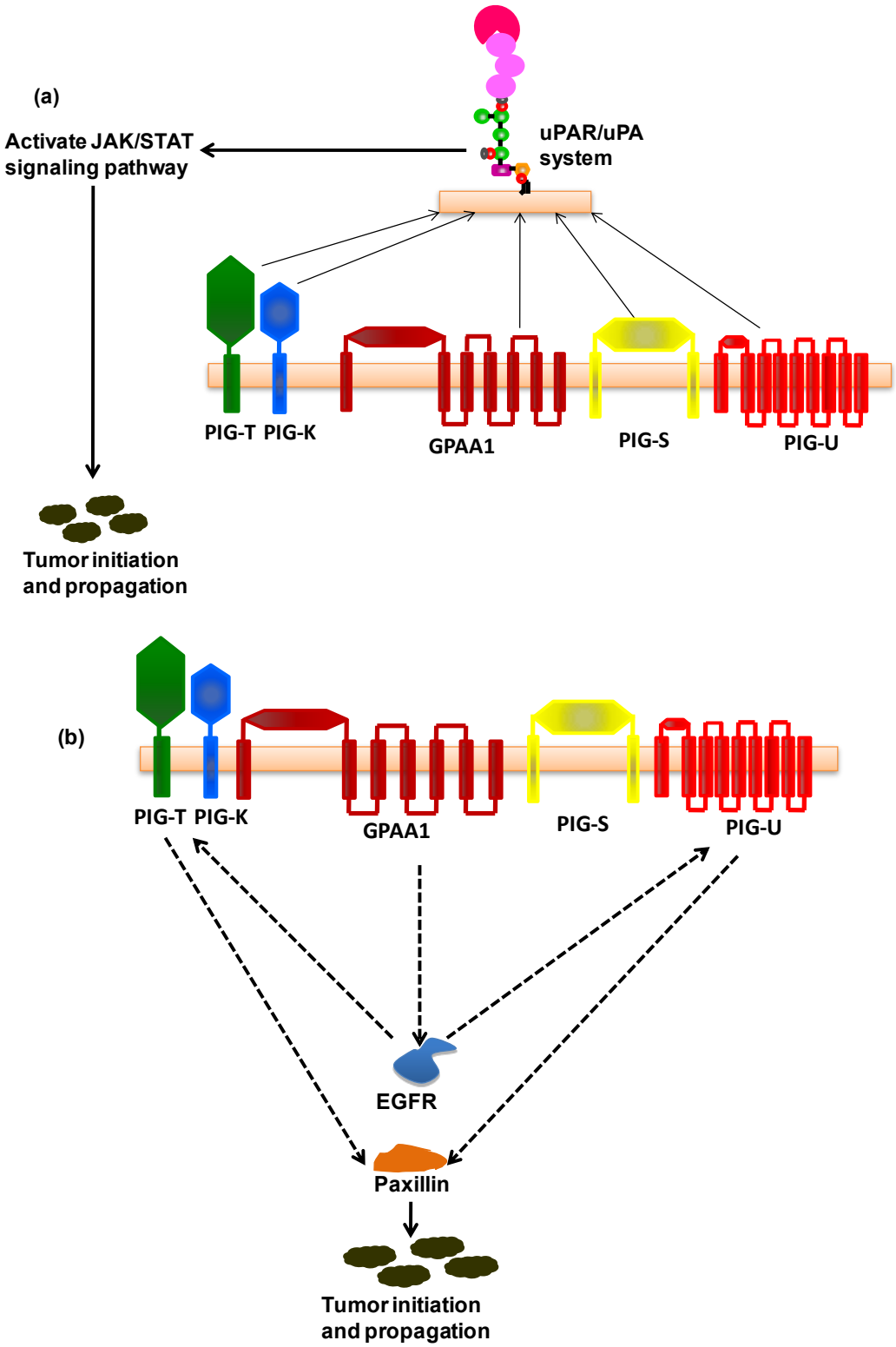
(a)
Activate JAK/STAT
signaling pathway
uPAR/uPA
system
PIG-T PIG-K
GPAA1
PIG-S
PIG-U
Tumor initiation
and propagation
(b)
PIG-T PIG-K
GPAA1
PIG-S
PIG-U
EGFR
Paxillin
Tumor initiation
and propagation

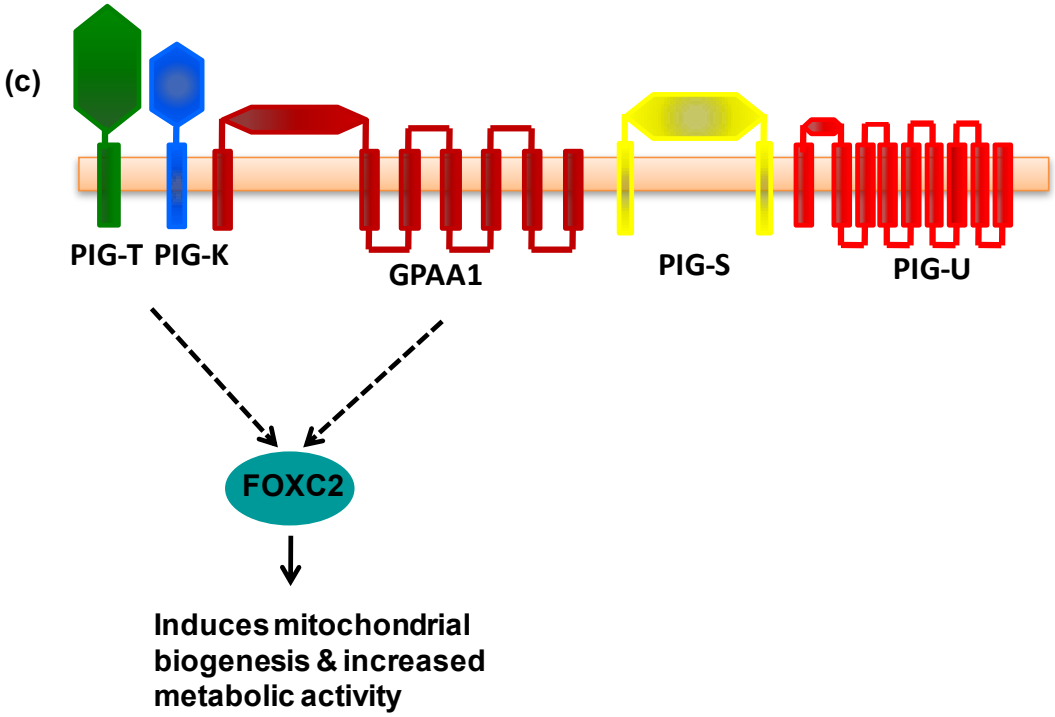

Figure 1.9: Proposed mechanisms for how GPI-T may participate in cancer: (a) Overexpression of uPAR to upregulate the JAK/STAT phosphorylation pathway; (b) Activation of paxillin phosphorylation; (c) Upregulation of FOXC2 expression and downstream signaling. The solid lines represent pathways that have more direct experimental support. The dashed lines represent pathways that likely involve intermediate steps that are currently uncharacterized.

mechanism that leads to these perturbations is not clear. The apparent recruitment of EGFR to the GPI-T complex upon GPAA1 overexpression is perhaps the most intriguing observation.[114] This association led to phosphorylate of both PIG-T and PIG-U. It isn't known how these phosphorylation events impact GPI-T activity, however expression of these different subunits and recruitment of EGFR correlated with paxillin phosphorylation.[114]

It is clear from these efforts that changes in GPI-T subunit overexpression impact the concentrations of different cell surface GPI anchored proteins and modulate signal transduction. The specific perturbations in GPI-T that lead to these consequences remain poorly understood. For example, is EGFR involved in the dedifferentiation of breast cancer after GPAA1 overexpression? Or do the GPAA1/EGFR interactions induce tumorigenesis via a mechanism that is different from GPAA1-induced dedifferentiation? And, at a more basic level, how does overexpression of each subunit impact GPI-T activity? It is easy to hypothesize that GPI-T activity is up-regulated in all cases, but this hypothesis is contraindicated by the fact that PIG-K, the catalytic subunit, is actually down-regulated in many tumors.

With respect to tumorigenesis and GPI-T, it is clear that we are still looking at only the tip of the iceberg. Further cell biology studies are needed, in addition to a careful assessment of the impact of subunit overexpression on GPI-T activity, which was one of the goals in this dissertation.

1.7 Functions of GPI anchored proteins relevant to tumorigenesis

GPI anchored proteins participate in diverse functions including immune responses, embryogenesis, fertilization, cell wall biosynthesis, signal transduction, and others.[127,128,129,130] The medical relevance of GPI anchored proteins is clear because specific GPI anchored proteins are crucial for tumor growth and invasion as well as other diseases like Creutzfeldt-Jakob disease, bovine spongiform encephalopathy, and African sleeping sickness.[4,7,131,132]

The following section discusses the physiological functions of a few GPI anchored proteins in cancer along with their potential relevance as oncogenes, biomarkers, and therapeutic targets. This section does not represent a comprehensive list of GPI anchored proteins in cancer. Instead, it is meant to highlight the different ways that GPI anchored proteins are known to participate in tumorigenesis and cancer progression. The importance of these proteins in cancer also implicates GPI-T, or its individual subunits, as targets for the development of new chemotherapies. The challenge with targeting GPI-T for cancer treatments, however, is that any suitable drug would likely have to access the ER to be effective. Thus, GPI-T may prove to be a difficult drug target, but changes in the expression of GPI anchored proteins in cancers, like those described below, offer an additional set of potential targets.

1.7.1 Urokinase plasminogen activated receptor (uPAR)

uPAR belongs to the urokinase plasminogen activating system (uPAS), which also includes the urokinase plasminogen activator (uPA), and two serine proteinase inhibitors, plasminogen activator inhibitor-1 (PAI-1) and -2 (PAI-2). uPAR is a ~60 kD glycoprotein that is GPI anchored.[133] It has three domains, D1, D2 and D3, linked together by conserved disulfide bonds.[107] In healthy tissues, uPAR is expressed at moderate levels; strong expression is seen in tissues undergoing extensive remodeling.[134] uPAR regulates extracellular proteolysis by binding to uPA and activating plasminogen-generating plasma.[135] Because of the above properties, uPAR is overexpressed in almost all cancer types; upregulation of uPAR causes downstream changes in a number of different cell signaling pathways (some of which are described below).[106,136,137,138,139,140]

Different expression levels of components of the uPA system act as biomarkers for different cancers and these receptors and enzymes can serve as therapeutic targets.[141,142] The most effective way to use this system is by inhibiting uPA using small molecule inhibitors or by interfering with the uPA/uPAR interaction. Small molecules such as 3-amidinophenylalanine negatively affect the uPA system and thereby limit the invasiveness of head and neck carcinoma cells, and cervical and breast cancer cell lines. Soluble uPAR inhibits cell proliferation in ovarian cancer.[143,144] Catalytically inactive uPA fragments and peptide constructs that can be used as antagonists or toxins were also useful in treating uPAR-activated cancer cells.[145,146]

1.7.2 Glypican-3

Glypicans are GPI anchored heparin sulfate proteoglycans that regulate the activity of heparin binding growth factor.[147] So far, six glypicans have been identified in mammals, all of similar size (60-70 kD).[147] Mutations that takes place in Glypican-3 can cause loss-of-function, leading to Simpson-Golabi-Behmel syndrome, a rare X-chromosome-linked overgrowth defect.[148] The expression levels of glypicans differ in growth stage and tissue specific manners, however expression predominates during development and in developmental morphogenesis.[149,150]

The ability of glypicans to regulate growth and survival indicates their relevance in tumor progression. The first relationship between cancer and glypicans was seen in human pancreatic cancer, where glypican-1 was overexpressed.[151] Glypican-3 is overexpressed in hepatocellular carcinoma and in the clear cell carcinoma of ovaries.[132,152] However, down-regulation of glypican-3 was observed in breast, lung and ovarian cancer cells.[153,154,155] The high expression levels of glypican-3 in both hepatocellular and ovarian clear cell carcinoma have led to the evaluation of this protein as a therapeutic target using cell- and antibody-based immunotherapies with some promising results.[156,157,158] Its differential overexpression in different cancers suggests that glypicans can be used as biomarkers using immunohistochemistry and they may be suitable as therapeutic targets.

1.7.3 Folate binding receptor

Two folate binding receptors (FR) are GPI anchored glycopeptides that have high affinity to folic acid (K_d ~ 1 pM).[159] Four different isoforms of FRs are known (α, β, γ andδ), however only the α and β isoforms are GPI anchored.[160,161] FR-α is the most widely studied isomer, which has limited expression levels in normal tissues but is overexpressed in a variety of cancer cell types including ovarian, lung, breast and others.[162,163,164] Due to its high affinity for folic acid, the FR/folate interaction has been used in radiopharmacology, chemotherapy, and magnetic resonance imaging.[165,166,167]

During the last two decades, folate-based radioconjugates have been developed to use in PET and SPECT imaging and tested in clinical trials in patients with folate receptor positive solid tumors.[168,169] Several radioisotopes have been used for PET imaging, including fluorine-18, gallium-68, terbium-152 and scandium-44.[170,171,172,173] The EC90 vaccine has been used in folate immune therapy and is in phase I studies for patients with renal cell cancer.[174] Several folate receptor targets have been synthesized to use in chemotherapeutics. For example, folate conjugate EC145 is in phase I clinical studies for patients with refractory tumors.[175,176] Overexpression of the folate receptor α in lung cancer (72% in adenocarcinomas and 51% in squamous cell carcinomas) indicates the importance of the folate receptor as a therapeutic agent and the need for more investigation of this GPI anchored protein.[162,177]

1.7.4 Prostasin

Prostasin is a serine protease highly expressed in the kidneys, prostate and lungs.[178] It is a GPI anchored protein that acts as a channel activating protease-1 (CAP-1) and activates epithelial sodium channels, which maintain the salt and fluid balance in the kidneys.[179,180] Prostasin is down-regulated in gastric and prostate cancer cells but it is overexpressed in pancreatic, breast and oral cancer cells.[181,182] Recently prostasin has been identified as a potential tumor marker for early stages of ovarian cancer.[183] Even though the role of prostasin in cancer cells is not well understood, the use of prostasin inhibitors such as protease nexin–1 (PN-1) have been investigated.[184]

1.8 Dissertation research

GPI anchored proteins play vital roles in different cancers and correlate to changes in GPI-T expression. Even though the importance of GPI anchored proteins in cancer is well established, the importance of GPI-T came into the picture only in 2004 with the discovery of PIG-U as an oncogene in bladder cancer. Since this discovery, several interesting findings have shown that the expression levels of different GPI-T subunits are highly variable in different cancer types and between patients. One key question that needs to be addressed is how the underexpression of PIG-K or Gpi8, the catalytic subunit, affects the GPI-T function in a way that promotes tumors. A detailed knowledge of GPI-T structure and function is needed in order to understand the role of this enzyme in cancer. To answer this difficulty, I have simplified the complexity of the

GPI-T core subunits to facilitate studies of this critical enzyme in my dissertation work. Here we used only the soluble domains of the core subunits to analyze the structure and function of each subunit alone and with respect to interactions with other core subunits.

Chapter 2 describes the characterization of Gpi8, the catalytic subunit of GPI-T. Here we looked at the dimerization of $Gpi8_{23-306}$, the effect of *N*-linked glycosylation on $Gpi8_{23-306}$ dimerization, and analysis of single point mutations along the predicted dimer interface of $Gpi8_{23-306}$ on dimerization. This chapter showed a robust $Gpi8_{23-306}$ dimerization when overexpressed and purified from both yeast and *E. coli.* Also, the *N*-linked glycosylation didn't have any effect on $Gpi8_{23-306}$ dimerization and the single point mutations done on the predicted dimer interface of $Gpi8_{23-306}$ couldn't disrupt the dimer completely.

Chapter 3 examines interactions between the three core subunit soluble domains ($Gpi8_{23-306}$, $Gaa1_{50-343}$ and $Gpi16_{20-551}$). Using co-immunoprecipitation and co-purification methods, we demonstrated that each pair of subunits can be isolated as a heterodimer and that the three soluble domains assemble into a heterotrimer.

Chapter 4 quantifies the impact of subunit overexpression on GPI–T activity *in vivo*. All five subunits overexpressed in cancer in varying levels. Therefore it is important to look at how each subunit overexpression affect on GPI-T activity. Here we use invertase reporter assay with three different Invertase variants having three *C*-terminal signal sequences to check the GPI-T activity when each of the core-subunits are overexpressed. For the three variants

overexpression of each GPI-T subunit showed a pattern of changes in GPI-T activity.

Chapter 5 concludes this dissertation with a discussion of the interesting questions about GPI-T that remains unanswered and could be examined in the future.

Two appendices are included that describe results from smaller, side projects. Appendix A describes our efforts in the synthesis of peptides and characterization of GPI-T *in vitro* assay products using ESI-MS. Appendix B summarizes our efforts to characterize the tetramer formation with yeast $Gpi8_{23-306}$ and $Gaa1_{50-343}$.

CHAPTER 2

GPI8$_{1-306}$ DIMERIZATION: EFFECTS OF *N*-LINKED GLYCOSYLATION AND ANALYSIS OF THE PREDICTED DIMER INTERFACE

2.1 Introduction

Being the catalytic subunit, Gpi8 plays an important role in the GPI-T complex. Even though Gpi8 is the most well characterized subunit in GPI-T, questions have been raised over the last five years about the structure and function of this subunit in terms of stoichiometry and its the catalytic activity.[83-84, 92, 185-186] Therefore further characterization of Gpi8 is still required for a complete understanding of GPI-T to be achieved.

Full-length yeast Gpi8$_{1-411}$ is a 47 kD protein that belongs to the C13 cysteine protease family. It contains a catalytic dyad (His 157 and Cys 199) that is believed to create a thioester intermediate with the ω-site residue of each protein substrates for GPI-T (see Figure 1.5). Rosetta software was used to construct a tertiary model of the soluble domain of Gpi8. This model overlaid nicely onto the structure of caspase-1 from *S. frugiperda*, even these two proteins share only very low level sequence similarity (~6%) (Figure 1.4).[83,187]

In order to better understand about this protein, yeast Gpi8$_{23-306}$ was first overexpressed and purified using *E. coli* to obtain higher levels of protein expression.[83] Here we used only the soluble domain I of Gpi8$_{23-306}$ without its *N*-terminal signal sequence, according to the Rosetta model. Purified Gpi8$_{23-306}$ was shown to exist as a mixture of homodimer and monomer, leading to the proposal that Gpi8 assembles into a homodimer analogous to caspases.[83] At this time, we hypothesize that the monomer was inadvertently formed either because of the

truncation of this subunit (e.g. the transmembrane domain would further drive dimerization) or as a result of heterologous expression in *E. coli* (e.g. glycosylation would help induce dimerization). This dimerization model was later questioned by a group of scientists from Singapore, who demonstrated that $Gpi8_{24-334}$ was monomeric.[84] However, this group purified $Gpi8_{24-334}$ by size exclusion chromatography (SEC), and apparently did not look for the dimer in their SEC experiment, suggesting that the dimerized fraction might have been lost during purification.

Here, we set out to more robustly characterize Gpi8 dimerization using native polyacrylamide gel electrophoresis (PAGE), SEC followed by native PAGE analysis and electrospray ionization ion mobility separation mass spectrometry (ESI-IMS-MS). Additionally because GPI-T is a eukaryotic enzyme, we hypothesized that expression in *E. coli* might fail to generate robustly folded proteins, leading to the mixture of monomer and dimer that we observed previously. Therefore we used *S. cerevisiae* to homologously overexpress and purify yeast $Gpi8_{1-306}$. In this case, Gpi8 was overexpressed with its *N*-terminal signal sequence (residues 1-22) to facilitate its processing through the secretory pathway. The above mentioned techniques were also used to analyze the effect of *N*-linked glycosylation on the dimerization of $Gpi8_{1-306}$ and to analyze the predicted dimer interface. Still when $Gpi8_{1-306}$ was expressed in yeast, a mixture of dimer and monomer was obtained. Dimerization was stable to mutations at the *N*-linked glycosylation site indicating that glycosylation does not drive

dimerization. Mutations at the predicted dimer interface only partially disrupted dimerization.

2.2 Results

2.2.1 Purification optimization of yeast $Gpi8_{23-306}$ over-expressed in yeast

During canonical protein secretion, proteins translocated into the lumen of the ER undergo glycosylation and folding with the assistance of chaperones and enzymes.[188] Misfolded proteins undergo ER associated degradation in the proteosome and folded proteins are transported through COPII (coat protein II) to their appropriate destinations.[188] Full length Gpi8 is located in the ER membrane, with its soluble active site domain in the ER lumen.

We imagined that the soluble domain I of $Gpi8_{1-306}$, when overexpressed without its transmembrane domain, might be secreted into the extracellular medium. To test this idea, yeast $Gpi8_{1-306}$-V5- His_6 (in pYES-DEST52 vector, InvSc1 cell line) was overexpressed in yeast and Ni-NTA affinity purification was used to isolate $Gpi8_{1-306}$-V5- His_6 from the cell pellet and the growth medium. (we assume that the *N*-terminal signal sequence, residues 1-22, have been cleaved from this construct, converting $Gpi8_{1-306}$-V5- His_6 into $Gpi8_{23-306}$-V5- His_6. (However, this cleavage has not verified.) $Gpi8_{23-306}$-V5- His_6 was not secreted into the growth medium, however it was isolated from cells in low amounts (Figure 2.1 (a)).

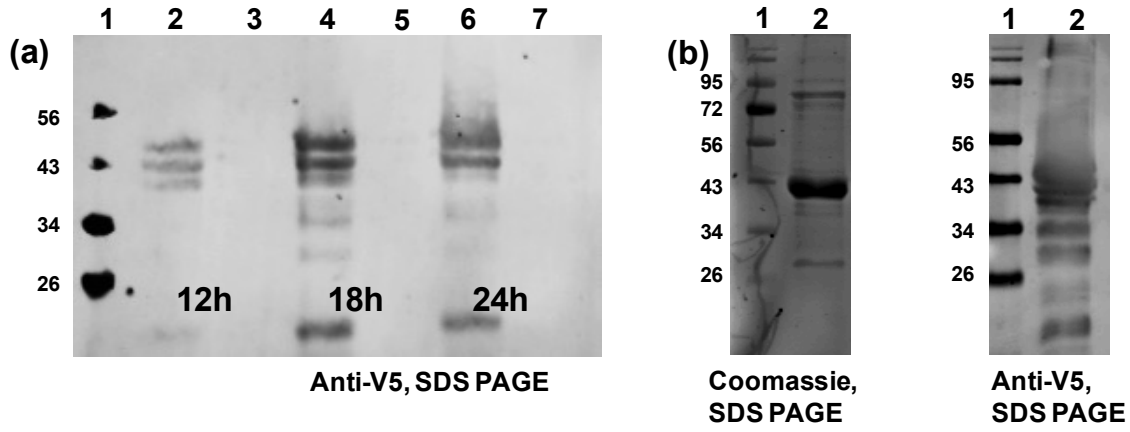

Figure 2.1: $Gpi8_{23\text{-}306}$-V5- His_6 is not secreted into the growth medium. (a) Anti-V5 blot of an SDS-PAGE gel (12%) showing $Gpi8_{23\text{-}306}$ expression levels in the cell pellet (P) versus the growth medium (M); both after Ni-NTA affinity purification. Lane 1: molecular weight markers, lanes 2, 4 and 6: purified proteins from pellets when overexpressed for 12, 18 and 24 hours after induction, lanes 3, 5 and 7: proteins purified from the growth medium after overexpressing for 12, 18 and 24 of induction. Three glycoforms of $Gpi8_{23\text{-}306}$ were observed in lanes 2, 4 and 6. Lanes 3, 5 and 7 did not contain any detectible $Gpi8_{23\text{-}306}$, indicating that this protein is not secreted to the growth medium. (b) Confirmation of the presence of $Gpi8_{23\text{-}306}$ using Coomassie stain (left) and anti-V5 blot (right). Purified yeast $Gpi8_{23\text{-}306}$-V5- His_6 was used to confirm the presence of $Gpi8_{23\text{-}306}$. The left panel shows a Coomassie stained gel of purified $Gpi8_{23\text{-}306}$ (lane 1: molecular weight markers, lane 2: purified protein) and the right panel shows the anti-V5 blot of the same protein sample (lane 1: molecular weight markers, lane 2: purified protein). The band corresponding to $Gpi8_{23\text{-}306}$ was excised from the Coomassie stained gel, digested with trypsin, and analyzed by mass spectrometry. (In collaboration with Dr. Chih-Wei Liu from professor Sarah Trimpin's lab.)

Following purification to homogeneity, the protein band believed to be $Gpi8_{23\text{-}306}$ was excised and treated with trypsin to confirm its identity. In-gel trypsin digestion and mass spectrometry were conducted by Dr. Chih-Wei Liu in Prof. Trimpin's lab. The protein bands were excised and cleaned (see materials and methods section), followed by the analysis of the samples using LC/MS/MS (Waters Inc.). The LC/MS/MS results were then uploaded to the Mascot server, to search for the matching sequences. An ion score was then calculated as the probability of each sequence compared to the matching sequence. The highest ion score corresponded to the best matched sequence. All ion scores were summed to give the protein score for one distinct sequence (Table 2.1, lane 1), which is proportional to the abundance of the protein in one particular sample.

The band corresponding to $Gpi8_{23\text{-}306}$ was identified as a combination of alcohol dehydrogenase (ADH1, ADH2 and ADH3) and low levels of $Gpi8_{23\text{-}306}$ (see both Figure 2.1 (b) and Table 2.1). Also ADH1, ADH2 and ADH3 have over 80% sequence homology. This result was unexpected because the native *S. cerevisiae* ADH is not histidine tagged and should not have been purified by Ni-NTA affinity purification. However, a published report has indicated that overexpression of ADH occurs when using the GAL1 promoter (as in our vector), with low levels of glucose.[189] ADH has two zinc binding motifs and a molecular weight of 37 kD which is similar in size to domain 1 of $Gpi8_{1\text{-}306}$.[95] Since there are no known interactions between ADH and Gpi8, we believe that ADH was non-specifically purified by Ni-NTA affinity chromatography. Therefore considering both the low expression levels of Gpi8 and the presence of ADH contamination,

Table 2.1: MS/MS analysis of the putative $Gpi8_{23-306}$ protein band indicates the presence of a contaminant, ADH. Protein scores were calculated using the probability for each of the sequences and the most abundant protein is ADH1. Along with ADH, Gpi8 is also present in low quantities.

Protein Score	Protein identification	Description
3417	ADH1	*S. cerevisiae*
1054	ADH3	*S. cerevisiae, Mitochodria*
947	ADH2	*Kluyveromyces marxianus*
763	Gpi8	*S. cerevisiae*
608	ADH2	*S. cerevisiae*

we have restricted our analysis to anti-V5 Western blots to specifically visualize and analyze protein samples containing $Gpi8_{23\text{-}306}$-V5-His_6.

2.2.2 Homo-dimerization of yeast $Gpi8_{23\text{-}306}$-V5- His_6 over-expressed in yeast versus *E. coli*

We previously reported that $Gpi8_{23\text{-}306}$ forms a mixture of homodimer and monomer when isolated from *E.coli*.[83] Here we set out to determine whether more robust dimerization would occur when $Gpi8_{23\text{-}306}$-V5-His_6 was expressed in *S. cerevisiae* and purified using Ni-NTA affinity chromatography. GST-$Gpi8_{23\text{-}306}$ was expressed in *E.coli* and purified by glutathione affinity chromatography for comparison. Purified proteins were analyzed using native PAGE and anti-GST and anti-V5 Western blots (Figure 2.2). As observed previously,[83] when purified from *E.coli*, GST-$Gpi8_{23\text{-}306}$ forms a monomer/homodimer mixture (Figure 2.2 (a)). Quantitatively, a higher ratio of dimer to monomer was observed when $Gpi8_{23\text{-}306}$ was purified from *S. cerevisiae* (Figure 2.2 (b)) compared to that from *E.coli*. Additionally, when purified from *S. cerevisiae*, three Gpi8 glycoforms were visible. These glycoforms hindered quantitative analysis of the extent of monomer versus dimer. The presence of dimer was confirmed by comparing bands to the monomer of $Gpi8_{23\text{-}306}$, which was obtained by heating the protein in sodium dodecyl sulfate (SDS) gel loading dye to denature the protein.

These observations were further corroborated by analyzing GST-$Gpi8_{23\text{-}306}$ purified from *E. coli* using SEC followed by native PAGE analysis of the elution fractions (Figure 2.3).

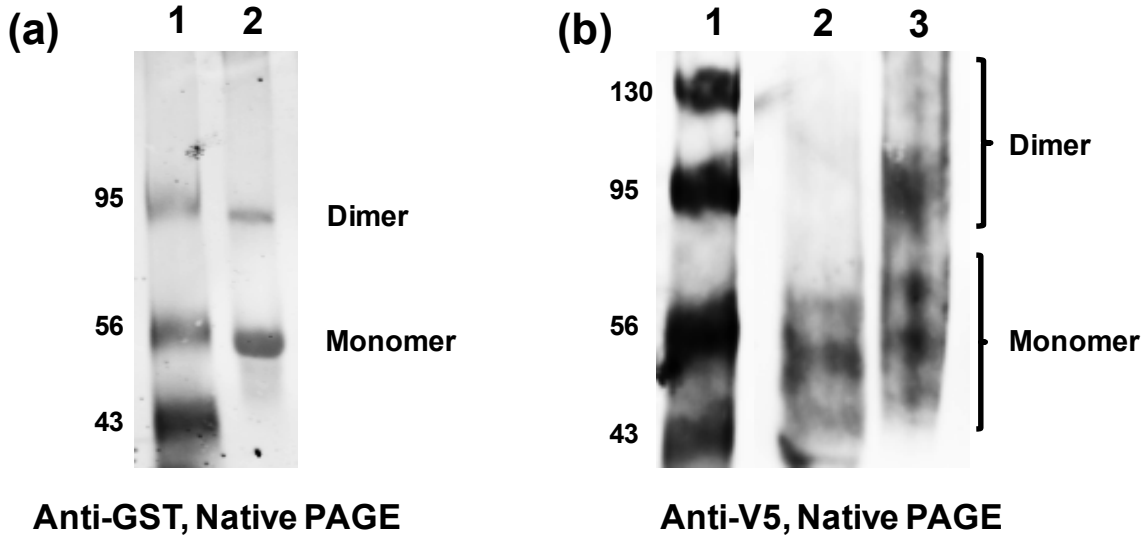

Figure 2.2: Yeast Gpi8$_{1\text{-}306}$ when overexpressed in *E. coli* or *S. cerevisiae* forms a mixture of homodimer and monomer. (a) Anti-GST blot of a native gel containing GST-Gpi8$_{23\text{-}306}$ when overexpressed and purified from *E. coli* using glutathione sepharose affinity purification. Lane 1: molecular weight markers, Lane 2: GST-Gpi8$_{23\text{-}306}$ labels indicate the presence of both dimer and monomer as labeled. (b) Anti-V5 blot of the native gel of Gpi8$_{23\text{-}306}$-V5-His$_6$ overexpressed in *S. cerevisiae* and purified using Ni-NTA affinity purification. Lane 1: molecular weight markers, lane 2: denatured Gpi8$_{23\text{-}306}$-V5-His$_6$ (see materials and methods), lane 3: native Gpi8$_{23\text{-}306}$-V5-His$_6$. Glycoforms are visible in both the monomer and the dimer bands. Both bands highlight the presence of a mixture of dimer and monomer.

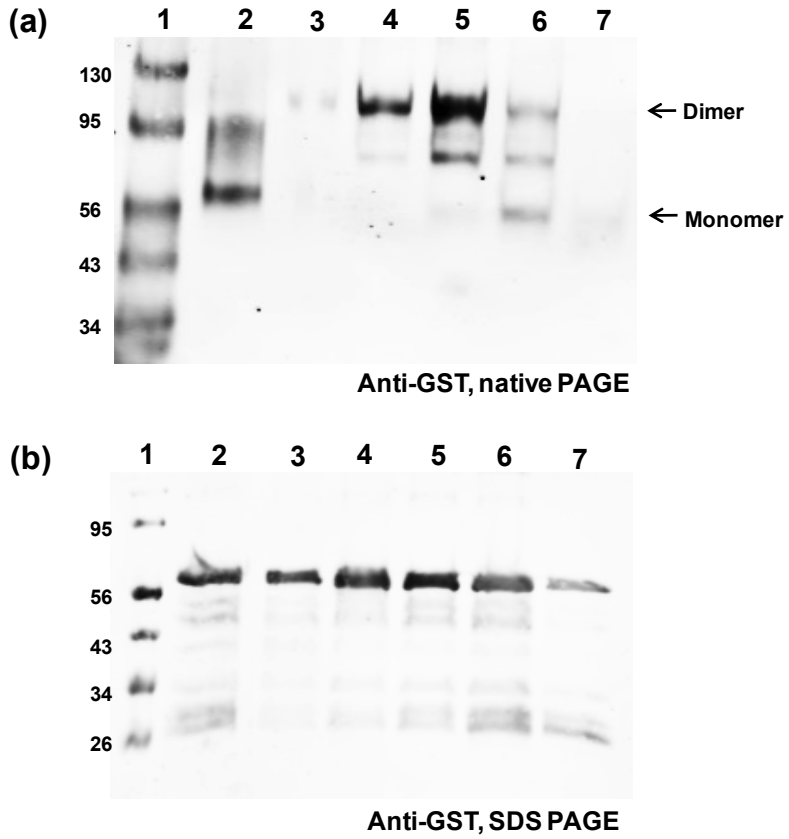

Figure 2.3: GST-Gpi8$_{23\text{-}306}$ purified from *E.coli* yields a higher amounts of dimer compared to monomer when analyzed by SEC. Analysis of each SEC fraction of GST-Gpi8$_{23\text{-}306}$ using native PAGE (a) and SDS PAGE (b). (a) An anti-GST blot of the native PAGE showing both the dimer and monomer for each of the SEC fractions. Lane 1: molecular weight markers, lane 2: Denatured protein sample, lanes 3-7: SEC fractions. (b) The anti-GST blot of the SDS PAGE for each of the fractions analyzed. Lanes are similar to the top (a) panel.

Unfortunately, individual peaks representing monomer versus dimer were not resolved by SEC. Since the expected dimer is 114 kD and the monomer is 57 kD, fractions from the SEC column were analyzed from the corresponding size range (compared to the SEC marker). Without SEC native gel analysis of the purified GST-Gpi8$_{23-306}$ (from *E. coli*) indicates higher amounts of monomer over dimer. However, when these proteins were injected into SEC and then evaluated, higher amounts of dimer were visible (Figure 2.3).

2.2.3 The effect of *N*-linked glycosylation on dimerization of Gpi8$_{23-306}$-V5-His$_6$.

N-linked glycosylation is an important post-translational modification that takes place in eukaryotic proteins that enter the secretory pathway and contain an aspargine (Asn) residue within an Asn(N)-X-Ser(S)/Thr(T) consensus sequence (X can be any amino acid other than proline).[190] Glycosylation is important for a wide variety of functions such as protein stability, folding, signal transduction, proper orientation, cellular trafficking and more.[191,192,193,194,195,196,197]

According to the UNIPROT database, full-length Gpi8$_{1-411}$ contains two predicted glycosylation sites at N256 and N346. N23 is also an appropriate consensus sequence, however, it was not listed as a glycosylation site since it is present immediately adjacent to the *N*-terminal signal peptide and so it was not predicted to be a valid site (Figure 2.4 (a)).[75] Therefore only the N256 site lays within the domain I (Gpi8$_{23-306}$), the region of interest herein. When Gpi8$_{23-306}$-V5-His$_6$ was overexpressed and purified from *S. cerevisiae*, three different bands

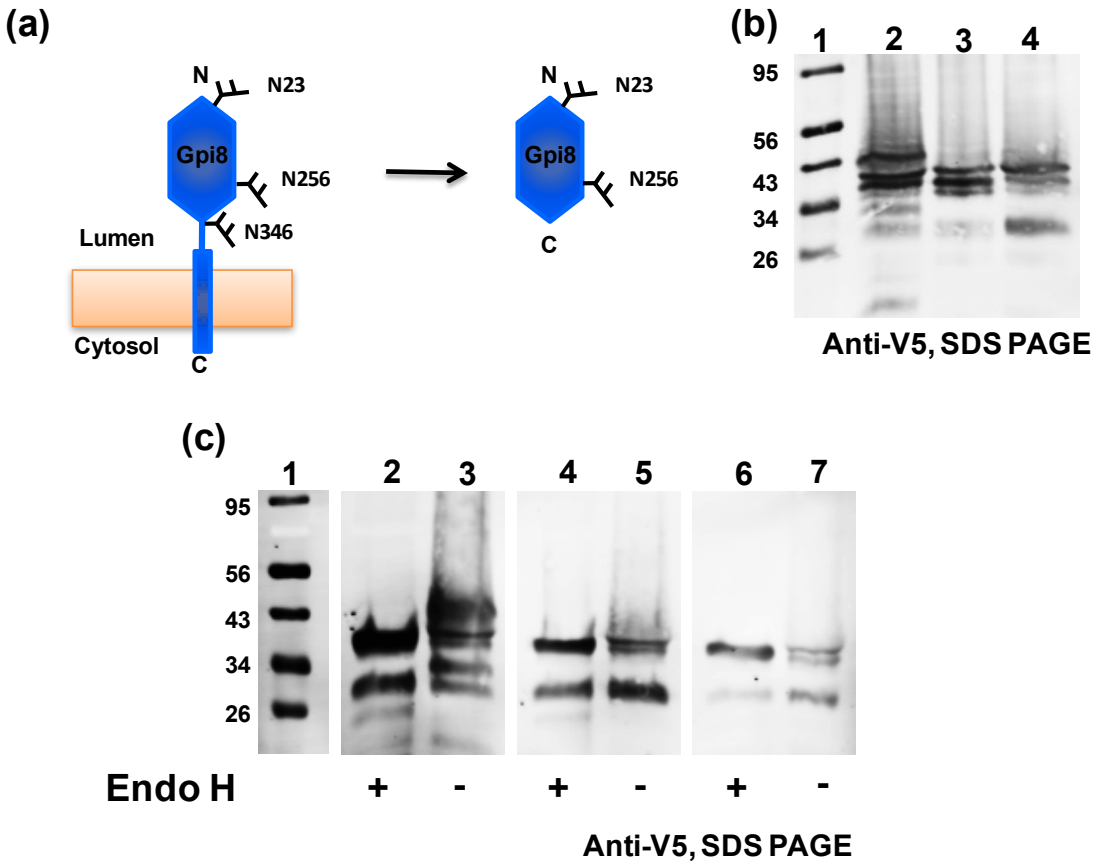

Figure 2.4: Gpi8$_{23\text{-}306}$-V5- His$_6$ has two *N*-linked glycosylation sites within the region of our interest. (a) A cartoon representation on the possible glycosylation sites of Gpi8. The full length Gpi8$_{1\text{-}411}$ has three glycosylation sites at N23, N256 and N346. Domain I contains N23 and N256 glycosylation sites. (b) Anti-V5 blot of an SDS PAGE gel showing the glycoforms found in Gpi8$_{23\text{-}306}$-V5-His$_6$ and the N256Q and N256A mutants. Lane 1: molecular weight markers, lane 2: wild type Gpi8$_{23\text{-}306}$-V5-His$_6$ lane 3: N256Q mutant and lane 4: N256A mutant. Wild type Gpi8$_{23\text{-}306}$-V5-His$_6$ shows three bands corresponding to glycosylation at N23, N256 and the unglycosylated form of this protein. Each mutant (N256Q and N256A) had two bands consistent with glycosylation at N23 and the unglycosylated form. (c) An anti-V5 blot of the SDS PAGE gel showing the impact of Endo H treatment on Gpi8 glycosylation. The wild type enzyme and two mutants were treated with Endo H (see materials and methods). Lane 1: molecular weight markers, lanes 2, 4 and 6: deglycosylated wild type Gpi8$_{23\text{-}306}$-V5-His$_6$, N256Q, and N256A, respectively, after Endo H treatment. Lanes 3,5 and 7: wild type Gpi8$_{23\text{-}306}$-V5-His$_6$, N256Q, and N256A, respectively, before Endo H treatment. All seven lanes are from one single blot.

were observed in the anti-V5 blot (Figures 2.2 & 2.4), suggesting the presence of two glycoforms and the non-glycosylated protein. The two glycoforms represent multiple glycoforms at N256 or glycosylation at both N256 and N23.

To evaluate the importance of glycosylation on Gpi8 dimerization, we mutated N256 to Gln (Q) and Ala (A). When overexpressed in *S. cerevisiae*, wild type $Gpi8_{23\text{-}306}$-V5-His_6 showed three bands in the anti-V5 blot, whereas N256 mutants only had two bands (Figure 2.4 (b)). When the wild type $Gpi8_{23\text{-}306}$-V5-His_6 and its two mutants were treated with Endoglycosidase H (Endo H), an enzyme that removes *N*-linked glycans[198] all glycoforms condensed into one deglycosylated band (Figure 2.4 (c)). These results strongly suggest that N23 is also glycosylated. To examine the effect of *N*-linked glycosylation on $Gpi8_{23\text{-}306}$ dimerization, wild type $Gpi8_{23\text{-}306}$-V5-His_6, the two mutants, and all Endo H treated fractions were analyzed using anti-V5 blots by native PAGE along (Figure 2.5). In each gel, the corresponding denatured protein was used as a marker. In all $Gpi8_{23\text{-}306}$ samples, the presence of both dimer and monomer was observed, indicating that glycosylation is not essential for dimerization.

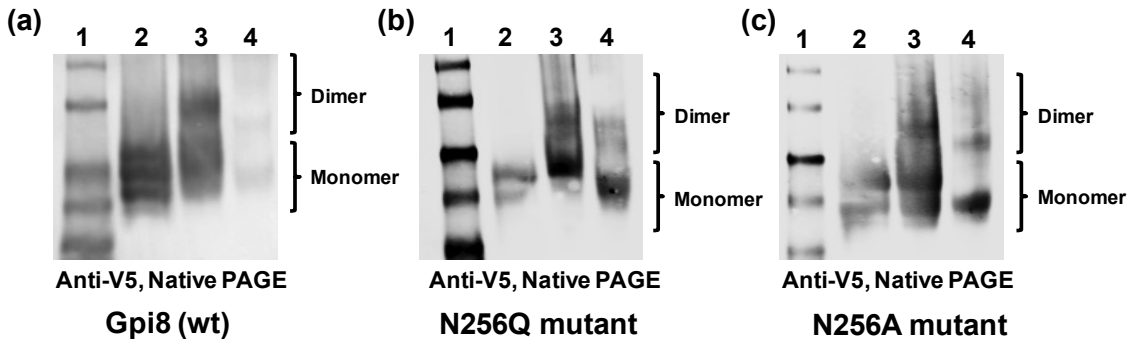

Figure 2.5: *N*-linked glycosylation does not affect Gpi8 dimerization. (a) Anti-V5 blot of a native PAGE gel of wild type $Gpi8_{23\text{-}306}$-V5-His_6. Lane1: molecular weight markers; lane 2: denatured $Gpi8_{23\text{-}306}$-V5-His_6 or mutant; lane 3: native $Gpi8_{23\text{-}306}$-V5-His_6 or mutant; lane 4: native $Gpi8_{23\text{-}306}$-V5-His_6 or mutant after treatment with Endo H. Both native forms show a mixture of dimer and monomer. (b) Anti-V5 blot of a native PAGE gel of the N256Q mutant. A mixture of dimer and monomer was observed even after treatment with Endo H. Lanes are the same as in (a) but only with the N256Q mutant. (c) Anti-V5 blot of a native PAGE gel of the N256A mutant. Results were similar to those in panel a and b. Lanes are the same as in (a) but with the N256A mutant. The presence of a mixture of dimer and monomer in wild type $Gpi8_{23\text{-}306}$-V5-His_6 and both mutants independent of Endo H treatment indicates that *N*-linked glycosylation does not affect dimerization.

The Oligomerization states of the N256Q and N256A mutants were also examined by SEC (Figure 2.6). Purified N256Q and N256A samples were injected into the SEC column. Fractions were analyzed by native PAGE and SDS PAGE. Both N256Q (Figure 2.6 (a)) and N256A (Figure 2.6 (b)) contained a mixture of dimer and monomer consistent with the gel analyses shown in Figure 2.5.

Additionally, ESI-IMS-MS was used to confirm the formation of the dimer in both $Gpi8_{23\text{-}306}$-V5-His_6 and the N256Q and N256A mutants. ESI-IMS-MS is ideal for this type of analysis because ions can be separated based on size (shape) and mass.[199,200,201,202,203] Nevertheless, it proved challenging to analyze the dimer and monomer of $Gpi8_{23\text{-}306}$ because of their higher molecular weights (unglycosylated dimer: 74 kD, unglycosylated monomer: 37 kD). Glycosylation of this protein, yielding the glycoforms shown in Figure 2.5, further complicated the analysis. Spectra were collected and analyzed in collaboration with Prof. Sarah Trimpin and of Dr. Ellen Inutan (Figure 2.7). The monomer and dimer mixtures were also examined by ion mobility separation for $Gpi8_{23\text{-}306}$-V5-His_6 and the N256Q and N256A mutants. Ni-NTA affinity purified proteins were buffer exchanged with ammonium acetate (see materials and methods for details) prior to analysis. Samples were injected onto the Synapt G2 mass spectrometer for ESI-IMS-MS analysis. Two dimensional plots of m/z vs drift time were constructed for each protein and are shown in the top panels of Figure 2.7 (a), (b) and (c). The middle and bottom panels show mass spectra that can be

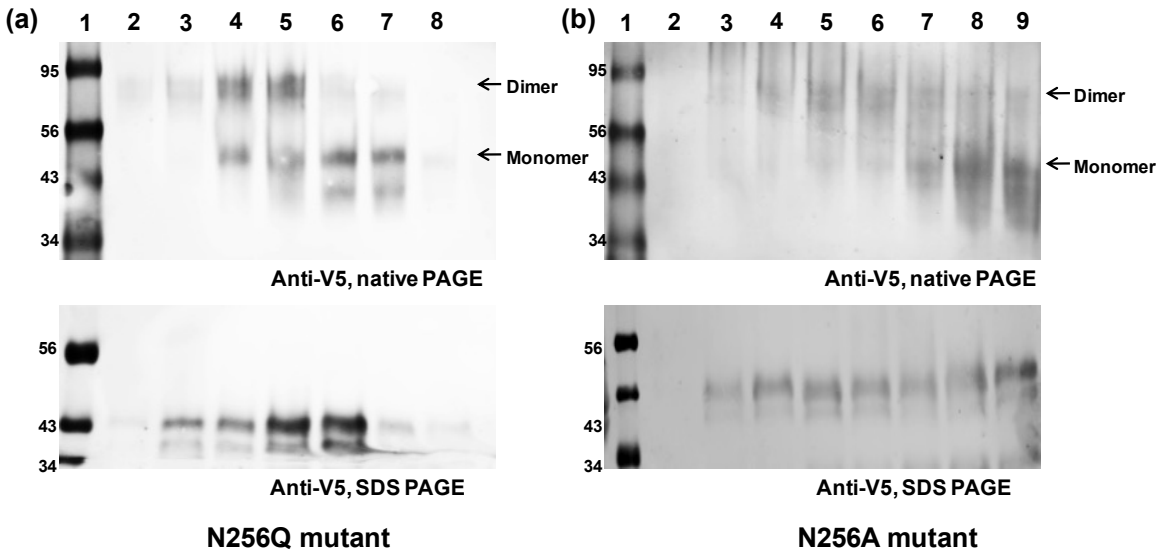

Figure 2.6: SEC analysis confirmed N256 mutagenesis does not affect dimerization. Anti-V5 blots of the native PAGE gel (top panel) and SDS PAGE gel (bottom panel) of SEC fractions for the N256Q mutant (a) and the N256A mutant (b). Concentrated SEC fractions were analyzed using native PAGE, which shows the presence of both dimer and monomer. Lane 1: molecular weight markers, lanes 2-9: SEC fractions. Both mutants show dimer and monomer consistent with the conclusion that *N*-linked glycosylation is not required for Gpi8 dimerization.

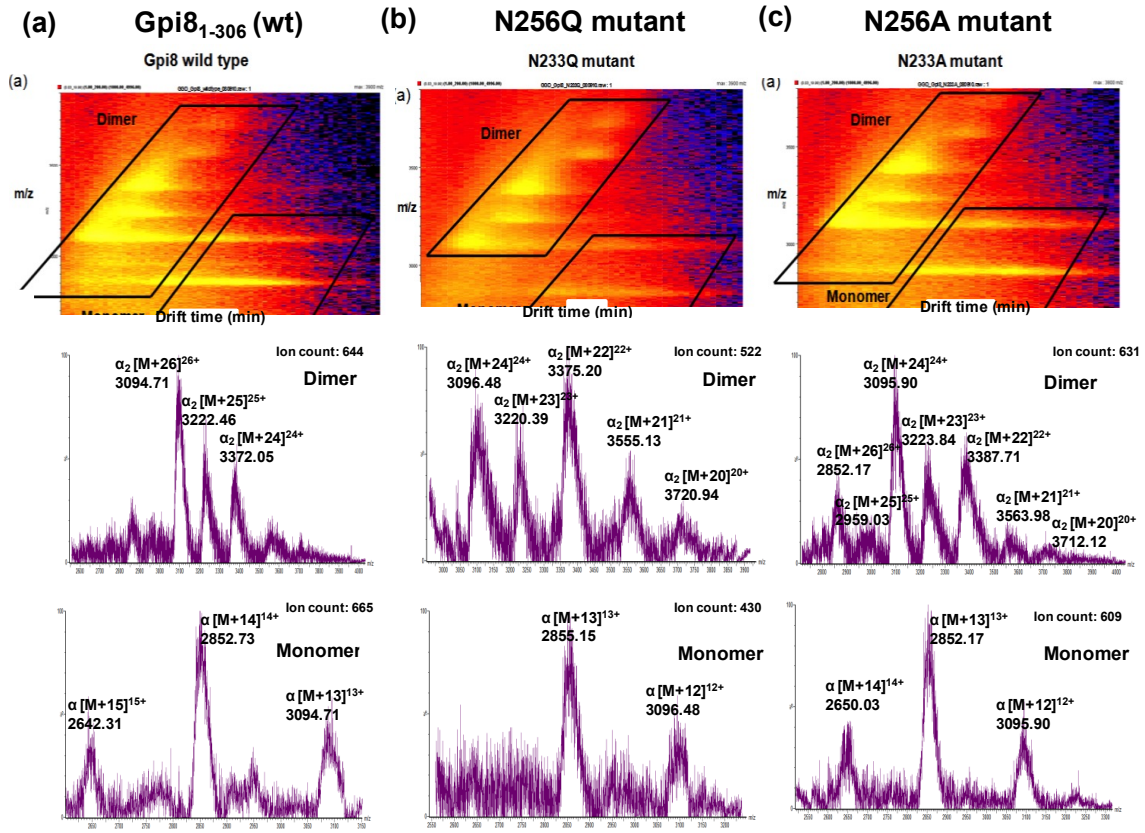

Figure 2.7. ESI-IMS-MS analysis to characterize the monomer and dimer forms of Gpi8$_{23-306}$-V5-His$_6$ and N256Q and N256A mutants. ESI-IMS-MS analysis of (a) wild type Gpi8$_{23-306}$-V5-His$_6$; (b) the N256Q mutant; and (c) the N256A mutant. In each case, the top panel shows a 2-D plot of m/z vs. drift time. Charge states corresponding to the monomer and dimer are noted. The middle panel shows an analysis of the mass spectrum from the dimer region in panel (a). The bottom panel shows the mass spectrum from the monomer region in (a). See Table 2.2 for additional analysis.

tentatively assigned as dimer and monomer ion clusters (boxed in panels a, b and c).

Different charge states were observed that are also consistent with separation of monomer and dimer for all three proteins (summarized in Table 2.2). However, presumably because of the higher molecular weights of the dimer and monomer and the different glycosylation states, broad peaks were observed and the ions were of very low abundance. Nevertheless, deconvolution of different ion clusters yielded interpretable molecular masses for the N256Q and N256A mutants. Using the masses calculated for the two mutants, the size of the glycans on N256 in wild-type $Gpi8_{23\text{-}306}$-V5-His_6 was calculated to be ~3000 g/mol (Table 2.2, Figure 2.7). These results are preliminary, given the low abundance of the observed ions. Efforts to improve ionization have been unsuccessful.

2.2.4 Predicted dimerization interface analysis using single point mutations

Activation of caspase 1, a cysteine protease, plays an important role in innate immune response.[204] Inactive monomeric pro-caspase-1 is activated inside the cell, after undergoing a process of dimerization and auto-proteolysis.[205] Structural similarities between our Rosetta model of domain 1 of Gpi8 ($Gpi8_{23\text{-}306}$) and *S. frugiperda* (Figure 1.4) led us to hypothesize that Gpi8 would also exist as a dimer.[83] We constructed a crude model of the $Gpi8_{23\text{-}306}$ dimer by overlaying the Rosetta model of $Gpi8_{23\text{-}306}$ onto the *S. frugiperda* caspase-1 dimer structure (Figure 2.8) to predict the dimer interface.

Table 2.2: Summary of the observed charge states for $Gpi8_{23\text{-}306}$-V5-His_6 and the N256Q and N256A mutants. Molecular weights were calculated from the different charge states for each protein's monomer and dimer using the m/z values assigned to each broad peak by the Drift Scope software. The X denotes changes in mass that presumably arise from glycosylation at N256.

Protein complex	Observed charge states	Calculated MW (Da)	Observed MW (Da)
N233Q dimer	20+, 21+,22+,23+,24+	74255	74321
N233Q monomer	12+,13+	37127	37125
N233A dimer	20, 21+,22+,23+,24+,25+,26+	74141	74291
N233A monomer	12+,13+,14+	37070	37097
Wild type dimer	24+,25+,26+	74227 + 2X	80626
Wild type monomer	13+,14+,15+	37113 + X	39921

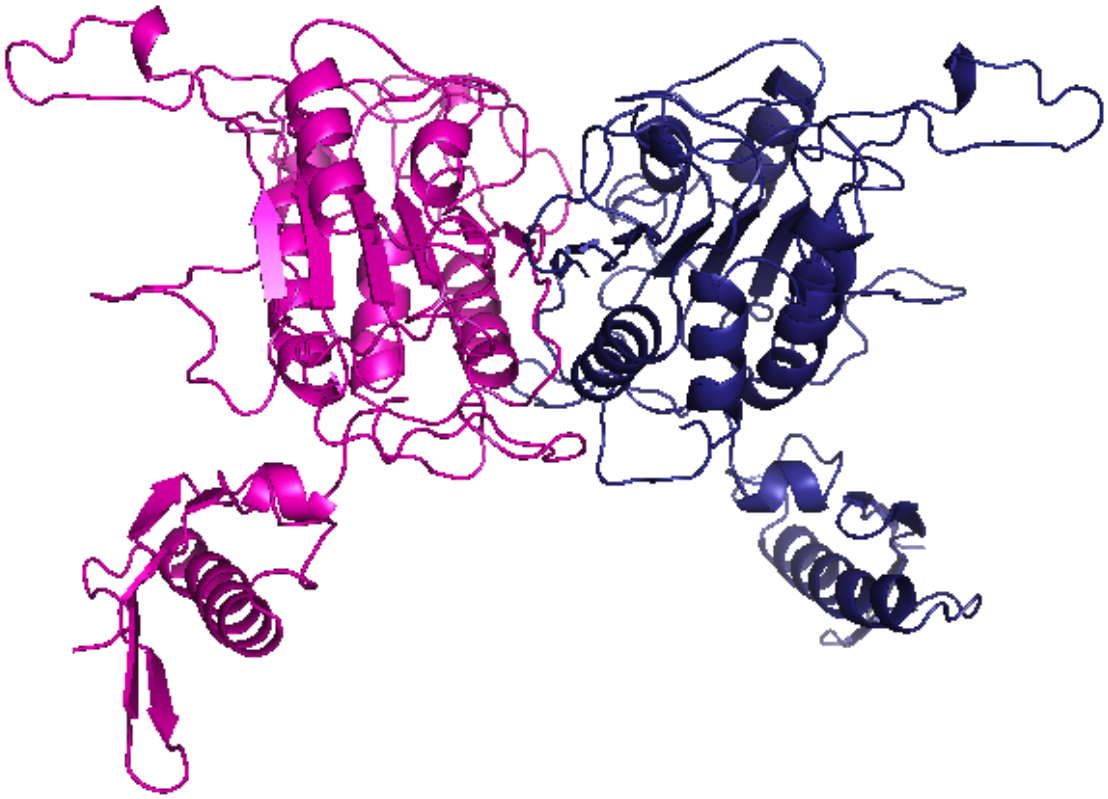

Figure 2.8: Dimer of Rosetta modeled $Gpi8_{1\text{-}360}$ created using caspase-1 dimer.

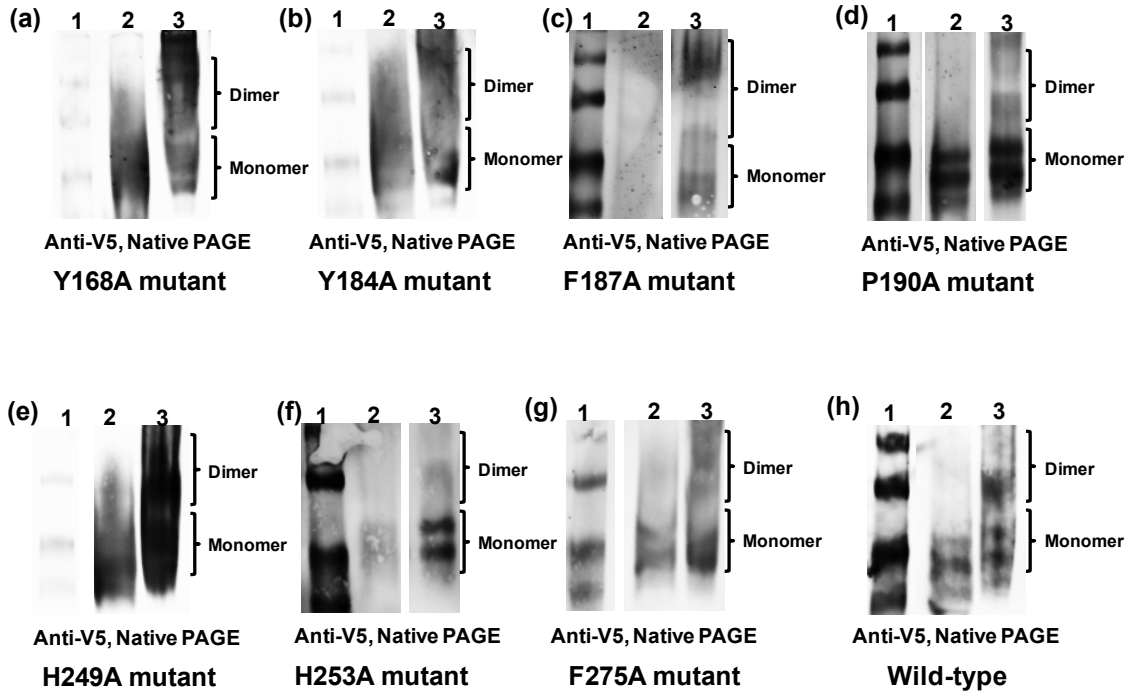

Figure 2.9: Single point mutation analysis on the predicted dimer interface. Each image is of an anti-V5 Western blot of native PAGE gels of each of the seven mutants: (a) Y168A mutant, (b) Y184A mutant, (c) F187A mutant, (d) P190A mutant, (e) H249A mutant, (f) H253A mutant and (g) F275A mutant. (h) is the wild type $Gpi8_{23\text{-}306}$-V5-His_6 for the comparison. For each gel, lane 1: molecular weight markers; lane 2: denatured protein; lane 3: native protein. For some images (F187A, P190A, H249A, H253A, and F275A), intervening lanes from the blot were removed for clarity. These changes are indicated by the presence of a white space separating the different lanes. The complete, unadulterated blots are included in an appendix (Appendix C, Figure C.1) at the end of this dissertation.

Seven single point mutations were created by Megan Ehrenwerth at the predicted dimer interface. After overexpression and purification from *S. cerevisiae,* each point mutation was analyzed using native PAGE (Figure 2.9). The glycoforms hindered our ability to quantify the amount of dimer and monomer for each mutant. However, qualitatively, different ratios of dimer to monomer were present for the different mutants. None of the point mutations completely disrupted $Gpi8_{23\text{-}306}$ dimerization. However, the P190A and H253A had the largest effects (Figures 2.9 (d) and (f)). Molecular weight markers and denatured proteins were used as controls.

2.3 Discussion

All the experiments described herein were conducted with $Gpi8_{23\text{-}306}$ that had either been expressed in *E. coli* (GST-$Gpi8_{23\text{-}306}$) or in *S. cerevisiae* ($Gpi8_{23\text{-}306}$-V5-His_6). Results confirming our earlier findings and clearly show that $Gpi8_{23\text{-}306}$ assembles into a homodimer.[2] Gpi8 dimer was observed by native PAGE and SEC. SEC analysis demonstrated that dimer predominates in this mixture. This was for $Gpi8_{23\text{-}306}$ that had been purified from *E. coli* using glutathione sepharose affinity purification (Figure 2.2 & 2.3) as well as for the N256 mutants of $Gpi8_{23\text{-}306}$-V5-His_6 mutants that were overexpressed in *S. cerevisiae* and purified using Ni-NTA affinity purification (Figure 2.5 & 2.6). These results strongly suggest that the dimer to monomer ratio observed *in vitro* depends on the protein's surrounding environment. However, complete dimerization was not observed

with any samples, suggesting that dimerization might be further driven by domain II or the transmembrane domain, which were deleted in our constructs.

As discussed, full-length yeast $Gpi8_{1-411}$ contains three possible glycosylation sites: N23, N256 and N346. However, N23 is immediately adjacent to the *N*-terminal signal sequence and so it was predicted that this site would not be glycosylated. The work presented herein represents the first efforts to characterize the N256 glycosylation site in terms of protein expression, stability, and its possible participation on dimerization. The elimination of *N*-linked glycans at 256, either by mutagenesis or Endo H treatment, did not eliminate dimerization, demonstrating that glycosylation and dimerization are separate, disconnected events. The results from this analysis also gave the first indication that N23 is glycosylated even though it is adjacent to the signal sequence. Presumably, glycosylation occurs prior to cleavage of residues 1-22 by signal peptidase. However, *N*-terminal signal sequence cleavage was not confirmed in this work.

None of the single point mutations that were made at the predicted dimer interface didn't completely dimerize (Figure 2.9). The P190A and H253A mutants noticeably disrupted dimerization in favor of monomer. It is possible that the structural changes introduced by these single point mutations are insufficient to completely disrupt dimerization. Analyses of double and even triple point mutations are expected to shed further light on this question.

2.4 Materials and methods

2.4.1 Buffers and solutions

Phosphate buffered saline (PBS): 10 mM Na_2HPO_4, 1.8 mM KH_2PO_4, 140 mM NaCl, 8.7 mM, pH 7.3. GSH elution buffer: 100 mM reduced glutathione (GSH), 50 mM Tris HCl, pH 8.0. Lysis buffer: 50 mM NaH_2PO_4, 300 mM NaCl, 10 mM imidazole, 5% glycerol, pH 7.4. Wash buffer: 50 mM NaH_2PO_4, 1 M NaCl, 50 mM imidazole, 5% glycerol, pH 7.4. Elution buffer: 50 mM NaH_2PO_4, 300 mM NaCl, 300 mM imidazole, 5% glycerol, pH 7.4. Tris glycine: 25 mM Tris base, 200 mM glycine, pH 8.3. 10X transfer buffer: 0.4 M glycine, 0.5 M Tris base, 13 mM sodium dodecyl sulfate (SDS). 1X transfer buffer: 10X transfer buffer was diluted to 1X in 20% aqueous methanol. Tris-Buffered Saline and Tween 20 (TBS-T): 10 mM Tris HCl, 150 mM NaCl, 0.05% Tween, pH 7.5). SEC buffer: 50 mM NaH_2PO_4, 300 mM NaCl. Minimal medium (4X Sc-ura): 26.8 g Yeast nitrogen base, 6.4 g dropout mix, 0.4 g each adenine, leucine, tryptophan and histidine in 1L of water and sterile filtered before use.

2.4.2 Over-expression and purification of yeast $Gpi8_{23-306}$ from *E. coli*

Plasmid pJLM008 (encoding GST-$Gpi8_{23-306}$) was transformed into BL21(DE3) RIL Codon Plus cells (Stratagene).[83] Protein overexpression was carried out with an overnight culture (30 mL) which was grown at 37 °C in Luria Bertani (LB) medium, and used to innoculate 1 L of LB medium that had been supplemented with 50 µg/mL ampicillin (Sigma-Aldrich). This culture was grown at 19 °C to an OD_{600} of 0.4-0.5, and then induced with 1 mM isopropyl-γ-D-1-

thiogalactopyranoside (IPTG, Gold Bio Inc). Cells were pelleted after two hours post-induction and stored at -80 °C until ready for use.

All purification steps were conducted at 4 °C unless otherwise noted. Cell pellets were resuspended in 15 mL PBS supplemented with 15 µL phenylmethanesulfonylfluoride (PMSF, from a saturated solution in isopropanol), and one quarter tablet of protease cocktail inhibitor (Roche). The suspension was lysed using an ultrasonic cell disrupter (Microsone) with six pulses for 20 sec each a power of 4 with 40 sec rest period in ice in between each pulse. The lysate was spun down at 14,000 rpm for 1 hr in a Beckman JA-20 rotor. The supernatant was supplemented with 500 µL (bed volume) pre-washed glutathione sepharose fast-flow resin (GE-Amersham Biosciences). The cell lysate supernatant and resin mixture was incubated for 1 hr at room temperature. The resin was washed ten times with 5 mL PBS each time. The expressed protein was eluted from the resin by treatment with 2 mL GSH elution buffer for 10 minutes at room temperature. The eluted protein solution was removed from the resin and concentrated to 250 µL. Elutions were loaded directly onto a 12% SDS-polyacrylamide gel for analysis before they were used for further subsequent experiments.

2.4.2 Over-expression and purification of yeast $Gpi8_{23\text{-}306}$ from yeast

All plasmids encoding for wild type $Gpi8_{23\text{-}306}$-V5-His_6, and the nine mutants studied herein (N256Q, N256A, Y168A, Y184A, F187A, P190A, H249A, H253A and F275A) were inserted into the pYES-DEST52 destination plasmid

using Gateway cloning technology (Invitrogen). These constructs were prepared by Megan Ehrenwerth. Briefly, the gene fragment coding wild type was amplified from genomic DNA using two primers flanking with AttB regions on either side. The resultant gene product was inserted into a donor vector (pDONR221) following the BP reaction according to the manufacturer's instructions (Invitrogen). This insert was sequenced in its entirety. The insert was then transferred into the destination vector (pYES-DEST52) using the LR reaction according to the manufacturer's instructions. This plasmid introduced the *C*-terminal V5 and six histidine tags onto $Gpi8_{1\text{-}306}$.This plasmid was used as the parent plasmid to create all the nine mutants using QuikChange site directed mutagenesis (Qiagen). The complete insert was resequenced after consruction of each mutant.

Plasmids were then transformed into the *S. cerevisiae* strain, INVSC1 (Invitrogen) using standard yeast transformation protocols (Invitrogen). In order to overexpress $Gpi8_{23\text{-}306}$ and each of the different mutants, an overnight culture (50 mL) was grown at 30 °C in Sc-Ura (minimal medium that lacks uracil) and 1% glucose. This culture was used to inoculate 1 L of Sc-Ura medium with 1% galactose in a 4 L flask. The culture was incubated at 30 °C. Cells were harvested after 12 hours and the final OD_{600} was noted for use in during purification.

All purifications were conducted at 4 °C. Typically, a cell pellet from a 4 X 1L growth was resuspended in 10 mL lysis buffer and lysed using glass beads using a bead beater (Invitrogen), for 8X30 s pulses with 30 s rest periods in ice in

between pulses. The lysate was centrifuged at 3000 rpm for 10 min to remove the cell debris and glass beads and the supernatant was centrifuged for 1 hour at 14,000 rpm in a Beckman JA-20 rotor. The filtered, clear supernatant was passed through a 1 mL Ni-NTA high trap column (GE Health care) followed by wash steps with 5 column volumes of lysis buffer and 50 column volumes of washing buffer. Finally, the protein was eluted using 5 mL of elution buffer and the eluted fraction was concentrated to 100 µL. The fractions were analyzed using 12% SDS-PAGE gel and other techniques.

2.4.3 Analysis of the oligomerization state of $Gpi8_{23-306}$ and its mutants by native PAGE and Western blots

All proteins were analyzed via an 12% SDS-PAGE or 10% native PAGE gels. Proteins were kept for 30 min on ice prior to loading onto the native gel. Electrophoresis was carried out with a 10% native polyacrylamide gel (39:1 Acrylamide:bisacrylamide, at pH 8.8) in tris-glycine buffer for 3 hours at 4 ºC at 100 V. Bands were visualized by Western blot using an anti-V5 antibody (Sigma-Aldrich).

For all Western blots, the proteins were transferred to the membrane (Immobilon-FL, Millipore) as follows:. The membrane was soaked in 100% methanol for 5 min and was transferred into 1X transfer buffer and incubated for 15 mins. For native PAGE 0.15% W/V SDS was added to the1x transfer buffer. The gel was also put in the 1X transfer buffer with the membrane for 15 min. Six blotting papers were cut to the same size as the gel and were immersed in the

same buffer prior to the transfer. A semi-dry Western blot apparatus (Thermo Scientific) was used for the transferring of proteins from the gel to the membrane. Three blotting papers were placed on the anode plate followed by the gel, membrane and another three blotting papers carefully without introducing any air bubbles. One gel (8.5 cm X 10 cm) was transferred to the membrane for 30 min at 200 mA.

The transferred membrane was incubated for two hours or overnight in 5% milk in TBS-T prior to incubation with the primary anti-V5 antibody (Sigma-Aldrich, 0.5 µg/mL in 1% BSA) or the anti-GST antibody (Anaspec, 0.5 µg/mL in 1% BSA) for 2 hr. The membrane was washed 3X with 50 mL TBS-T incubating for 5 min each time. The membrane was then incubated with anti-mouse IgG Hilyte Plus 647 (Anaspec, 0.5 µg/mL in 1% BSA) for 1 hr. the membrane was washed again 3X with 50 mL TBS-T with an incubation of 5 min each time and then the blot was visualized using a Typhoon 9210 (Red 633 nm excitation laser, 670 nm emission filter).

2.4.4 Analysis of $Gpi8_{23\text{-}306}$ protein secretion to media in yeast

Cells were grown at 30 ºC as described above. For each time point, a 500 mL aliquot of the cell culture was removed. Cells were harvested at 3500 rpm for 5 min using a Beckman F-500 rotor. The medium was transferred to a 1 L flask and NaH_2PO_4 and NaCl were added to final concentrations of 50 mM and 300 mM respectively. The pH was adjusted to 7.0 and one half of a protease cocktail inhibitor tablet (Roche) was added to inhibit any proteolytic activity. A precipitate

formed as the pH was adjusted. The mixture was filtered using a 0.2 µm filter and the precipitate was discarded (after verification that it did not contain Gpi8 by SDS-PAGE, data not shown). The filtered medium was treated with Ni-NTA resin as described above to purify any secreted $Gpi8_{23-306}$. For comparison, Gpi8 was also purified and analyzed from cell pellets.

2.4.5 Removal of glycans using Endo H

Purified Gpi8 and mutant samples were treated with Endo H to remove any *N*-linked glycans. For 30 µL of a protein sample, 0.5 µL of Endo H_f (1000 U/µL, Invitrogen) were added. The digestion was carried out for 2 hours at 30 ºC. Proteins were incubated at 4 ºC for at least 30 min prior to analysis by native PAGE.

2.4.6 Evaluation of dimers using size exclusion chromatography (SEC)

A sample of 100 µL of protein (~50 µM) was buffer exchanged with SEC buffer, filtered using a 0.22 µm filter, and injected onto an ultra high resolution SEC column (14 mL, Waters) using a BioRad FPLC system. The column was run with 3X column volume with a flow rate of 0.25 mL/min or 0.3 mL/min. Fractions were collected, concentrated and analyzed using 12% SDS-PAGE and 10% native PAGE followed by corresponding blot analysis as described above. A gel filtration standard (100 µg, SEC marker, BioRad) was used to generate a standard curve.

2.4.7 Use of ESI/IMS/MS to evaluate dimer formation by $Gpi8_{23-306}$

Samples for mass spectrometric analysis were quantified using a Bradford assay (BioRad). Each protein was diluted to a concentration of 5 pmol/μL in 25 mM ammonium acetate buffer with 10% methanol for the analysis by the ESI-IMS-MS using a SYNAPT G2 HDMS from Waters Inc. Each sample was injected at a flow rate of 10 μL/min and drift time and m/z (mass to charge ratio) data were collected for 20 min. Driftscope 2.1 (Waters) was used to visualize the 2D plot of drift time vs m/z ratio using a black background and hot metal color code for the third dimension (ion intensity). The data were further processed by extracting mass spectral information for the ion peaks of interest. The spectra were adjusted one time using the Savitzky-Golay smoothing method with a value of ± 10. Baselines in all spectra were subtracted to provide a baseline level close to 0%.

2.4.8 In-gel trypsin digestion for protein confirmation

Protein bands were excised from the gel manually, and washed several times with destaining buffer (10% Acetic acid. 45% methanol and 45% water) to remove the Coomassie stain. The gel was then cut into small pieces and washed twice for five minutes each time with 50 μL of 50% acetonitrile (ACN) in water. Next, the pieces were washed in 50 μL of 200 mM NH_4HCO_3. The gel pieces then were shrunk with 100% ACN until they turned white and were dried for 5 min in an vacuum evaporator (Genevac).

The following steps as well as acquiring spectra were done by Dr. Chih-Wei Liu from Prof Sarah Trimpin's lab. The gel pieces were rehydrated in 15 µL of 50 mM NH_4HCO_3 at 37 °C for 4 min prior to trypsin digestion. An equivalent volume (15 µL) of 20 ng/µL trypsin (Trypsin Gold, Promega) in 50 mM NH_4HCO_3 was added to the gel pieces, and they were incubated at 37 °C for at least 16 h for complete digestion. The digests were extracted using 0.1% formic acid in 50% ACN. All extracts were dried and dissolved in 50% ACN:water with 1% formic acid and analyzed using (LC/MS/MS). The resultant mass spectra were uploaded into the Mascot server to analyze proteins.

2.5 Acknowledge

I sincerely thank, Dr. Jennifer Meizler and Ms Megan Eherenwerth for providing me plasmids. Special thanks to Travis Ness and Aaron Sieg for helping me in growth and purifications of Gpi8 and its mutants. Special thanks goes to Dr Ellen Eutan, Dr Chih-Wei Liu and Dr Sarah Trimpin assisting us with ESI-MS.

CHAPTER 3

CO-EXPRESSION AND CHARACTERIZATION OF THE SOLUBLE DOMAINS OF CORE SUBUNITS OF GPI-T

3.1 Introduction

Gab1 was the first subunit of GPI-T discovered to be oncogenic, highlighting the importance of this enzyme in cancer.[206] However, the complexity of the membrane-bound GPI-T enzyme has hindered progress towards understanding how it functions. In 2001, the Conzelmann group discovered that the full-length GPI-T core subunits, Gpi8, Gpi16 and Gaa1, could be co-purified as an intact complex.[18] Even though Gpi17 and Gab1 are also essential for GPI-T activity, they do not form a stable complex with Gpi8, Gpi16, and Gaa1 in yeast.[89] Unfortunately, 10 years later, scientists still have not determined the function of each subunit or the stoichiometry of the complex. These types of results would be of general interest because of this enzyme's medical and scientific importance. Also, development of a facile assay to investigate GPI-T activity has proved to be challenging.

In order to understand the structure and organization of the GPI-T subunits, we want to determine the stoichiometry of each subunit in the GPI-T complex. Evidence suggests that GPI-T contains more than one copy of each subunit.[18,187] We focused only on the core heterotrimeric GPI-T subunits, Gpi8, Gpi16, and Gaa1. Our lab has demonstrated dimer formation of the soluble domain of $Gpi8_{23-306}$ and several other labs have observed that GPI-T is significantly larger (440-660 kD) than the sum of the molecular weights of the core

subunits (186 kD, not considering the impact of glycosylation).[18,83,85] Combined, these observations suggest that GPI-T is at least a Symmetrical dimer, perhaps further modified with different glycoforms. The possibility that GPI-T is a dimer cannot be entirely ruled out at this point. Despite these observations by us and others, our evidence for dimerization of $Gpi8_{23-306}$ was questioned recently, in favor of Gpi8 existing as a monomer.[84] In response, in chapter 2 of this thesis, we further characterized the dimer of $Gpi8_{23-306}$ when overexpressed and purified from both yeast and *E. coli*.

The approach we used in Chapter 2 eliminated the complexities introduced by working with the full-length, membrane-soluble subunits. The native transmembrane (TM) regions Gpi8 (1 TM), Gpi16 (1 TM), and Gaa1 (6 TMs) make it difficult to purify and analyze these subunits. Therefore, as in chapter 2, we used molecular modeling and TM domain predictions to focus only on the soluble domain regions of these subunits, *i.e.* $Gpi8_{1-306}$, $Gaa1_{50-343}$ and $Gpi16_{1-551}$.[83,207] As a precursor to characterizing the stoichiometry of these subunits, we first looked at the assembly of each soluble domain into heterodimeric and heterotrimeric complexes using co-immunoprecipitation studies. In this chapter we show that each possible pair of these soluble domains assemble into stable isolable heterodimeric complexes. Additionally, we show that the heterotrimer containing at least one copy of $Gpi8_{23-306}$, $Gaa1_{50-343}$, and $Gpi16_{20-551}$, can be purified by tandem affinity purification (TAP), laying the foundation for future studies to characterize the stoichiometry of this complex. This complex was tested initially for GPI-T activity using an *in vitro* assay under development in our

lab (Appendix A). We observed an increase in fluorescence over time, even in the absence of the nucleophile hydroxylamine. Further studies are underway to characterize the catalytic activity of this soluble core complex as well as to evaluate its stoichiometry.

3.2 Results

3.2.1 Plasmid design and construction

Yeast Gpi8 contains a larger luminal domain (residues 23-380) that was used to create a model using Rosetta software.[75,208] (In full-length Gpi8, residues 1-22 contain the *N*-terminal ER localization signal sequence, residues 377-397 contain the TM domain, and residues 398-411 represent a short cytoplasmic peptide.)[75] The model was built with two domains, domain I (the caspase-like domain, residues 23-306) and domain II (a smaller domain, residues 307-376) (Figure 3.1).[83] The overlay of domain I to that of caspase-1 from *Spodoptera frugiperda* led us to conclude that domain I would likely be sufficient for dimerization studies (Figure 1.4). Indeed, our previous publication[83] and the results in chapter 2 clearly demonstrate that domain 1 assembles into a homodimer.

Similar to Gpi8, Rosetta produced a plausible model for Gaa1, taking into account only this subunit's large soluble domain (50-343 residues) (Figure 3.1). (Full-length Gaa1 contains six TM domains; one is *N*-terminal (residues 20-40) and the remaining five are C-terminal (residues 357-598)).[75] After expression, the *N*-terminus of wild-type Gaa1 lies in the cytosol. Thus, to express our

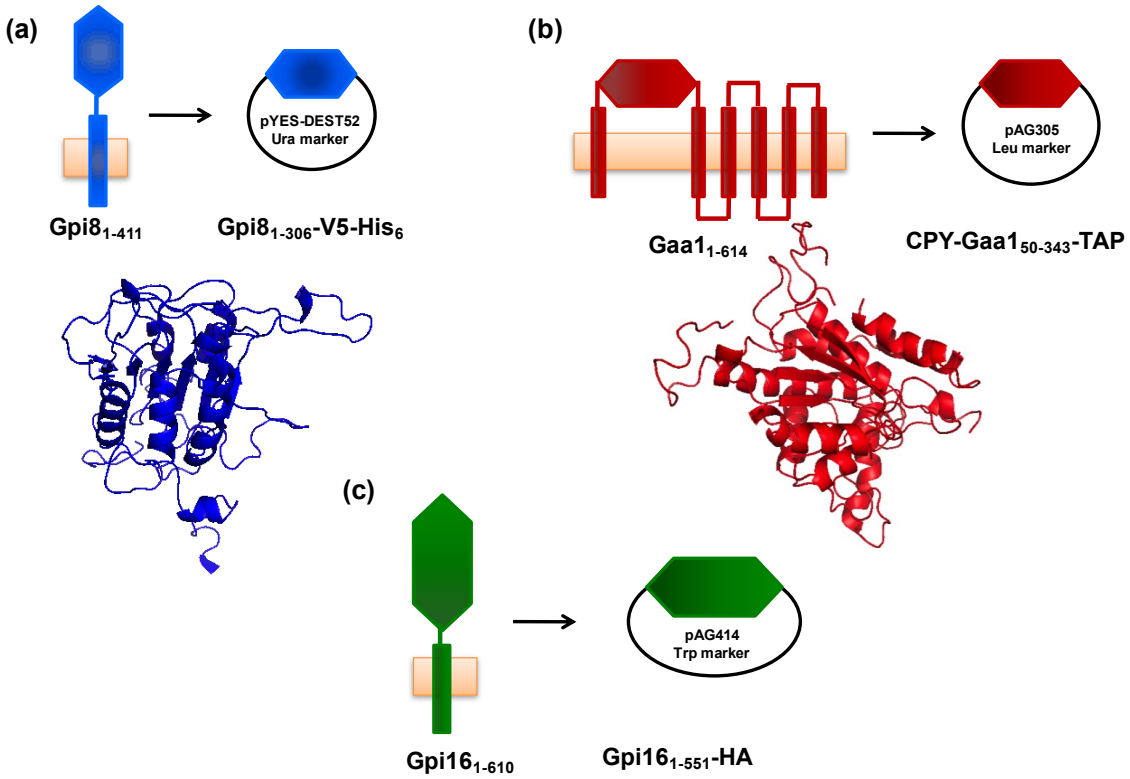

Figure 3.1: Rosetta modeling and design of soluble domain constructions to overexpress Gpi8$_{1-306}$, Gaa1$_{50-343}$ and Gpi16$_{1-551}$. In all three panels, a cartoon is shown for each full-length subunit (left) followed by a cartoon of the soluble domain construct (or constructs) studied herein. See the accompanying text for additional information about the plasmids used to express these vectors. (a) A Rosetta model of the soluble domain I of Gpi8 (blue) is shown. Building from this model, we cloned the portion of the *gpi8* gene coding residues 1-306 into the pYES-DEST52 vector. (b) A Rosetta model of the soluble domain of Gaa1 (red) is shown. Gaa1$_{50-343}$ was cloned into the pAG305-TAP destination vector. After *N*-terminal processing, this vector produces Gaa1$_{50-343}$-TAP. (Note: Another Gaa1 construct was also used but proved significantly less essential so it is not shown here. See text below for details). (c) A useful Rosetta model was not obtained from our modeling efforts. Gpi16$_{1-551}$ was cloned into the pAG414-HA expression vector. After processing, this plasmid is expected to produce Gpi16$_{20-551}$-HA.

truncated version with processing through the ER, we introduced the vacuolar protein carboxypeptidase Y (CPY) signal sequence[207] to the *N*-terminus of $Gaa1_{50\text{-}343}$.

The soluble domain of Gpi16 (residues 1-551) was similarly analyzed with Rosetta after eliminating the single, predicted *C*-terminal TM domain (Figure 3.1). Unfortunately, the model returned by Rosetta was not strong. These Rosetta analyses were conducted by Prof. Tamara Hendrickson, Dr. Jennifer Meitzler, Dr. Yug Varma, and Megan Ehrenwerth. [83,207]

Dr. Meitzler, Dr. Varma and Ms. Ehrenwerth also constructed the original plasmids for the overexpression of these soluble domains. These plasmids are described in detail below. Plasmids were constructed using Gateway cloning technology. $Gpi8_{1\text{-}306}$ and $Gpi16_{1\text{-}551}$ were cloned with their native *N*-terminal signal sequences; $Gaa1_{50\text{-}343}$ was cloned with the CPY signal sequence appended onto its *N*-terminus. Each gene was initially put into the pDONR221 entry vector (Invitrogen). The resultant donor vectors were used to transfer these genes into the desired destination vectors as outlined in Figure 3.1. Destination vectors were selected to contain three different, compatible selection markers (for co-expression studies) and for the tags that they would append onto each subunit. Protein expression is induced with galactose with all three final destination vectors used herein.

$Gpi8_{1\text{-}306}$ was transferred into pYES-DEST52 (Invitrogen) to append V5 and His_6 tags onto the *C*-terminus of this protein. These tags were used for immunoblotting and visualization. The pYES-DEST52 vector contains a Ura

selection marker. $Gpi16_{1-551}$ was transferred into pAG414-GAL (Addgene), which adds a *C*-terminal HA tag for immunoblotting experiments. This vector contains a Trp selection marker.

CPY-$Gaa1_{50-343}$ was transferred into either pAG414-GAL, which appends a C- terminal HA tag and contains Trp selection marker, or into pAG305-GAL (Addgene), which adds a C-terminal TAP tag and contains a Ura marker. As described below, challenges arose when expressing Gaa1 from the pAG414-GAL vector. Consequently, all subsequent experiments used the pAG305-GAL vector coding for $Gaa1_{50-343}$-TAP.

3.2.2 $Gaa1_{50-343}$-HA binds to Ni^{2+} and Co^{2+} resin.

The characterization of $Gpi8_{23-306}$ and $Gaa1_{50-343}$ were conducted using proteins purified from InvSc1 cells, an *S. cerevisiae* cell line. Initial experiments (conducted by Dr. Jennifer Meitzler) characterized yeast His_6-$Gaa1_{50-343}$ alone and with GST-$Gpi8_{23-306}$ after overexpression in and purification from *E. coli*. Several observations were made, namely that expression of His_6-Gaa1 alone is toxic to *E. coli* and that the low levels of His_6-$Gaa1_{50-343}$ that were present could be co-purified with GST-$Gpi8_{23-306}$ by glutathione affinity chromatography.[207,209] To better characterize this heterodimeric complex, we switched from *E. coli* to *S. cerevisiae*. The plasmids encoding GPY-$Gaa1_{50-343}$-HA and $Gpi8_{1-306}$-V5-His_6 were transformed individually or together into InvSc1, *S. cerevisiae* and were overexpressed using galactose induction. Co-purification studies were initially carried out with Ni-NTA affinity purification, to determine whether or not

purification of $Gpi8_{23\text{-}306}$-V5-His_6 would result in co-purification of $Gaa1_{50\text{-}343}$-HA, confirming what Dr. Meitzler had seen when variations of these two constructs were co-expressed in *E. coli*. Unexpectedly, after purification, Western blots with α-HA antibody demonstrated that $Gaa1_{50\text{-}343}$-HA was purified by Ni-NTA affinity without co-purification of $Gpi8_{23\text{-}306}$-V5-His_6 (Figure 3.2 (a)). A control experiment was conducted with $Gpi8_{23\text{-}306}$-V5-His_6 in the absence of Gaa1. In this case, $Gpi8_{23\text{-}306}$-V5-His_6 was purified as expected. Further analysis revealed that the purification of $Gaa1_{50\text{-}343}$ was not due to interactions with $Gpi8_{1\text{-}306}$; instead, this protein showed affinity for Ni-NTA resin (lane 2 of Figure 3.2 (b)) and also with Co^{2+} resin (Figure 3.2, lanes 3-7). These results were surprising because our $Gaa1_{50\text{-}343}$ construct did not contain a His_6 tag. Sequence alignments with full-length Gaa1 (not shown) suggest that it is an M28 type aminopeptidase with one metal binding site, presumably for Zn^{2+}.[186] Perhaps its ability to bind to Ni^{2+} and Co^{2+} resin arises from this metal binding site. Because of this unexpected obstacle, we reversed our approach and used an anti-HA antibody to examine $Gpi8_{23\text{-}306}$-V5-His_6 and $Gaa1_{50\text{-}343}$-HA interactions by co-immunoprecipitation analyses.

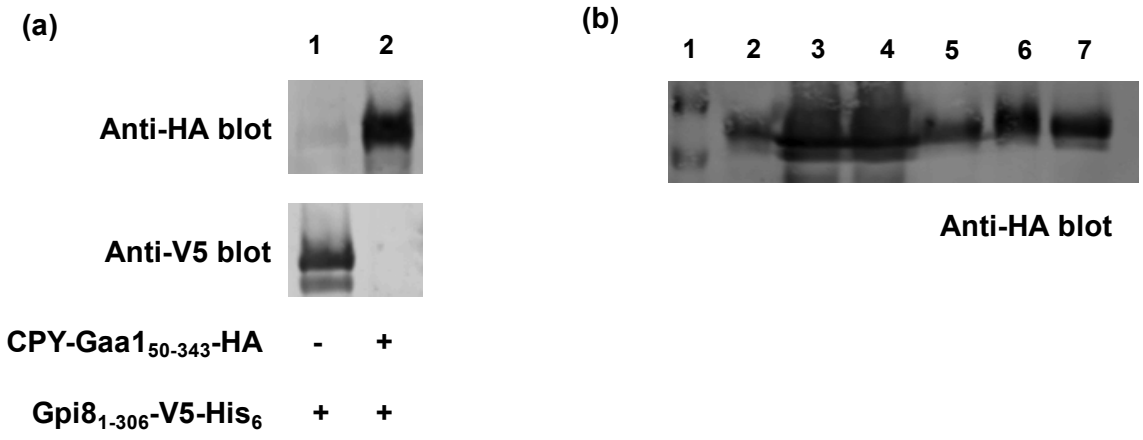

Figure 3.2: CPY-Gaa1$_{50-343}$-HA can be purified by Ni^{2+} and Co^{2+} resin without a His$_6$ affinity tag. (a) Co-purification of CPY-Gaa1$_{50-343}$-HA and Gpi8$_{23-306}$-V5-His$_6$ using Ni-NTA affinity purification. Top panel: An anti HA blot to confirm the presence of Gaa1. Bottom panel: An anti-V5 blot to confirm the presence of Gpi8. For both panels, lane 1: Gpi8$_{23-306}$-V5-His$_6$ alone; lane 2: Co-purification of CPY-Gaa1$_{50-343}$-HA and Gpi8$_{23-306}$-V5-His$_6$. (b) Results from a mock purification of Gaa1$_{50-343}$-HA using Ni-NTA resin. Cell lysate containing overexpressed CPY-Gaa1$_{50-343}$-HA were incubated with Ni-NTA resin. The results of this purification were examined by Western blot using an α-HA antibody. The lanes in this blot are as follows: lane 1: molecular weight markers; Lane 2: Gaa1$_{50-343}$-HA purified by Ni-NTA affinity chromatography; lanes 3-7 show the results of this mock purification using Co^{2+} resin; lane 3: cell lysate; lane 4: flow through; Lane 5: wash; Lane 6: eluted fraction (300 mM imidazole); lane 7: resin after elution. The anti HA blot confirms the purification of Gaa1$_{50-343}$ by metal (Ni^{2+} and Co^{2+}) affinity purification without a His$_6$ tag. A picture of the complete blot is shown in Appendix C, Figure C.2.

3.2.3 $Gpi8_{23\text{-}306}$-V5-His_6 co-immunoprecipitation with $Gaa1_{50\text{-}343}$-HA

An HA antibody was used to see if $Gpi8_{23\text{-}306}$-V5-His_6 would co-immunoprecipitate with $Gaa1_{50\text{-}343}$-HA. As controls, we carried out parallel immunoprecipitation studies with each subunit alone as well (Figure 3.3). As expected, $Gpi8_{23\text{-}306}$-V5-His_6 alone did not immunoprecipitate from total cell lysates with the HA antibody in the absence of $Gaa1_{50\text{-}343}$-HA (Figure 3.3, lane 1); $Gaa1_{50\text{-}343}$-HA alone was immunoprecipitated with the HA antibody (Figure 3.3, lane 2). When both $Gpi8_{1\text{-}306}$-V5-His_6 and CPY-$Gaa1_{50\text{-}343}$-HA were overexpressed together, immunoprecipitation of $Gaa1_{50\text{-}343}$-HA led to the co-precipitation of $Gpi8_{23\text{-}306}$-V5-His_6 (Figure 3.3, lane 3). These results confirm that $Gpi8_{23\text{-}306}$-V5-His_6 interacts with $Gaa1_{50\text{-}343}$-HA non-covalently. Consequently, it can also be concluded that the interactions between these two subunits do not require other GPI-T subunits or transmembrane domains.

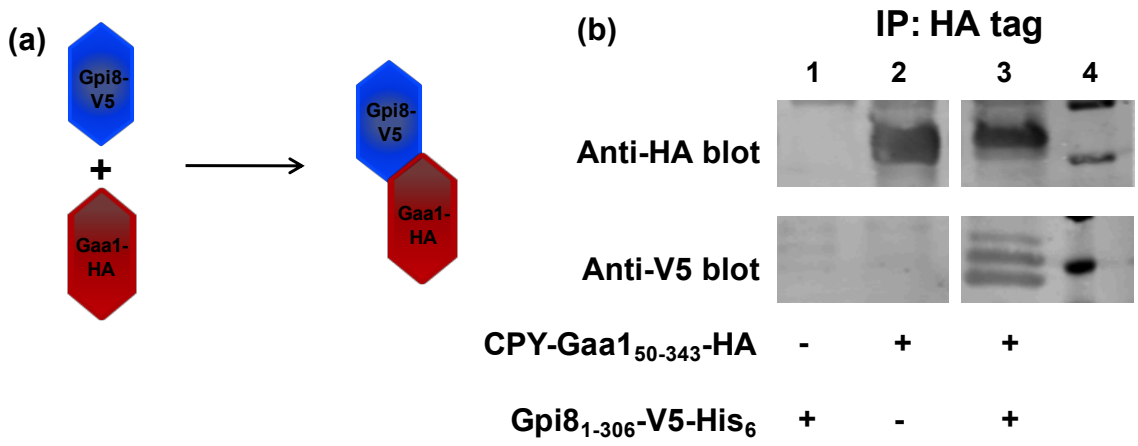

Figure 3.3: Gpi8$_{23-306}$ interacts with Gaa1$_{50-343}$ without its transmembrane domains or the Gpi16 subunit. (a) A cartoon representation of the interactions between the soluble domains of Gpi8 and Gaa1. Gpi8$_{23-306}$ co-immunoprecipitated with Gaa1$_{50-343}$ when both Gpi8$_{23-306}$-V5-His$_6$ and Gaa1$_{50-343}$-HA were overexpressed together in yeast. (b) Western blot analysis of immunoprecipitation results using HA antibodies. Top panel: an anti-HA blot confirming the presence of Gaa1$_{50-343}$-HA in different samples after co-immunoprecipitation. Bottom panel: an anti-V5 blot examining the presence of Gpi8$_{23-306}$-V5-His$_6$ in different fractions. Blots were generated from the same sets of samples from two different SDS-PAGE gels that were run in parallel. Lane 1: Gpi8$_{23-306}$-V5-His$_6$ alone; lane 2: Gaa1$_{50-343}$-HA alone; lane 3: Co-immunoprecipitation of Gpi8$_{23-306}$-V5-His$_6$ with Gaa1$_{50-343}$-HA; lane4: molecular weight markers. For the image, intervening lanes from the blot were removed for clarity. These changes are indicated by the presence of a white space separating the different lanes. A complete gel picture is shown in Appendix C, Figure C.3. These results indicate that the soluble domains of Gpi8$_{23-306}$ Gaa1$_{50-343}$ interact with each other *in vivo*.

3.2.4 $Gpi8_{23-306}$ co-immunoprecipitates with $Gpi16_{20-551}$.

The Gpi16 subunit is covalently connected to Gpi8 through a disulfide bond, and this interaction has been proposed to maintain complex stability.[210] In yeast GPI-T, the residues Cys85 of Gpi8 and Cys202 of Gpi16 form this disulfide bond.[211-212] Even though the exact function of Gpi16 is not known, It has been proposed that its lumenal domain of Gpi16 has a β-propeller structure that acts as a funnel that directs the protein substrate into the Gpi8 active site.[213-214]

To gain further insight into the interactions between Gpi8 and Gpi16, a Gpi16 soluble domain was constructed as described above using Gateway cloning technology for overexpression in yeast with galactose induction. Gpi16 has a single *C*-terminal TM domain (residues 546-568). The Gpi16 construct ($Gpi16_{1-551}$) was designed by removing this TM domain leaving the native *N*-terminal ER signal sequence intact. $Gpi16_{1-551}$ was cloned into pAG414-GAL such that a C-terminal HA tag was added for visualization by Western blot. The same Gpi8 construct ($Gpi8_{1-306}$-V5-His_6), as described above (Section 3.2, Chapter 3), was used here.

We used an anti-HA antibody for these studies. $Gpi8_{1-306}$-V5-His_6 and $Gpi16_{1-551}$-HA were overexpressed and immunoprecipitated separately and together, the results are shown in Figure 3.4. $Gpi8_{23-306}$-V5-His_6 did not show any non-specific interactions with either the resin or the antibody (Figure 3.4 (b), lane 4). As expected, $Gpi16_{20-551}$ alone was successfully immunoprecipitated using an anti-HA antibody (Figure 3.4 (b),lane 5).

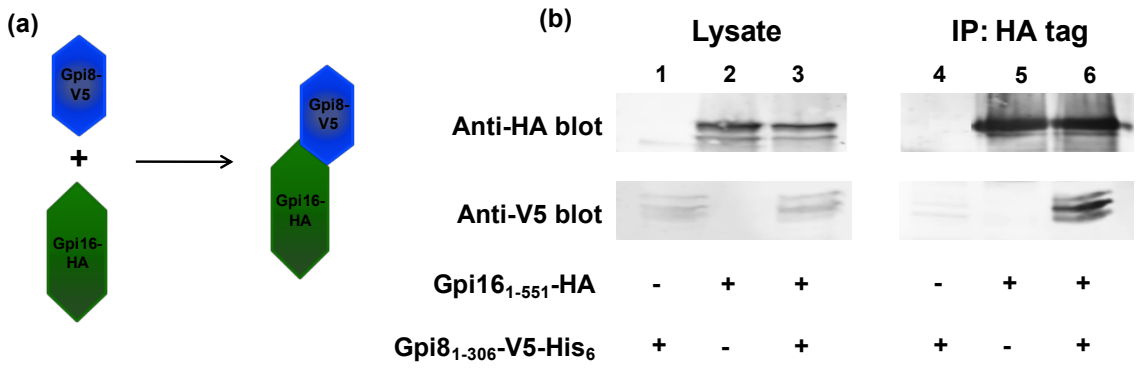

Figure 3.4: Gpi8$_{23-306}$ specifically co-immunoprecipitates with Gpi16$_{20-551}$ indicating formation of a heterodimer between these two subunits. (a) A cartoon representation of the putative interactions between the soluble domains of Gpi8 and Gpi16 of interest herein. (b) Western blot results from immunoprecipitation studies conducted with anti-HA antibodies. The top panels show an anti-HA blot to visualize Gpi16$_{20-551}$-HA. The bottom panels show results from an anti-V5 blot to visualize Gpi8$_{23-306}$-V5-His$_6$. Lanes 1-3 contain the lysates used in these studies, before immunoprecipitation. Lanes 4-6 show the results after immunoprecipitation. Lanes 1 and 4: Gpi8$_{23-306}$-V5-His$_6$ alone;lanes 2 and 5: Gpi16$_{20-551}$-HA alone; lanes3 and 6: Co-immunoprecipitation of Gpi8$_{23-306}$-V5-His$_6$. A complete gel picture is shown in Appendix C, Figure C.4.

In contrast, when $Gpi8_{1-306}$ was co-expressed with $Gpi16_{1-551}$, these subunits co-immunoprecipitated as a complex under oxidizing conditions (Figure 3.4, lane 6). Co-immunoprecipitation of $Gpi8_{23-306}$-V5-His_6 with $Gpi16_{20-551}$-HA as a complex is in contrast to previous findings with human GPI-T that showed that interactions between these two subunits require their TM domains.[215]

In wild-type GPI-T, the disulfide bond between Gpi8 and Gpi16 is formed between C85 (Gpi8) and C202 (Gpi16). To test the importance of these residues for assembly of the $Gpi8_{23-306}$:$Gpi16_{20-551}$ complex, each cysteine residue was mutated to alanine and the co-immunoprecipitation studies described in the previous paragraph were repeated. These mutations would eliminate the possibility of disulfide bond formation between Gpi8 and Gpi16. Co-expression and co-immunoprecipitation studies were conducted with the following protein combinations: C85A $Gpi8_{23-306}$ with WT-$Gpi16_{20-551}$, WT-$Gpi8_{23-306}$ with C202A $Gpi16_{20-551}$, and C85A $Gpi8_{23-306}$ with C202A-$Gpi16_{20-551}$ (Figure 3.5). In all cases, immunoprecipitation of $Gpi16_{20-551}$-HA using an anti-HA antibody led to co-immunoprecipitation of $Gpi8_{23-306}$-V5-His_6 (Figure 3.5). These results demonstrate that the disulfide bond between Gpi8 and Gaa1 is not essential for the interactions between the soluble domains of these two subunits.

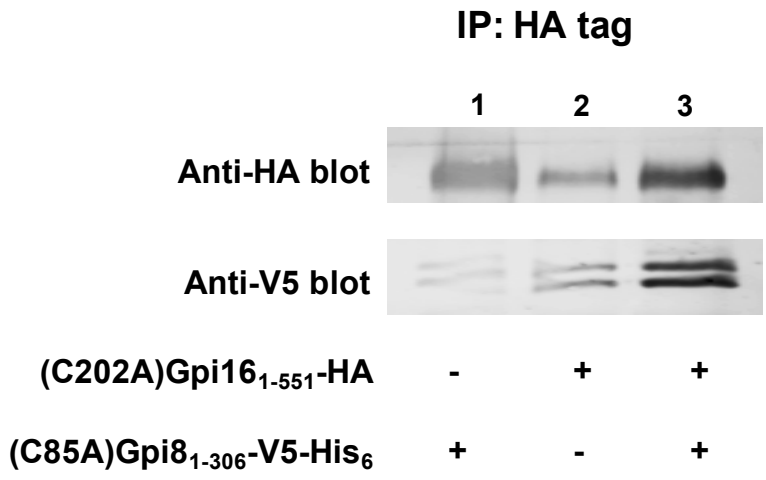

Figure 3.5: The disulfide bond between Gpi8 and Gpi16 is not essential for Gpi8$_{23-306}$ and Gpi16$_{20-551}$ interactions. Immunoprecipitation studies were conducted using anti-HA antibody under oxidizing conditions. Each of the lane contains both Gpi16$_{20-551}$-HA and Gpi8$_{23-306}$-V5-His$_6$ either with or without the mutant. Lane1: Co-immunoprecipitation of C85A Gpi8$_{23-306}$-V5-His$_6$ with WT Gpi16$_{20-551}$-HA. Lane 2: Co-immunoprecipitation of WT Gpi8$_{23-306}$-V5-His$_6$ with C202A Gpi16$_{20-551}$-HA. Lane 3: Co-immunoprecipitation of C85A Gpi8$_{23-306}$-V5-His$_6$ with WT Gpi16$_{20-551}$-HA. The complete picture of this blot is shown in Appendix C, Figure C.5. Results indicate that Gpi16$_{20-551}$ interacts with Gpi8$_{23-306}$ even in the absence of the disulfide bond between these two subunits.

3.2.5 $Gaa1_{50-343}$ assembles into a heterodimeric complex with $Gpi16_{20-551}$

We also examined the hypothesis that $Gpi16_{20-551}$ and $Gaa1_{50-343}$ could form a stable heterodimer in the absence of Gpi8. Gateway cloning technology was used and a plasmid expressing $Gpi16_{20-551}$ was constructed with a V5 and a His_6 tag added to its *C*-terminal. Another plasmid was constructed in which $Gaa1_{50-343}$ was modified to contain an *N*-terminal CPY signal sequence and a *C*-terminal tandem affinity purification (TAP) tag. Co-immunoprecipitation with IgG resin (targeting the TAP tag) demonstrated that these two subunits also directly interact with each other, in this case in the absence of Gpi8 (Figure 3.6). However, additional controls needed to be done to confirm that $Gpi16_{20-551}$-V5-His_6 does not have any non-specific affinity for this IgG resin.

3.2.6 The three core subunits of GPI-T co-purify with each other without their transmembrane regions

The results described above demonstrate that the soluble domains of the core subunits of GPI-T stably interact with each other in heterodimeric pairs. Building on these results, we set out to isolate these three soluble domains as a single complex (Figure 3.7 (a)). Such an accomplishment would open up innumerable new avenues to further and better characterize GPI-T. It would be of particular interest to determine if such a complex was catalytically active. We overexpressed and set out to purify the core complex, containing $Gpi8_{1-306}$-V5-His_6, $Gpi16_{1-551}$-HA and CPY-$Gaa1_{50-343}$-TAP using the InvSc1 strain of *S. cerevisiae* and the plasmids described in previous sections.

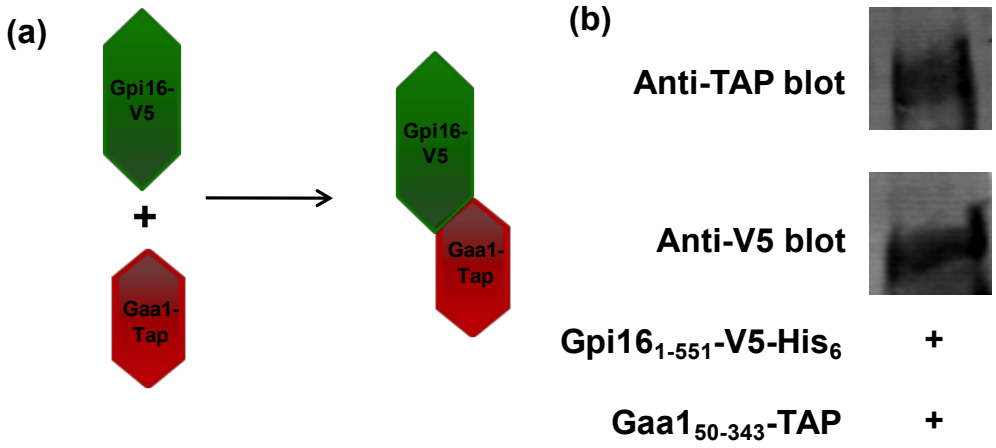

Figure 3.6: Gpi16$_{20-551}$-V5-His$_6$ co-immunoprecipitates with Gaa1$_{50-343}$–TAP. (a) A cartoon representation of the putative interaction between Gpi16$_{1-551}$ and Gaa1$_{50-343}$. (b) Results from immunoprecipitation with IgG resin. The top panel shows an anti-TAP blot indicating the presence of Gaa1$_{50-343}$-TAP after precipitation with IgG resin. The bottom panel shows an anti-V5 blot demonstrating that Gpi16$_{23-551}$-V5-His$_6$ was isolated with Gaa1. Additional controls will be run to confirm that this result arose from specific interactions between the two subunits rather than via non-specific interactions between Gpi16 and the IgG resin. The complete picture of this blot is shown in Appendix C, Figure C.6.

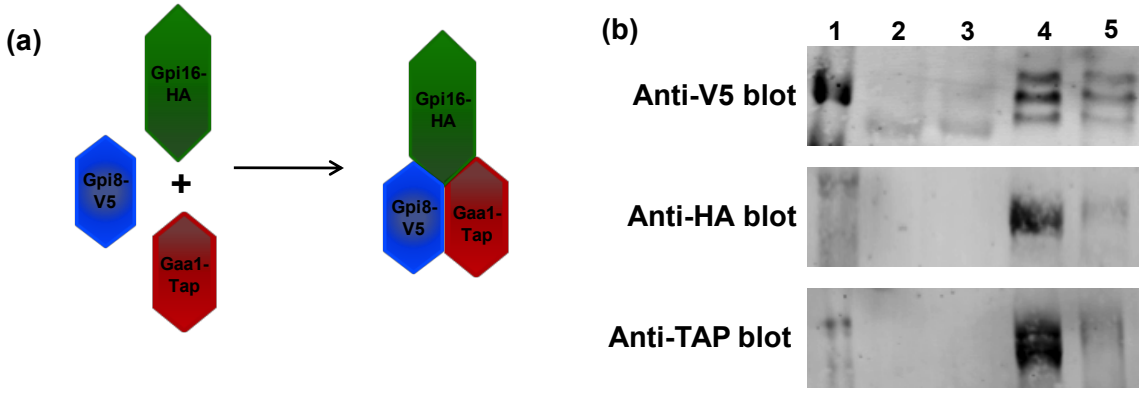

Figure 3.7: Tandem affinity purification of $Gaa1_{50-343}$-TAP results in the co-purification of $Gpi16_{23-551}$-HA and $Gpi8_{23-306}$-V5-His_6. (a) A cartoon representation of the putative interactions between $Gpi8_{23-306}$, $Gpi16_{20-551}$, and $Gaa1_{50-343}$ of interest herein. (b) Evaluation of the co-purification of $Gpi16_{20-551}$-HA, $Gpi8_{23-306}$-V5-His_6, and $Gaa1_{50-343}$-TAP. Each fraction along the purification was tested for the presence of the individual subunits using specific antibodies for Gpi8 (top), Gpi16 (middle), and Gaa1 (bottom). In all three panels, lane 1: molecular weight markers; lane 2: cell lysate prior to purification; lane 3: flow through after lysate was incubated with the calmodulin binding resin; lane 4: $Gaa1_{50-343}$-TAP after elution from the resin, with its co-purified protein partners; lane 5: anti-protein A resin after elution. The complete picture of this blot is shown in Appendix C, Figure C.7.

This heterotrimeric complex was isolated by TAP tag purification *in vitro* using calmodulin binding resin (see materials and methods). The presence of all three soluble domains was verified by Western blots for each subunits (Figure 3.7). Lanes 2-5 of Figure 3.7 indicates analysis of each fractions along the purification. When purified using TAP tag, both $Gpi8_{23\text{-}306}$-V5-His_6 and $Gpi16_{20\text{-}551}$-HA purified along with $Gaa1_{50\text{-}343}$-TAP as an intact complex (Figure 3.7, lane 4). These results indicate that the core subunits interact with each other without their transmembrane regions.

3.2.7 The heterotrimer of the soluble domains of GPI-T has catalytic activity

With a method in hand to purify the three core subunits of GPI-T as a single complex, we were uniquely positioned to begin to characterize this complex *in vitro* for the first time. The foremost goal in our mind was to determine whether or not this truncated soluble complex retained catalytic activity. Such a discovery would dramatically improve the ability of researches, including us to characterize GPI-T.

Our lab has developed a reliable FRET assay that would not only will help to analyze GPI-T activity as a whole complex, but could also facilitate analysis of single subunit contributions to GPI-T activity.[216] This assay relies on synthetic peptides modified with a fluorophore (Abz, 2-aminobenzoic acid) and a quencher (Y*, nitrotyrosine) flanking the ω site amino acid. Our main substrate for this assay is based on the human campath-1 antigen, or CD52 (Figure 3.8), the smallest known substrate for GPI-T. After cleavage of its *N*-terminal ER signal

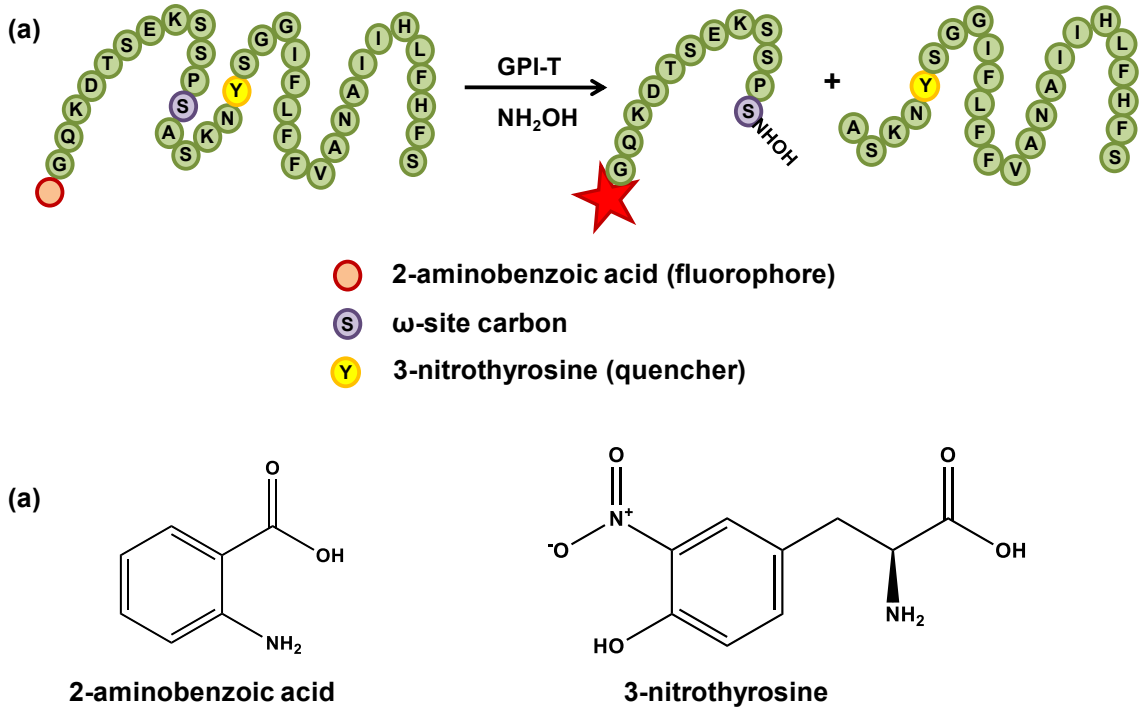

Figure 3.8: Transamidation reaction takes place in CD52. (a) Transamidation reaction. Red color amino acid indicates the fluorophore (Abz or 2-aminobenzoic acid) and the yellow color amino acid indicates the quencher (3-nitrotyrosine), which are flanking the ω-site serine shown in pale purple color. The right hand side contains the two products obtained from the transamidase reaction when incubated with GPI-T and hydroxylamine (NH_2OH). First product is the hydroxamate that contain the fluorophore and the second product is the part contains the quencher. (b) Chemical structures of the fluorophore (Abz) and the quencher (3-nitrotyrosine).

sequence, CD52 is only 37 amino acids long.[217,218,219] We synthesized this peptide with the addition of the fluorophore (red) and the quencher (yellow) on either side of the ω-site (pale purple).

When this peptide is incubated with purified GPI-T from yeast with a GPI anchor mimic such as hydroxylamine,[220] the peptide is cleaved at the ω-site amide, which results in increase Abz fluorescence over time. Previous experiments carried out to develop this assay were conducted by Dr. Sandamali Ekanayaka (see Appendix A for more *in vitro* assay details).[216] Dr Ekanayaka demonstrated that this peptide is a substrate for GPI-T and that GPI-T activity is dependant on hydroxylamine as a replacement for the full-length GPI anchor (Figure 3.9 (a).

CD52 was used as the basis for the design and synthesis of two additional peptides, peptides 2 and 8 (Table 3.1). Several modifications were introduced into this peptide (shown in bold letters for both peptides, Table 3.1) to avoid any *N*-linked glycosylations[221] or any oxidations[222] (when using the crude lysates) to make the peptide substrate less complicated. Including these modifications, peptide 2 was synthesized with an 2-aminobenzoic acid (Abz) group on the *N*-terminus amino acid and the 3-nitrotyrosine group on the 17th amino acid from the *N*-terminus (Table 3.1). Peptide 8 was similar to that of peptide 2 without its hydrophobic signal sequence.

Using the same protocol developed by Dr. Sandamali Ekanayaka, we tested the soluble domains of the core subunits for GPI-T activity (Figure 3.9).[216]

Table 3.1: Peptide substrates to test GPI-T activity. The peptide substrates used in this chapter were built from the sequence of CD52. Changes are highlighted in bold. A 2-aminobenzoic acid (Abz) group was introduced at the *N*-terminus and a 3-nitrotyrosine (Y*) was inserted in place of Ile17. Peptide 8 is similar to peptide 2 however it lacks the hydrophobic region of the *C*-terminal GPI-T signal sequence.

Peptide	***N* – terminus**	***N*-terminal sequence**	**ω site**	**Signal sequence**	**C-terminus**
WT-CD52	H_2N	GQNDTSETSSP	S	ASSNISGGIFLFFVANAIIHLFCFS	COOH
Peptide 02	Abz	GQ**K**DTSE**K**SSP	S	AS**KN**Y*SGGIFLFFVAVAIIHLF**H**FS	COOH
Peptide 08	Abz	GQ**K**DTSE**K**SSP	S	AS**KN**Y*SGGIFL	COOH

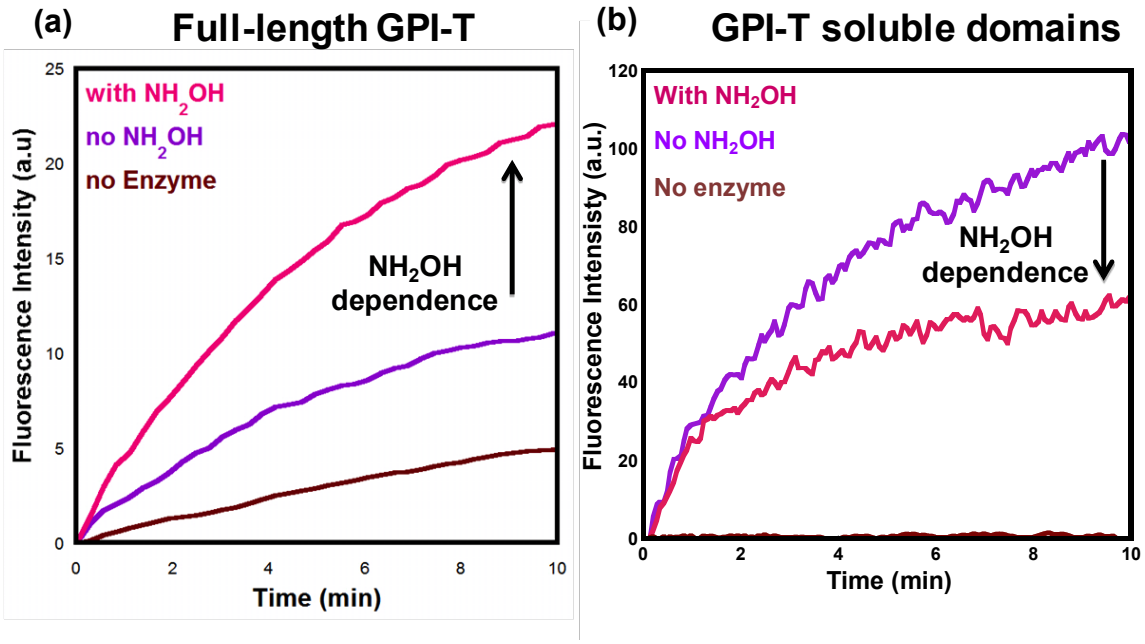

Figure 3.9: The soluble domains of the core subunits show nucleophile independent activity. (a) Fluorescence measurements from an *in vitro* GPI-T assay conducted with the peptide 2 for the full length GPI-T in the presence (red) and absence (blue) of 10 mM hydroxylamine. (b) Fluorescence measurements from an *in vitro* GPI-T assay conducted with the peptide 2 for the soluble domains of the core GPI-T subunits in the presence (red) and absence (blue) of 10 mM hydroxylamine. Full length GPI-T shows an NH_2OH dependence where as soluble domains of the core GPI-T subunits show an reduction of NH_2OH dependence.

Surprisingly, when incubated with peptide 2, a time-dependent increase in fluorescence was observed but this rate was independent of hydroxylamine; this result is in contrast to assays with full-length GPI-T, in which measurable activity was only obtained in the presence of hydroxylamine (Figure 3.9). However, as observed with wild-type GPI-T, our assay of the solubilized heterotrimer with the truncated peptide 8 revealed a much slower rate (data not shown). These preliminary data suggests that the pure soluble hetrotrimer retains some catalytic activity, however this activity is nucleophile-independent. The most likely explanation for this activity is that truncation of GPI-T has disrupted the active site of Gpi8 in a way that is sufficient to convert this enzyme's normal transamidation activity into proteolytic activity. However, additional experiments are need to confirm this scenario.

To better understand these results and to further explore the activity of this heterotrimeric complex, a carboxyfluorescein (CF) labeled CD52 is being synthesized. This peptide will be assayed as a substrate for our miniaturized, soluble GPI-T and any product produced by GPI-T will be characterized by LC-MS to confirm that either transamidation or hydrolysis has occurred at the ω site.

3.3 Discussion

We designed and overexpressed soluble domains for each of the three core subunits of GPI-T to facilitate experiments to examine the structure and organization of this enzyme. Here we've demonstrated that each pair of subunits can be isolated by immunoprecipitation or by purification, even in the absence of

the third subunit or any transmembrane domains. We were also able to co-purify these three soluble domains together in a heterotrimetric complex using only the TAP tag appended onto the *C*-terminus of $Gaa1_{50-343}$. Preliminary assays suggest that this solubilized complex has retained some GPI-T-like catalytic activity however this activity is nucleophile-independent (unlike full-length, wild-type GPI-T, which requires a nucleophile).

In yeast, the full lengths forms of the core subunits Gpi8, Gpi16 and Gaa1 purify as one complex.[18] But the complexity of this complex and the low levels of purified protein obtained have hindered efforts to further characterize this enzyme. Here we were able to confirm interactions between the soluble domains of the core subunits, which will simplify additional analyses. These results represent just the beginning of a new era for understanding about GPI-T. Using these interactions, we can now determine the oligomerization states of these different complexes and, eventually, characterize the different contributions of each subunit towards GPI-T activity, providing insight into this complicated enzyme complex that had previously been inaccessible.

3.4 Materials and methods

3.4.1 Buffers and solutions

Minimal medium (4X Sc-ura): 26.8 g Yeast nitrogen base, 6.4 g dropout mix, 0.4 g each adenine, leucine, tryptophan and histidine in 1L of water and sterile filtered before use. Minimal medium (4X Sc-trp): 26.8 g Yeast nitrogen base, 6.4 g dropout mix, 0.4 g each adenine, leucine, uracil and histidine in 1L of

water and sterile filtered before use. Minimal medium (4X Sc-ura-trp): 26.8 g Yeast nitrogen base, 6.4 g dropout mix, 0.4 g each adenine, leucine and histidine in 1L of water and sterile filtered before use. Lysis buffer: 50 mM NaH_2PO_4, 300 mM NaCl, 10 mM imidazole, pH 7.2. Wash buffer: 50 mM NaH_2PO_4, 1 M NaCl, 50 mM imidazole, pH 7.2. Imidazole elution buffer: 50 mM NaH_2PO_4, 300 mM NaCl, 300 mM imidazole, pH 7.2. Phosphate buffered saline (PBS) buffer: 10 mM Na_2HPO_4, 1.8 mM KH_2PO_4, 2.7 mM KCl, 137 mM NaCl, 1 mM $CaCl_2$, 0.5 mM $MgCl_2$, pH 7.2. Radioimmunoprecipitation assay (RIPA) buffer: 50 mM Tris-HCl, 150 mM NaCl, 0.25 % w/v deoxycholate, 1 % igepal, 1 mM (Ethylenediaminetetraacetic acid) EDTA, pH 7.4. Calmodulin binding buffer: 10 mM Tris-HCl, 150 mM NaCl, 1 mM Mg-acetate, 1 mM β-mercaptoethanol (BME), 2 mM $CaCl_2$, pH 8.0. Ethyleneglycoltetraacetic acid (EGTA) elution buffer: 5 mM Tris-HCl, 10 mM EGTA, 5 mM EDTA, pH 8.0. FRET assay buffer: 50 mM Tris-HCl, 0.1 M NaCl, 1 mM $MgCl_2$, 1 mM $CaCl_2$, 1 mM $MnCl_2$, 1 mM dithiothreitol (DTT), 1 mM phenylmethylsulfonylfluoride (PMSF), and 20 mM reduced glutathione (GSH), pH 7.4.

3.4.2 Co-purification of the $Gpi8_{23\text{-}306}$-V5-His_6:$Gaa1_{50\text{-}343}$-HA complex using Ni-NTA affinity purification

Plasmids were constructed using Gateway cloning technology as described in section 3.2.1, by Dr Yug Varma and Ms Megan Ehrenwerth. Each gene was amplified using primers with appended AttB sites along with their native or CPY *N*-terminal signal sequences. PCR products were transferred into

the pDONR221 donor vector using standard *E. coli* transformation protocols and DH5α competent cells. After sequencing of each construct, genes were transferred into the appropriate destination vectors using the LR recombination mix (Invirtogen). $Gpi8_{1\text{-}306}$ was inserted into pYES-DEST52 (Invitrogen) and CPY-$Gaa1_{50\text{-}343}$ into pAG414-GAL (Addgene). Both destination plasmids were transformed individually or together into InvSc1 competent cells using standard lithium acetate transformation (Invitrogen, pYES-DEST52 Gateway vector manual).

A 50 mL overnight culture of $Gpi8_{1\text{-}306}$-V5-His_6:CYP-$Gaa1_{50\text{-}343}$-HA or each single subunit was grown overnight and then transferred into a 1 L cell culture of the appropriate minimal medium (Sc-ura for $Gpi8_{1\text{-}306}$-V5-His_6, Sc-trp for CYP-$Gaa1_{50\text{-}343}$-HA and Sc-ura-trp for $Gpi8_{1\text{-}306}$-V5-His_6:CYP-$Gaa1_{50\text{-}343}$-HA. Ultimately, cells from a 4 L culture were used for the each experiment. The cultures were grown in the minimal medium either lacking uracil or tryptophan or both, depending on the selection markers present in the plasmids used. Galactose (1%) was added to each large culture (overnight cultures were grown in 1% glucose) and each culture was grown for 12 hours prior to harvesting of the cells by centrifugation (3000 rpm for 5 min). Lysis buffer was added to the harvested cell pellet from a single 4 L cell culture, along with a quarter of a protease cocktail inhibitor tablet (Roche). An equal volume of glass beads (10 mL) was added to the cell suspension, which was subsequently treated by vortexing for 30 sec followed by 30 sec on ice for 8 cycles. The cell lysate was centrifuged at 14,000 rpm for one hour using a JA20 rotor (Beckman Coulter).

The cleared supernatant was used for protein purification by Ni-NTA affinity purification. A 1 mL HisTrap HP column (GE Healthcare) was used for each purification. The columns were pre-equlibriated by washing each with 10 column volumes of lysis buffer. Each lysate was passed through a column at a rate of 0.5 mL/min. Then the columns were washed with 5 column volumes lysis buffer followed by 50 column volumes wash buffer and another 5 column volumes lysis buffer. Proteins were eluted with 4 mL imidazole elution buffer and the eluent was concentrated using a 30,000 MW cutoff (Millipore) to a final volume of ~ 150 µL.

Western blots of SDS-PAGE gels were run to confirm the presence of the protein using the same protocol described in the materials and methods section of the Chapter 2. $Gpi8_{23-306}$ was visualized using an anti-V5 primary antibody (Sigma-Aldrich) and $Gaa1_{50-343}$ was visualized using an anti-HA primary antibody (Sigma-Aldrich).

3.4.3 Co-immunoprecipitation using an HA tag (To evaluate $Gpi8_{23-306}$-V5-His_6: $Gaa1_{50-343}$-HA and $Gpi8_{23-306}$-V5-His_6:$Gpi16_{20-551}$-HA complexes)

Cell lysate from a 100 mL cell culture was used for immunoprecipitation assays. Cells were overexpressed as described above, with appropriate adjustments to the media and volumes. Each cell pellet was resuspended in 1 mL PBS buffer with the addition of a quarter tablet of a Roche protease cocktail inhibitor. The cells were broken with glass beads as described above (section 3.4.2) and the cell lysate was obtained. An Anti-HA antibody (20 µg from a 1

mg/mL solution, Sigma Aldrich) was added and the solution was incubated overnight on a wheel at 4 °C. A 20 µL sample of protein A agarose resin (Sigma-Aldrich) was used for the immunoprecipitation studies. The resin was pelleted at 12,000 rpm for 1 min and washed three times with 1 mL RIPA buffer. The resin was pelleted in between each wash before adding to the lysate/antibody mixture. The lysate/antibody/resin mixture was incubated with the resin at 4 °C for 2 hours. The beads were pelleted by centrifugation at 12,000 rpm for 1 min. The beads were washed four times with 1 mL RIPA buffer each time and one time with PBS buffer. The beads were pelleted again and then resuspended in 25 µL 2X SDS gel loading dye. This suspension was boiled for 5 min and analyzed using SDS PAGE gels followed by Western blots as described in Chapter 2, section 2.4.3. $Gpi8_{23-306}$ was visualized using an anti-V5 primary antibody (Sigma-Aldrich) and $Gaa1_{50-343}$ and $Gpi16_{20-551}$ were visualized using an anti-HA primary antibody (Sigma-Aldrich).

3.4.4 TAP tag purification to isolate heterotrimer

Cells were grown in Sc-ura-trp-leu minimal medium with galactose induction, essentially as described above. The cells were harvested at 3000 rpm for 5 min and were lysed using calmodulin binding buffer with the addition of a quarter tablet of a Roche protease cocktail inhibitor. Cell lysate from a 4 L cell culture was used for each purification. A 100 µL bed volume of calmodulin sepharose beads (Sigma-Aldrich), which had been pre-equilibriated by washing with 20 mL calmodulin binding buffer, was added to a column (Bio-Rad) at 4 ºC.

The cell lysate was added onto these beads and the slurry was incubated for 2 hours at 4 °C on a rotating wheel. The beads were then washed with 30 mL ice-cold calmodulin binding buffer at 4 °C. The proteins were eluted with 4 mL EGTA elution buffer and were concentrated using a 30,000 MW cutoff to a final volume of ~150 µL. The eluted proteins were analyzed using SDS-PAGE gels followed by Western blot analysis as described in the materials and methods in chapter 2. $Gpi8_{23-306}$ was visualized using an anti-V5 primary antibody (Sigma-Aldrich), $Gpi16_{20-551}$ was visualized using an anti-HA primary antibody (Sigma-Aldrich), and $Gaa1_{50-343}$ was visualized using an anti-TAP primary antibody (Sigma-Aldrich).

3.4.5 FRET assay for the soluble domains

The FRET assay was carried out essentially using the protocol described in Dr. Sandamali Ekanayaka's thesis.[216] A 20 µL aliquot of a 1 mM peptide solution (dissolved in DMSO, either peptide 2 or 8) was added to 1.93 mL of FRET assay buffer. A Cary Eclipse spectrofluorimeter set to the following parameters: 321 nm excitation wavelength, 417 nm emission wavelength, 10 nm excitation slit width, 5 nm emission slit width. Each assay was conducted at 30 °C. The assays were initiated by adding 50 µL of the soluble GPI-T heterotrimer enzyme and fluorescence emission was monitored over time.

3.5 Acknowledgment

I sincerely thank Dr Yug Varma and Ms Megan Ehrenwerth for providing plasmids and Dr Sandamali Ekanayaka for teaching me the *in vitro* assay.

CHAPTER 4

EFFECT OF GPI-T CORE SUBUNIT OVEREXPRESSION ON TRANSAMIDASE ACTIVITY *IN VIVO*

4.1 Introduction

The overexpression of different GPI-T subunits and the upregulation of certain GPI anchored proteins (e.g. urokinase plasminogen activated receptor; (uPAR),[133] mesothelin, folate receptor alpha, and testisin) in various cancers make GPI-T a target for chemotherapies.[103, 126] In 2008, the Trink group reported a profile of the expression patterns for the human GPI-T subunits, PIG-K (Gpi8), GPAA1 (Gaa1), PIG-S (Gpi17), PIG-T (Gpi16), PIG-U (Gab1) (with their corresponding yeast names in parenthesis) in 19 different cancers.[110,187] All five subunits of GPI-T appear to play a role in different types of cancer propagation.[223] However, the catalytic subunit, Gpi8, is the only subunit that is frequently downregulated in certain cancers. In this chapter, we describe the use of an *in vivo* assay in yeast to assess the contribution of each GPI-T subunit towards GPI transamidase activity.[66] This approach is allowing us to develop yeast as a cancer model system to understand how changes in GPI-T subunit expression levels impact the presentation of GPI-anchored proteins on the cell surface.[224-230]

We used an *in vivo* invertase assay that had been previously developed in our lab,[66] to quantify changes in cell surface expression of GPI-anchored invertase in cell lines that were overexpressing Gpi8, Gpi16, or Gaa1. Different levels of GPI-T activity were observed based on the subunit that was overexpressed and the identity of the C-terminal signal sequence appended onto

invertase. Three signal sequences were examined based on the yeast yapsin 2 protease (Y21), the campath-1 antigen (CA25) and UPAR (UP30). When Gpi8 was overexpressed**.**

4.2 Results

4.2.1 Invertase assay development

Invertase is commonly used as a reporter assay because it hydrolyzes sucrose to fructose and glucose and the glucose produced can be measured using an enzyme coupled colorimetric assay.[231]

Dr. Rachel Morrisette (an alumna of our lab) previously developed three Invertase variants that carry different *C*-terminal GPI-T signal sequences on them, each with a flag tag for immunoblotting (Figure 4.1 (a)).[66] The signal sequences we used were from the following proteins: *S. cerevisiae* Yapsin 2 protease (Y21), human campath-1 antigen (CA25) and human urokinase-type plasminogen-activated receptor (UP30). The plasmids coding these variants were transformed into an invertase knockout strain (*SUC2*-).[66,209] In wild-type strains, endogenous invertase is highly secreted as a soluble cytoplasmic protein in yeast. When invertase is fused with GPI signal sequences and expressed in the *SUC2*- strain, GPI anchored invertase is translocated to the outer surface of the yeast cell membrane (Figure 4.2). The amount of cell surface invertase can be measured using a standard glucose assay.[231] Importantly, this assay is

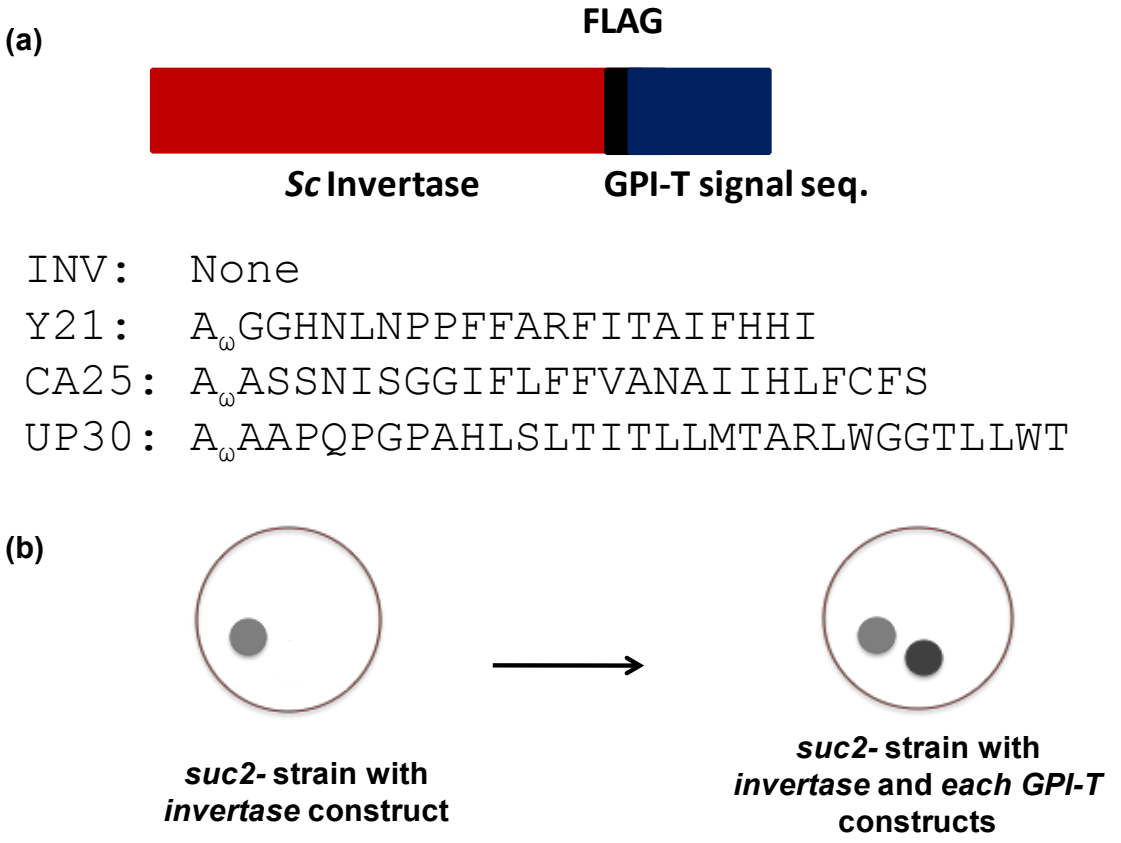

Figure 4.1: Invertase variants were constructed with three different GPI-T signal sequences. (a) Arrangement of invertase variants used herein. Top panel: cartoon representation of each construct. *S. cerevisiae* invertase was modified with a FLAG tag followed by different *C*-terminal GPI-T signal sequences. Bottom: the sequences used were from the *S. cerevisiae* Yapsin 2 protease (Y21), the human campath-1 antigen (CA25) and human UPAR (UP30). (b) The *SUC2*- strain was transformed with an invertase construct (right) and a plasmid coding for overexpression of one GPI-T subunit (left).

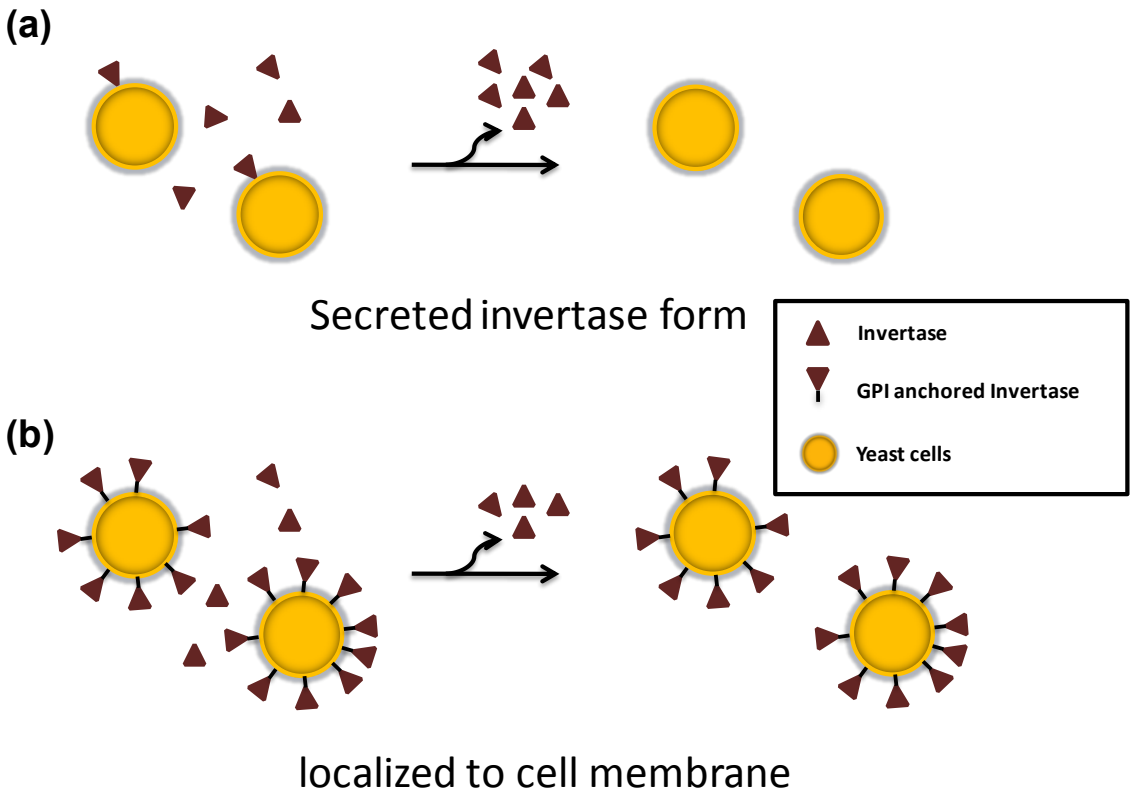

Figure 4.2: GPI anchored invertase localized to the outer cell membrane through its GPI anchor. (a) Invertase constructed without GPI signal sequence secreted out in yeast cells. When the cells were washed Invertase can be removed from the cells. (b) GPI anchored Invertase is localized in the cell membrane. When washed, Invertase that are not attached with the GPI anchor washed away leaving GPI anchored Invertase onto the cell membrane.

conducted on live cells simply by adding sucrose and then measuring glucose production.

4.2.2 The effect of endogenous expression of GPI-T on transamidase activity.

We first recapitulated our previous results using this assay and endogenous levels of each GPI-T subunit.[66,209] The Y21 *C*-terminal signal sequence yielded the highest levels of GPI-anchored invertase on the surface of cells. The activity of the UP30 and CA25 GPI-T signal sequences were normalized to that of Y21 (Figure 4.3). As we've previously reported, the two human GPI-T signal sequences (UP30 and CA25) are less effective as substrates for GPI-T. These results suggest species specificity, with yeast GPI-T favoring *C*-terminal signal sequences from yeast proteins over those from human proteins. However, this dataset is too small to draw such a conclusion with any certainty.

4.2.3 Effect of $Gpi8_{1-441}$ overexpression on GPI-T activity

The full-length $Gpi8_{1-414}$ gene was amplified by PCR with AttB sites included within the primers (Appendix C, Table C.1). The product was incorporated into the destination vector pAG414-GAL-Trp using Gateway cloning technology. This plasmid appended an HA tag onto the *C*-terminus of Gpi8 that was useful for immunoblotting purposes. This plasmid was transformed into the three *SUC2*- strains that were carrying the different invertase variants. Gpi8 was overexpressed by the induction of galactose for 12 hours and the harvested cells

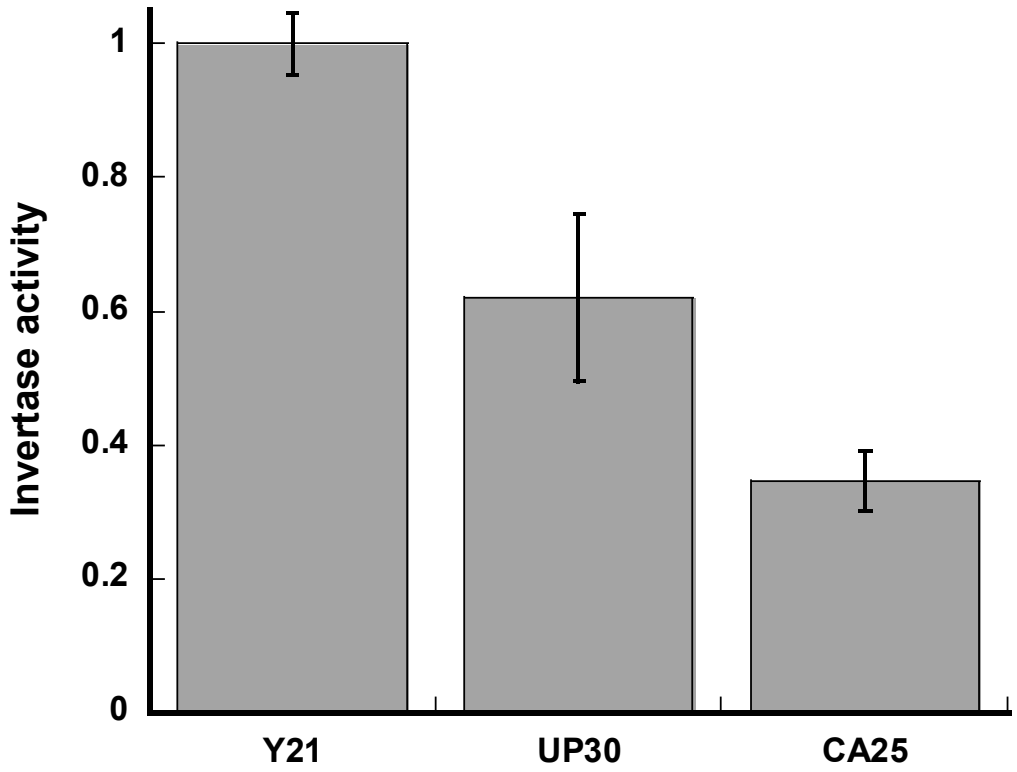

Figure 4.3: Y21 shows highest GPI-T activity when GPI-T is expressed in endogenous levels. Bar graph representing the GPI-T activity at endogenous levels of GPI-T expression. Y21 shows the highest GPI-T activity. UP30 and CA25 are normalized to that of Y21. Both CA25 and UP30 are weaker substrates for GPI-T. Raw data are shown in the Appendix C, Figure C.8.

were assayed immediately for invertase on their cell surface (see materials and methods).

Overexpression of $Gpi8_{1-414}$ showed some interesting results (Figure 4.4). The amount of invertase presented on the extracellular plasma membrane was quantified for each of our three signal sequences under endogenous levels (no overexpression) and then under conditions where Gpi8 was overexpressed. Results were normalized against the endogenous levels for each signal sequence in Figure 4.4 (a) and only against the Y21 levels in Figure 4.4 (b). Overexpression of Gpi8 had no effect on invertase activity with the constructs containing either the Y21 or the UP30 GPI-T signal sequence. In contrast, overexpression of Gpi8 doubled the amount of GPI anchored invertase when the CA25 GPI-T signal sequence was used. Without Gpi8 overexpression, the CA25 signal sequence was the poorest of the three tested herein. With Gpi8 overexpression, the amount of GPI anchored invertase produced with the CA25 signal sequence rose to levels equivalent to those observed with the UP30 signal sequence.

We designed our original invertase construct so that, once modified, the GPI anchored invertase would be the same no matter what signal sequence was used. Consequently, the amount of invertase presented on the cell surface is directly correlated to the ability of GPI-T to recognize and process each signal sequence as a substrate. We had not anticipated the possibility overexpression of one subunit would show signal sequence dependent changes on GPI-T activity. Nevertheless, the results in Figure 4.4 clearly show overexpression of

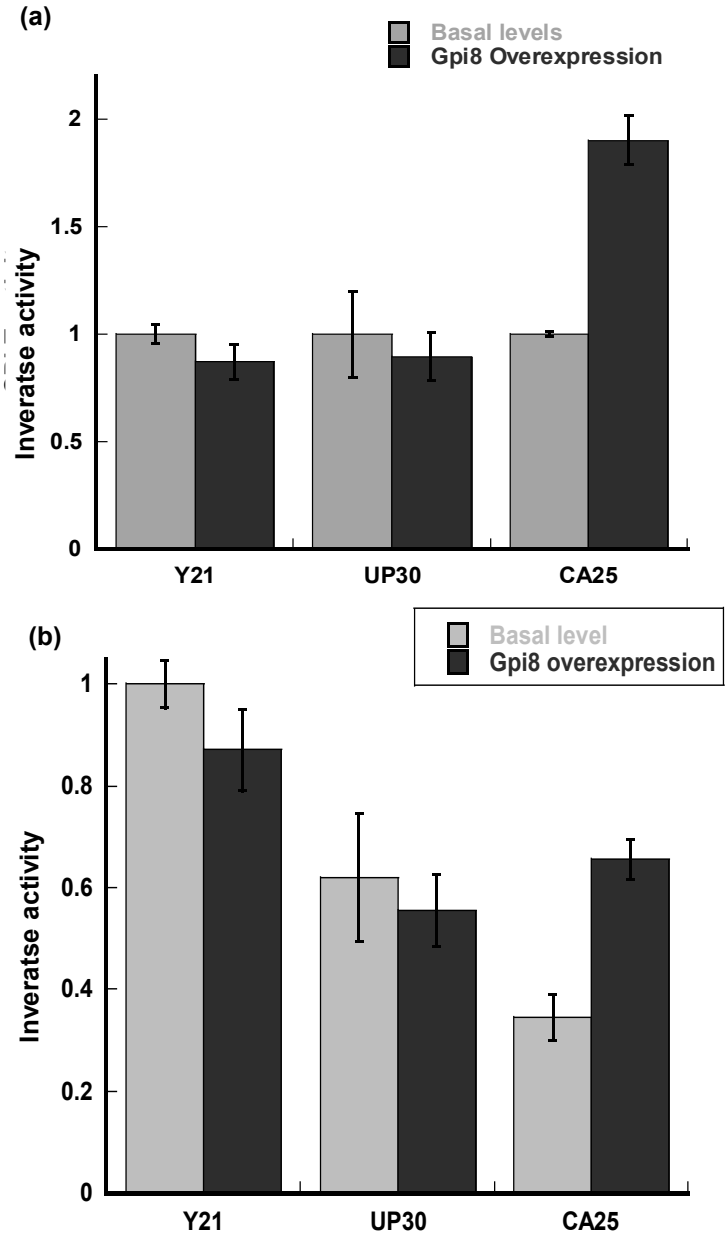

Figure 4.4: Overexpression of Gpi8 causes an increase in GPI anchoring of invertase with the CA25 signal sequence specifically. (a) GPI-T anchoring of invertase normalized to basal level expression levels for each signal sequence. (b) GPI-T anchoring of invertase normalized specifically to Y21 basal levels. Raw data are shown in the Appendix C, Figure C.9.

Gpi8 specifically enhances GPI-T activity when the CA25 signal sequence is present. These results suggest that Gpi8 recognizes at least part of the C-terminal signal sequence, a scenario that has not previously been considered to our knowledge.

4.2.4 The effect of $Gpi16_{1-610}$ overexpression on GPI-T activity.

As described above for Gpi8, the full length Gpi16 subunit of GPI-T was also overexpressed and the impact of this overexpression was assessed by measuring changes in the amount of GPI anchored invertase present on the cell surface (Figure 4.5). Compared to cells expressing endogenous levels of the GPI-T subunits, the overexpression of Gpi16 diminished the amount of GPI anchored invertase presented on the cell surface with all three GPI-T signal sequences. Invertase levels dropped by about 30% when the Y21 signal sequence was used and by about 60% when either the UP30 or the CA25 signal sequence was used.

The role of Gpi16 in GPI-T is not known although it has been proposed that this subunit enhances the stability of the complex.[232] Here we demonstrate that excess Gpi16 diminishes the catalytic competence of GPI-T, perhaps contradicting this stability hypothesis. In Chapter 3 of this dissertation, we showed that the soluble domain of Gpi16 forms stable dimeric complexes with Gpi8 and with Gaa1. Presumably excess Gpi16 leads to saturation of these dimeric complexes (e.g. all Gpi8 is bound to Gpi16) leaving extra Gpi16 to either bind to Gaa1 and prevent trimer complex formation or to interact with other proteins in the cell, disrupting normal cell function. The latter scenario is not unprecedented.

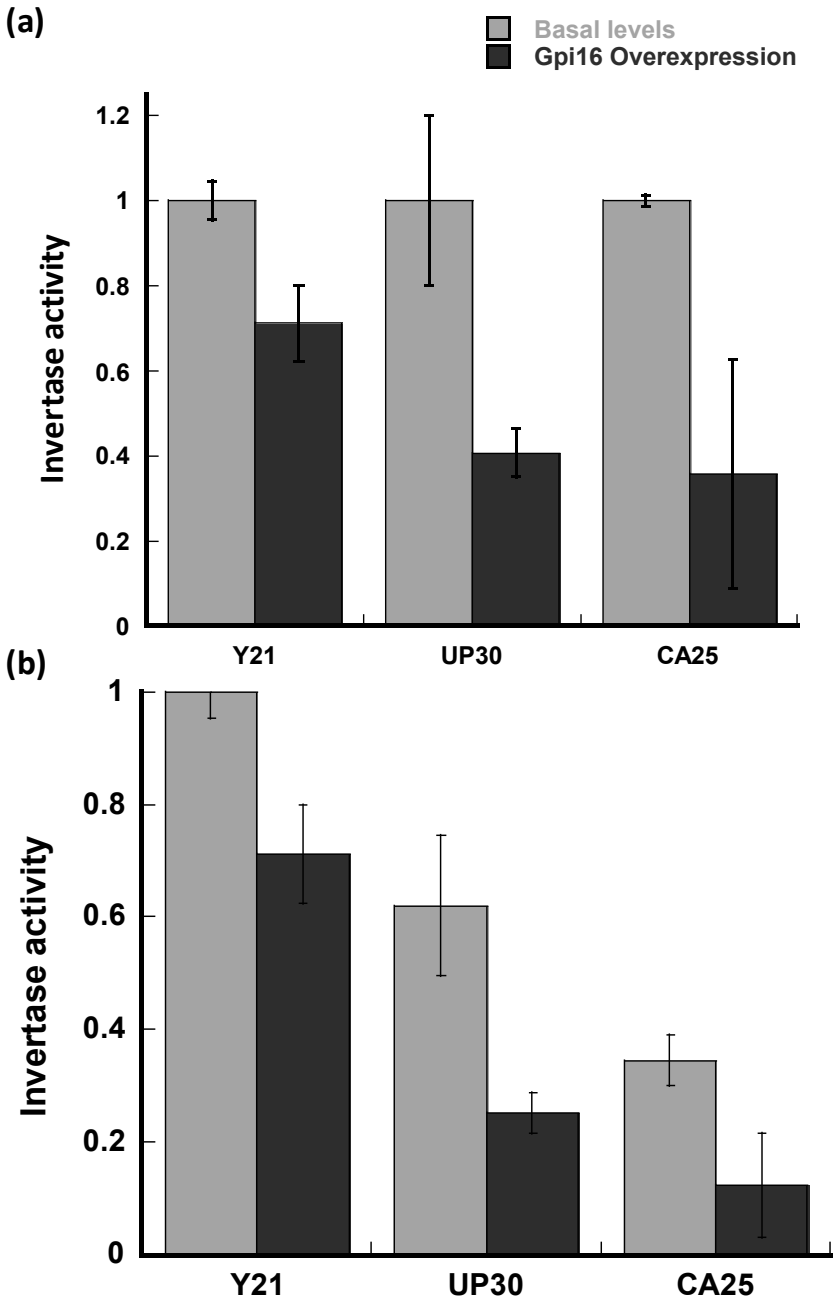

Figure 4.5: Gpi16 overexpression reduces the cell surface expression of GPI anchored invertase. (a) GPI-T anchoring of invertase normalized to basal level expression levels for each signal sequence. (b) GPI-T anchoring of invertase normalized specifically to Y21 basal levels. Raw data are shown in the Appendix C, Figure C.10.

In humans, Gpi16 is known to activate several different signal transduction pathways (see Figure 1.9).

4.2.5 Effect of $Gaa1_{1-614}$ overexpression on GPI-T activity.

Similar to Gpi16, Gaa1 overexpression leads to reduced activity overall In this case, the impact of individual signal sequences was more varied (Figure 4.6). A reduction of approximately 45% was observed with the Y21 signal sequence, 65% with the UP30 signal sequence, and 80% with the CA25 signal sequence. Similar arguments as those proposed for the impact of Gpi16 overexpression can be made for Gaa1 as well.

4.3 Discussion

Using the invertase assay developed in our lab, we were able to quantitatively examine the impact of overexpression of the three core GPI-T subunits on GPI anchoring *in vivo*. Overexpression of each full-length GPI-T subunit caused altered levels of GPI anchored invertase that were dependent on the C-terminal GPI-T signal sequence presented in each construct. The data presented in Figures 4.4 – 4.6 can be further analyzed in a number of different ways. Figure 4.7 shows a comparison of these data organized by overexpressed subunit and Figure 4.8 shows these same data rearranged by signal sequence so that the impact of each subunit on a specific signal sequence can be easily observed.

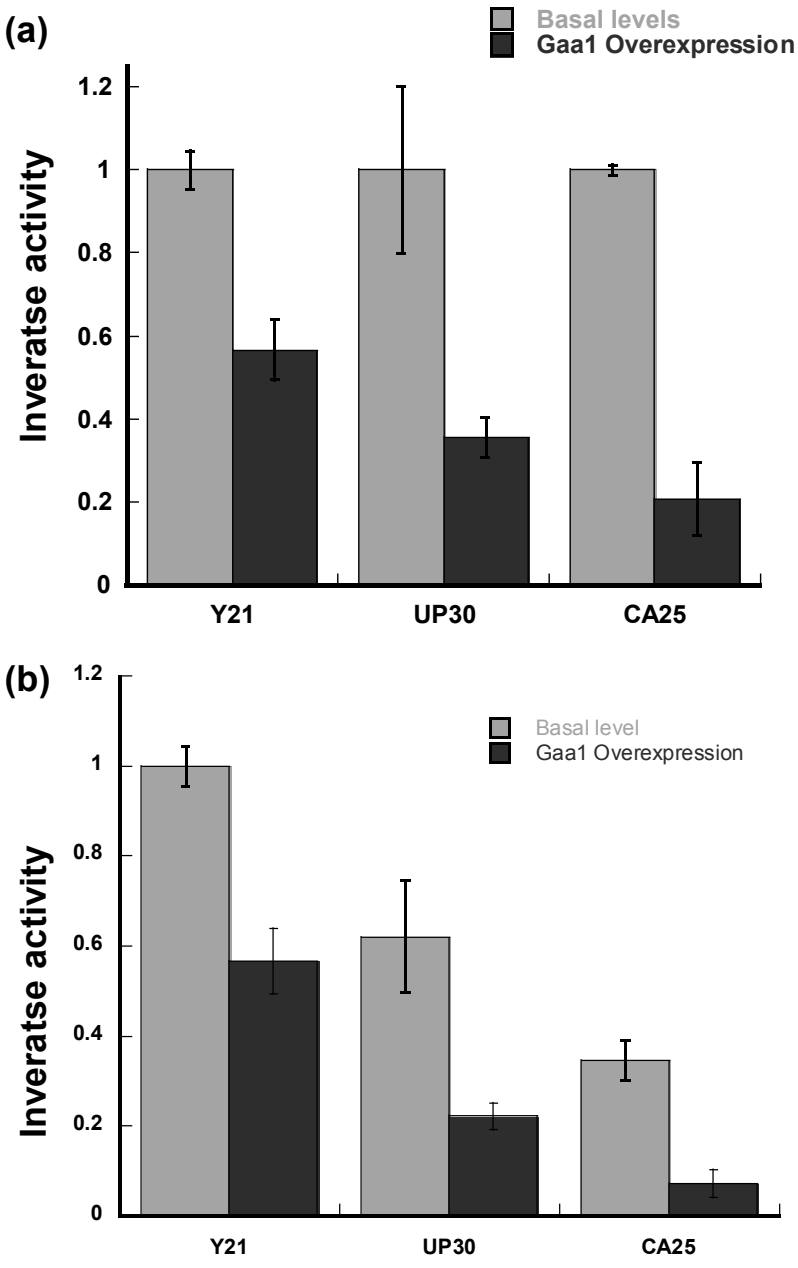

Figure 4.6: Gaa1 overexpression reduces the cell surface expression of GPI anchored invertase. (a) GPI-T anchoring of invertase normalized to basal level expression levels for each signal sequence. (b) GPI-T anchoring of invertase normalized specifically to Y21 basal levels. Raw data are shown in the Appendix C, Figure C.11.

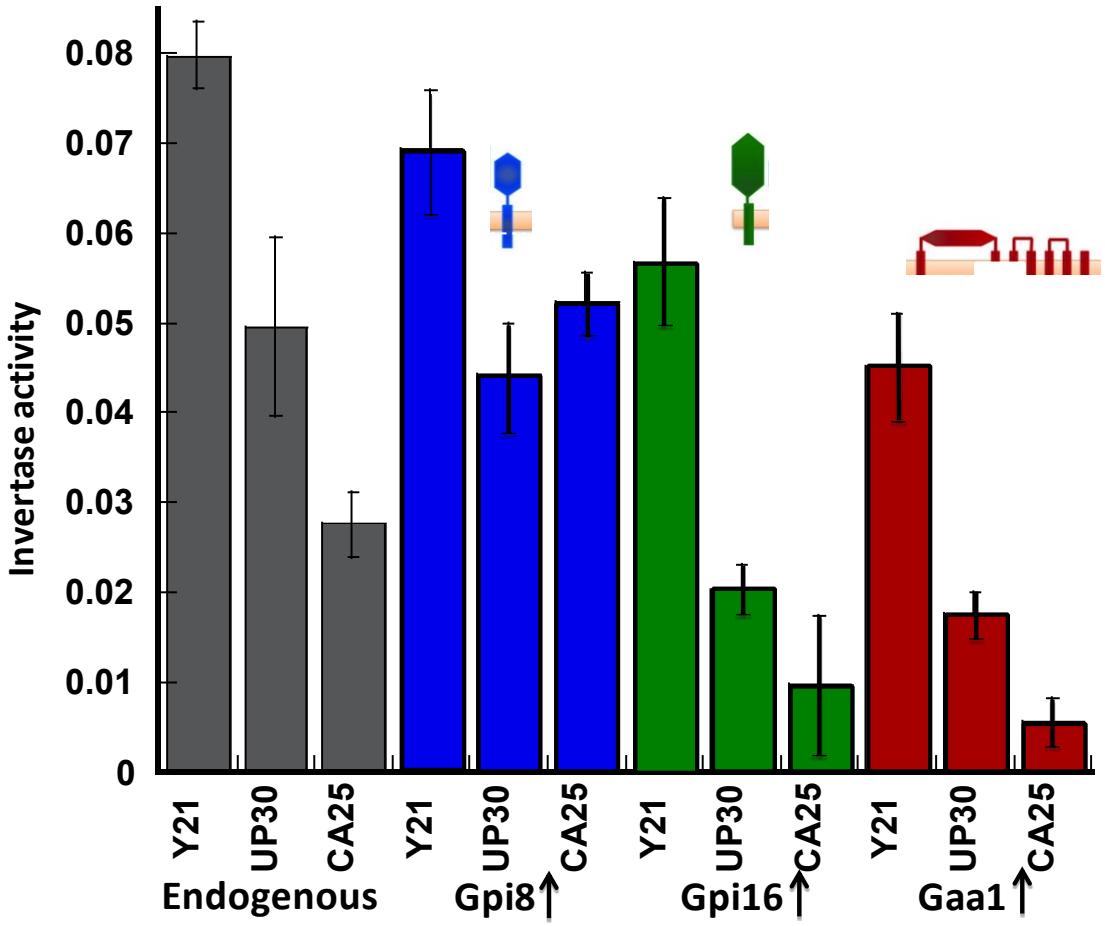

Figure 4.7: Comparison of overall GPI-T activity on single subunit overexpression. GPI-T activity was measured for basal, Gpi8, Gpi16 and Gaa1 expression. Y21 shows the highest activity on all Invertase variants. UP30 and CA25 have lower activity compared to Y21. Color coded bars represent each subunit overexpression.

The Y21 signal sequence always led to the highest levels of GPI anchored invertase. Overexpression of Gpi8 and Gpi16 had only nominal effects on GPI anchoring of invertase with either the Y21 or UP30 signal sequences (compared to endogenous levels with these signal sequences). In contrast, overexpression of Gaa1 caused a notable reduction in the amount of GPI anchored invertase presented on the cell surface.

Like the Y21 signal sequence, overexpression of Gpi8 had little effect on the amount of GPI anchored invertase present on the cell surface when the UP30 signal sequence was used. In contrast, this signal sequence was sensitive to overexpression of both Gpi16 and Gaa1, upon which the extent of GPI anchoring of invertase was diminished.

Finally, the CA25 signal sequence was sensitive to overexpression of all three GPI-T subunits. Unexpectedly, Gpi8 overexpression doubled the efficacy of this weak signal sequence; however overexpression of either Gpi16 or Gaa1 reduced anchoring of invertase with this signal sequence.

Overexpression of GPI-T subunits occurs to varying extents in different types of cancers and between patients. The only subunit that is ever underexpressed in cancer is Gpi8, the catalytic subunit of GPI-T. Here we show the first correlations between subunit overexpression and GPI-T activity. It is possible that subunit overepression can lead to tumorigenesis by altering signal transduction pathways.

The connection between subunit overexpression and increases in tumor growth could arise from one of three mechanisms. First, overexpression of a

single could lead to efficient complex assembly, thereby increasing the overall activity of GPI-T. Alternatively, subunit overexpression could actually decrease GPI-T complex assembly by oversaturating dimeric subunit intermediates. Finally, overexpression could lead to GPI-T subunits that are no in complexes with their normal protein partners and are therefore free to participate in other signal transduction pathways (e.g. uPAR in JAKS/STAT pathway).[187] Our results with Gpi16 and Gaa1 clearly favor one of the latter two scenarios because we see a drop in GPI-T activity. Future efforts will be directed towards examining the distribution of these overexpressed subunits *in vivo* to determine whether or not they are completely free of GPI-T or in complexes with specific GPI-T subunits.

4.4 Materials and methods

4.4.1 Plasmid construction

Each GPI-T plasmid was constructed similarly using Gateway cloning technology. Each gene was amplified using gene specific primers flanking attB overhangs. (These primers are listed in Appendix C, Table C.1) Each gene product was inserted into the pDONR221 vector (Invitrogen) following the manufacturer's instructions. The resulting donor vector was used to transfer the genes into then with the destination vector, pAG414-Trp-GAL (Addgene) according to Invitrogen's protocol for an LR reaction. The inserts were sequenced prior to use. Each was transformed into our *SUC2*- cell line using standard LiAc transformation protocols (Invitrogen, pYES-DEST52 Gateway vector manual).

4.4.2 *In vivo* Invertase assay

For each assay, 5 mL cell cultures were used. Cells were grown at 30 °C with 1% fructose (for *SUC2*- cells only with invertase plasmids), or with both 1% fructose and 1% galactose (for SUC2- cells with both the invertase plasmid and a plasmid for subunit overexpression) in Sc-Ura or Sc-Ura-Trp media, respectively. Cultures were grown for 12 hours and then immediately assayed. The OD_{600} was measured for each cell culture, and a volume equivalent to 1.0 absorbance unit was used for each assay. Cells were washed three times with pre-chilled autoclaved water. To the cells 40 µL of a 1 M NaOAc (pH 4.9) solution was added and was diluted to 400 µL with autoclaved water. This solution was incubated at 30 °C for 30 min. A separate 0.5 M sucrose (in 1 M NaOAc, pH 4.9) sample was also incubated at 30 ºC prior to use. Next, sucrose (100 µL, 0.5 M solution) was added to each cell suspension. Time points (50 µL each) were removed at 1, 2, 3, 4, 5, 8, 11 and 16 min and quenched immediately into 75 µL of 0.2 M K_2HPO_4 (pH 10.0) followed by boiling for 3 min. The amount of glucose present in each time point was measures as previously described. [66,209]

4.5 Acknowledgement

I sincerely thank Dr Rachel Morrissette for providing me *SUC2*- strains with invertase variants.

CHAPTER 5

CONCLUSIONS AND FUTURE DIRECTIONS

GPI membrane anchoring of proteins is an important post-translational modification for eukaryotes. This process and the enzyme that is responsible for this modification, GPI-T, are poorly understood, particularly relative to their roles in human cancer. GPI-T contains 5 known subunits: Gpi8, Gpi16, Gaa1, Gab1 and Gpi17. Even after 20 years of study, our understanding of the structure and function of these subunits remain in its infancy. Therefore, in this dissertation, we set out to look at the structure, stoichiometry, and contributions of these three core subunits towards GPI-T activity to better understand this enzyme.

Chapters 2, 3 and Appendix B describe our efforts to structurally characterize the soluble domains of the three core GPI-T subunits ($Gpi8_{23-306}$, $Gpi16_{20-551}$ and $Gaa1_{50-343}$). These three subunits were chosen for study herein because they are found in all eukarya (Gab1 and Gpi17 are missing in trypanosomes)[74] and they can be isolated as a complex from *S. cerevisiae*. We focused our studies on the soluble domains of these subunits in order to simplify their purification and overexpression.

There is precedent for working with soluble domains in isolation and this strategy is a common method for characterizing complicated membrane-associated proteins.[233,234,235] For example, the toll/interleukin-1 receptor (TIR) is a membrane protein that resides on the plasma membrane and plays an important role in inflammation and innate immune response. The crystal structure obtained from the soluble domain of the TIR10 receptor demonstrated that this receptor

assembles into a dimer, providing important insight into the function the full-length, membrane-associated protein.[236]

We evaluated the soluble domains of these core subunits to understand how they interact with each other and to reconstitute an active, soluble enzyme for future studies. This approach is powerful because it reduces the complexity of GPI-T. In addition, in trypanosomes, the catalytic subunit of GPI-T, Gpi8, is naturally a soluble protein without a TM domain, offering an interesting precedent for our approach.[81] However, we were mindful of the fact that removing the TM domains from each subunit could change their behavior *in vitro* in terms of oligomerization or activity.

The catalytic subunit, Gpi8, shares weak sequence similarity to caspase-1. Caspases are catalytically active as simple homodimers or as homodimers in complex with specific activating proteins.[20] Analogously, $Gpi8_{23\text{-}306}$ assembles into a mixture of homodimer and monomer (Chapter 2). These results suggested that the transmembrane domain of Gpi8 and/or other subunits are necessary for complete dimerization. This monomer/dimer $Gpi8_{23\text{-}306}$ mixture binds to peptide substrate but is catalytically inert, leading us to further hypothesize that either complete dimerization or the presence of one or more additional subunits is necessary for activity.[83] Consistently, our characterization of the trimeric assembly of $Gpi8_{23\text{-}306}$, $Gaa1_{50\text{-}343}$ and $Gpi16_{20\text{-}551}$ shows that is has proteolytic activity, demonstrating that the addition of Gaa1 and/or Gpi16 is sufficient to activate Gpi8, even in the absence of the native TM domains.

Also the results obtained from analyses of $Gpi8_{23-306}$ variants with mutations at N256 offer the first evidence that N23 might be glycosylated, even though it lies next to the *N*-terminal signal sequence. Moreover, elimination of *N*-linked glycosylation at N256 (via either mutagenesis or the Endo H treatment) had little effect on the oligomerization state of Gpi8 indicating that *N*-linked glycosylation is not critical for Gpi8 dimerization.

With $Gpi8_{23-306}$ as a homodimer, it is logical to hypothesize that the heterotrimer, containing all three core subunits, would also dimerize (to a dimer of the heterotrimer, in other words a heterohexamer) (Figure 5.1). In fact, the preliminary results presented in Appendix B are most consistent with the conclusion that the $Gpi8_{23-306}$:$Gaa1_{50-343}$ heterodimer is a dimer of dimers (a heterotrimer) offering additional support for this hypothesis. Thus, work in this dissertation argues that the three core subunits of GPI-T assemble into a dimer of trimers.

Data from Chapter 3 show that each pair of subunits assembles into heterodimeric complexes, offering the first direct evidence that all subunits are in contact with each other. Furthermore, all three subunits assemble into a heterotrimer that can be purified by tandem affinity purification. Using a FRET assay previously developed in our lab,[216] we have shown that the soluble heterotrimer (presumably containing two copies each of $Gpi8_{23-306}$, $Gpi16_{20-551}$ and $Gaa1_{50-343}$) is catalytically active but, surprisingly, its activity is not dependant on hydroxylamine. The most likely explanation for this activity is that truncation of GPI-T has disrupted the active site of Gpi8 in a way that is sufficient to convert

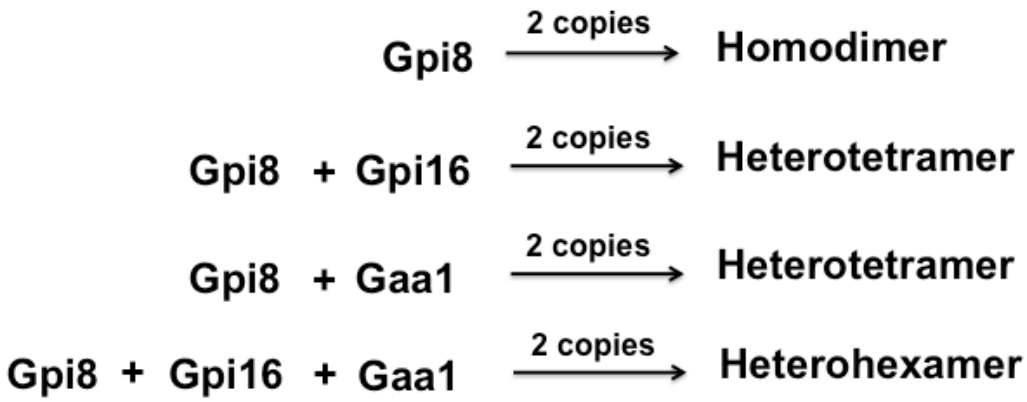

Figure 5.1: The expected stoichiometry for each of the complexes studied in this dissertation. The stoichiometry was predicted based on the observations that $Gpi8_{23\text{-}306}$ assembles as a mixture of monomer and homodimer and that $Gpi8_{23\text{-}306}$:$Gaa1_{50\text{-}343}$ is likely to exist as a dimer of dimers (heterotetramer).

this enzyme's normal transamidation activity into proteolytic activity. In fact, full-length GPI-T also has proteolytic activity.[92]

In the future, we would like to further characterize the stoichiometry of each subunit pair and of the heterotrimer as these experiments will allow us to map, at least partially, the 3D organization of GPI-T. Our lab will use SEC, native PAGE and mass spectrometry to examine these soluble subunit mixtures for the presence of heterotetramer and heterohexamer. We also hope to use covalent crosslinking coupled to mass spectrometry to map the interfaces between each subunit. This type of crosslinking approach, coupled to our Rosetta models for each subunit, will paint a picture of GPI-T's structure in the absence of any crystallographic information. As we increase our understanding of the structure of this enzyme, our ultimate goal will be to obtain a crystal structure of these three soluble domains in a complex.

It will also be important to use our FRET assay, peptide binding and crosslinking experiments to evaluate each subunit's contributions to GPI-T activity. The FRET assay developed in our lab will be used to determine which subunits are necessary for a functional GPI-T enzyme. Each subunit pair will be used to test for GPI-T activity, as we have reported for the heterotrimer in Chapter 3. The cleaved peptides product(s) will be analyzed using mass spectrometry to confirm that peptide cleavage occurred at the ω-site. Currently only the function of Gpi8 is known: this subunit contains the catalytic active site. And alone, the soluble domain of Gpi8 is inactive.[83] To understand which subunit is responsible for the recognition of the *C*-terminal signal sequence, our lab will

use peptides that contain a photoactivated crosslinker (e.g. benzoylphenylalanine or p-azidophenylalanine) and a tag for co-immunoprecipitation studies. The peptide will be incubated with the heterotrimer, and irradiated with UV light to induce crosslinking. The subunits that interact with the peptide can be immunoprecipitated using the tag on the peptide (e.g. a biotinylated residue) and analyzed using western blots. The different bands corresponding to each subunit will be excised and analyzed using mass spectrometry after treating with trypsin.

Chapter 4 and Appendix A of this dissertation describe the use of *in vivo* and *in vitro* assays developed in our lab to functionally characterize GPI-T. As in Appendix A, a FRET assay was used to examine GPI-T activity *in vitro*. This assay is the first reliable *in vitro,* quantitative assay developed for GPI-T.[216] Unfortunately we are still struggling to confirm the formation of the correct hydroxamate, indicating cleavage and modification at the ω-site residue, due to complications from the buffer system, such as the presence of digitonin. Once we confirm the *in vitro* assay, our lab will use small GPI anchor mimics that were synthesized by Dr. Franklin John,[29] a former member from our lab, as GPI anchor mimics to test activity. These GPI anchor mimics have structures that are more similar to the GPI anchor and are likely to be better substrates than hydroxylamine. Ultimately, our lab will use this assay to examine the impact of subunit overexpression on GPI-T activity, as an *in vitro* model for cancer.

Our lab has also developed an *in vivo* assay using invertase as a reporter enzyme.[66] In chapter 4, this assay was used to assess the impact of overexpression of each core subunit on GPI-T activity. Our data show two

unexpected results; first, that activity increases for Gpi8 overexpression specifically for the signal sequence based on the CD52 protein substrate; and secondly, GPI-T activity went down upon overexpression of either Gpi16 or Gaa1 independent of the signal sequence tested. These observations have led us to consider two possible mechanisms for subunit overexpression that could explain the connections between GPI-T and cancer (Figure 5.2): 1) catalytic subunit (Gpi8) overexpression is sequence dependent and increases GPI anchoring of some substrates that will specifically perturb signal transduction pathways; and 2) overexpression of Gpi16 and Gaa1 apparently leads to disruption of the GPI-T complex, possibly freeing one or more subunits to activate signaling cascades. In both cases, perturbations of signal transduction pathways would lead to tumor initiation and propagation. In the future, overexpression of the Gpi17 and Gab1 subunits will also be examined.

This *in vivo* assay needs to be expanded to include a broader array of GPI-T signal sequences. Our lab will use more GPI-T signal sequences from humans (e.g. Glypican 1, Prostatin, Cripto 1 etc.) and yeast (e.g. Yapsin 2, Phospholipase PLB1 etc.) to better understand how the nature of the substrate signal sequence and subunit overexpression are connected. Ultimately, it is important to establish this assay in human cells to more directly examine the relationship between subunit overexpression and cancer.

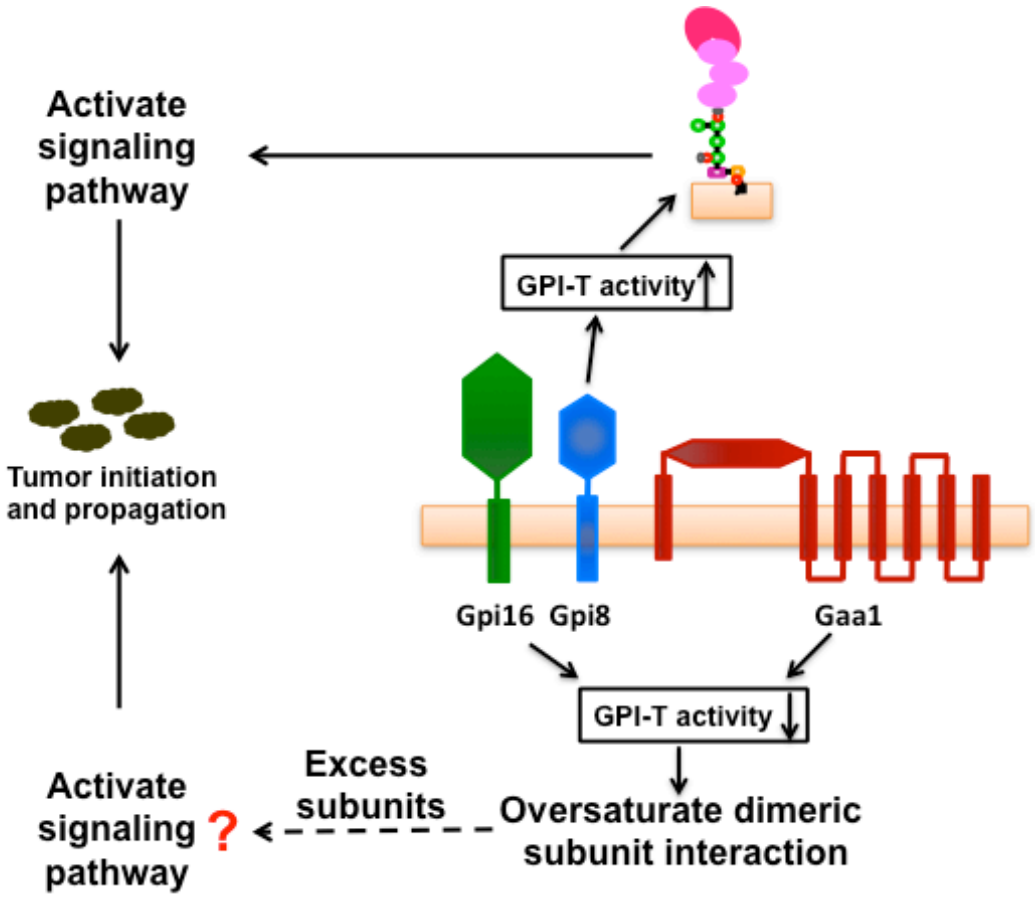

Figure 5.2: Possible mechanism for signal transduction perturbations based on our results. The overexpression of Gpi8, the catalytic subunit increases the cell presentation of some GPI anchored proteins that can perturbate signaling pathways (top). The overexpression of Gpi16 and Gaa1 reduces the cell presentation of GPI anchored proteins by reducing GPI-T activity. This bottom pathway might be due to the oversaturation of some subunit interactions leading to excess subunits participating in signal transduction. These pathways remain poorly understood.

The work in this dissertation takes an important step forward, providing new insights into GPI-T and new tools to better characterize this complicated and important enzyme. We are only looking at the tip of the iceberg; there is significant more work to be done.

APPENDIX A

GPI-T *IN VITRO* ASSAY PRODUCT CHARACTERIZATION

A.1 Introduction

The complexity of GPI-T has hindered a reliable quantitative assay that would allow researchers to analyze the kinetics of the protein. Even though there are many *in vivo* and *in vitro* experiments being developed to characterize GPI-T, the majority of them remain qualitative.[81,215,96,55] Placental alkaline phosphatase (preproPLAP) and its miniature version, prepromini PLAP have been used over the last few decades in this capacity.[55,54,56,237,238] The only *in vitro* quantitative assay reported to date is a fluorescence assay that uses a tetrapeptide containing the ω-3 to ω residues of a GPI-T substrate with an aminomethylcoumarin attached to the *C*-terminus of the ω amino acid.[81] Several limitations were evident in this assay that included long incubation times and the absence of the *C*-terminal signal sequences for GPI-T in the synthetic, tetrapeptide substrate. There is a significant need for better assays with more comprehensive substrates to completely understand the behavior of GPI-T.

Our lab has been developing a reliable assay base on fluorescence resonance energy transfer (FRET) that we expect not only to help us analyze GPI-T, but also to assess the contributions of individual substrates on GPI-T activity.[216] Here we describe the solid-phase synthesis of peptides that are based on a known substrate for GPI-T (CD52) and have been modified to contain a fluorophore (2-aminobenzoic acid) and a quencher (nitrotyrosine) flanking the ω-site amino acid (Figure 3.9, Chapter 3).[216] CD52 is one of the shortest known

substrate for GPI-T: this protein is only 37 amino acids long with its *C*-terminal signal sequence and once the signal sequence is cleaved the protein is only 12 amino acids in length.[217,64,218]

When this peptide is incubated with purified GPI-T from yeast with a GPI anchor mimic like hydroxylamine,[220] a time-dependent increase in fluorescence was observed. These experiments were conducted by Dr. Sandamali Ekanayaka (data not shown).[216] This fluorescence response was consistent with transamidation by GPI-T. In this appendix, synthesis of two peptide substrates for this GPI-T assay will be described. These peptides were based on CD52 and on a yeast substrate for GPI-T called Yapsin 2. Our efforts to confirm that transamidation had occurred by isolating the hydroxamate peptide product from this assay will be described. This project is ongoing and is therefore provided as an appendix.

A.2 Results

A.2.1 Synthesis of peptide substrates using solid phase peptide synthesis

A modified version of our CD52 substrate peptide was synthesized with a biotin tag added to the side chain of Lys3, the 3rd amino acid from the *N*-terminus (peptide 3). Compared to the peptide 2 (Chapter 3) that used to characterize GPI-T,[216] the only modification done onto peptide 3 was the addition of the biotin tag. This biotin was inserted to facilitate the evaluation of peptide products from our assay. Additionally, several modifications were introduced into this peptide

compared to its native form to avoid *N*-linked glycosylations (when using crude yeast lysates)[221] or complications that could arise from oxidations[222] similar to peptide 2 (Chapter 3) (Table A.1).

Yapsin 2 is a yeast aspartyl protease, and is a GPI-T substrate with a validated ω-site.[239] Yeast Yapsin 2 also known as Aspartic proteinase MKC7 with 596 aminoacids carrying a molecular weight of 64 kD. It has a *N*-terminal signal sequence (residues 1-22) that target the ER localization and a *C*-terminal signal sequence (residues 576-596) recognized and modified using GPI-T.[75] We have chosen 21 amino acid long *C*-terminal signal sequence of Yapsin 2 to create peptide 11 with additional five amino acid residues towards the *N*-terminus. We introduced the Abz, fluorophore to the Lys4, the 4th amino acid from the *N*-terminus and the 3-nitrotyrosine, quencher onto the 11th amino acid from the *N*-terminus. We have positioned the fluorophore and the quencher more closely compared to CD52 to increase the sensitivity of the assay. Also, the *N*-terminus of this peptide was acetylated to inhibit any additional modifications that could take place (Table A.1).

Both peptide substrates were synthesized by solid phase peptide synthesis using either a Prelude peptide synthesizer or by manual synthesis. Each substrate was cleaved from the resin, purified by HPLC and characterized by ESI-MS prior to applications to the study of GPI-T (See materials and methods).

Table A.1: The peptides synthesized compared with their native form. Red colored amino acids are the changes that's being done compared to the wild type sequence. Peptide 3 is designed to represent CD52 and peptide 11 was designed to represent Yapsin 2.

Peptide	*N*-terminal sequence	ω	GPI-T signal sequence
CD52	GQNDTSETSSP	S	ASSNISGGIFLFFVANAIIHLFCFS
Peptide 3	Abz-GQK(biotin)DTSEKSSP	S	ASKNY*SGGIFLFFVANAIIHLFHFS
Yapsin 2	STRKE	N	GGHNLNPPFFARFITAIFHHI
Peptide 11	(Acetylated)STRK(Abz)E	N	GGHNY*NPPFFARFITAIFHHI

A.2.2 Purification of GPI-T and *in vitro* assay for Yapsin2.

Professor Andreas Conzelmann kindly provided us with yeast strain FBY656. In this strain, the wild-type *gpi8* gene has been disrupted with a kanamycin cassette. Viability of the strain is supported by plasmid YCplac22, which contains a GST-tagged version of the *gpi8* gene. The GST was inserted into the gene such that it is encoded immediately after the *N*-terminal ER localization sequence and before the beginning of the soluble domain of Gpi8 such that the final expressed protein contains the GST sequence followed by $Gpi8_{23\text{-}441}$. GPI-T was purified by glutathione affinity purification according to the protocol of Fraering et al.[216,18] Affinity purification of GST-$Gpi8_{1\text{-}411}$ was confirmed by SDS-PAGE and anti-GST blot, which visualized the presence of $Gpi8_{1\text{-}411}$-GST (Figure A.1). Insufficient protein was obtained to confirm the co-purification of Gpi16 and Gaa1 (in contrast to the results of Fraering et. al.).[18]

Dr. Ekanayaka's assay development and optimization experiments were conducted using our synthetic CD52 peptide substrate (peptide 2). Because this peptide is based on a human substrate for GPI-T, we set out to develop a substrate based on the yapsin protease, a substrate for S. cerevisiae GPI-T.[216,75] Our expectations were that this peptide would be a stronger substrate for GPI-T. Therefor, we carried out the *in vitro* assay with varying peptide concentrations of peptide 11 (Figure A.2 (a)). Data was normalized to peptide 2, representing CD52 (Figure A.2 (b)). The red line indicates the background fluorescence for the assay done without any enzyme. However, even at 5X the concentration of peptide 2 (the CD52 substrate), activity with our Yapsin 2

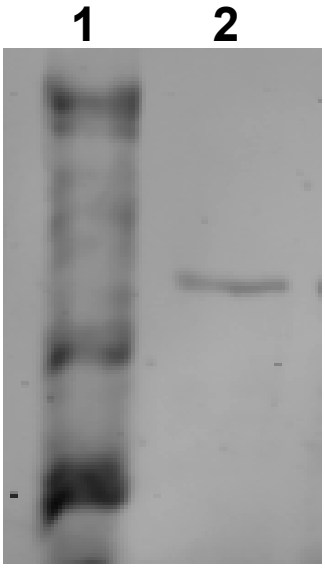

Figure A.1: Purification of GST-Gpi8$_{23-411}$. An anti-GST blot to confirm the presence of GST-Gpi8$_{23-411}$. Lane 1: Molecular weight markers, Lane 2: Purified GST-Gpi8$_{23-411}$, this construct has a calculated molecular weight of 72 kD.

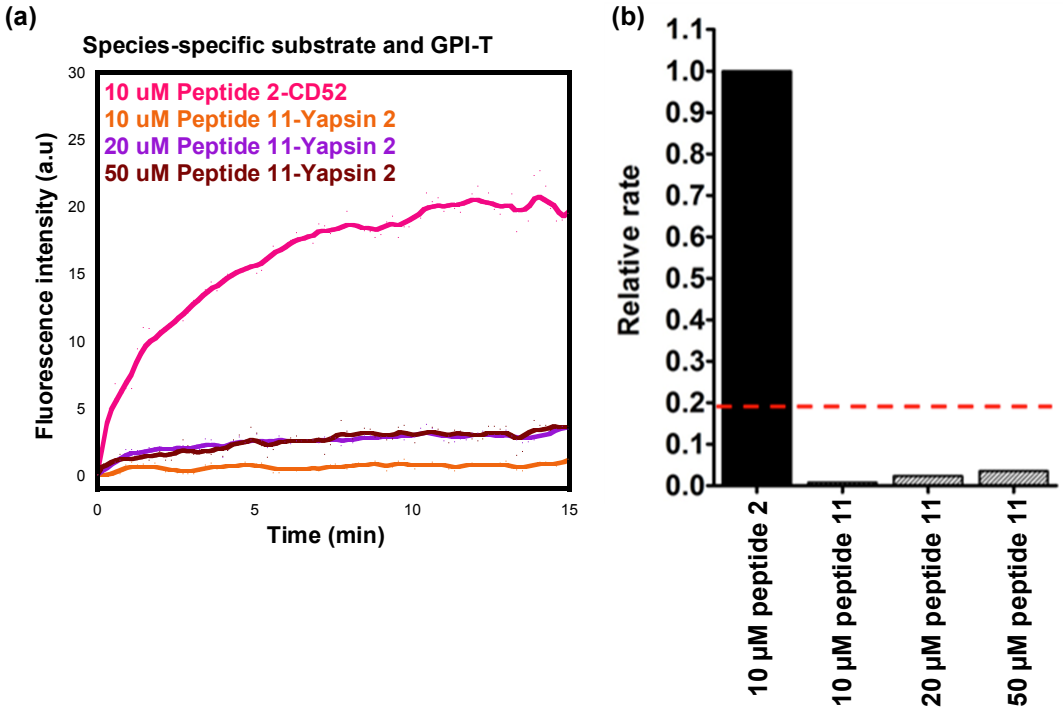

Figure A.2: The synthetic Yapsin 2 peptide is not a good substrate for yeast GPI-T. (a) Initial rates to compare the GPI-T activity on peptide 2 (CD52) and peptide 11 (Yapsin 2) peptide substrates with different concentrations.(b)The bar graph shows a comparison of the initial rates obtained from our assay using our synthetic peptide 2 and peptide 11 peptides. Our peptide11, did not show activity even at 5X higher concentrations than our typical CD52 assay. The red line indicates the background fluorescence, the assay conducted without GPI-T (No enzyme control).

peptide (peptide 11) was not observed (Figure A.2). (Figure courtesy of Dr. Sandamali Ekanayaka).[216]

A.2.3 Analysis of the peptide products from our GPI-T assay

We used peptide 3 (biotynilated version of CD52) (Table A.1) to facilitate characterization of the peptide products of our GPI-T assay. After an extended incubation of this peptide with purified GPI-T in the presence of hydroxylamine, streptavidin purification was carried out to purify all biotin tagged peptides. Different peptides were separated by high performance liquid chromatography (HPLC) and then analyzed by ESI-MS. The predicted ω-site of CD52 is Ser12. Therefore we expected to isolate a peptide containing the 12-*N*-terminal amino acids, with the *C*-terminal serine modified with hydroxylamine to the hydroxamate by GPI-T. This putative product has a calculated exact mass of 1610 g/mol. The calculated masses for this peptide as well as other possible biotynilated peptides are summarized in Table A.2.

However, only masses that roughly matches to the hydroxamates of 4^{th} , 7^{th} and 8^{th} amino acids from the *N*-terminus were seen (807, 1124 and 1253 D). Also we were able to observe two prominent peaks that we initially resembles as the hydroxyl product of 8^{th} amino acid (1250 D) and it's hydroxamate product (1237 D) (Figure A.3). We were surprised to observe multiple cleavage sites and the predicted ω site was not cleaved. Further analysis of these products confirmed that the peaks corresponding to 8^{th} amino acid are due to the presence of digitonin. We used digitonin as a detergent, which will solubilize

Table A.2: The calculated molecular weights for hydroxamate and hydroxyl products. Red colored amino acids are the changes that's being done compared to the wild type sequence. Molecular weights for both hydroxyl and hydroxamate products were calculated for assuming cleavage takes place on the 4th, 7th, 8th or on the 12th amino acid from the *N*-terminus. All the MW are in g/mol.

Peptide product	Sequence	Calculated MW of the hydroamate product	Calculated MW of the hydroxyl product
12 mer	Abz-GQK(biotin)DTSEKSSPS	1611	1624
8 mer	Abz-GQK(biotin)DTSEK	1237	1250
7 mer	Abz-GQK(biotin)DTSE	1124	1137
4 mer	Abz-GQK(biotin)D	807	820

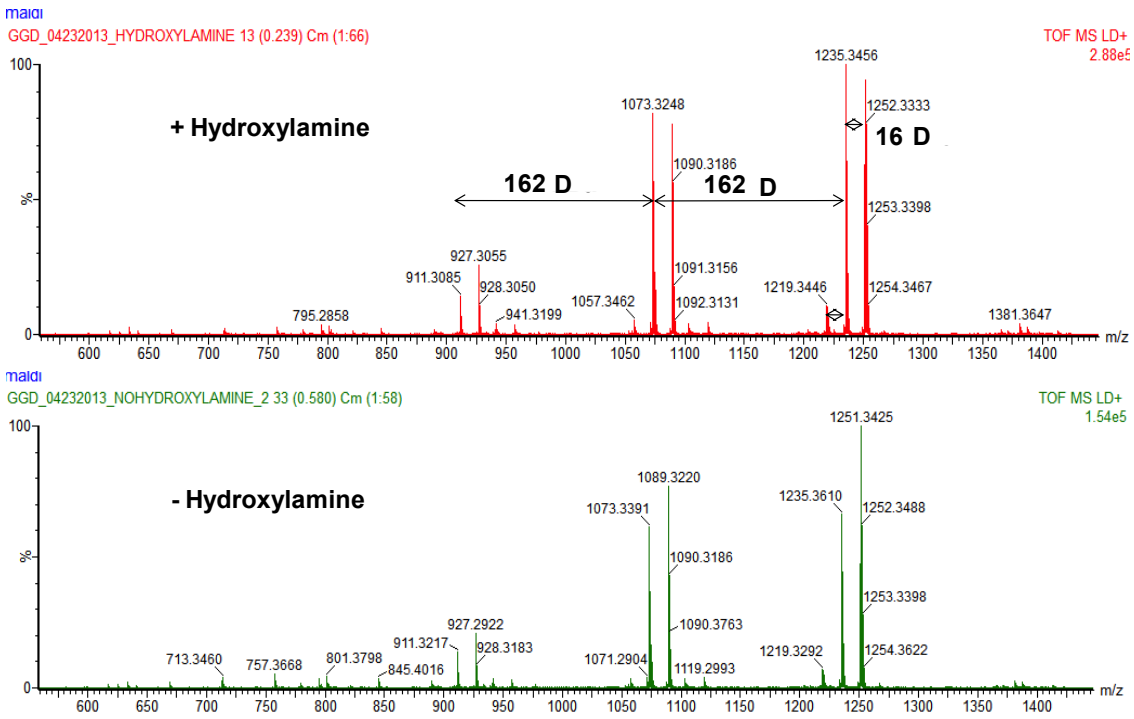

Figure A.3: Mass spectra of assay product analysis. Two mass spectra are shown which were acquired from assays conducted in the presence (top) and absence (bottom) of hydroxylamine.

GPI-T, the transmembrane protein complex. Digitonin is a glycoside with a molecular weight of 1229 g/mol. When digitonin is present in a sample, mass spectrum gives a well-known[240,241] pattern with a difference of 162 g/mol between peaks (Figure A.3). This difference corresponds to the loss of one glucose molecule.

Next, we introduced a water:chloroform:$MgCl_2$ extraction step into our assay workup (see materials and methods) to more completely extract the digitonin from our samples prior to analysis. After extraction, both the aqueous and organic layers were analyzed in a peptide gel (Figure A.4) and by thin layer chromatography (Figure A.5) to verify that peptides partitioned into the aqueous layer with the digitonin in the organic layer. In this case, we used our biotinylated peptide (see Table A.1) so that partitioning could be visualized by Western blot after separation in a 20% tris-tricine peptide gel (Figure A.4). As hoped, the peptide was separated into the aqueous layer. A comparison of lanes 1 and 3 in Figure A.4 reveals the presence of a shorter peptide in lane 1 that is not present in lane 4. While it is clear that cleavage of the parent peptide was poor and incomplete, this smaller peptide may represent the cleavage product from our assay. In fact, this biotinylated CD52 peptide appears to be a poor substrate for GPI-T, as judged by the low fluorescence increase observed over time in our standard assay.

Thin layer chromatography in hexane:ethylacetate with a carbohydrate specific stain was used to check for the presence of digitonin in the aqueous and organic layers after extraction. Digitonin and mannitol were tested as controls as

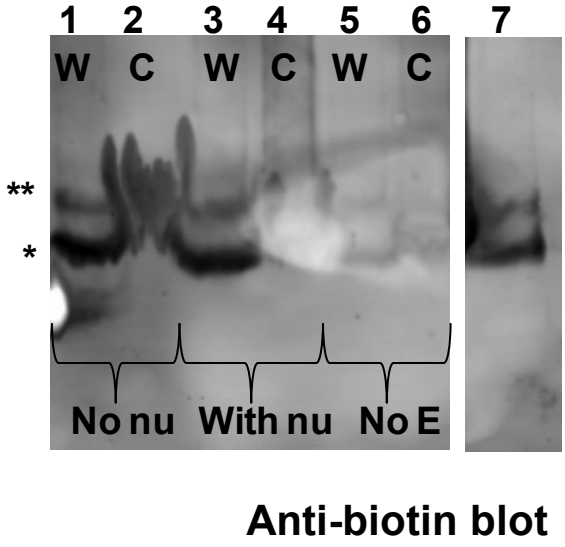

Figure A.4: Analysis of extraction step to separate our peptide substrate from digitonin. A 20% tris-tricine peptide gel was run to analyze the aqueous (lanes 1, 3, and 5) and organic (lanes 2, 4, and 6) layers from this extraction. The samples in lanes 1 and 2 are from an assay conducted with hydroxylamine; Lanes 3 and 4 are from an assay in the absence of hydroxylamine. Lanes 5 and 6 are from a mock assay without GPI-T. Lane 7 contains the biotinylated CD52 peptide as a positive control. *Indicates the band that corresponds to our CD52 substrate. **Indicates a new band that may represent the product peptide from our assay.

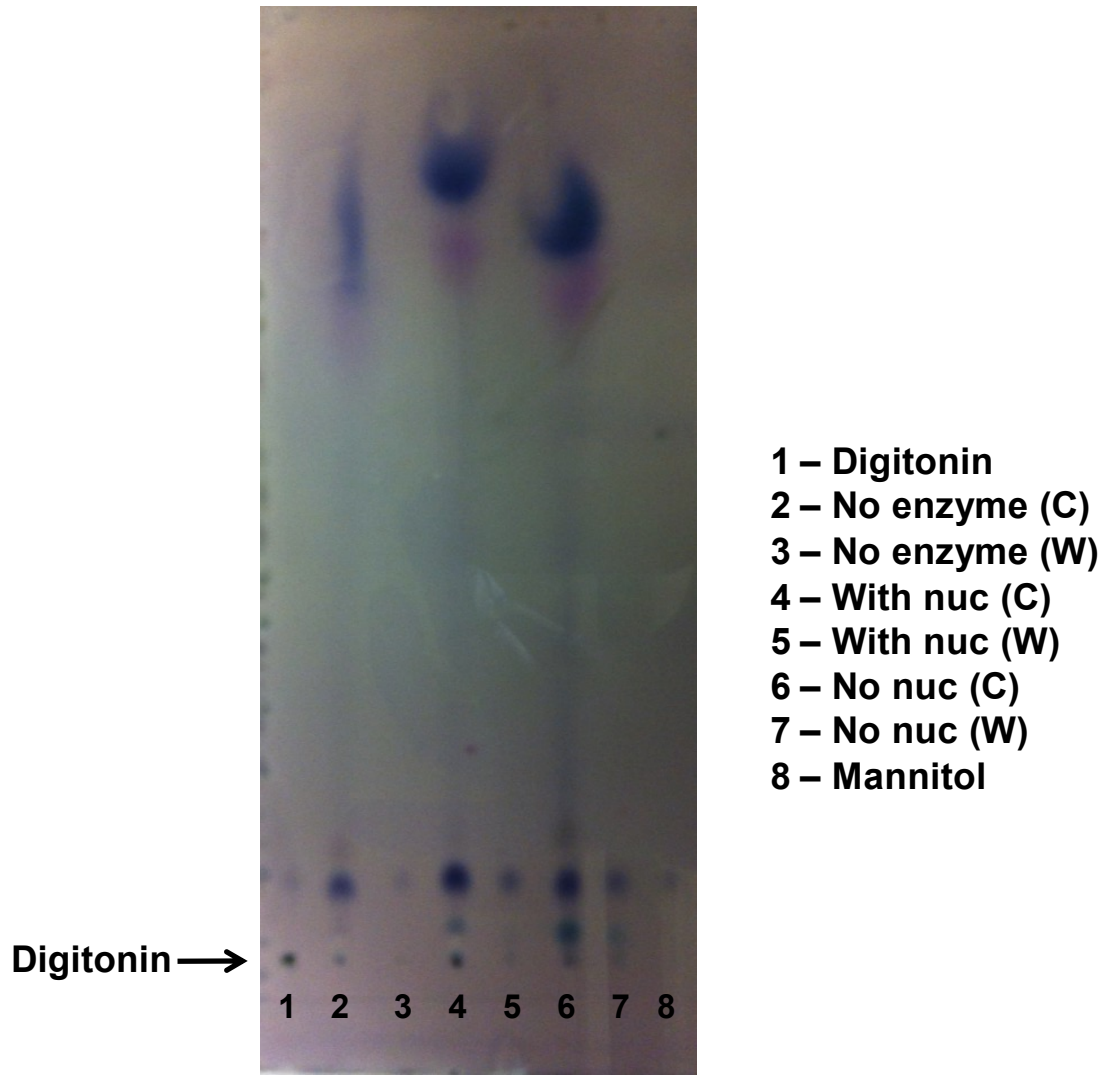

Figure A.5: Digitonin can be removed from assay samples by organic extraction. Peptide samples were separated from digitonin by water:chloroform:$MgCl_2$ extraction and the organic and aqueous layers were analyzed by thin layer chromatographic separation. Lanes 2, 4, and 6, represent the aqueous layers from these extractions; lanes 3, 5, and 7 represent the corresponding organic layers. Lane 1 shows digitonin without extraction. Lanes 2 and 3 are from a mock assay conducted without enzyme. Lanes 4 and 5 are from an assay conducted with hydroxylamine. Lanes 6 and 7 are from an assay conducted in the absence of hydroxylamine.

both were used in our buffers. Using this method we confirmed that digitonin is extracted into the chloroform layer, suggesting that peptides in the aqueous layer are more suitable for analysis by ESI-MS. Efforts are underway to optimize this method to purify the assay products obtained with peptide 2 (without the biotin tag), followed by LC-MS to characterize the products.

A.3 Discussion

The importance of GPI-T in human cancer has created an urgent need for a reliable quantitative assay for this enzyme. A FRET assay was first developed in our lab using crude microsomes and then with pure GPI-T.[216,209] This assay relies on hydroxylamine as a GPI anchor mimic and reduced activity was seen in the absence of hydroxylamine, confirming the nucleophilic dependence of this assay.[216]

Even using the yeast GPI-T, activity was reduced when a peptide based on yeast Yapsin 2 was used as a substrate, compared to our human CD52 substrate. However, the Yapsin 2 peptide substrate was synthesized with only three amino acids downstream of the ω-site. It is possible that this truncation explains the poor substrate behavior of this peptide. A peptide containing a longer *N*-terminal sequence is currently being synthesized for testing as a substrate.

The last step required for the development of our GPI-T assay is to confirm that transamidation has occurred by demonstrating the formation of a hydroxamate product. Complications arose due to the presence of digitonin in our

assay buffer and the biotin tag added on to our CD52 peptide substrate. We have now developed an extraction protocol to remove the digitonin from our assay. Efforts to characterize these peptide products are ongoing.

A.4 Materials and methods

A.4.1 Buffers and solutions

HBTU: *O*-(Benzotriazol-1-yl)-*N,N,N′,N′*-tetramethyluronium hexafluorophosphate, DIPEA: N,N-diisopropylethylamine, NMP: N-methyl-2-pyrrolidone, cleavage solution: 1.35 mL of Trifluoro Acetic acid (TFA), 50 uL of Anisole and 95 uL of Thioanisole. Anisaldehyde stain for TLC: 9.2 mL anisaldehyde, 3.75 mL Acetic acid, 338 mL 95% Ethanol, 12.5 mL concentrated sulfuric acid.

Peptide gel (20%) preparation:

Gel buffer (3X, pH 8.5), 3 M Tris base, 1 M HCl, and 0.3 % SDS. Separating layer, 15 mL 39:1 Acrylamide/Bis acrylamide, 10 mL of 3X gel buffer, 2.4 mL of glycerol, 2.5 mL of water, 100 uL of Ammonium peroxodisulfate (APS), 10 uL of Tetramethylethylenediamine (TEMED).

Stacking layer, 1 mL of 39:1 Acrylamide/Bis acrylamide, 3 mL of 3X gel buffer, 8 mL of water, 90 uL of APS, 10 uL of TEMED.

2X gel loading dye, 2 mL of Tris HCl pH 6.8, 2 mL of 10% Sodium dodecyl sulfate (SDS), 4 mL of glycerol, 1.8 mL of water and 5 uL of β-mercaptoethanol (BME).

10X Cathode buffer at pH 8.25, 1 M Tris base, 1 M Tricine, and 1% SDS. 10X Anode buffer, 1 M Tris base, 0.225 M HCl.

A.4.2 Solid phase peptide synthesis

All the peptides were synthesized manually or on a Prelude peptide synthesizer (Proteins technology). Pre-substituted Fmoc-Ile-Wang resin (for Yapsin 2 peptides, 100-200 mesh, 0.6 mmol/g) or Fmoc-Ser(tBu)-Wang resin (for CD52, with a 100-200 mesh, 0.6 mmol/g) were used. All the amino acids were coupled from 200 mM stock solutions with 400 mM HBTU and 200 mM DIPEA using NMP as the solvent. The peptides were either doubly coupled as needed. Manual coupling was performed after testing each amino acid coupling and deprotection using standard nynhydrin test. Deprotection was achieved with 20% piperidine in NMP for 20 min to remove the Fmoc group protecting group from each *N*-terminal amino acid. The peptides were cleaved from the resin using peptide cleavage solution, with mixing at room temperature for two hours. Cold ether was used to precipitate the cleaved peptide. The precipitate was then lyophilized from water. Each sample was purified by reverse phase HPLC (Beckman coulter) using a C3 column and ACN: water as the solvent system with 1% TFA. The identity of each peptide confirmed by ESI-MS in collaboration with the Trimpin Lab).

A.4.3 Purification and assay of GPI-T

The growth, purification and the *in vitro* assay of GPI-T was conducted according to the protocols developed by Dr. Sandamali Ekanayaka.[216] The

concentrated proteins were then analyzed using 10% SDS PAGE gel followed by Western blot. The presence of GST-Gpi8 was visualized by Western blot as described in the materials and methods of chapter 2.

A.4.4 *In vitro* assay product analysis for the biotynilated peptide.

After the biotinylated CD52 peptide was incubated with GPI-T under our standard assay conditions with NH_2OH for six hours, the resultant mixture was loaded onto streptavidin resin (1 mL bed volume) after washing, biotinylated peptides were eluted with hot.[216] The resultant eluent was lyophilized and analyzed by MAIV, a mass spectroscopic method developed in Dr Trimpin's lab and was ran by Dr. Ellen Inutan using 3-Nitrobenzonitrile (3-NBN) as the matrix.[242]

A.4.5 Assay product separation using water:chloroform separation

Two milliliter assay samples were used for the extractions. A 3:2:1 ratio of chloroform:methanol:$MgCl_2$ (4 mM) was added to each assay to become 6 mL total volumn. Each sample was vortexed for two minutes and then let it to stand until the layers are settled. The chloroform layer was separated and collected into a new tube and a second extraction was carried out for the water layer. Both the water and chloroform layers were separately collected, dried or lyophilized and frozen until further characterization.

A.4.6 Peptide gel for product analysis

Samples from the extractions described in the previous section were analyzed for peptide content using a 20% peptide gel followed by a Western blot using anti-biotin to detect the biotin tag on our peptide. A 20% separating layer and a 4% stacking layer were used to prepare the gels (see above). Samples were loaded onto the gels with 2X gel loading dye (after heat denaturation) and each gel was ran at 100 V for two hours. The peptide gel was transferred onto PVDF membrane using similar protocols as in chapter 2 and visualized using anti-biotin (1 mg/mL, Sigma-Aldrich) followed by secondary anti-mouse antibodies.

A.4.7 Thin layer chromatographic analysis

TLC was performed with hexane:ethylacetate 50:50 solvent system. The solvent chamber was saturated first before running the TLC. After elution, the plate was dried and stained with anisaldehyde to visualize digitonin. To this end, the TLC plate was sprayed with the stain and then it was heated gently until spots were visible. Different sugars light up in different colors. A control spot with pure digitonin was included as a positive control.

A.5 Acknowledgement

I sincerely thank Dr Sandamali Ekanayaka for the guidance in protein purification and providing with peptides and samples for analysis. Special thanks goes to Dr Ellen Eutan and Dr Sarah Trimpin assisting us with ESI-MS.

APPENDIX B

STRUCTURAL CHARACTERIZATION OF YEAST GPI8$_{23-306}$:GAA1$_{50-343}$ SOLUBLE DOMAINS IN *E. COLI*

B.1 Introduction

From the five known subunits of GPI-T, Gpi8, Gpi16 and Gaa1 co-purify as a core-heterotrimer in yeast,[18] we consider these three subunits the "core" components of GPI-T. Even though each subunit is known to be essential for transamidase activity, the exact contribution of each subunit to activity is unknown in terms of structure, connectivity, stoichiometry and function.[12,19,5, 232] An initial characterization of the soluble domain of the catalytic subunit, Gpi8$_{23-306}$, revealed that it is inactive due either to the absence of one or more of the other subunits or a requirement for soluble domain II and its TM domain. Nevertheless, this subunit does bind peptide substrates.[83] Therefore, as the next step, efforts have been initiated to characterize the structural and functional involvement of the other two core subunits, Gpi16 and Gaa1 (see Chapter 3) . This appendix describes our efforts towards the structural characterization of yeast Gpi8$_{23-306}$:Gaa1$_{50-343}$ overexpressed and purified from *E. coli*.

Gaa1 has a single, large soluble domain with six transmembrane helices.[75] Sequence alignments and the three dimensional structural predictions by us and others Show an evolutionary connection between Gaa1 and a metal-dependant aminopeptidase.[185,186] However, when grown in *E. coli*, overexpression of Gaa1$_{50-343}$ is toxic.[207] To overcome this problem, we examined the impact of co-expression of Gaa1$_{50-343}$ with GST-Gpi8$_{23-306}$ in *E.*

coli. Our hypothesis was that complex formation between these two subunits would alleviate the toxicity of Gaa1 overexpression. This appendix explains our efforts towards optimizing growth to maximized the yields of both subunits ($Gpi8_{23-306}$ and $Gaa1_{50-343}$ and to determine the stoichiometry of this complex.

B.2 Results

B.2.1 Overexpression and purification of $Gpi8_{23-306}$:$Gaa1_{50-343}$

The plasmid pJLM017 ($Gaa1_{50-343}$) was transformed into BL21(DE3)RIL Codon Plus cells (Stratagene); this plasmid adds a His_6 tag onto the *N*-terminus of $Gaa1_{50-343}$. Since $Gaa1_{50-343}$ alone is toxic to *E. coli*, GST-$Gpi8_{23-306}$ (pJLM008) was co-transformed into this strain in an effort to alleviate toxicity.[207] Co-expression was conducted at low temperature. The protein complex was purified using glutathione affinity purification, which will purify GST-$Gpi8_{23-306}$ along with $Gaa1_{50-343}$. The purified proteins were analyzed using an anti-GST Western blot, anti-His blots and Coomassie-stained gels (Figure B.1). Further, these purified proteins were analyzed using size exclusion chromatography (SEC) and native PAGE.

B.2.2 Analysis of $Gpi8_{23-306}$:$Gaa1_{50-343}$ complex by SEC.

Native PAGE gels were used to analyze the complex formation between $Gpi8_{23-306}$ and $Gaa1_{50-343}$; however, they were unsuccessful (data not shown). Next we injected the purified putative protein complex onto an SEC column.

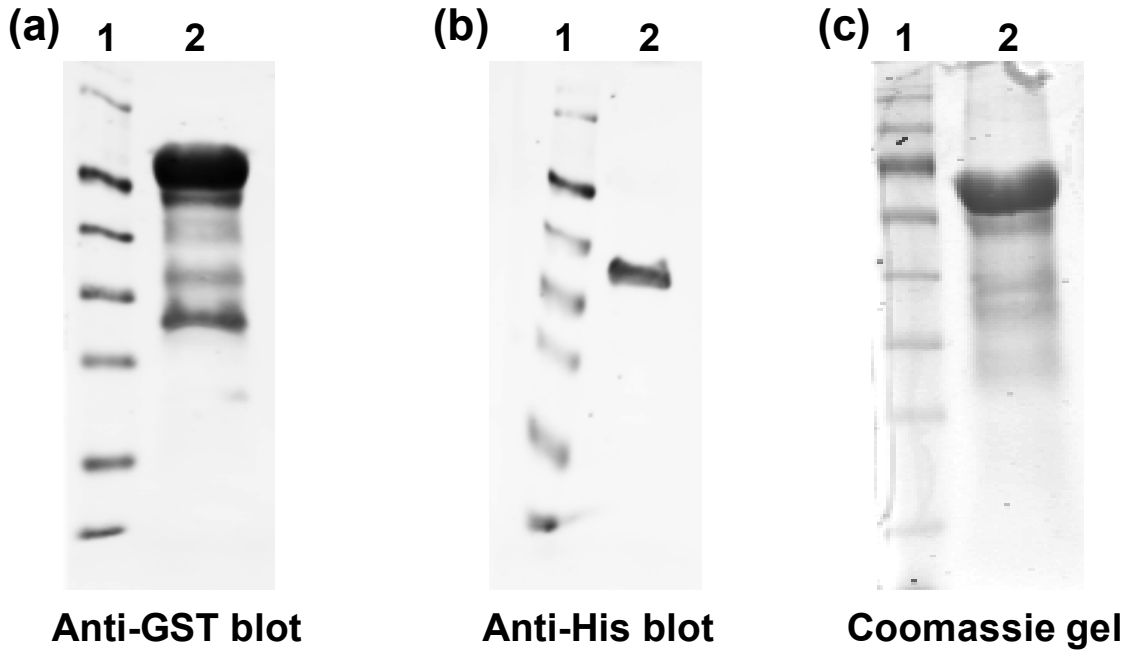

Figure B.1: Glutathione sepharose purification of GST-Gpi8$_{23-306}$ results in the co-purification of His$_6$-Gaa1$_{50-343}$. GST-Gpi8$_{23-306}$ and His$_6$-Gaa1$_{50-343}$ were simultaneously overexpressed in BL21(DE3)RIL codon plus cells the GST tag on GST-Gpi8$_{23-306}$ was used to purify both proteins. (a) Anti-GST Western blot (b) Anti-His$_6$ blot. (c) Coomassie stained gel. In all three panels, lane 1 molecular weight markers, Lane 2: purified protein.

(Figure B.2). Since the amount of protein were not enough to analyze using native PAGE, the SEC spectra of the complex was overlaid with the SEC molecular weight marker (Figure B.2 (a)).

Fractions were collected, concentrated and analyzed using SDS-PAGE gels followed by Western blot visualization using anti-GST and anti-His_6 antibodies

SEC exclusion revealed three peaks (Figure B.2 (a)). The first peak (fractions 4-6) presumably represents aggregates. Western blot analysis demonstrated that these fractions did not contain either GST-$Gpi8_{23-306}$ or His_6-$Gaa1_{50-343}$. The second peak (fractions 7-9) was not baseline resolved and appeared as a shoulder to the first peak. This peak contained both GST-$Gpi8_{23-306}$ or His_6-$Gaa1_{50-343}$ (Figure B.2. (b)) and eluted with a molecular weight range of 252-164, which is most consistent with the formation of an α2β2 complex, containing two copies of both GST-$Gpi8_{23-306}$(α) and His6-$Gaa1_{50-343}$ (β). The third peak eluted with a calculated MW range of 164-70 (fractions 9-10). These fractions predominantly contain GST-$Gpi8_{23-306}$ and are most consistent with a homodimer of this subunit. To further confirm the formation of an $\alpha_2\beta_2$ heterotetramer, we set out to optimize the yields of the $Gpi8_{23-306}$:$Gaa1_{50-343}$ expression.

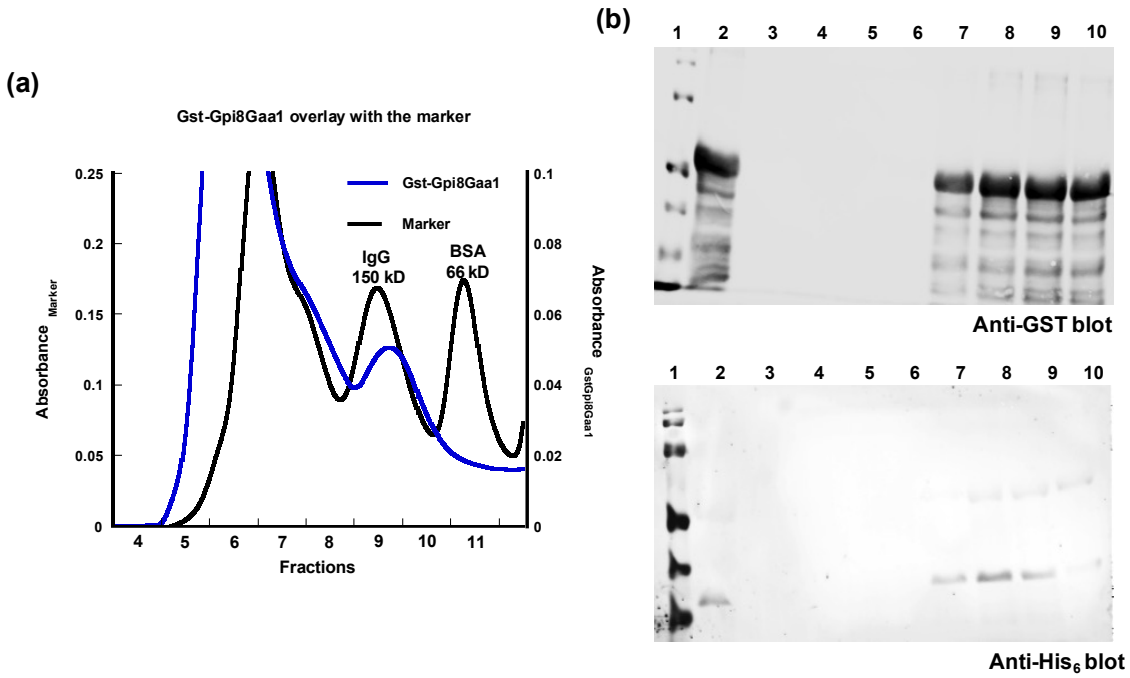

Figure B.2: SEC analysis of GST-Gpi8$_{23\text{-}306}$:His$_6$-Gaa1$_{50\text{-}343}$ complex forms a heterotetramer. GST-Gpi8$_{23\text{-}306}$:His$_6$-Gaa1$_{50\text{-}343}$ was overexpressed and purified using glutathione affinity purification. The purified protein was injected into the SEC column. (a) Spectrum of the complex overlaid with the SEC marker. Blue color is the spectrum of the complex. Black color id the spectrum of the molecular weight marker. The eluted fractions were concentrated and analyzed using western blots of anti-GST and anti-His blots. (b) Top panel: anti-GST western blot, bottom panel: anti-His western blot. For each lanes, lane 1: molecular weight marker, lane 2: the injected protein sample, lane 3-10: concentrated protein fractions collected from the SEC column. If GST-Gpi8$_{23\text{-}306}$ is α and His$_6$-Gaa1$_{50\text{-}343}$ is β, αβ~ 94 kD, $\alpha_2\beta$~ 153 kD and $\alpha_2\beta_2$~ 188 kD. The protein complex was observed at a higher molecular weight greater than 150 kD indicates that the complex is the heterotetramer.

B.2.3 Impact of small molecule additives on protein expression and purification

A number of different small molecules can be added to growth media and purification buffers to increase protein stability and solubility and to reduce aggregation of proteins.[243] Several additives such as sugars, osmolytes, amino acids and their derivatives, detergents (non ionic, zwitter ionic and ionic), salts (mild and strong chaotropes and kosmotropes), alcohols, polyols and polymers have been used to increase protein stability.[243,244,245,246,247] We tested a series of additives first to increase the solubility of GST-Gpi8$_{23\text{-}306}$ and to see the effect of the small molecules on GST-Gpi8$_{23\text{-}306}$ dimerization (Figures B.3 & B.4).

GST-Gpi8$_{23\text{-}306}$ was first grown in small scale (25 mL) in the presence of different small molecules, (erythritol, mannitol, xylitol, trehalose, gly-gly, glycerol and proline) added to the growth media (see materials and methods). The final OD_{600} was measured and each culture was divided into two. One half was purified in the presence of the same additive and the second half was purified in the absence. The production of GST-Gpi8$_{23\text{-}306}$ was examined using Western blots with anti-GST antibodies (Figure B.3), native PAGE gels were also used to test the effect of each additive on protein solubility and protein dimerization (Figure B.4). However, little effects were observed in terms of protein stability and solubility for GST-Gpi8$_{23\text{-}306}$.

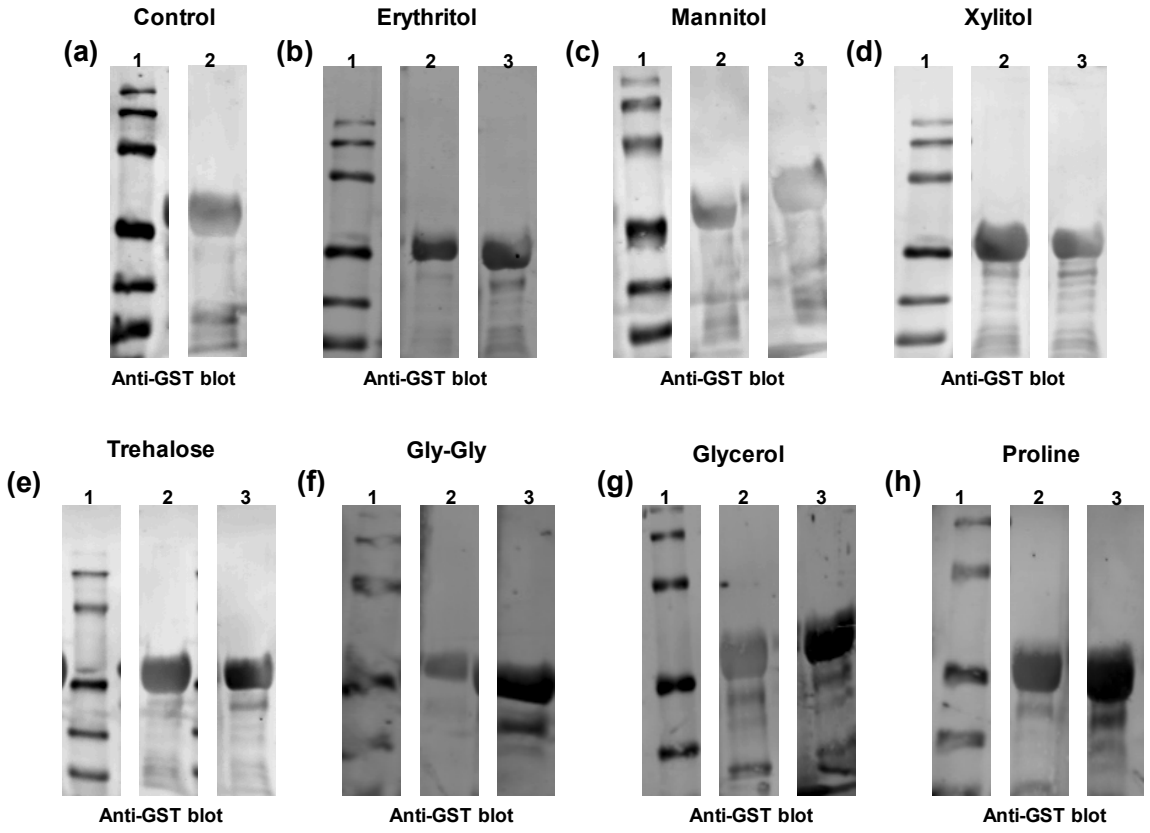

Figure B.3: The impact of small molecules on the production and stability of GST-Gpi8$_{23\text{-}306}$. Small molecules were used to growth media and purification buffers in an effort to enhance the overproduction and solubility of GST-Gpi8$_{23\text{-}306}$. (a) Control growth without any additional small molecules. (b)-(h) Growth media were supplemented with small molecules, as follows; (b) erythritol, (c) mannitol, (d) xylitol (e) trehalose (f) gly-gly (g) glycerol and (h) proline. In (a) lane 1: molecular weight markers, and lane 2: affinity purified protein. For panels (b)-(h), lane 1: molecular weight markers, lane 2: small molecule was added only to the growth medium, lane 3: small molecule was added to both the growth medium and to the lysis buffer used in the purification.

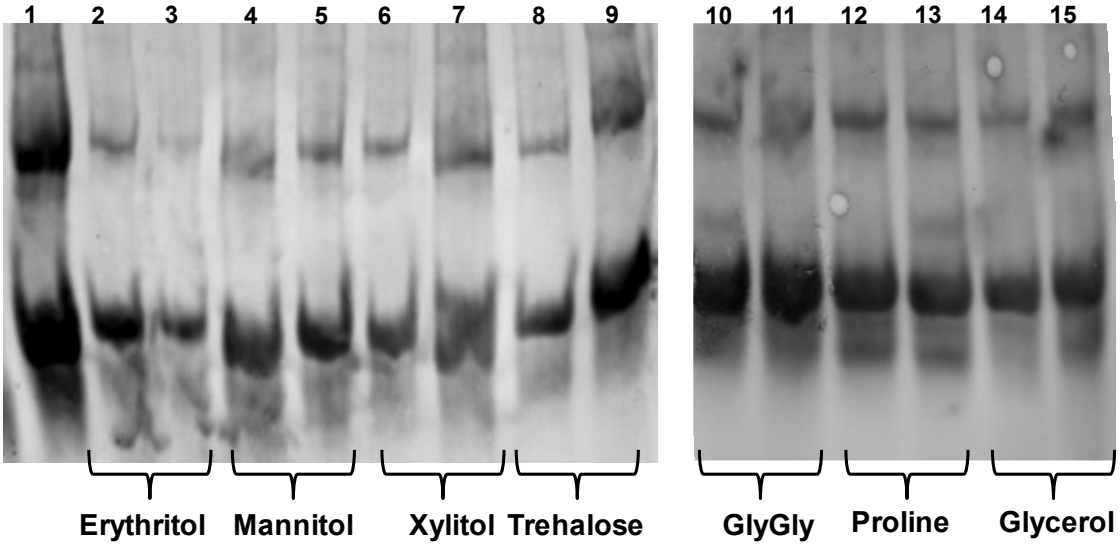

Figure B.4: Small molecules additives do not enhance dimerization of GST-Gpi8$_{23\text{-}306}$. GST-Gpi8$_{23\text{-}306}$ purified from cultures containing different small molecule additives was loaded onto a native PAGE gel to analyze the amount of dimer formed. Lane 1: control protein without any small molecule additive, lanes 2, 4, 6, 8, 10, 12, and 14: Each small molecule was added only to the growth medium. Lanes 3, 5, 7, 9, 11, 13, and 15: Each small molecule was added to both the growth medium and the lysis buffer.

We also tested these small molecules on the overproduction of GST-Gpi8$_{23-306}$: His$_6$-Gaa1$_{50-343}$. Cultures were grown separately with each of the small molecule additives as described above for GST-Gpi8$_{23-306}$. Each cell pellet was purified with or without the same additive in the purification buffer using glutathione sepharose affinity purification. The presence of GST-Gpi8$_{23-306}$: His$_6$-Gaa1$_{50-343}$ were analyzed using anti-GST and anti-His Western blots, respectively (Figure B.5).

Gaa1$_{50-343}$ was observed in protein samples, with erythritol added into both growth medium and to the purification, with trehalose added to the growth medium and purified even in the presence and absence of trehalose and with xylitol was added only into the growth medium. However, when trehalose was added onto the large growth medium (1 L), no protein was overexpressed indicating this protein complex should grown and purify in small scale cultures.

B.2.4 Switching the tags to increase expression of Gaa1$_{50-343}$

Since the overexpression of Gaa1$_{50-343}$ alone is toxic to the cells and we couldn't grow the complex in larger cultures, we assumed by altering the tags it would help the overexpression of the complex. Therefore we switched tags in Gpi8$_{23-306}$ to His$_6$ and Gaa1$_{50-343}$ to GST. The individual overexpression and purification of each protein yield a reasonable quantity of proteins. However, when both the proteins were expressed in same cell and purified using glutathione affinity purification, only GST-Gaa1$_{50-343}$ was purified and His$_6$-Gpi8$_{23-306}$ was washed during the washing step (Figure B.6).

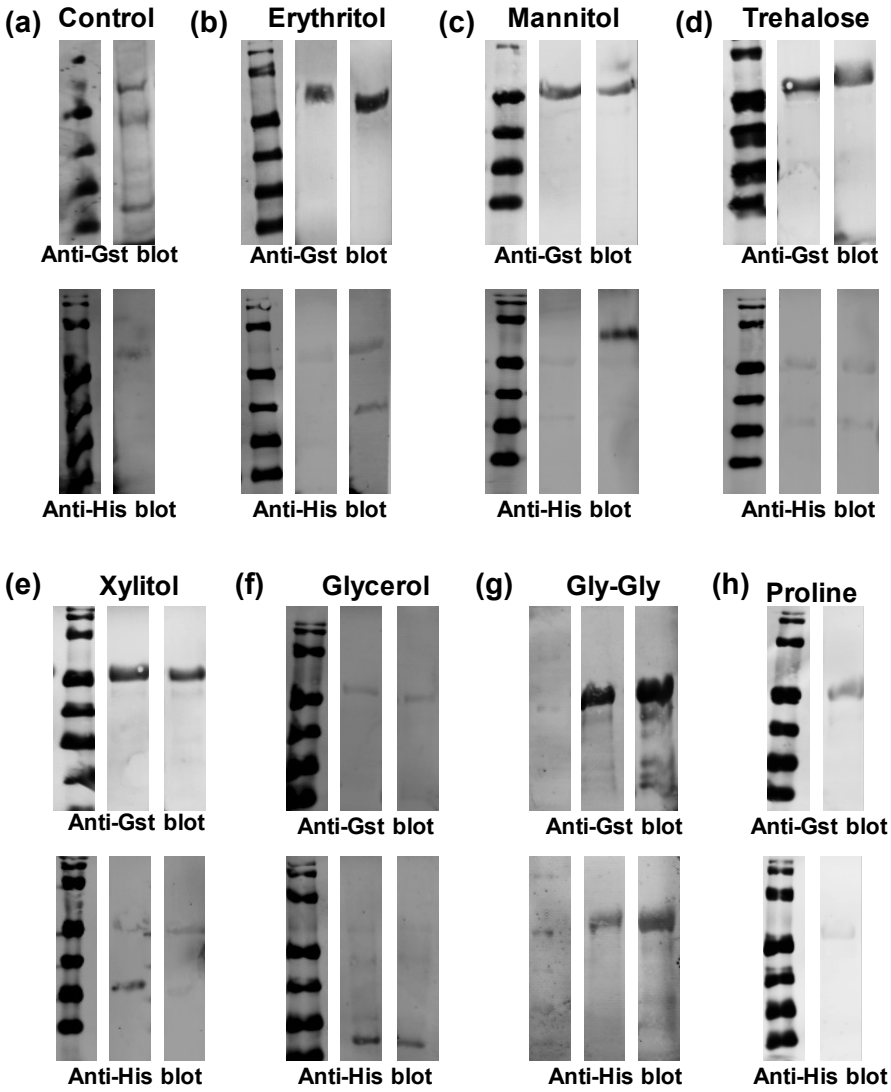

Figure B.5: Effect of small molecules on overexpression and purification of GST-Gpi8$_{23\text{-}306}$:His$_6$-Gaa1$_{50\text{-}343}$ Both GST-Gpi8$_{23\text{-}306}$ and His$_6$-Gaa1$_{50\text{-}343}$ was overexpressed in BL1(DE3)RIL codon plus cells in the presence of small molecules. Glutathione affinity purified proteins in the presence or absence of small molecules were analyzed using western blots of anti-GST and anti-His. (a)-(h) Top panel: anti-GST blot to visualize GST-Gpi8$_{23\text{-}306}$ and bottom panel: anti-His blot to visualized His$_6$-Gaa1$_{50\text{-}343}$. (a) Control sample without any sugar. Lane 1: Molecular weight marker, Lane 2: purified protein (b)-(h) Overexpressed and purified samples with addition of sugar molecules. Lane 1: Molecular weight maker, Lane 2: Purified protein in the absence of small molecules, Lane 3: Proteins were purified in the presence of each small molecule.

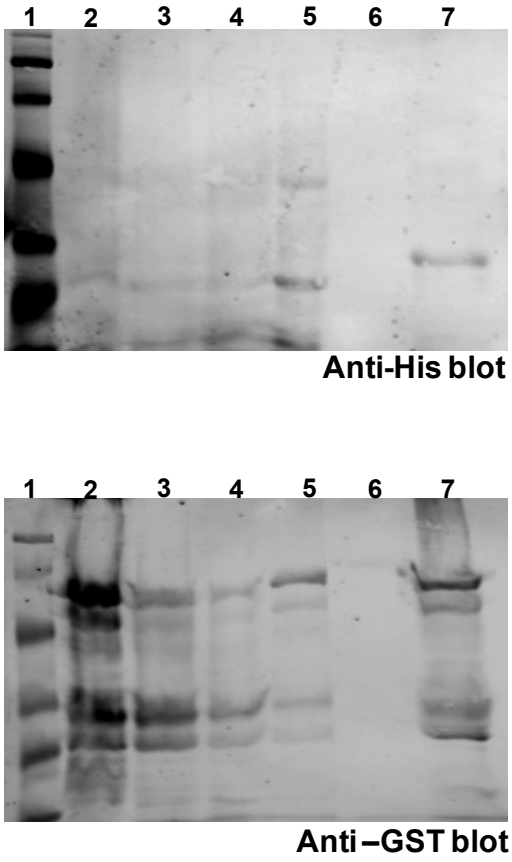

Figure B.6: Glutathione affinity purified GST-Gaa1$_{50-343}$ complex didn't co-purify His$_6$-Gpi8$_{23-306}$. Both His$_6$-Gpi8$_{23-306}$ and GST-Gaa1$_{50-343}$ was overexpressed in BL1(DE3)RIL codon plus cells and purified using glutathione affinity purification. Top panel: Anti-His blot to indicate the presence of His$_6$-Gpi8$_{23-306}$, Bottom panel: Anti-GST blot to confirm the presence of GST-Gaa1$_{50-343}$. For both the gels lane 1: molecular weight marker, lane 2: pellet, lane 3: lysate, lane 4: flow through, lane 5: wash 1, lane 6: wash 5, lane 7: eluted protein. Lane 5 of the anti-His blot indicate Gpi8$_{23-306}$ has washed and didn't participate in forming the complex.

These results suggest that His_6-$Gpi8_{23-306}$ is not binding to GST-$Gaa1_{50-343}$ may due to the GST-tag interfering with the $Gpi8_{23-306}$ and $Gaa1_{50-343}$ binding interface.

B.3 Discussion

Even thought preliminary native PAGE and ESI-IMS-MS results indicate the presence of the heterotetramer of GST-$Gpi8_{23-306}$: His_6-$Gaa1_{50-343}$, we wanted observe a robust tetramer of this complex. The toxicity of $Gaa1_{50-343}$ when grown in *E.coli* has hindered the isolation of the complex in a higher yield. Therefore we had to carry out optimization of the growth and purification of this protein complex to increase the yield.

Attempts were carried out to characterize GST-$Gpi8_{23-306}$: His_6-$Gaa1_{50-343}$ using SEC, but repetitions were unsuccessful. Therefore to increase the yield of the protein complex, small molecules were added to the growth medium. Even thought the addition of small molecules onto the growth medium, didn't enhance the solubility and stability of the $Gpi8_{23-306}$-GST, in GST-$Gpi8_{23-306}$: His_6-$Gaa1_{50-343}$ a higher yield of the complex was obtained with erythritol, trehalose and xylitol in small growth cultures. When small molecules were used in larger cultures protein complex was not overexpressed leading us to think that may be amount of air and the cell crowding may effect on the protein's expression. Therefore, growth should carryout in small scale, to obtain a higher yield of the protein and re-analyze for the heterotetramer should done using native PAGE and SEC.

B.4 Materials and methods

B.4.1 Overexpression and purification of GST-Gpi8$_{23-306}$: His$_6$-Gaa1$_{50-343}$

Plasmids were constructed by Dr Y. Varma and Dr R. Morissette.[207,209] Overexpression and purifications were carried according to Dr. Varma's protocols.[207] The presence of proteins was confirmed by SDS-PAGE gels followed by Western blots. Anti-GST Western blots done similar to Chapter 2, materials and methods. Anti-His western blots were carried out with a 1 µg/mL concentrations of anti-His primary antibody from mouse (AnaSpec) followed by the secondary anti-mouse antibodies (Sigma-Aldrich) with a working concentration of 1 µg/mL.

B.4.2 Use of small molecules in overexpression and purification of GST-Gpi8$_{23-306}$ and GST-Gpi8$_{23-306}$: His$_6$-Gaa1$_{50-343}$ complex

Overnight pre-cultures were grown without any small molecules. A volume of 1 mL pre-culture was added to a 25 mL culture with appropriate antibiotics and 1% glucose, along with small molecules to obtain the following final concentrations. erythritol: 0.5 M, mannitol: 0.5 M, xylitol: 1 M, trehalose: 0.75 M, gly-gly: 0.1 M and glycerol: 5%, proline, 0.5 M.[243] Samples were grown at 19 ^{o}C until it reaches the OD_{600} to ~0.5. Once the desired OD_{600} was obtained, a final concentration of 1 mM IPTG was added and was induced for another two hours. The final OD_{600} was measured prior to the purification. The cell pellet was dissolved to obtain a similar concentration of cells and was purified following the same protocols for GST purifications as described in Dr Varma's thesis.[207]

The purified cells were analyzed using SDS-PAGE gels and native PAGE gels where appropriate followed by anti-GST and anti His Western blots as described in materials and methods of Chapter 2.

B.4.3 Switching tags to obtain His_6-$Gpi8_{23-306}$: GST-$Gaa1_{50-343}$ complex

Plasmids pJLM008 (GST-$Gpi8_{23-306}$) and pJLM017 (His_6-$Gaa1_{50-343}$) was used to obtain the His_6-$Gpi8_{23-306}$ and GST-$Gaa1_{50-343}$ plasmids. The restriction enzyme cleavage was done to get $Gpi8_{23-306}$ and $Gaa1_{50-343}$ gene products and was inserted into pCDF-1B and to pGEX-4T3 plasmids respectively to switch the tags.

Glutathione sepharose affinity purification was used to purify the complex. The protocols for overexpression and purification of these proteins are similar to previous.

APPENDIX C

EXPANDED FIGURES AND TABLES

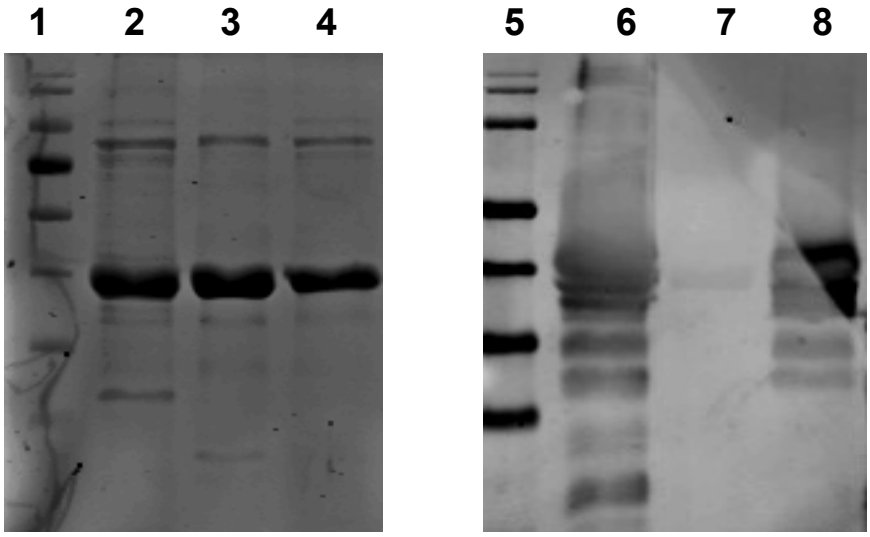

Figure C.1: Extended gel pictures with respect to Figure 2.1.

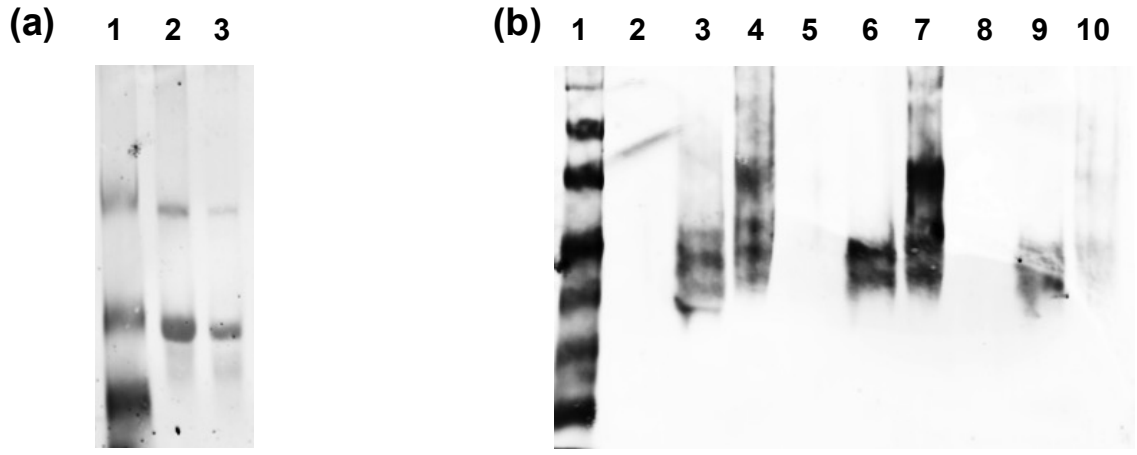

Figure C.2: Extended gel pictures with respect to Figure 2.2.

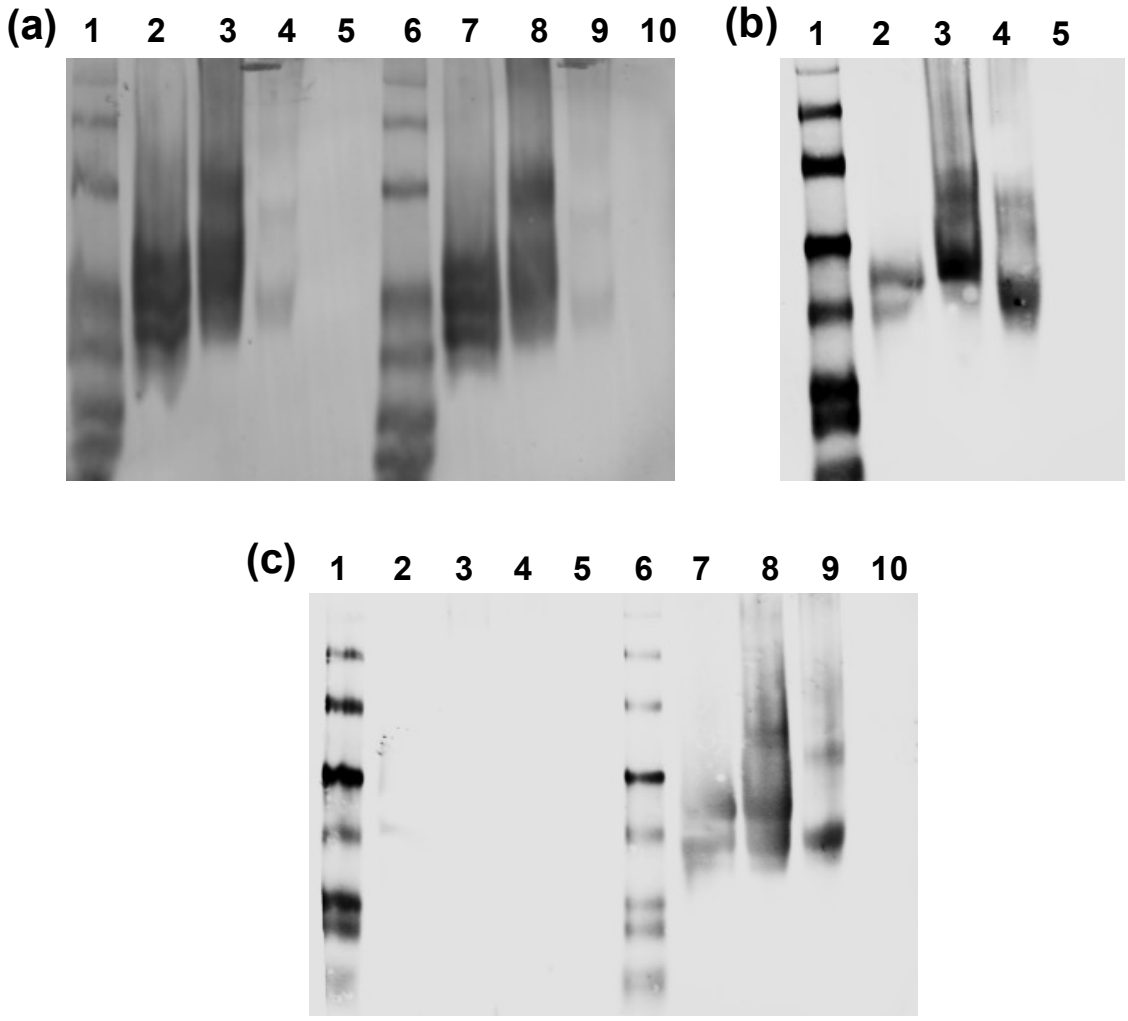

Figure C.3: Extended gel pictures with respect to Figure 2.5.

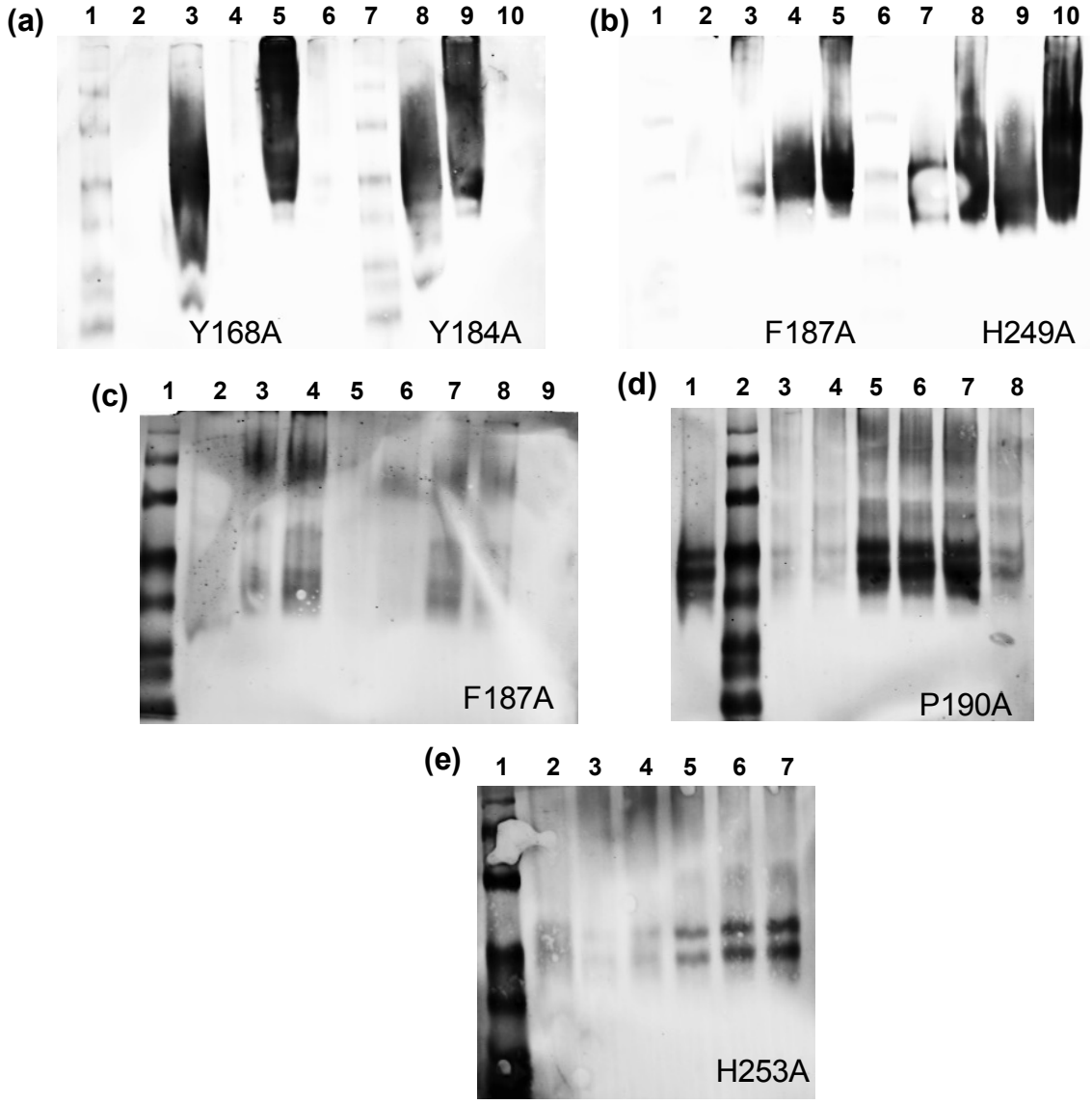

Figure C.4: Extended gel pictures with respect to Figure 2.9.

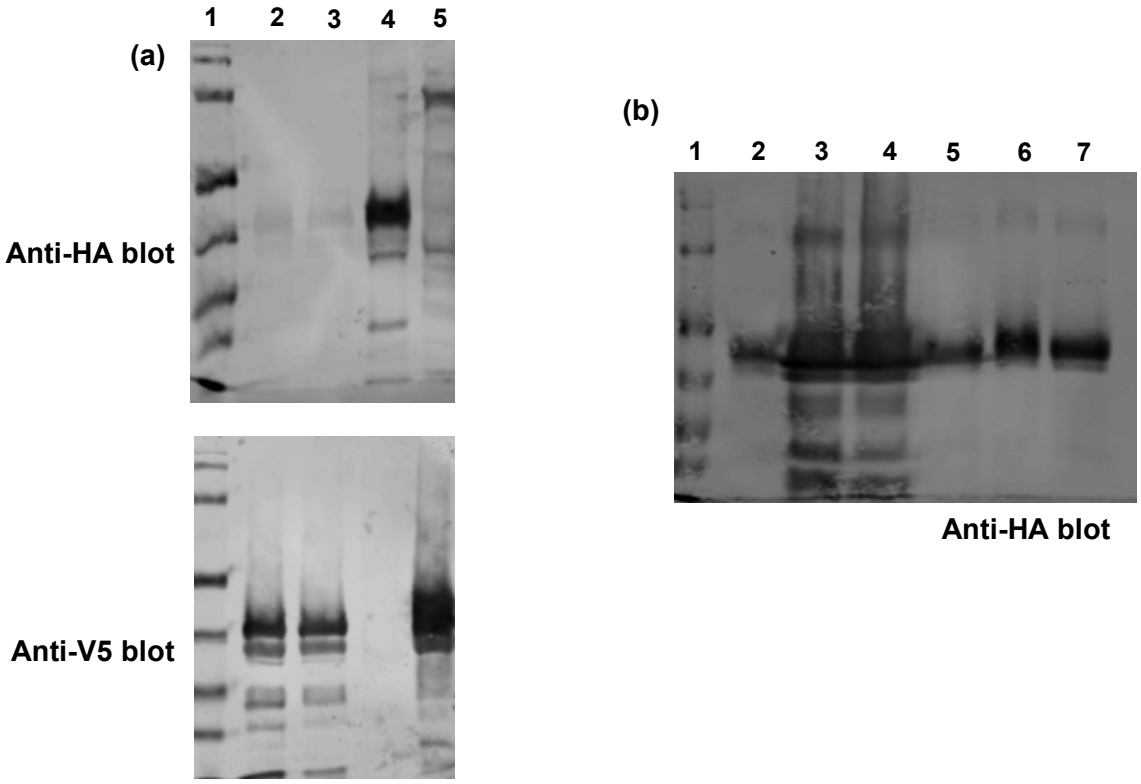

Figure C.5: Extended gel pictures with respect to Figure 3.2.

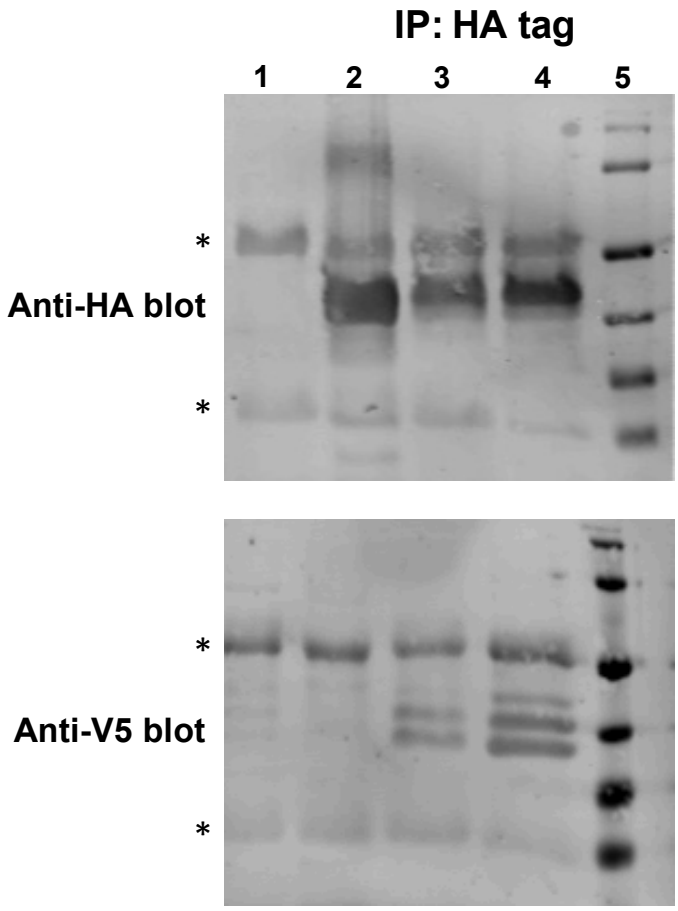

Figure C.6: Extended gel pictures with respect to Figure 3.3.

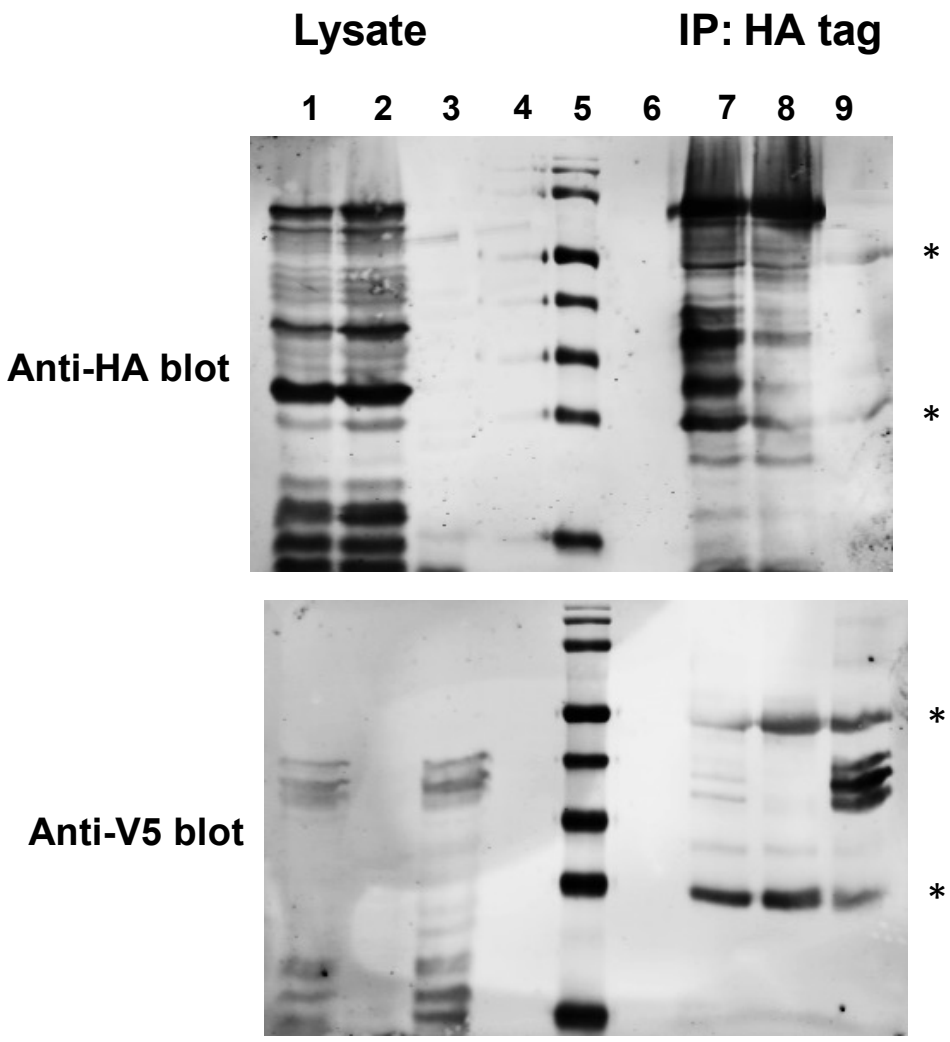

Figure C.7: Extended gel pictures with respect to Figure 3.4.

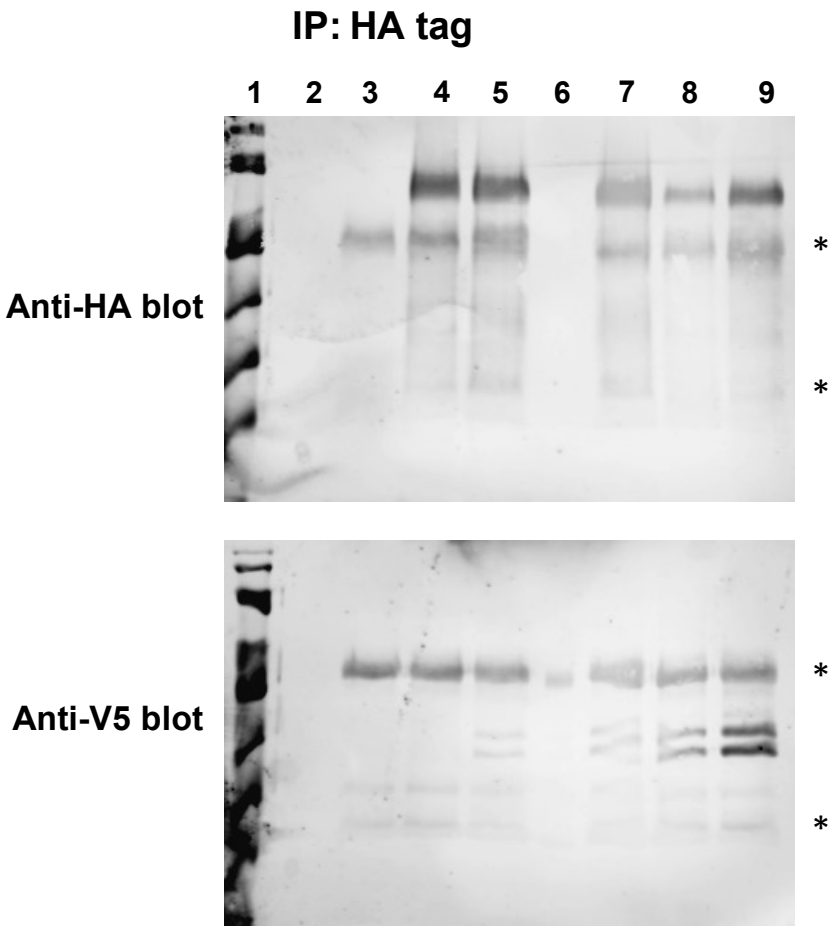

Figure C.8: Extended gel pictures with respect to Figure 3.5.

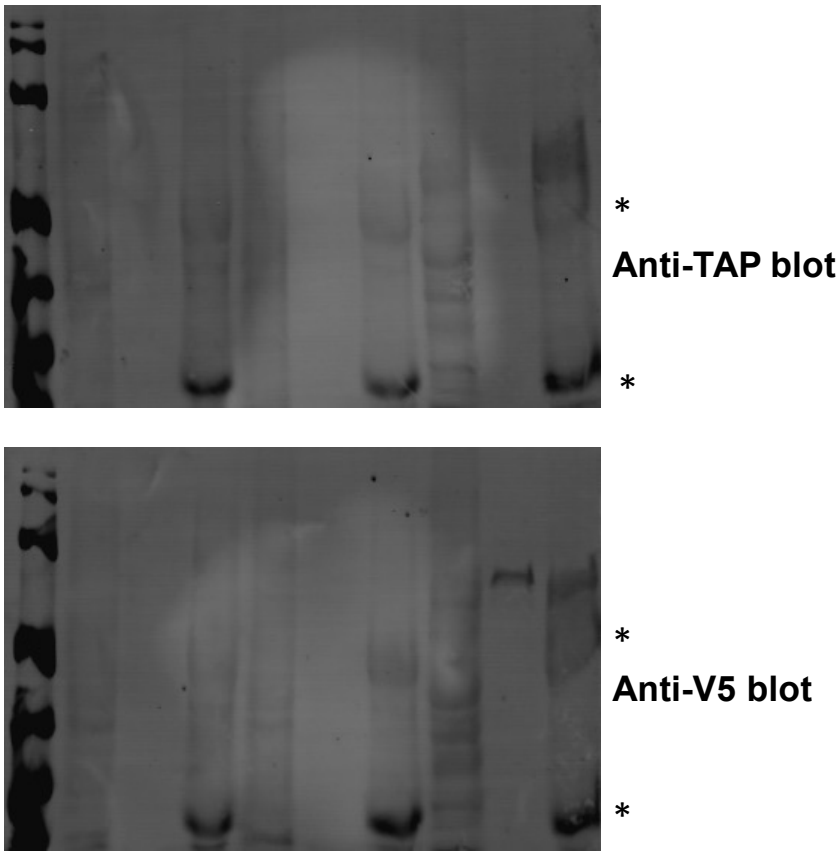

Figure C.9: Extended gel pictures with respect to Figure 3.6.

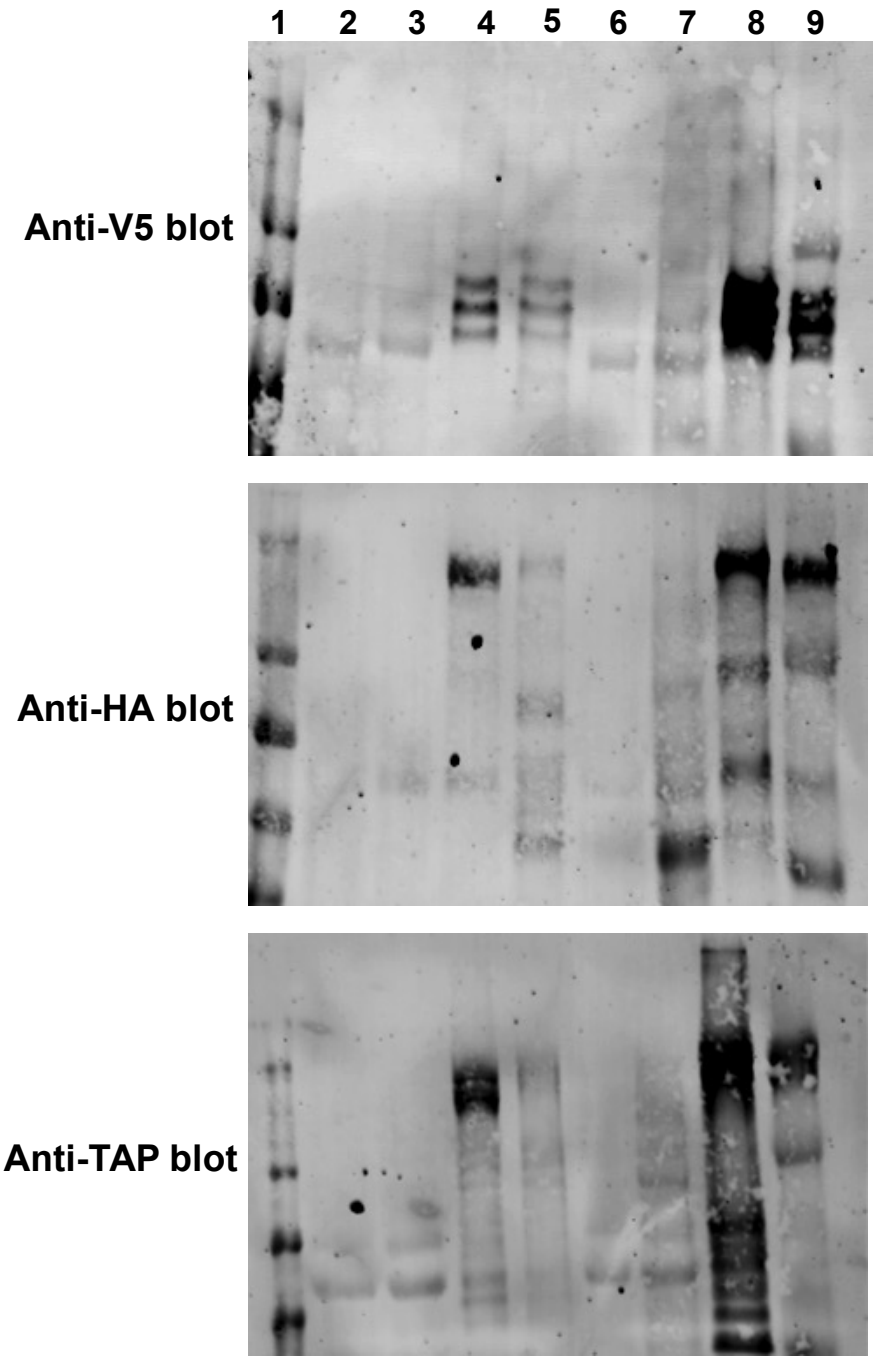

Figure C.10: Extended gel pictures with respect to Figure 3.7.

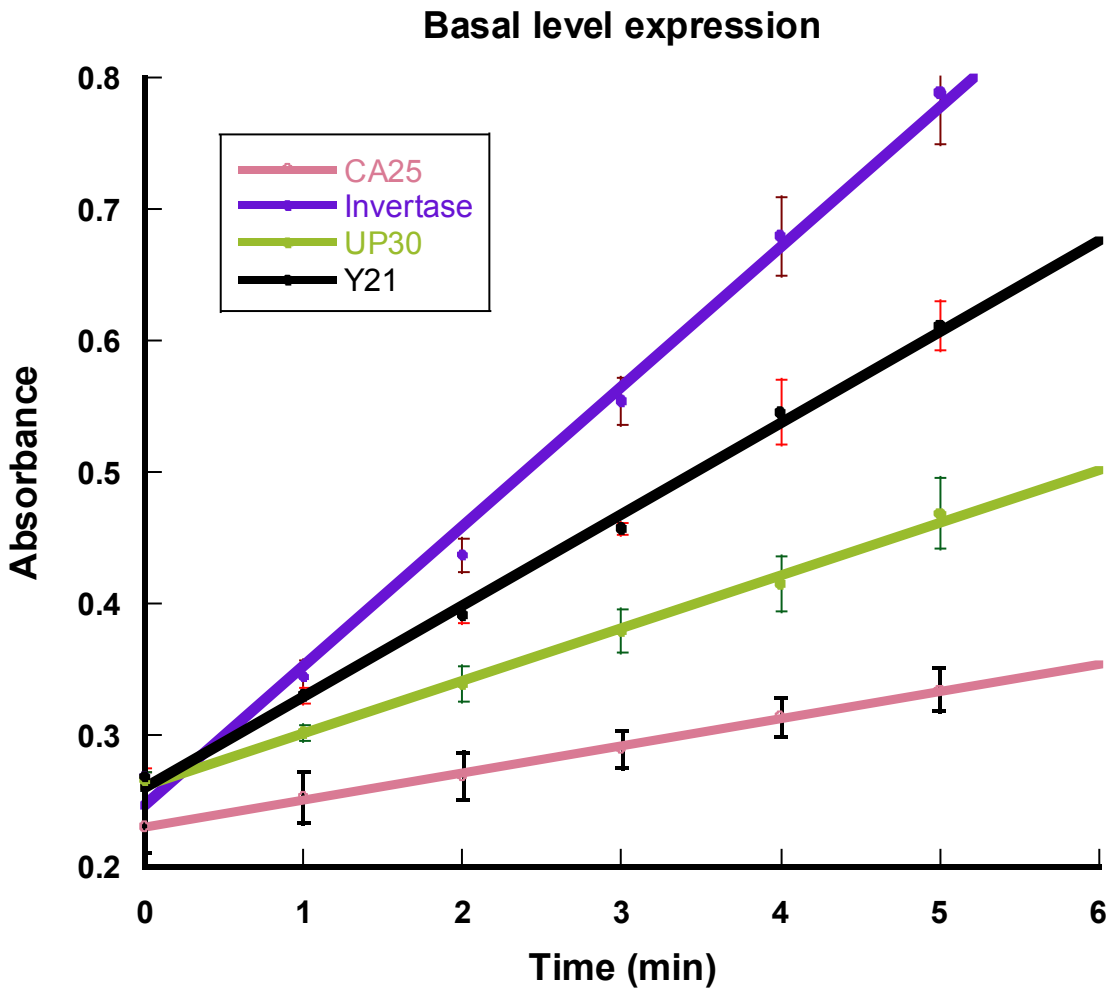

Figure C.11: Raw data, for Figure 4.3.

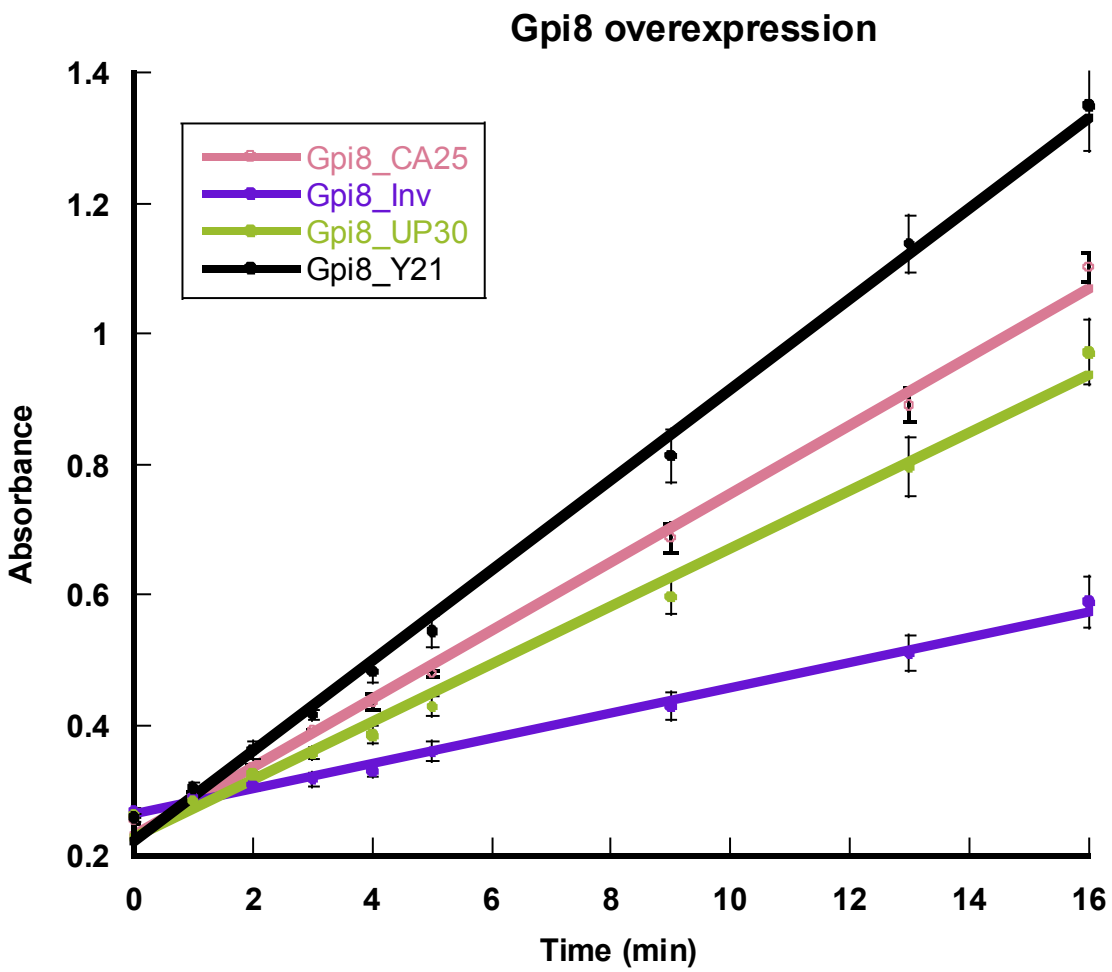

Figure C.12: Raw data for Figure 4.4.

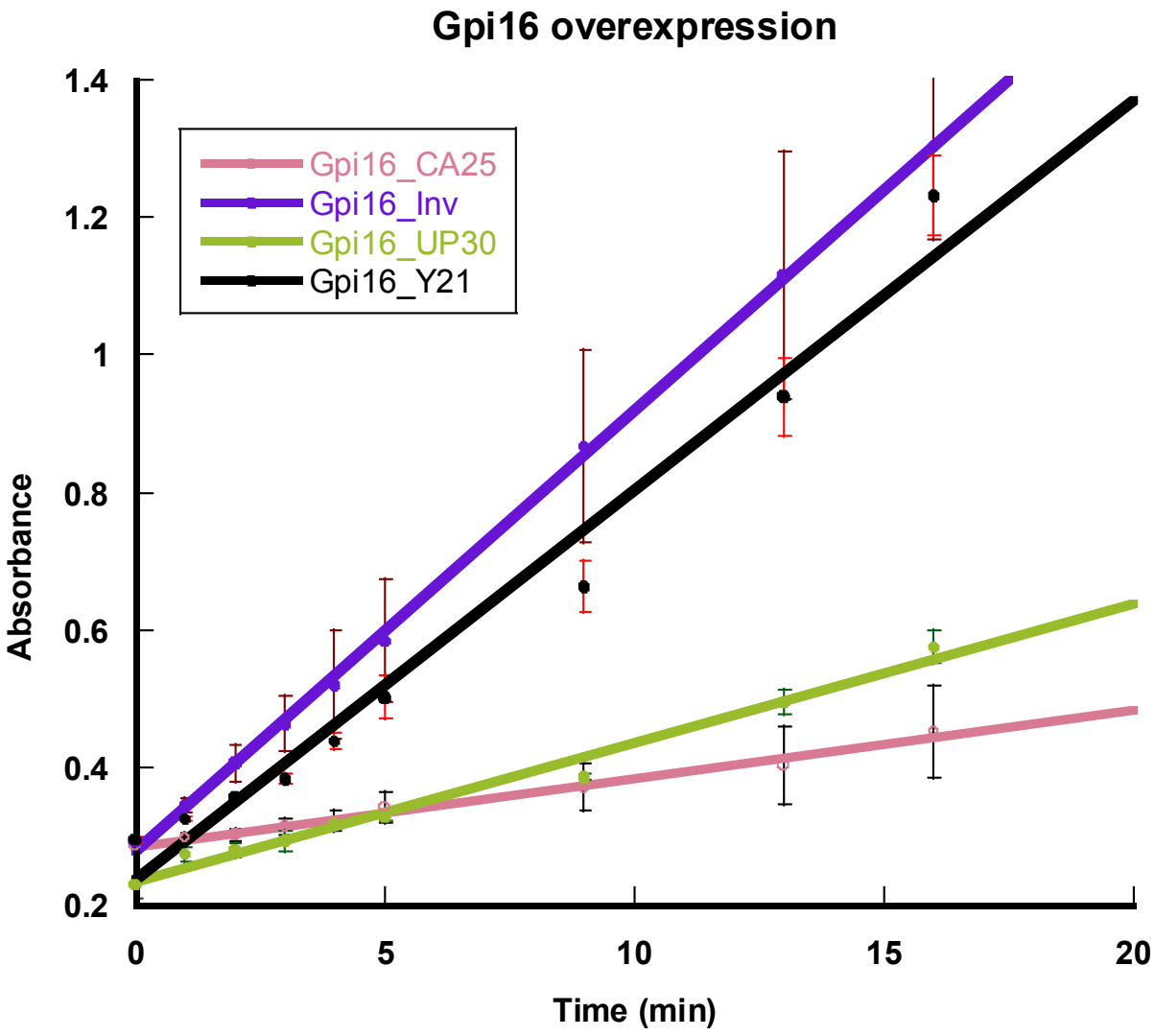

Figure C.13: Raw data for Figure 4.5.

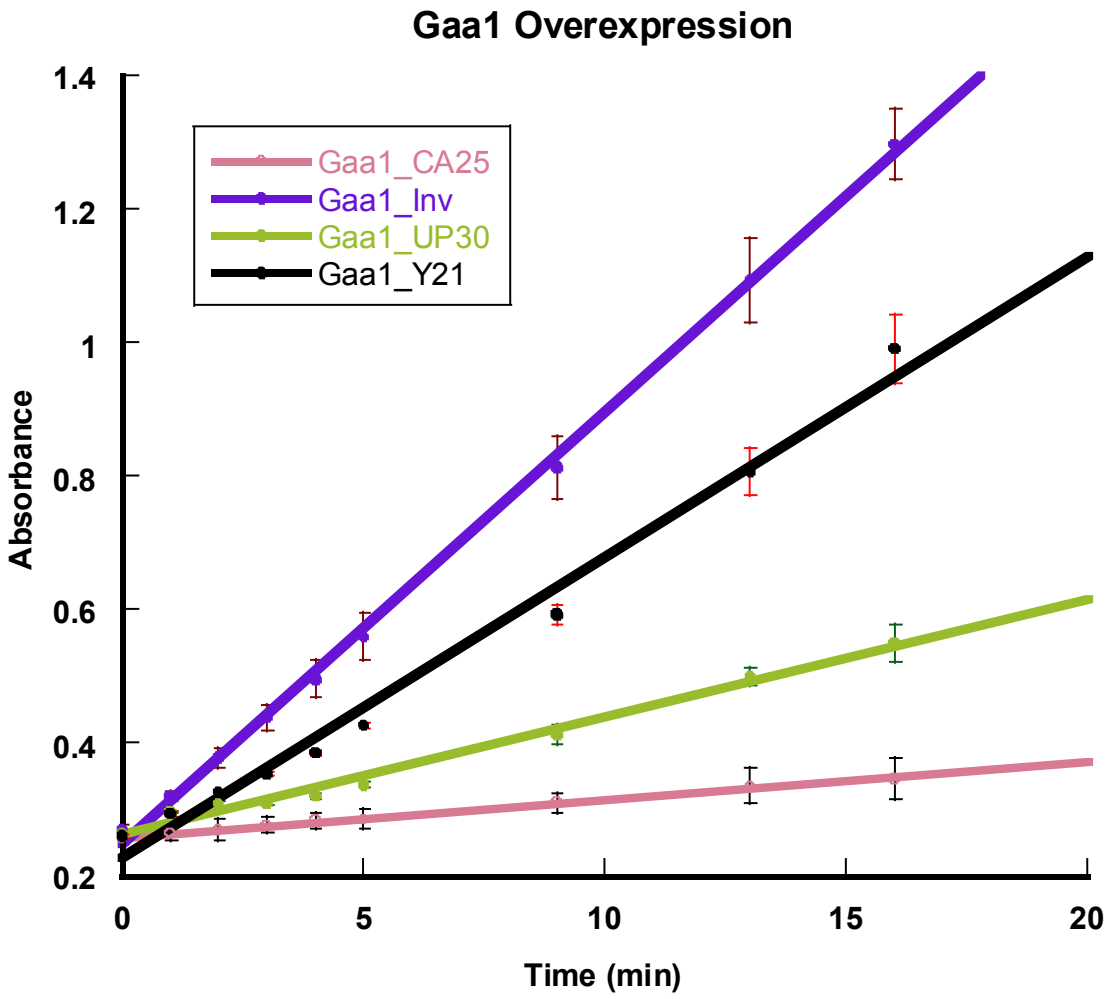

Figure C.14: Raw data for Figure 4.6.

REFERENCES

1. Global Cancer Facts & Figures, 2nd Edition. http://www.cancer.org/acs/groups/content/@epidemiologysurveilance/documents/document/acspc-027766.pdf (accessed May 31, 2013).

2. Lacey, S. W.; Sanders, J. M.; Rothberg, K. G.; Anderson, R. G.; Kamen, B. A., Complementary DNA for the folate binding protein correctly predicts anchoring to the membrane by glycosyl-phosphatidylinositol. *The Journal of Clinical Investigation* **1989,** *84* (2), 715-720.

3. Ploug, M.; Rønne, E.; Behrendt, N.; Jensen, A. L.; Blasi, F.; Danø, K., Cellular receptor for urokinase plasminogen activator. Carboxyl-terminal processing and membrane anchoring by glycosyl-phosphatidylinositol. *Journal of Biological Chemistry* **1991,** *266* (3), 1926-1933.

4. Guo, Z.; Linn, J.; Wu, G.; Anzick, S.; Eisenberger, C.; Halachmi, S.; Cohen, Y.; Fomenkov, A.; Hoque, M.; Okami, K.; Steiner, G.; Engles, J.; Osada, M.; Moon, C.; Ratovitski, E.; Trent, J.; Meltzer, P.; Westra, W.; Kiemeney, L.; Schoenberg, M.; Sidransky, D.; Trink, B., CDC91L1 (PIG-U) is a newly discovered oncogene in human bladder cancer. *Nat Med* **2004,** *10*, 374 - 381.

5. Hong, Y.; Ohishi, K.; Kang, J.; Tanaka, S.; Inoue, N.; Nishimura, J.; Maeda, Y.; Kinoshita, T., Human PIG-U and yeast Cdc91p are the fifth subunit of GPI transamidase that attaches GPI-anchors to proteins. *Mol Biol Cell* **2003,** *14*, 1780 - 1789.

6. Eisenhaber, B.; Bork, P.; Eisenhaber, F., Post-translational GPI lipid anchor modification of proteins in kingdoms of life: analysis of protein sequence data from complete genomes. *Protein Engineering* **2001,** *14* (1), 17-25.

7. Ferguson, M. A., The structure, biosynthesis and functions of glycosylphosphatidylinositol anchors, and the contributions of trypanosome research. *Journal of Cell Science* **1999,** *112* (17), 2799-2809.

8. Fujita, M.; Jigami, Y., Lipid remodeling of GPI-anchored proteins and its function. *Biochimica et Biophysica Acta (BBA) - General Subjects* **2008,** *1780* (3), 410-420.

9. Fujita, M.; Kinoshita, T., GPI-anchor remodeling: Potential functions of GPI-anchors in intracellular trafficking and membrane dynamics. *Biochimica et Biophysica Acta (BBA) - Molecular and Cell Biology of Lipids* **2012,** *1821* (8), 1050-1058.

10. M, N.; K, O.; N, Y.; T, K.; A, N.; J, T., Developmental abnormalities of glycosylphosphatidylinositol-anchor-deficient embryos revealed by Cre/loxP system. *Lab Invest* **1999,** *79* (3), 293-299.

11. Paulick, M. G.; Bertozzi, C. R., The Glycosylphosphatidylinositol Anchor: A Complex Membrane-Anchoring Structure for Proteins†. *Biochemistry* **2008,** *47* (27), 6991-7000.

12. Benghezal, M.; Benachour, A.; Rusconi, S.; Aebi, M.; Conzelmann, A., Yeast Gpi8p is essential for GPI anchor attachment onto proteins. *Embo J* **1996,** *15*, 6575 - 6583.

13. Leidich, S. D.; Drapp, D. A.; Orlean, P., A conditionally lethal yeast mutant blocked at the first step in glycosyl phosphatidylinositol anchor synthesis. *Journal of Biological Chemistry* **1994,** *269* (14), 10193-6.

14. Brodsky, R. A.; Hu, R., PIG-A mutations in paroxysmal nocturnal hemoglobinuria and in normal hematopoiesis. *Leukemia & Lymphoma* **2006,** *47* (7), 1215-1221.

15. Krawitz, Peter M.; Murakami, Y.; Rieß, A.; Hietala, M.; Krüger, U.; Zhu, N.; Kinoshita, T.; Mundlos, S.; Hecht, J.; Robinson, Peter N.; Horn, D., PGAP2 Mutations, Affecting the GPI-Anchor-Synthesis Pathway, Cause Hyperphosphatasia with Mental Retardation Syndrome. *American journal of human genetics* **2013,** *92* (4), 584-589.

16. Kvarnung, M.; Nilsson, D.; Lindstrand, A.; Korenke, G. C.; Chiang, S. C. C.; Blennow, E.; Bergmann, M.; Stödberg, T.; Mäkitie, O.; Anderlid, B.-M.; Bryceson, Y. T.; Nordenskjöld, M.; Nordgren, A., A novel intellectual disability syndrome caused by GPI anchor deficiency due to homozygous mutations in PIGT. *Journal of Medical Genetics* **2013**.

17. Ohishi, K.; Inoue, N.; Kinoshita, T., PIG-S and PIG-T, essential for GPI anchor attachment to proteins, form a complex with GAA1 and GPI8. *EMBO J* **2001,** *20* (15), 4088-4098.

18. Fraering, P.; Imhof, I.; Meyer, U.; Strub, J.; van Dorsselaer, A.; Vionnet, C.; Conzelmann, A., The GPI transamidase complex of Saccharomyces cerevisiae contains Gaa1p, Gpi8p, and Gpi16p. *Mol Biol Cell* **2001,** *12*, 3295 - 3306.

19. Hamburger, D.; Egerton, M.; Riezman, H., Yeast Gaa1p is required for attachment of a completed GPI anchor onto proteins. *The Journal of Cell Biology* **1995,** *129* (3), 629-639.

20. Meyer, U.; Benghezal, M.; Imhof, I.; Conzelmann, A., Active site determination of Gpi8p, a caspase-related enzyme required for glycosylphosphatidylinositol anchor addition to proteins. *Biochemistry* **2000,** *39*, 3461 - 3471.

21. Fujita, M.; Kinoshita, T., Structural remodeling of GPI anchors during biosynthesis and after attachment to proteins. *FEBS Letters* **2010,** *584* (9), 1670-1677.

22. Conzelmann, A.; Puoti, A.; Lester, R. L.; Desponds, C., Two different types of lipid moieties are present in glycophosphoinositol-anchored membrane proteins of Saccharomyces cerevisiae. *EMBO J* **1992,** *11* (2), 457-66.

23. Englund, P. T., The Structure and Biosynthesis of Glycosyl Phosphatidylinositol Protein Anchors. *Annual Review of Biochemistry* **1993,** *62* (1), 121-138.

24. Ferguson, M.; Homans, S.; Dwek, R.; Rademacher, T., Glycosyl-phosphatidylinositol moiety that anchors Trypanosoma brucei variant surface glycoprotein to the membrane. *Science* **1988,** *239* (4841), 753-759.

25. McConville, M. J.; Ferguson, M. A., The structure, biosynthesis and function of glycosylated phosphatidylinositols in the parasitic protozoa and higher eukaryotes. *Biochemical Journal* **1993,** *294* (2), 305-0.

26. Eisenhaber, B.; Maurer-Stroh, S.; Novatchkova, M.; Schneider, G.; Eisenhaber, F., Enzymes and auxiliary factors for GPI lipid anchor biosynthesis and post-translational transfer to proteins. *BioEssays* **2003,** *25* (4), 367-385.

27. Masterson, W. J.; Doering, T. L.; Hart, G. W.; Englund, P. T., A novel pathway for glycan assembly: Biosynthesis of the glycosyl-phosphatidylinositol anchor of the trypanosome variant surface glycoprotein. *Cell* **1989,** *56* (5), 793-800.

28. Ramalingam, S.; Maxwell, S. E.; Medof, M. E.; Chen, R.; Gerber, L. D.; Udenfriend, S., COOH-terminal processing of nascent polypeptides by the glycosylphosphatidylinositol transamidase in the presence of hydrazine is governed by the same parameters as glycosylphosphatidylinositol addition. *Proceedings of the National Academy of Sciences* **1996,** *93* (15), 7528-7533.

29. John, F.; Hendrickson, T. L., Synthesis of Truncated Analogues for Studying the Process of Glycosyl Phosphatidylinositol Modification. *Organic Letters* **2010,** *12* (9), 2080-2083.

30. Paulick, M. G.; Wise, A. R.; Forstner, M. B.; Groves, J. T.; Bertozzi, C. R., Synthetic Analogues of Glycosylphosphatidylinositol-Anchored Proteins and Their Behavior in Supported Lipid Bilayers. *Journal of the American Chemical Society* **2007,** *129* (37), 11543-11550.

31. Burgula, S.; Swarts, B. M.; Guo, Z., Total Synthesis of a Glycosylphosphatidylinositol Anchor of the Human Lymphocyte CD52 Antigen. *Chemistry – A European Journal* **2012,** *18* (4), 1194-1201.

32. Shao, N.; Xue, J.; Guo, Z., Chemical Synthesis of a Skeleton Structure of Sperm CD52—A GPI-Anchored Glycopeptide. *Angewandte Chemie International Edition* **2004,** *43* (12), 1569-1573.

33. Kamena, F.; Tamborrini, M.; Liu, X.; Kwon, Y.-U.; Thompson, F.; Pluschke, G.; Seeberger, P. H., Synthetic GPI array to study antitoxic malaria response. *Nat Chem Biol* **2008,** *4* (4), 238-240.

34. Schofield, L.; Hewitt, M. C.; Evans, K.; Siomos, M.-A.; Seeberger, P. H., Synthetic GPI as a candidate anti-toxic vaccine in a model of malaria. *Nature* **2002,** *418* (6899), 785-789.

35. Vainauskas, S.; Cortes, L. K.; Taron, C. H., In vivo incorporation of an azide-labeled sugar analog to detect mammalian glycosylphosphatidylinositol molecules isolated from the cell surface. *Carbohydrate Research* **2012,** *362* (0), 62-69.

36. Almeida, A.; Layton, M.; Karadimitris, A., Inherited glycosylphosphatidyl inositol deficiency: A treatable CDG. *Biochimica et Biophysica Acta (BBA) - Molecular Basis of Disease* **2009,** *1792* (9), 874-880.

37. Caras, I. W.; Weddell, G. N.; Williams, S. R., Analysis of the signal for attachment of a glycophospholipid membrane anchor. *The Journal of Cell Biology* **1989,** *108* (4), 1387-1396.

38. Ast, T.; Cohen, G.; Schuldiner, M., A Network of Cytosolic Factors Targets SRP-Independent Proteins to the Endoplasmic Reticulum. *Cell* **2013,** *152* (5), 1134-1145.

39. Murakami, Y.; Siripanyaphinyo, U.; Hong, Y.; Tashima, Y.; Maeda, Y.; Kinoshita, T., The Initial Enzyme for Glycosylphosphatidylinositol Biosynthesis Requires PIG-Y, a Seventh Component. *Molecular Biology of the Cell* **2005,** *16* (11), 5236-5246.

40. Watanabe, R.; Inoue, N.; Westfall, B.; Taron, C. H.; Orlean, P.; Takeda, J.; Kinoshita, T., The first step of glycosylphosphatidylinositol biosynthesis is mediated by a complex of PIG-A, PIG-H, PIG-C and GPI1. *EMBO J* **1998,** *17* (4), 877-885.

41. Watanabe, R.; Ohishi, K.; Maeda, Y.; Nakamura, N.; Kinoshita, T., Mammalian PIG-L and its yeast homologue Gpi12p are N-acetylglucosaminylphosphatidylinositol de-N-acetylases essential in glycosylphosphatidylinositol biosynthesis. *Biochemical Journal* **1999,** *339* (1), 185-192.

42. Tiede, A.; Nischan, C.; Schubert, J.; Schmidt, R. E., Characterisation of the enzymatic complex for the first step in glycosylphosphatidylinositol biosynthesis. *The International Journal of Biochemistry & Cell Biology* **2000,** *32* (3), 339-350.

43. Vainauskas, S.; Menon, A. K., A Conserved Proline in the Last Transmembrane Segment of Gaa1 Is Required for Glycosylphosphatidylinositol (GPI) Recognition by GPI Transamidase. *Journal of Biological Chemistry* **2004,** *279* (8), 6540-6545.

44. Murakami, Y.; Siripanyapinyo, U.; Hong, Y.; Kang, J. Y.; Ishihara, S.; Nakakuma, H.; Maeda, Y.; Kinoshita, T., PIG-W Is Critical for Inositol Acylation

but Not for Flipping of Glycosylphosphatidylinositol-Anchor. *Molecular Biology of the Cell* **2003,** *14* (10), 4285-4295.

45. Ashida, H.; Hong, Y.; Murakami, Y.; Shishioh, N.; Sugimoto, N.; Kim, Y. U.; Maeda, Y.; Kinoshita, T., Mammalian PIG-X and Yeast Pbn1p Are the Essential Components of Glycosylphosphatidylinositol-Mannosyltransferase I. *Molecular Biology of the Cell* **2005,** *16* (3), 1439-1448.

46. Maeda, Y.; Watanabe, R.; Harris, C. L.; Hong, Y.; Ohishi, K.; Kinoshita, K.; Kinoshita, T., PIG-M transfers the first mannose to glycosylphosphatidylinositol on the lumenal side of the ER. *EMBO J* **2001,** *20* (1/2), 250-261.

47. Kang, J. Y.; Hong, Y.; Ashida, H.; Shishioh, N.; Murakami, Y.; Morita, Y. S.; Maeda, Y.; Kinoshita, T., PIG-V Involved in Transferring the Second Mannose in Glycosylphosphatidylinositol. *Journal of Biological Chemistry* **2005,** *280* (10), 9489-9497.

48. Hong, Y.; Maeda, Y.; Watanabe, R.; Ohishi, K.; Mishkind, M.; Riezman, H.; Kinoshita, T., Pig-n, a Mammalian Homologue of Yeast Mcd4p, Is Involved in Transferring Phosphoethanolamine to the First Mannose of the Glycosylphosphatidylinositol. *Journal of Biological Chemistry* **1999,** *274* (49), 35099-35106.

49. Takahashi, M.; Inoue, N.; Ohishi, K.; Maeda, Y.; Nakamura, N.; Endo, Y.; Fujita, T.; Takeda, J.; Kinoshita, T., PIG-B, a membrane protein of the endoplasmic reticulum with a large lumenal domain, is involved in transferring the third mannose of the GPI anchor. *EMBO J* **1996,** *15* (16), 4254-4261.

50. Taron, B. W.; Colussi, P. A.; Wiedman, J. M.; Orlean, P.; Taron, C. H., Human Smp3p Adds a Fourth Mannose to Yeast and Human Glycosylphosphatidylinositol Precursors in Vivo. *Journal of Biological Chemistry* **2004,** *279* (34), 36083-36092.

51. Hong, Y.; Maeda, Y.; Watanabe, R.; Inoue, N.; Ohishi, K.; Kinoshita, T., Requirement of PIG-F and PIG-O for Transferring Phosphoethanolamine to the Third Mannose in Glycosylphosphatidylinositol. *Journal of Biological Chemistry* **2000,** *275* (27), 20911-20919.

52. Eisenhaber, B.; Bork, P.; Eisenhaber, F., Sequence properties of GPI-anchored proteins near the omega-site: constraints for the polypeptide binding site of the putative transamidase. *Protein Engineering* **1998,** *11* (12), 1155-1161.

53. Moran, P.; Caras, I. W., A nonfunctional sequence converted to a signal for glycophosphatidylinositol membrane anchor attachment. *The Journal of Cell Biology* **1991,** *115* (2), 329-336.

54. Kodukula, K.; Micanovic, R.; Gerber, L.; Tamburrini, M.; Brink, L.; Udenfriend, S., Biosynthesis of phosphatidylinositol glycan-anchored membrane proteins. Design of a simple protein substrate to characterize the enzyme that cleaves the COOH-terminal signal peptide. *Journal of Biological Chemistry* **1991,** *266* (7), 4464-70.

55. Varma, Y.; Hendrickson, T., Methods to Study GPI Anchoring of Proteins. *ChemBioChem* **2010,** *11* (5), 623-636.

56. Micanovic, R.; Kodukula, K.; Gerber, L. D.; Udenfriend, S., Selectivity at the cleavage/attachment site of phosphatidylinositol-glycan anchored membrane

proteins is enzymatically determined. *Proceedings of the National Academy of Sciences* **1990,** *87* (20), 7939-7943.

57. Moran, P.; Raab, H.; Kohr, W. J.; Caras, I. W., Glycophospholipid membrane anchor attachment. Molecular analysis of the cleavage/attachment site. *Journal of Biological Chemistry* **1991,** *266* (2), 1250-1257.

58. Eisenhaber, B.; Bork, P.; Eisenhaber, F., Prediction of Potential GPI-modification Sites in Proprotein Sequences. *Journal of Molecular Biology* **1999,** *292* (3), 741-758.

59. Gerber, L. D.; Kodukula, K.; Udenfriend, S., Phosphatidylinositol glycan (PI-G) anchored membrane proteins. Amino acid requirements adjacent to the site of cleavage and PI-G attachment in the COOH-terminal signal peptide. *Journal of Biological Chemistry* **1992,** *267* (17), 12168-12173.

60. Coyne, K. E.; Crisci, A.; Lublin, D. M., Construction of synthetic signals for glycosyl-phosphatidylinositol anchor attachment. Analysis of amino acid sequence requirements for anchoring. *Journal of Biological Chemistry* **1993,** *268* (9), 6689-6693.

61. Galian, C.; Björkholm, P.; Bulleid, N.; von Heijne, G., Efficient Glycosylphosphatidylinositol (GPI) Modification of Membrane Proteins Requires a C-terminal Anchoring Signal of Marginal Hydrophobicity. *Journal of Biological Chemistry* **2012,** *287* (20), 16399-16409.

62. De Groot, P. W. J.; Ram, A. F.; Klis, F. M., Features and functions of covalently linked proteins in fungal cell walls. *Fungal Genetics and Biology* **2005,** *42* (8), 657-675.

63. Lu, C. F.; Kurjan, J.; Lipke, P. N., A pathway for cell wall anchorage of Saccharomyces cerevisiae alpha-agglutinin. *Molecular and Cellular Biology* **1994,** *14* (7), 4825-4833.

64. Xia, M.-Q.; Hale, G.; Lifely, M. R.; Ferguson, M. A. J.; Campbell, D.; Packman, L.; Waldmann, H.; Xia, M.-Q.; Hale, G.; Lifely, M. R.; Ferguson, M. A. J.; Campbell, D.; Packman, L.; Waldmann, H., Structure of the CAMPATH-1 antigen, a glycosylphosphatidylinositol-anchored glycoprotein which is an exceptionally good target for complement lysis. *Biochemical Journal* **1993,** *293 (Pt 3)*, 633-640.

65. Moran, P.; Caras, I., Requirements for glycosylphosphatidylinositol attachment are similar but not identical in mammalian cells and parasitic protozoa. *J Cell Biol* **1994,** *125*, 333 - 343.

66. Morissette, R.; Varma, Y.; Hendrickson, T. L., Defining the boundaries of species specificity for the Saccharomyces cerevisiae glycosylphosphatidylinositol transamidase using a quantitative in vivo assay. *Bioscience Reports* **2012,** *32* (6), 577-586.

67. Takos, A. M.; Dry, I. B.; Soole, K. L., Glycosyl-phosphatidylinositol-anchor addition signals are processed in Nicotiana tabacum. *The Plant Journal* **2000,** *21* (1), 43-52.

68. Fankhauser, N.; Maser, P., Identification of GPI anchor attachment signals by a Kohonen self-organizing map. *Bioinformatics* **2005,** *21*, 1846 - 1852.

69. Pierleoni, A.; Martelli, P.; Casadio, R., PredGPI: a GPI-anchor predictor. *BMC Bioinformatics* **2008,** *9* (1), 392.

70. Poisson, G.; Chauve, C.; Chen, X.; Bergeron, A., FragAnchor: a large-scale predictor of glycosylphosphatidylinositol anchors in eukaryote protein sequences by qualitative scoring. *Genomics Proteomics Bioinformatics* **2007,** *5*, 121 - 130.

71. Mukai, Y.; Sasaki, T.; Oura, O.; Ikeda, M. In *Identification of mammalian GPI-anchored proteins based on amino acid propensities in their GPI attachment signal sequences*, Trendz in Information Sciences & Computing (TISC), 2010, 17-19 Dec. 2010; 2010; pp 106-110.

72. Mukai, Y.; Ikeda, M.; Tanaka, H.; Konishi, T.; Oura, O.; Sasaki, T., Discrimination of Mammalian GPI-Anchored Proteins by Hydropathy and Amino Acid Propensities. *Bioscience, Biotechnology, and Biochemistry* **2013,** *advpub*.

73. Inoue, N.; Ohishi, K.; Endo, Y.; Fujita, T.; Takeda, J.; Kinoshita, T., Human and mouse GPAA1 (Glycosylphosphatidylinositol anchor attachment 1) genes: genomic structures, chromosome loci and the presence of a minor class intron. *Cytogenetic and Genome Research* **1999,** *84* (3-4), 199-205.

74. Nagamune, K.; Ohishi, K.; Ashida, H.; Hong, Y.; Hino, J.; Kangawa, K.; Inoue, N.; Maeda, Y.; Kinoshita, T., GPI transamidase of Trypanosoma brucei has two previously uncharacterized (trypanosomatid transamidase 1 and 2) and three common subunits. *Proc Natl Acad Sci USA* **2003,** *100*, 10682 - 10687.

75. Consortium., T. U., Reorganizing the protein space at the universal protein resource (uniprot). *Nucleic Acids Res* **2012,** *40*, D71-D75.

76. Hiroi, Y.; Komuro, I.; Chen, R.; Hosoda, T.; Mizuno, T.; Kudoh, S.; Georgescu, S.; Medof, M.; Yazaki, Y., Molecular cloning of human homolog of

yeast GAA1 which is required for attachment of glycosylphosphatidylinositols to proteins. *FEBS Lett* **1998,** *421*, 252 - 258.

77. Chen, R.; Jiang, X.; Sun, D.; Han, G.; Wang, F.; Ye, M.; Wang, L.; Zou, H., Glycoproteomics Analysis of Human Liver Tissue by Combination of Multiple Enzyme Digestion and Hydrazide Chemistry. *Journal of Proteome Research* **2009,** *8* (2), 651-661.

78. Benghezal, M.; Benachour, A.; Rusconi, S.; Aebi, M.; Conzelmann, A., Yeast Gpi8p is essential for GPI anchor attachment onto proteins. *The EMBO journal* **1996,** *15* (23), 6575-6583.

79. Hamburger, D.; Egerton, M.; Riezman, H., Yeast Gaa1p is required for attachment of a completed GPI anchor onto proteins. *J Cell Biol* **1995,** *129*, 629 - 639.

80. Fraering, P.; Imhof, I.; Meyer, U.; Strub, J.-M.; van Dorsselaer, A.; Vionnet, C.; Conzelmann, A., The GPI Transamidase Complex of Saccharomyces cerevisiae Contains Gaa1p, Gpi8p, and Gpi16p. *Molecular Biology of the Cell* **2001,** *12* (10), 3295-3306.

81. Kang, X.; Szallies, A.; Rawer, M.; Echner, H.; Duszenko, M., GPI anchor transamidase of Trypanosoma brucei: in vitro assay of the recombinant protein and VSG anchor exchange. *Journal of Cell Science* **2002,** *115* (12), 2529-2539.

82. Nagamune, K.; Ohishi, K.; Ashida, H.; Hong, Y.; Hino, J.; Kangawa, K.; Inoue, N.; Maeda, Y.; Kinoshita, T., GPI transamidase of Trypanosoma brucei has two previously uncharacterized (trypanosomatid transamidase 1 and 2) and

three common subunits. *Proceedings of the National Academy of Sciences* **2003,** *100* (19), 10682-10687.

83. Meitzler, J. L.; Gray, J. J.; Hendrickson, T. L., Truncation of the caspase-related subunit (Gpi8p) of Saccharomyces cerevisiae GPI transamidase: Dimerization revealed. *Archives of Biochemistry and Biophysics* **2007,** *462* (1), 83-93.

84. Toh, Y. K.; Kamariah, N.; Maurer-Stroh, S.; Roessle, M.; Eisenhaber, F.; Adhikari, S.; Eisenhaber, B.; Grüber, G., Structural insight into the glycosylphosphatidylinositol transamidase subunits PIG-K and PIG-S from yeast. *Journal of Structural Biology* **2011,** *173* (2), 271-281.

85. Vainauskas, S.; Maeda, Y.; Kurniawan, H.; Kinoshita, T.; Menon, A. K., Structural Requirements for the Recruitment of Gaa1 into a Functional Glycosylphosphatidylinositol Transamidase Complex. *Journal of Biological Chemistry* **2002,** *277* (34), 30535-30542.

86. Ohishi, K.; Nagamune, K.; Maeda, Y.; Kinoshita, T., Two Subunits of Glycosylphosphatidylinositol Transamidase, GPI8 and PIG-T, Form a Functionally Important Intermolecular Disulfide Bridge. *Journal of Biological Chemistry* **2003,** *278* (16), 13959-13967.

87. Ohishi, K.; Nagamune, K.; Maeda, Y.; Kinoshita, T., Two subunits of glycosylphosphatidylinositol transamidase, GPI8 and PIG-T, form a functionally important intermolecular disulfide bridge. *J Biol Chem* **2003,** *278*, 13959 - 13967.

88. Ohishi, K.; Inoue, N.; Kinoshita, T., PIG-S and PIG-T, essential for GPI anchor attachment to proteins, form a complex with GAA1 and GPI8. *Embo J* **2001,** *20*, 4088 - 4098.

89. Zhu, Y.; Fraering, P.; Vionnet, C.; Conzelmann, A., Gpi17p does not stably interact with other subunits of glycosylphosphatidylinositol transamidase in Saccharomyces cerevisiae. *Biochimica et Biophysica Acta (BBA) - Molecular and Cell Biology of Lipids* **2005,** *1735* (1), 79-88.

90. Vainauskas, S.; Menon, A., A conserved proline in the last transmembrane segment of Gaa1 is required for glycosylphosphatidylinositol (GPI) recognition by GPI transamidase. *J Biol Chem* **2004,** *279*, 6540 - 6545.

91. Ohishi, K.; Inoue, N.; Maeda, Y.; Takeda, J.; Riezman, H.; Kinoshita, T., Gaa1p and Gpi8p Are Components of a Glycosylphosphatidylinositol (GPI) Transamidase That Mediates Attachment of GPI to Proteins. *Molecular Biology of the Cell* **2000,** *11* (5), 1523-1533.

92. Zacks, M. A.; Garg, N., Recent developments in the molecular, biochemical and functional characterization of GPI8 and the GPI-anchoring mechanism [Review]. *Molecular Membrane Biology* **2006,** *23* (3), 209-225.

93. Meyer, U.; Benghezal, M.; Imhof, I.; Conzelmann, A., Active Site Determination of Gpi8p, a Caspase-Related Enzyme Required for Glycosylphosphatidylinositol Anchor Addition to Proteins†. *Biochemistry* **2000,** *39* (12), 3461-3471.

94. Saw, W. G.; Eisenhaber, B.; Eisenhaber, F.; Grüber, G., Low resolution structure of the soluble domain GPAA1 (yGPAA170-247) of the

glycosylphosphatidylinositol transamidase subunit GPAA1 from Saccharomyces cerevisiae. *Biosci Rep* **2013**.

95. Reorganizing the protein space at the Universal Protein Resource (UniProt). In *Nucleic Acids Research*, The UniProt Consortium: 2012; Vol. 40, pp D71-D75.

96. Chen, R.; Anderson, V.; Hiroi, Y.; Medof, M. E., Proprotein interaction with the GPI transamidase. *Journal of Cellular Biochemistry* **2003,** *88* (5), 1025-1037.

97. Bishop, J. M., Molecular themes in oncogenesis. *Cell* **1991,** *64* (2), 235-248.

98. Guan, X.-Y.; Xu, J.; Anzick, S. L.; Zhang, H.; Trent, J. M.; Meltzer, P. S., Hybrid Selection of Transcribed Sequences from Microdissected DNA: Isolation of Genes within an Amplified Region at 20q11–q13.2 in Breast Cancer. *Cancer Research* **1996,** *56* (15), 3446-3450.

99. Kallioniemi, A.; Kallioniemi, O. P.; Piper, J.; Tanner, M.; Stokke, T.; Chen, L.; Smith, H. S.; Pinkel, D.; Gray, J. W.; Waldman, F. M., Detection and mapping of amplified DNA sequences in breast cancer by comparative genomic hybridization. *Proceedings of the National Academy of Sciences* **1994,** *91* (6), 2156-2160.

100. Kallioniemi, A.; Kallioniemi, O.-P.; Citro, G.; Sauter, G.; Devries, S.; Kerschmann, R.; Caroll, P.; Waldman, F., Identification of gains and losses of DNA sequences in primary bladder cancer by comparative genomic hybridization. *Genes, Chromosomes and Cancer* **1995,** *12* (3), 213-219.

101. Pere, H.; Tapper, J.; Wahlström, T.; Knuutila, S.; Butzow, R., Distinct Chromosomal Imbalances in Uterine Serous and Endometrioid Carcinomas. *Cancer Research* **1998,** *58* (5), 892-895.

102. Wilting, S. M.; Snijders, P. J. F.; Meijer, G. A.; Ylstra, B.; van den Ijssel, P.; Snijders, A. M.; Albertson, D. G.; Coffa, J.; Schouten, J. P.; van de Wiel, M. A.; Meijer, C.; Steenbergen, R. D. M., Increased gene copy numbers at chromosome 20q are frequent in both squamous cell carcinomas and adenocarcinomas of the cervix. *The Journal of Pathology* **2006,** *209* (2), 220-230.

103. Nagpal, J. K.; Dasgupta, S.; Jadallah, S.; Chae, Y. K.; Ratovitski, E. A.; Toubaji, A.; Netto, G. J.; Eagle, T.; Nissan, A.; Sidransky, D.; Trink, B., Profiling the expression pattern of GPI transamidase complex subunits in human cancer. *Mod Pathol* **2008,** *21* (8), 979-991.

104. Zhao, P.; Nairn, A. V.; Hester, S.; Moremen, K. W.; O'Regan, R. M.; Oprea, G.; Wells, L.; Pierce, M.; Abbott, K. L., Proteomic Identification of Glycosylphosphatidylinositol Anchor-dependent Membrane Proteins Elevated in Breast Carcinoma. *Journal of Biological Chemistry* **2012,** *287* (30), 25230-25240.

105. Schoenberg, M.; Kiemeney, L.; Walsh, P. C.; Griffin, C. A.; Sidransky, D., Germline Translocation t(5;20)(p15;q11) and Familial Transitional Cell Carcinoma. *The Journal of Urology* **1996,** *155* (3), 1035-1036.

106. Andres, S. A.; Edwards, A. B.; Wittliff, J. L., Expression of Urokinase-Type Plasminogen Activator (uPA), its Receptor (uPAR), and Inhibitor (PAI-1) in Human Breast Carcinomas and Their Clinical Relevance. *Journal of Clinical Laboratory Analysis* **2012,** *26* (2), 93-103.

107. Mekkawy, A. H.; Morris, D. L.; Pourgholami, M. H., Urokinase plasminogen activator system as a potential target for cancer therapy. *Future Oncology* **2009,** *5* (9), 1487-1499.

108. Schultz, I. J.; Kiemeney, L. A.; Witjes, J. A.; Schalken, J. A.; Willems, J. L.; Swinkels, D. W.; de Kok, J. B., CDC91L1 (PIG-U) mRNA expression in urothelial cell carcinomas. *International Journal of Cancer* **2005,** *116* (2), 282-284.

109. Shen, Y.-J.; Ye, D.-W.; Yao, X.-D.; Trink, B.; Zhou, X.-Y.; Zhang, S.-L.; Dai, B.; Zhang, H.-L.; Zhu, Y.; Guo, Z.; Wu, G.; Nagpal, J., Overexpression of CDC91L1 (PIG-U) in bladder urothelial cell carcinoma: correlation with clinical variables and prognostic significance. *BJU International* **2008,** *101* (1), 113-119.

110. Wu, G.; Guo, Z.; Chatterjee, A.; Huang, X.; Rubin, E.; Wu, F.; Mambo, E.; Chang, X.; Osada, M.; Sook Kim, M.; Moon, C.; Califano, J.; Ratovitski, E.; Gollin, S.; Sukumar, S.; Sidransky, D.; Trink, B., Overexpression of glycosylphosphatidylinositol (GPI) transamidase subunits phosphatidylinositol glycan class T and/or GPI anchor attachment 1 induces tumorigenesis and contributes to invasion in human breast cancer. *Cancer Res* **2006,** *66*, 9829 - 36.

111. Huang, C.; Jacobson, K.; Schaller, M. D., A Role for JNK-Paxillin Signaling in Cell Migration. *Cell Cycle* **2004,** *3* (1), 3-5.

112. Conway, W. C.; Van der Voort van Zyp, J.; Thamilselvan, V.; Walsh, M. F.; Crowe, D. L.; Basson, M. D., Paxillin modulates squamous cancer cell adhesion and is important in pressure-augmented adhesion. *Journal of Cellular Biochemistry* **2006,** *98* (6), 1507-1516.

113. Lidell, M. E.; Seifert, E. L.; Westergren, R.; Heglind, M.; Gowing, A.; Sukonina, V.; Arani, Z.; Itkonen, P.; Wallin, S.; Westberg, F.; Fernandez-Rodriguez, J.; Laakso, M.; Nilsson, T.; Peng, X.-R.; Harper, M.-E.; Enerbäck, S., The Adipocyte-Expressed Forkhead Transcription Factor Foxc2 Regulates Metabolism Through Altered Mitochondrial Function. *Diabetes* **2011,** *60* (2), 427-435.

114. Yiping, H.; Jatin, N.; Barry, T.; Edward, R., Tobacco Smoke Activates Protein Association and Tyrosine Phosphorylation of the GPI-Transamidase Complex Subunits in Human Cancers. *Journal of Epithelial Biology and Pharmacology* **2009,** *2*, 14-22.

115. Balsara, B. R.; Sonoda, G.; du Manoir, S.; Siegfried, J. M.; Gabrielson, E.; Testa, J. R., Comparative Genomic Hybridization Analysis Detects Frequent, Often High-Level, Overrepresentation of DNA Sequences at 3q, 5p, 7p, and 8q in Human Non-Small Cell Lung Carcinomas. *Cancer Research* **1997,** *57* (11), 2116-2120.

116. Sonoda, G.; Palazzo, J.; du Manoir, S.; Godwin, A. K.; Feder, M.; Yakushiji, M.; Testa, J. R., Comparative genomic hybridization detects frequent overrepresentation of chromosomal material from 3q26, 8q24, and 20q13 in human ovarian carcinomas. *Genes, Chromosomes and Cancer* **1997,** *20* (4), 320-328.

117. Yokota, T.; Yoshimoto, M.; Akiyama, F.; Sakamoto, G.; Kasumi, F.; Nakamura, Y.; Emi, M., Frequent multiplication of chromosomal region 8q24.1

associated with aggressive histologic types of breast cancers. *Cancer letters* **1999,** *139* (1), 7-13.

118. Tsuchiya, N.; Kondo, Y.; Takahashi, A.; Pawar, H.; Qian, J.; Sato, K.; Lieber, M. M.; Jenkins, R. B., Mapping and Gene Expression Profile of the Minimally Overrepresented 8q24 Region in Prostate Cancer. *The American Journal of Pathology* **2002,** *160* (5), 1799-1806.

119. Jiang, W.-W.; Zahurak, M.; Zhou, Z.-T.; Park, H.; Guo, Z.-M.; Wu, G.-J.; Sidransky, D.; Trink, B.; Califano, J., Alterations of GPI transamidase subunits in head and neck squamous carcinoma. *Molecular Cancer* **2007,** *6* (1), 74.

120. Kurokawa, Y.; Matoba, R.; Nakamori, S.; Takemasa, I.; Nagano, H.; Dono, K.; Umeshita, K.; Sakon, M.; Monden, M.; Kato, K., PCR-array gene expression profiling of hepatocellular carcinoma. *J. Exp. Clin. Cancer Res.* **2004,** *23* (1), 135-41.

121. Ho, J. C.; Cheung, S. T.; Patil, M.; Chen, X.; Fan, S. T., Increased expression of glycosyl-phosphatidylinositol anchor attachment protein 1 (GPAA1) is associated with gene amplification in hepatocellular carcinoma. *International Journal of Cancer* **2006,** *119* (6), 1330-1337.

122. Chen, H.-Y.; Shen, C.-H.; Tsai, Y.-T.; Lin, F.-C.; Huang, Y.-P.; Chen, R.-H., Brk Activates Rac1 and Promotes Cell Migration and Invasion by Phosphorylating Paxillin. *Molecular and Cellular Biology* **2004,** *24* (24), 10558-10572.

123. Rooney, P. H.; Murray, G. I.; Stevenson, D. A. J.; Haites, N. E.; Cassidy, J.; McLeod, H. L., Comparative genomic hybridization and chromosomal instability in solid tumours. *Br J Cancer* **1999,** *80* (5-6), 862-873.

124. Santanu, D.; Prodipto, P.; D., M. N.; Yumei, F.; A., R.; Chul-So, M.; Mohammad, O. H.; B., F. P.; Barry, T., A single nucleotide polymorphism in the human PIGK gene associates with low PIGK expression in colorectal cancer patients. *International Journal of Oncology* **2012,** *41* (4), 1405-1410.

125. Grimme, S. J.; Gao, X.-D.; Martin, P. S.; Tu, K.; Tcheperegine, S. E.; Corrado, K.; Farewell, A. E.; Orlean, P.; Bi, E., Deficiencies in the Endoplasmic Reticulum (ER)-Membrane Protein Gab1p Perturb Transfer of Glycosylphosphatidylinositol to Proteins and Cause Perinuclear ER-associated Actin Bar Formation. *Molecular Biology of the Cell* **2004,** *15* (6), 2758-2770.

126. Wu, G.; Guo, Z.; Chatterjee, A.; Huang, X.; Rubin, E.; Wu, F.; Mambo, E.; Chang, X.; Osada, M.; Sook Kim, M.; Moon, C.; Califano, J. A.; Ratovitski, E. A.; Gollin, S. M.; Sukumar, S.; Sidransky, D.; Trink, B., Overexpression of Glycosylphosphatidylinositol (GPI) Transamidase Subunits Phosphatidylinositol Glycan Class T and/or GPI Anchor Attachment 1 Induces Tumorigenesis and Contributes to Invasion in Human Breast Cancer. *Cancer Research* **2006,** *66* (20), 9829-9836.

127. Kawagoe, K.; Kitamura, D.; Okabe, M.; Taniuchi, I.; Ikawa, M.; Watanabe, T.; Kinoshita, T.; Takeda, J., Glycosylphosphatidylinositol-anchor-deficient mice: implications for clonal dominance of mutant cells in paroxysmal nocturnal hemoglobinuria. *Blood* **1996,** *87* (9), 3600-3606.

128. Hazenbos, W. L. W.; Clausen, B. E.; Takeda, J.; Kinoshita, T., GPI-anchor deficiency in myeloid cells causes impaired FcγR effector functions. *Blood* **2004,** *104* (9), 2825-2831.

129. Pittet, M.; Conzelmann, A., Biosynthesis and function of GPI proteins in the yeast Saccharomyces cerevisiae. *Biochimica et Biophysica Acta (BBA) - Molecular and Cell Biology of Lipids* **2007,** *1771* (3), 405-420.

130. Ueda, Y.; Yamaguchi, R.; Ikawa, M.; Okabe, M.; Morii, E.; Maeda, Y.; Kinoshita, T., PGAP1 Knock-out Mice Show Otocephaly and Male Infertility. *Journal of Biological Chemistry* **2007,** *282* (42), 30373-30380.

131. Prusiner, S., Molecular biology of prion diseases. *Science* **1991,** *252* (5012), 1515-1522.

132. Nakatsura, T.; Yoshitake, Y.; Senju, S.; Monji, M.; Komori, H.; Motomura, Y.; Hosaka, S.; Beppu, T.; Ishiko, T.; Kamohara, H.; Ashihara, H.; Katagiri, T.; Furukawa, Y.; Fujiyama, S.; Ogawa, M.; Nakamura, Y.; Nishimura, Y., Glypican-3, overexpressed specifically in human hepatocellular carcinoma, is a novel tumor marker. *Biochemical and Biophysical Research Communications* **2003,** *306* (1), 16-25.

133. Aceto, J.; Kieber-Emmons, T.; Cines, D. B., Carboxy-Terminal Processing of the Urokinase Receptor: Implications for Substrate Recognition and Glycosylphosphatidylinositol Anchor Addition†. *Biochemistry* **1998,** *38* (3), 992-1001.

134. Solberg, H.; Ploug, M.; Høyer–Hansen, G.; Nielsen, B. S.; Lund, L. R., The Murine Receptor for Urokinase-Type Plasminogen Activator Is Primarily

Expressed in Tissues Actively Undergoing Remodeling. *Journal of Histochemistry & Cytochemistry* **2001,** *49* (2), 237-246.

135. Ellis, V.; Pyke, C.; Eriksen, J.; Solberg, H.; DanØ, K., The Urokinase Receptor: Involvement in Cell Surface Proteolysis and Cancer Invasion. *Annals of the New York Academy of Sciences* **1992,** *667* (1), 13-31.

136. Almasi, C. E.; Brasso, K.; Iversen, P.; Pappot, H.; Høyer-Hansen, G.; Danø, K.; Christensen, I. J., Prognostic and predictive value of intact and cleaved forms of the urokinase plasminogen activator receptor in metastatic prostate cancer. *The Prostate* **2011,** *71* (8), 899-907.

137. Park, J. S.; Park, J. H.; Khoi, P. N.; Joo, Y. E.; Jung, Y. D., MSP-induced RON activation upregulates uPAR expression and cell invasiveness via MAPK, AP-1 and NF-κB signals in gastric cancer cells. *Carcinogenesis* **2011,** *32* (2), 175-181.

138. Asuthkar, S.; Gondi, C. S.; Nalla, A. K.; Velpula, K. K.; Gorantla, B.; Rao, J. S., Urokinase-type Plasminogen Activator Receptor (uPAR)-mediated Regulation of WNT/β-Catenin Signaling Is Enhanced in Irradiated Medulloblastoma Cells. *Journal of Biological Chemistry* **2012,** *287* (24), 20576-20589.

139. Waldron, N. N.; Oh, S.; Vallera, D. A., Bispecific targeting of EGFR and uPAR in a mouse model of head and neck squamous cell carcinoma. *Oral oncology* **2012,** *48* (12), 1202-1207.

140. Bujanda, L.; Sarasqueta, C.; Cosme, A.; Hijona, E.; Enríquez-Navascués, J. M.; Placer, C.; Villarreal, E.; Herreros-Villanueva, M.; Giraldez, M. D.;

Gironella, M.; Balaguer, F.; Castells, A., Evaluation of Alpha 1-Antitrypsin and the Levels of mRNA Expression of Matrix Metalloproteinase 7, Urokinase Type Plasminogen Activator Receptor and COX-2 for the Diagnosis of Colorectal Cancer. *PLoS ONE* **2013,** *8* (1), e51810.

141. Ossowski, L.; Reich, E., Antibodies to plasminogen activator inhibit human tumor metastasis. *Cell* **1983,** *35* (3), 611-619.

142. Rea, V. E. A.; Lavecchia, A.; Di Giovanni, C.; Rossi, F. W.; Gorrasi, A.; Pesapane, A.; de Paulis, A.; Ragno, P.; Montuori, N., Discovery of new small molecules targeting the vitronectin binding site of the urokinase receptor that block cancer cell invasion. *Molecular Cancer Therapeutics* **2013**.

143. Wilhelm, O.; Weidle, U.; Höhl, S.; Rettenberger, P.; Schmitt, M.; Graeff, H., Recombinant soluble urokinase receptor as a scavenger for urokinase-type plasminogen activator (uPA): Inhibition of proliferation and invasion of human ovarian cancer cells. *FEBS Letters* **1994,** *337* (2), 131-134.

144. Ertongur, S.; Lang, S.; Mack, B.; Wosikowski, K.; Muehlenweg, B.; Gires, O., Inhibition of the invasion capacity of carcinoma cells by WX-UK1, a novel synthetic inhibitor of the urokinase-type plasminogen activator system. *International Journal of Cancer* **2004,** *110* (6), 815-824.

145. Jankun, J., Antitumor Activity of the Type 1 Plasminogen Activator Inhibitor and Cytotoxic Conjugate in Vitro. *Cancer Research* **1992,** *52* (20), 5829-5832.

146. Ploug, M.; Østergaard, S.; Gårdsvoll, H.; Kovalski, K.; Holst-Hansen, C.; Holm, A.; Ossowski, L.; Danø, K., Peptide-Derived Antagonists of the Urokinase

Receptor. Affinity Maturation by Combinatorial Chemistry, Identification of Functional Epitopes, and Inhibitory Effect on Cancer Cell Intravasation†. *Biochemistry* **2001,** *40* (40), 12157-12168.

147. Filmus, J.; Selleck, S. B., Glypicans: proteoglycans with a surprise. *The Journal of Clinical Investigation* **2001,** *108* (4), 497-501.

148. Pilia, G.; Hughes-Benzie, R. M.; MacKenzie, A.; Baybayan, P.; Chen, E. Y.; Huber, R.; Neri, G.; Cao, A.; Forabosco, A.; Schlessinger, D., Mutations in GPC3, a glypican gene, cause the Simpson-Golabi-Behmel overgrowth syndrome. *Nat Genet* **1996,** *12* (3), 241-247.

149. Li, M.; Choo, B.; Wong, Z.-M.; Filmus, J.; Buick, R. N., Expression of OCI-5/Glypican 3 during Intestinal Morphogenesis: Regulation by Cell Shape in Intestinal Epithelial Cells. *Experimental Cell Research* **1997,** *235* (1), 3-12.

150. Litwack, E. D.; Ivins, J. K.; Kumbasar, A.; Paine-Saunders, S.; Stipp, C. S.; Lander, A. D., Expression of the heparan sulfate proteoglycan glypican-1 in the developing rodent. *Developmental Dynamics* **1998,** *211* (1), 72-87.

151. Kleeff, J.; Ishiwata, T.; Kumbasar, A.; Friess, H.; xFc; chler, M. W.; Lander, A. D.; Korc, M., The cell-surface heparan sulfate proteoglycan glypican-1 regulates growth factor action in pancreatic carcinoma cells and is overexpressed in human pancreatic cancer. *The Journal of Clinical Investigation* **1998,** *102* (9), 1662-1673.

152. Umezu, T.; Shibata, K.; Shimaoka, M.; Kajiyama, H.; Yamamoto, E.; Ino, K.; Nawa, A.; Senga, T.; Kikkawa, F., Gene silencing of glypican-3 in clear cell

carcinoma of the ovary renders it more sensitive to the apoptotic agent paclitaxel in vitro and in vivo. *Cancer Science* **2010,** *101* (1), 143-148.

153. De Rienzo, A.; Ferriola, P. C.; Filmus, J.; Jhanwar, S. C.; Lee, W.-C.; Mossman, B. T.; Murthy, S. S.; Shen, T.; Testa, J. R., Expression of GPC3, an X-linked recessive overgrowth gene, is silenced in malignant mesothelioma. *Oncogene* **2000,** *19*, 410.

154. Yun-Yan, X.; Virginia, L.; Jorge, F., Glypican-3 expression is silenced in human breast cancer. *Oncogene* **2001,** *20* (50).

155. Kim, H.; Xu, G.-L.; Borczuk, A. C.; Busch, S.; Filmus, J.; Capurro, M.; Brody, J. S.; Lange, J.; D'Armiento, J. M.; Rothman, P. B.; Powell, C. A., The Heparan Sulfate Proteoglycan GPC3 Is a Potential Lung Tumor Suppressor. *American Journal of Respiratory Cell and Molecular Biology* **2003,** *29* (6), 694-701.

156. Nakatsura, T.; Komori, H.; Kubo, T.; Yoshitake, Y.; Senju, S.; Katagiri, T.; Furukawa, Y.; Ogawa, M.; Nakamura, Y.; Nishimura, Y., Mouse Homologue of a Novel Human Oncofetal Antigen, Glypican-3, Evokes T-Cell–Mediated Tumor Rejection without Autoimmune Reactions in Mice. *Clinical Cancer Research* **2004,** *10* (24), 8630-8640.

157. Ishiguro, T.; Sugimoto, M.; Kinoshita, Y.; Miyazaki, Y.; Nakano, K.; Tsunoda, H.; Sugo, I.; Ohizumi, I.; Aburatani, H.; Hamakubo, T.; Kodama, T.; Tsuchiya, M.; Yamada-Okabe, H., Anti–Glypican 3 Antibody as a Potential Antitumor Agent for Human Liver Cancer. *Cancer Research* **2008,** *68* (23), 9832-9838.

158. Ho, M.; Kim, H., Glypican-3: A new target for cancer immunotherapy. *European Journal of Cancer* **2011,** *47* (3), 333-338.

159. Vastag, B. B., Folate gains momentum as a vehicle for drug delivery. *J Natl Cancer Inst* **2000,** *92* (22), 1800-1801.

160. Shen, F.; Wu, M.; Ross, J. F.; Miller, D.; Ratnam, M., Folate Receptor Type .gamma. Is Primarily a Secretory Protein Due to Lack of an Efficient Signal for Glycosylphosphatidylinositol Modification: Protein Characterization and Cell Type Specificity. *Biochemistry* **1995,** *34* (16), 5660-5665.

161. Yan, W.; Ratnam, M., Preferred Sites of Glycosylphosphatidylinositol Modification in Folate Receptors and Constraints in the Primary Structure of the Hydrophobic Portion of the Signal. *Biochemistry* **1995,** *34* (44), 14594-14600.

162. Cagle, P. T.; Zhai, Q. J.; Murphy, L.; Low, P. S., Folate Receptor in Adenocarcinoma and Squamous Cell Carcinoma of the Lung: Potential Target for Folate-Linked Therapeutic Agents. *Archives of Pathology & Laboratory Medicine* **2012,** *137* (2), 241-244.

163. O'Shannessy, D.; Somers, E.; Maltzman, J.; Smale, R.; Fu, Y.-S., Folate receptor alpha (FRA) expression in breast cancer: identification of a new molecular subtype and association with triple negative disease. *SpringerPlus* **2012,** *1* (1), 22.

164. Leung, F.; Dimitromanolakis, A.; Kobayashi, H.; Diamandis, E. P.; Kulasingam, V., Folate-receptor 1 (FOLR1) protein is elevated in the serum of ovarian cancer patients. *Clinical Biochemistry* **2013,** (0).

165. Goren, D.; Horowitz, A. T.; Tzemach, D.; Tarshish, M.; Zalipsky, S.; Gabizon, A., Nuclear Delivery of Doxorubicin via Folate-targeted Liposomes with Bypass of Multidrug-resistance Efflux Pump. *Clinical Cancer Research* **2000,** *6* (5), 1949-1957.

166. Konda, S. D.; Aref, M.; Wang, S.; Brechbiel, M.; Wiener, E. C., Specific targeting of folate–dendrimer MRI contrast agents to the high affinity folate receptor expressed in ovarian tumor xenografts. *Magnetic Resonance Materials in Physics, Biology and Medicine* **2001,** *12* (2–3), 104-113.

167. Leamon, C. P.; Parker, M. A.; Vlahov, I. R.; Xu, L.-C.; Reddy, J. A.; Vetzel, M.; Douglas, N., Synthesis and Biological Evaluation of EC20: A New Folate-Derived, 99mTc-Based Radiopharmaceutical. *Bioconjugate Chemistry* **2002,** *13* (6), 1200-1210.

168. Siegel, B. A.; Dehdashti, F.; Mutch, D. G.; Podoloff, D. A.; Wendt, R.; Sutton, G. P.; Burt, R. W.; Ellis, P. R.; Mathias, C. J.; Green, M. A.; Gershenson, D. M., Evaluation of 111In-DTPA-Folate as a Receptor-Targeted Diagnostic Agent for Ovarian Cancer: Initial Clinical Results. *Journal of Nuclear Medicine* **2003,** *44* (5), 700-707.

169. Fisher, R. E.; Siegel, B. A.; Edell, S. L.; Oyesiku, N. M.; Morgenstern, D. E.; Messmann, R. A.; Amato, R. J., Exploratory Study of 99mTc-EC20 Imaging for Identifying Patients with Folate Receptor–Positive Solid Tumors. *Journal of Nuclear Medicine* **2008,** *49* (6), 899-906.

170. Fani, M.; Tamma, M.-L.; Nicolas, G. P.; Lasri, E.; Medina, C.; Raynal, I.; Port, M.; Weber, W. A.; Maecke, H. R., In Vivo Imaging of Folate Receptor

Positive Tumor Xenografts Using Novel 68Ga-NODAGA-Folate Conjugates. *Molecular Pharmaceutics* **2012,** *9* (5), 1136-1145.

171. Fischer, C. R.; Müller, C.; Reber, J.; Müller, A.; Krämer, S. D.; Ametamey, S. M.; Schibli, R., [18F]Fluoro-Deoxy-Glucose Folate: A Novel PET Radiotracer with Improved in Vivo Properties for Folate Receptor Targeting. *Bioconjugate Chemistry* **2012,** *23* (4), 805-813.

172. Koumarianou, E.; Loktionova, N. S.; Fellner, M.; Roesch, F.; Thews, O.; Pawlak, D.; Archimandritis, S. C.; Mikolajczak, R., 44Sc-DOTA-BN[2-14]NH2 in comparison to 68Ga-DOTA-BN[2-14]NH2 in pre-clinical investigation. Is 44Sc a potential radionuclide for PET? *Applied Radiation and Isotopes* **2012,** *70* (12), 2669-2676.

173. Müller, C.; Zhernosekov, K.; Köster, U.; Johnston, K.; Dorrer, H.; Hohn, A.; van der Walt, N. T.; Türler, A.; Schibli, R., A Unique Matched Quadruplet of Terbium Radioisotopes for PET and SPECT and for α- and β−-Radionuclide Therapy: An In Vivo Proof-of-Concept Study with a New Receptor-Targeted Folate Derivative. *Journal of Nuclear Medicine* **2012,** *53* (12), 1951-1959.

174. Amato, R. J.; Shetty, A.; Lu, Y.; Ellis, R.; Low, P. S., A Phase I Study of Folate Immune Therapy (EC90 Vaccine Administered With GPI-0100 Adjuvant Followed by EC17) in Patients With Renal Cell Carcinoma. *Journal of Immunotherapy* **2013,** *36* (4), 268-275 10.1097/CJI.0b013e3182917f59.

175. Ak, G.; Sanlıer, S. H., Synthesis of folate receptor- targeted and Doxorubicin coupled chemotherapeutic nanoconjugate and research into its

medical application. *Preparative Biochemistry and Biotechnology* **2012,** *42* (6), 551-563.

176. LoRusso, P. M.; Edelman, M. J.; Bever, S. L.; Forman, K. M.; Pilat, M.; Quinn, M. F.; Li, J.; Heath, E. I.; Malburg, L. M.; Klein, P. J.; Leamon, C. P.; Messmann, R. A.; Sausville, E. A., Phase I Study of Folate Conjugate EC145 (Vintafolide) in Patients With Refractory Solid Tumors. *Journal of Clinical Oncology* **2012,** *30* (32), 4011-4016.

177. Wood, L. D., *Folate Receptor Alpha: A New Tool in the Diagnosis and Treatment of Lung Cancer*. 2012; Vol. 3.

178. Chen, L.-M.; Skinner, M. L.; Kauffman, S. W.; Chao, J.; Chao, L.; Thaler, C. D.; Chai, K. X., Prostasin Is a Glycosylphosphatidylinositol-anchored Active Serine Protease. *Journal of Biological Chemistry* **2001,** *276* (24), 21434-21442.

179. Schild, L.; Kellenberger, S., Structure function relationships of ENaC and its role in sodium handling. In *Hypoxia*, Roach, R.; Wagner, P.; Hackett, P., Eds. Springer US: 2001; Vol. 502, pp 305-314.

180. Rossier, B. C., The Epithelial Sodium Channel. *Proceedings of the American Thoracic Society* **2004,** *1* (1), 4-9.

181. Takahashi, S.; Suzuki, S.; Inaguma, S.; Ikeda, Y.; Cho, Y.-M.; Hayashi, N.; Inoue, T.; Sugimura, Y.; Nishiyama, N.; Fujita, T.; Chao, J.; Ushijima, T.; Shirai, T., Down-regulated expression of prostasin in high-grade or hormone-refractory human prostate cancers. *The Prostate* **2003,** *54* (3), 187-193.

182. Sakashita, K.; Mimori, K.; Tanaka, F.; Tahara, K.; Inoue, H.; Sawada, T.; Ohira, M.; Hirakawa, K.; Mori, M., Clinical significance of low expression of

Prostasin mRNA in human gastric cancer. *Journal of Surgical Oncology* **2008,** *98* (7), 559-564.

183. Costa, F. P.; Batista Junior, E. L.; Zelmanowicz, A.; Svedman, C.; Devenz, G.; Alves, S.; Silva, A. S. M. d.; Garicochea, B., Prostasin, a potential tumor marker in ovarian cancer: a pilot study. *Clinics* **2009,** *64*, 641-644.

184. Selzer-Plon, J.; Bornholdt, J.; Friis, S.; Bisgaard, H.; Lothe, I.; Tveit, K.; Kure, E.; Vogel, U.; Vogel, L., Expression of prostasin and its inhibitors during colorectal cancer carcinogenesis. *BMC Cancer* **2009,** *9* (1), 201.

185. Kinoshita, T., Enzymatic mechanism of GPI anchor attachment clarified. *Cell Cycle* **2014,** *13* (12), 1838-1839.

186. Eisenhaber, B.; Eisenhaber, S.; Kwang, T. Y.; Grüber, G.; Eisenhaber, F., Transamidase subunit GAA1/GPAA1 is a M28 family metallo-peptide-synthetase that catalyzes the peptide bond formation between the substrate protein's omega-site and the GPI lipid anchor's phosphoethanolamine. *Cell Cycle* **2014,** *13* (12), 1912-1917.

187. Gamage, D. G.; Hendrickson, T. L., GPI Transamidase and GPI anchored proteins: Oncogenes and biomarkers for cancer. *Critical Reviews in Biochemistry and Molecular Biology* **2013,** *48* (5), 446-464.

188. Delic, M.; Valli, M.; Graf, A. B.; Pfeffer, M.; Mattanovich, D.; Gasser, B., The secretory pathway: exploring yeast diversity. *FEMS Microbiology Reviews* **2013,** *37* (6), 872-914.

189. Bertram, G.; Swoboda, R. K.; Gooday, G. W.; Gow, N. A. R.; Brown, A. J. P., Structure and regulation of the Candida albicans ADH1 gene encoding an immunogenic alcohol dehydrogenase. *Yeast* **1996,** *12* (2), 115-127.

190. Kornfeld, R.; Kornfeld, S., Assembly of Asparagine-Linked Oligosaccharides. *Annual Review of Biochemistry* **1985,** *54* (1), 631-664.

191. Karaivanova, V. K.; Spiro, R. G., Effect of proteasome inhibitors on the release into the cytosol of free polymannose oligosaccharides from glycoproteins. *Glycobiology* **2000,** *10* (7), 727-735.

192. Helenius, A.; Aebi; Markus, Intracellular Functions of N-Linked Glycans. *Science* **2001,** *291* (5512), 2364-2369.

193. Rudd, P. M.; Elliott, T.; Cresswell, P.; Wilson, I. A.; Dwek, R. A., Glycosylation and the Immune System. *Science* **2001,** *291* (5512), 2370-2376.

194. Jakimowicz, D.; Majka, J.; Konopa, G.; Węgrzyn, G.; Messer, W.; Schrempf, H.; Zakrzewska-Czerwińska, J., Architecture of the streptomyces lividans DnaA protein-replication origin complexes. *Journal of Molecular Biology* **2000,** *298* (3), 351-364.

195. Grakoui, A.; Bromley, S. K.; Sumen, C.; Davis, M. M.; Shaw, A. S.; Allen, P. M.; Dustin, M. L., The Immunological Synapse: A Molecular Machine Controlling T Cell Activation. *Science* **1999,** *285* (5425), 221-227.

196. Zhou, F.; Xu, W.; Hong, M.; Pan, Z.; Sinko, P. J.; Ma, J.; You, G., The Role of N-Linked Glycosylation in Protein Folding, Membrane Targeting, and Substrate Binding of Human Organic Anion Transporter hOAT4. *Molecular Pharmacology* **2005,** *67* (3), 868-876.

197. Sriram, V.; Willard, C. A.; Liu, J.; Brutkiewicz, R. R., Importance of N-linked glycosylation in the functional expression of murine CD1d1. *Immunology* **2008,** *123* (2), 272-281.

198. Maley, F.; Trimble, R. B.; Tarentino, A. L.; Plummer Jr, T. H., Characterization of glycoproteins and their associated oligosaccharides through the use of endoglycosidases. *Analytical Biochemistry* **1989,** *180* (2), 195-204.

199. Woods, L. A.; Radford, S. E.; Ashcroft, A. E., Advances in ion mobility spectrometry–mass spectrometry reveal key insights into amyloid assembly. *Biochimica et Biophysica Acta (BBA) - Proteins and Proteomics* **2013,** *1834* (6), 1257-1268.

200. Williams, D. M.; Pukala, T. L., Novel insights into protein misfolding diseases revealed by ion mobility-mass spectrometry. *Mass Spectrometry Reviews* **2013,** *32* (3), 169-187.

201. Bernstein, S. L.; Dupuis, N. F.; Lazo, N. D.; Wyttenbach, T.; Condron, M. M.; Bitan, G.; Teplow, D. B.; Shea, J.-E.; Ruotolo, B. T.; Robinson, C. V.; Bowers, M. T., Amyloid-β protein oligomerization and the importance of tetramers and dodecamers in the aetiology of Alzheimer's disease. *Nat Chem* **2009,** *1* (4), 326-331.

202. Young, L. M.; Cao, P.; Raleigh, D. P.; Ashcroft, A. E.; Radford, S. E., Ion Mobility Spectrometry–Mass Spectrometry Defines the Oligomeric Intermediates in Amylin Amyloid Formation and the Mode of Action of Inhibitors. *Journal of the American Chemical Society* **2013,** *136* (2), 660-670.

203. Inutan, E.; Trimpin, S., Laserspray Ionization (LSI) Ion Mobility Spectrometry (IMS) Mass Spectrometry. *Journal of the American Society for Mass Spectrometry* **2010,** *21* (7), 1260-1264.

204. Broz, P.; von Moltke, J.; Jones, J. W.; Vance, R. E.; Monack, D. M., Differential Requirement for Caspase-1 Autoproteolysis in Pathogen-Induced Cell Death and Cytokine Processing. *Cell Host & Microbe* **2010,** *8* (6), 471-483.

205. Martinon, F.; Mayor, A.; Tschopp, J., The Inflammasomes: Guardians of the Body. *Annual Review of Immunology* **2009,** *27* (1), 229-265.

206. Guo, Z.; Linn, J. F.; Wu, G.; Anzick, S. L.; Eisenberger, C. F.; Halachmi, S.; Cohen, Y.; Fomenkov, A.; Hoque, M. O.; Okami, K.; Steiner, G.; Engles, J. M.; Osada, M.; Moon, C.; Ratovitski, E.; Trent, J. M.; Meltzer, P. S.; Westra, W. H.; Kiemeney, L. A.; Schoenberg, M. P.; Sidransky, D.; Trink, B., CDC91L1 (PIG-U) is a newly discovered oncogene in human bladder cancer. *Nat Med* **2004,** *10* (4), 374-381.

207. Varma, Y. Structural and biochemical characterization of components of the fungal GPI transamidase. Johns Hopkins University, Maryland, 2011.

208. Rohl, C. A.; Strauss, C. E. M.; Chivian, D.; Baker, D., Modeling structurally variable regions in homologous proteins with rosetta. *Proteins: Structure, Function, and Bioinformatics* **2004,** *55* (3), 656-677.

209. Morissette, R. Methods to characterize and assay the S. cerevisiae GPI tansamidase- a membrane bound, multi subunit, enzyme that post translationally modifies proteins. John Hopkins University, Maryland, 2007.

210. Ohishi, K.; Nagamune, K.; Maeda, Y.; Kinoshita, T., Two subunits of glycosylphosphatidylinositol transamidase, GPI8 and PIG-T, form a functionally important intermolecular disulfide bridge. *J Biol Chem* **2003,** *278* (16), 13959-67.

211. Meyer, U.; Benghezal, M.; Imhof, I.; Conzelmann, A., Active site determination of Gpi8p, a caspase-related enzyme required for glycosylphosphatidylinositol anchor addition to proteins. *Biochemistry* **2000,** *39* (12), 3461-71.

212. Ohishi, K.; Inoue, N.; Kinoshita, T., PIG-S and PIG-T, essential for GPI anchor attachment to proteins, form a complex with GAA1 and GPI8. *Embo J* **2001,** *20* (15), 4088-98.

213. Bowman, S. M.; Piwowar, A.; Arnone, E. D.; Matsumoto, R.; Koudelka, G. B.; Free, S. J., Characterization of GPIT-1 and GPIT-2, two auxiliary components of the Neurospora crassa GPI transamidase complex. *Mycologia* **2009,** *101* (6), 764-72.

214. Eisenhaber, B.; Maurer-Stroh, S.; Novatchkova, M.; Schneider, G.; Eisenhaber, F., Enzymes and auxiliary factors for GPI lipid anchor biosynthesis and post-translational transfer to proteins. *Bioessays* **2003,** *25* (4), 367-85.

215. Vidugiriene, J.; Vainauskas, S.; Johnson, A.; Menon, A., Endoplasmic reticulum proteins involved in glycosylphosphatidylinositol-anchor attachment: photocrosslinking studies in a cell-free system. *Eur J Biochem* **2001,** *268*, 2290 - 2300.

216. Ekanayaka, S. A. Development and optimization of the first high throughput *in vitro* assay to characterize the *S. cerevisiae* GPI-T. Wayne State University, Detroit, Michigan, 2013.

217. Hale, G., Synthetic peptide mimotope of the CAMPATH-1 (CD52) antigen, a small glycosylphosphatidylinositol-anchored glycoprotein. *Immunotechnology* **1995,** *1* (3–4), 175-187.

218. Xia, M.-Q.; Tone, M.; Packman, L.; Hale, G.; Waldmann, H., Characterization of the CAMPATH-1 (CDw52) antigen: biochemical analysis and cDNA cloning reveal an unusually small peptide backbone. *European Journal of Immunology* **1991,** *21* (7), 1677-1684.

219. Xia, M. Q. H., G; Lifely, M. R.; Ferguson, M.A., Campbell, D; Packman, L; Waldmann, H, Structure of the CAMPATH-1 antigen, a glycosylphosphatidylinositol-anchored glycoprotein which is an exceptionally good target for complement lysis. *Biochem. J.* **1993,** *293*, 633-640.

220. Edwards, J. O.; Pearson, R. G., The Factors Determining Nucleophilic Reactivities. *Journal of the American Chemical Society* **1962,** *84* (1), 16-24.

221. Dalley, J. A.; Bulleid, N. J., The Endoplasmic Reticulum (ER) Translocon Can Differentiate between Hydrophobic Sequences Allowing Signals for Glycosylphosphatidylinositol Anchor Addition to Be Fully Translocated into the ER Lumen. *Journal of Biological Chemistry* **2003,** *278* (51), 51749-51757.

222. Chen, R.; Knez, J. J.; Merrick, W. C.; Medof, M. E., Comparative efficiencies of C-terminal signals of native glycophosphatidylinositol (GPI)-

anchored proproteins in conferring GPI-anchoring. *Journal of Cellular Biochemistry* **2002,** *84* (1), 68-83.

223. G, G. D.; L, H. T., GPI Transamidase and GPI anchored proteins: Oncogenes and biomarkers for cancer. *Critical Reviews in Biochemistry and Molecular Biology* **2013,** *0* (0), 1-19.

224. Strome, E. D.; Plon, S. E., Utilizing Saccharomyces cerevisiae to identify aneuploidy and cancer susceptibility genes. *Methods Mol Biol* **2010,** *653*, 73-85.

225. Motegi, A.; Myung, K., Measuring the rate of gross chromosomal rearrangements in Saccharomyces cerevisiae: A practical approach to study genomic rearrangements observed in cancer. *Methods* **2007,** *41* (2), 168-76.

226. Tosato, V.; Gruning, N. M.; Breitenbach, M.; Arnak, R.; Ralser, M.; Bruschi, C. V., Warburg effect and translocation-induced genomic instability: two yeast models for cancer cells. *Frontiers in oncology* **2012,** *2*, 212.

227. Pereira, C.; Coutinho, I.; Soares, J.; Bessa, C.; Leao, M.; Saraiva, L., New insights into cancer-related proteins provided by the yeast model. *The FEBS journal* **2012,** *279* (5), 697-712.

228. Daee, D. L.; Mertz, T. M.; Shcherbakova, P. V., A cancer-associated DNA polymerase delta variant modeled in yeast causes a catastrophic increase in genomic instability. *Proceedings of the National Academy of Sciences of the United States of America* **2010,** *107* (1), 157-62.

229. Madia, F.; Gattazzo, C.; Fabrizio, P.; Longo, V. D., A simple model system for age-dependent DNA damage and cancer. *Mechanisms of ageing and development* **2007,** *128* (1), 45-9.

230. Brozmanova, J.; Manikova, D.; Vlckova, V.; Chovanec, M., Selenium: a double-edged sword for defense and offence in cancer. *Archives of toxicology* **2010,** *84* (12), 919-38.

231. Darsow, T.; Odorizzi, G.; Emr, S. D., Invertase fusion proteins for analysis of protein trafficking in yeast. *Methods Enzymol.* **2000,** *327*, 95-106.

232. Ohishi, K.; Inoue, N.; Kinoshita, T., *PIG−S and PIG−T, essential for GPI anchor attachment to proteins, form a complex with GAA1 and GPI8*. 2001; Vol. 20, p 4088-4098.

233. Craig, T. A.; Kumar, R., Synthesis and Purification of Soluble Ligand Binding Domain of the Human Vitamin D3Receptor. *Biochemical and Biophysical Research Communications* **1996,** *218* (3), 902-907.

234. Paterson, R. G.; Lamb, R. A., Conversion of a class II integral membrane protein into a soluble and efficiently secreted protein: multiple intracellular and extracellular oligomeric and conformational forms. *The Journal of Cell Biology* **1990,** *110* (4), 999-1011.

235. Wu, C. C.; MacCoss, M. J.; Howell, K. E.; Yates, J. R., A method for the comprehensive proteomic analysis of membrane proteins. *Nat Biotech* **2003,** *21* (5), 532-538.

236. Nyman, T.; Stenmark, P.; Flodin, S.; Johansson, I.; Hammarström, M.; Nordlund, P., The Crystal Structure of the Human Toll-like Receptor 10 Cytoplasmic Domain Reveals a Putative Signaling Dimer. *Journal of Biological Chemistry* **2008,** *283* (18), 11861-11865.

237. Kodukula, K.; Gerber, L. D.; Amthauer, R.; Brink, L.; Udenfriend, S., Biosynthesis of glycosylphosphatidylinositol (GPI)-anchored membrane proteins in intact cells: specific amino acid requirements adjacent to the site of cleavage and GPI attachment. *The Journal of Cell Biology* **1993,** *120* (3), 657-664.

238. Berger, J.; Micanovic, R.; Greenspan, R. J.; Udenfriend, S., Conversion of placental alkaline phosphatase from a phosphatidylinositol-glycan-anchored protein to an integral transmembrane protein. *Proceedings of the National Academy of Sciences* **1989,** *86* (5), 1457-1460.

239. Komano, H.; Rockwell, N.; Wang, G. T.; Krafft, G. A.; Fuller, R. S., Purification and Characterization of the Yeast Glycosylphosphatidylinositol-anchored, Monobasic-specific Aspartyl Protease Yapsin 2 (Mkc7p). *Journal of Biological Chemistry* **1999,** *274* (34), 24431-24437.

240. Hsu, N.-Y.; Yang, W.-B.; Wong, C.-H.; Lee, Y.-C.; Lee, R. T.; Wang, Y.-S.; Chen, C.-H., Matrix-assisted laser desorption/ionization mass spectrometry of polysaccharides with 2′,4′,6′-trihydroxyacetophenone as matrix. *Rapid Communications in Mass Spectrometry* **2007,** *21* (13), 2137-2146.

241. Domon, B.; Costello, C., A systematic nomenclature for carbohydrate fragmentations in FAB-MS/MS spectra of glycoconjugates. *Glycoconjugate J* **1988,** *5* (4), 397-409.

242. Inutan, E. D.; Trimpin, S., Matrix Assisted Ionization Vacuum (MAIV), a New Ionization Method for Biological Materials Analysis Using Mass Spectrometry. *Molecular & Cellular Proteomics* **2013,** *12* (3), 792-796.

243. Leibly, D. J.; Nguyen, T. N.; Kao, L. T.; Hewitt, S. N.; Barrett, L. K.; Van Voorhis, W. C., Stabilizing Additives Added during Cell Lysis Aid in the Solubilization of Recombinant Proteins. *PLoS ONE* **2012,** *7* (12), e52482.

244. Churion, K.; Bondos, S., Identifying Solubility-Promoting Buffers for Intrinsically Disordered Proteins Prior to Purification. In *Intrinsically Disordered Protein Analysis*, Uversky, V. N.; Dunker, A. K., Eds. Springer New York: 2012; Vol. 896, pp 415-427.

245. Shukla, D.; Schneider, C. P.; Trout, B. L., Molecular level insight into intra-solvent interaction effects on protein stability and aggregation. *Advanced Drug Delivery Reviews* **2011,** *63* (13), 1074-1085.

246. Golovanov, A. P.; Hautbergue, G. M.; Wilson, S. A.; Lian, L.-Y., A Simple Method for Improving Protein Solubility and Long-Term Stability. *Journal of the American Chemical Society* **2004,** *126* (29), 8933-8939.

247. Bondos, S. E.; Bicknell, A., Detection and prevention of protein aggregation before, during, and after purification. *Analytical Biochemistry* **2003,** *316* (2), 223-231.

ABSTRACT

BIOCHEMICAL AND STRUCTURAL CHARACTERIZATION OF THE CORE SUBUNITS OF GPI TRANSAMIDASE

by

DILANI G GAMAGE

May 2015

Advisor: Prof. Tamara L. Hendrickson

Major: Chemistry (Biochemistry)

Degree: Doctor of Philosophy

Glycosylphosphatidylinositol transamidase (GPI-T) is a complicated, membrane-bound, multi-subunit enzyme that catalyzes an essential post-translational modification. This enzyme attaches GPI anchors to the *C*-termini of various proteins that contain a proper GPI-T signal sequence. Gpi8, Gaa1, Gpi16, Gpi17 and Gab1 are the five known subunits that may encompass the fungal GPI-T; Gpi8 is the catalytic subunit, but the functions of the other subunits remain essentially unknown. In humans, different GPI-T subunits are upregulated in different cancers, making GPI-T a target for cancer research. However, in spite of the importance of this enzyme, little is known about how it assembles into an active enzyme complex, the stoichiometry of this complex, or the roles of the different components. Here we use soluble domains of the three core subunits (Gpi8, Gpi16 and Gaa1) to investigate the stoichiometry of the enzyme as well as to study the functions of each subunit *in vitro*. Additionally, overexpression of the

full-length core subunits was used to study the enzyme's behavior on transamidation *in vivo*.

Due to the complex nature of this protein and the fact that it is membrane associated, we set out to simply this enzyme into a more tractable system. In chapters 2 and 3 of this thesis, we focused on the soluble domains of the core subunits, $Gpi8_{1\text{-}306}$, $Gaa1_{50\text{-}343}$ and $Gpi16_{1\text{-}551}$. These soluble domains were overexpressed and their interactions and stoichiometry were characterized. Gpi8, the catalytic subunit, has weak sequence similarity to caspase-1 and assembles into a homodimer. Also, *N*-linked glycosylation of one asparagine in this subunit is not essential for dimerization. Co-immunoprecipitation of the soluble domains of $Gpi8_{1\text{-}306}$:$Gaa1_{50\text{-}343}$, $Gpi8_{1\text{-}306}$:$Gpi16_{1\text{-}551}$ and $Gpi16_{1\text{-}551}$:$Gaa1_{50\text{-}343}$ demonstrated that these subunits interact with each other at least in heterodimeric complexes. Initial characterization of the $Gpi8_{23\text{-}306}$:$Gaa1_{50\text{-}343}$ complex is consistent with the formation of an $\alpha_2\beta_2$ heterotetramer. Also, these three subunits $Gpi8_{1\text{-}306}$:$Gaa1_{50\text{-}343}$:$Gpi16_{1\text{-}551}$ can be co-purified as an intact complex. Preliminary results show that this core heterotrimer has nucleophile-independent activity. Our results will help to elucidate the function and resolve the complexity of GPI-T. Efforts are underway to determine the stoichiometry of each subunit and the contribution of each subunit towards transamidase activity.

To better understand how changes in expression affect GPI-T activity, and as a model for this enzyme in cancer, we have developed an *in vivo* strategy to monitor and quantify the effect of subunit overexpression on cell surface presentation of GPI-anchored proteins in *Saccharomyces cerevisiae*. Here we

used Invertase as a reporter enzyme. Three GPI-T signal sequences were appended to the *C*-terminus of invertase and the amount of cell surfaced, GPI anchored invertase was measured. Overexpression of Gpi8, the catalytic subunit had little effect on GPI anchoring of invertase with two of these three signal sequences; however, the amount of cell surface invertase was nearly doubled when the weakest signal sequence was used. Compared to Gpi8, overexpression of either Gpi16 or Gaa1 downregulated GPI-T activity with all three signal sequences. To our knowledge, these results represent the first direct examination of the impact of subunit overexpression directly on GPI-T activity. Our results suggest that overexpression of a single GPI-T subunit either disrupts assembly of active GPI-T or frees these subunits to participate different cellular functions.

The results presented in this dissertation represent the beginning of a new era aimed at understanding GPI-T and provide new tools and approaches to achieve this important goal.

AUTOBIOGRAPHICAL STATEMENT

EDUCATION:

Ph. D. Candidate (Chemistry) **2009 - present**
Wayne State University, Detroit, MI, USA,Advisor: Professor Tamara L. Hendrickson
M. Sc. In Chemistry (Biochemistry) **2007- 2009**
Eastern Illinois University, Charleston, IL, USA, Advisor: Dr Gopal R Periyannan
Bachelor of Science (B. Sc.) **2002 – 2005**
Institute of Chemistry, Sri Lanka
Bachelor of Science (B. Sc.) **2002 – 2006**
University of Colombo, Colombo, Sri Lanka

RESEARCH EXPERIENCE

Graduate Research
Wayne State University, Detroit, MI, USA **2009 - present**
Department of Chemistry, Advisor: Professor Tamara L. Hendrickson
Eastern Illinois University, Charleston, IL, USA **2007 - 2009**
Department of Chemistry, Advisor: Dr. Gopal R. Periyannan
Undergraduate Research
University of Colombo **2002 - 2006**
Department of Chemistry, Advisor: Dr. Jayantha Wijebandara

PUBLICATIONS

Invited review: **Gamage, D. G.** and Hendrickson, T. L. "GPI transamidase and GPI anchored proteins: oncogenes and biomarkers for cancer." **2013**,*Crit. Rev. Biochem. Mol Biol.* 48(5):446-64.

POSTER PRESENTATIONS:

Dilani G. Gamage, Tamara L. Hendrickson, "Reconstitution of the core domains of GPI transamidase into a soluble complex without their transmembrane region." ASBMB annual meeting, San Diego, California, **2014.**
Dilani G. Gamage, Sandamali Ekanayaka, Yug Varma, Sairaman Seetharaman & Tamara L. Hendrickson, "Breaking the boundaries of the GPI transamidase complex." 8th Midwest Carbohydrate Research Symposium, Detroit, Michigan, **2012.**
Dilani G. Gamage; Gopal R. Periyannan; Pramodha S. Liyanage, "Homology modeling: Molecular evolution of glutamate carboxypeptidase II." 38th ACS Regional Meeting & Exposition at Chicago, **2009**
Dilani G. Gamage; Timothy Russell; Gopal R. Periyannan, "Instability Index as an indicator of *in vitro* protein stability." 236th ACS National Meeting & Exposition at Philadelphia, **2008**.

AWARDS:

Herbert K. Livingston Award for Excellence in Teaching, WSU, 2014

Honors Citation for Excellence in Teaching, WSU, 2013

Outstanding International Student Award, EIU, 2009

Outstanding Teaching Assistant Award in Chemistry, EIU, 2009

Distinguished Graduate Student Award in Chemistry, EIU, 2008

Shireen Jayasuriya Gold medal for best performance, I.Chem, 2005